UNIVERSITY OF STAVANGER

Uncompensated and compensated backgrounds in homeostatic controllers: Analogies to retinal light adaptation

by

Melissa Nygård

Master Thesis in Biological Chemistry

submitted to the
Faculty of Science and Technology
Department of Biology, Chemistry and Environmental Engineering

June 2023

UNIVERSITY OF STAVANGER

Abstract

Faculty of Science and Technology
Department of Biology, Chemistry and Environmental Engineering

Master Thesis in Biological Chemistry

by Melissa Nygård

Integral controllers with single negative feedbacks were subjected to a step-perturbation at constant but different backgrounds. Response amplitudes of the controlled variable, here called A, decreased monotonically with increasing backgrounds, which was opposed and corrected for by compensatory actions of the manipulated variable E. The controllers divided equally into two classes, in which the compensatory fluxes were either based on derepression or activation. Controllers with derepression-based compensatory fluxes showed decreased sensitivity but accelerated response kinetics, which is analogous to the resetting kinetics seen in vertebrate photoreceptors. Retinal light adaptation also involves compensating backgrounds according to remarks in the literature. We therefore became interested in understanding the underlying feedback mechanisms of background compensation. As such, we created controllers or oscillators that show robust background compensation independent of the applied background. These controllers need a second feedback layer, where the additional integral controllers (I_1 and I_2) feed directly or coherently back to the controlled variable. These feedback conditions were termed "coherent feedback" in analogy to a similar feedback mechanism used in quantum control theory and optics. Finally, simple three-neuron retinal light adapation (RLA) models, representing the retina as a whole, were subjected to the same perturbations. It was the feedback organization in the two-layered oscillator that was responsible for eliminating backgrounds. Robust background compensation, here described theoretically, could be of interest in terms of regulatory properties. Although, no biological relevanse of the concept has been identified.

Acknowledgements

I would like to express my deepest appreciation to my supervisor Prof. Dr. Peter Ruoff at the University of Stavanger for guiding me through the work of this thesis. He has gladly offered his expertice and support on countless occasions, and it has been a real joy working alongside with him.

I would also like to thank my fiancé Egil Tunheim for encouraging me to succeed and for his endless support.

A special thanks goes to my father Knut Arvid Nygård for always being there for me and inspiring me to believe in myself.

Contents

List of Figures

Chapter 1

Introduction

1.1 About the thesis

This thesis is a computational study on models for photoadaptation. A certain set of negative feedback loops, also called controllers, were studied and they showed robust homeostasis. These controllers respond to perturbations in a coordinated and regulated way, and keep their variables within narrow limits due to the application of integral control. It was found that the controllers have the same type of resetting kinetics (i.e., background and/or frequency compensations) as certain retinal cells, and are therefore analyzed with regards to photoadaptation.

1.2 Cannon's concept of homeostasis

Homeostasis is the property of a physiological system to maintain its internal stability while being subjected to external perturbations. This is made possible by coordinated responses that keep these disturbances within narrow limits. The presence of (homeostatic) defense mechanisms in animals and plants is crucial for their health and survival. Different physiological variables, such as body temperature, blood glucose levels, and hormones in animals, are kept within an optimal, functional, and healthy range of values. By not maintaining homeostasis the internal stability weakens and the organism can experience damage, disease, and even death [9, 10].

The original concept of homeostasis took many years to develop. In the eighteenth century, Charles Blagden [11, 12] and John Hunther [13] came to understand that body temperature remains constant over a wide range of external temperature values, indicating that it is internally stable. This idea of internal stability was further established

in the nineteenth century by scientists such as Charles Robin, Claude Bernard, Leon Fredericq, and Charles Richet [10]. Bernard, in particular, realized that the internal environment is stable and not dependent on external conditions. He also recognized that the internal stability, or as he called it: "Le milieu interieur", is vital for the organism's health and survival [14–16]. Richet, who was a student of Bernard, stressed that the internal environment is dynamically regulated and can be modified to oppose the changes caused by external stimuli [17]. The physician Walter B. Cannon built on ideas like these and eventually coined the term "homeostasis" in 1929, which describes a self-regulatory process in living systems that adapts to external perturbations and maintains stability [9, 10, 16, 17].

The constant conditions of homeostasis can be explained by maintaining a steady state. This is because a complex and (open) biological system might have some variations, in which the internal environment is held within narrow limits without being constant and rigid. Cannon therefore acknowledged that the prefix "stasis" in homeostasis could be misleading. He tried to explain the variations by using the prefix "homeo" instead of "homo", which indicates similar instead of like, respectively [10].

1.3 Alternative definitions of homeostasis

Even though Cannon mentioned that homeostasis can show some variations, the term is today often recognized in its most simplistic form. As a result, alternative names and definitions have been suggested to account for the more complex and dynamic homeostasis (i.e., oscillations) that is known to occur in (open) biological systems.

Moore-Ede recognized that the classical concept of homeostasis is reactive, i.e., deviations from the set-point are measured before being corrected for by negative feedback. He suggested to expand Cannon's definition to include **predictive homeostasis**. This would account for circadian timing systems, which first anticipate and then adapts to environmental changes [18].

The term **allostasis** was introduced by Sterling and Eyer [19] and means "stability through change". They argued that the classical concept of homeostasis fails to explain that an organism may benefit from a non-constant internal environment. Instead it adapts to perceived and anticipated challenges by changing the internal milieu [19–21]. This is true when a bear prepares for hibernation by gaining fat, or when a cow undergoes morphological, physiological and behavioural changes in order to produce lactate for a calf [22].

Also, Lloyd suggested to use the term **homeodynamics** instead of homeostasis since adaptation mechanisms are very dynamic. In fact, he stated that it is the dynamic organization of having a homeodynamic system that makes the organized complexitiy of life possible [23].

Lastly, Mrosovosky introduced **rheostasis** to consider shifting set-points. He explained that an organism is under homeostastic control at all times, but that the regulated set-point may change over time. This is the case when we are running a fever, and the body experiences a sustained and controlled rise in temperature [24]. Another example is when an animal adapts to a change in season by gaining fat. Mrosovsky argued that environmental changes like this could explain the physiological plasticity that an organism experiences during evolution [25].

These alternative definitions to homeostasis are not necessary, according to Carpenter [26]. Homeostatic principles are often used in an oversimplified way, and deviations from this are rediscovered and wrongly treated as something new and distinct from homeostasis. Carpenter further argues that Cannon's definition of homeostasis can take onto different and more complex forms by allowing the cooporation of different feedback mechanisms, and that the term **homeostasis** can still stand as an unified approach.

1.4 The apperance of cybernetics

Regardless of the definition that is used, we now know that homeostatic processes involve a complex combination of feedback mechanisms, i.e., feedback loops, that respond to environmental changes in an automatic and coordinated way. A negative feedback loop is able to maintain the preferred set-point of its physiological variable (i.e., body temperature, blood glucose level, and hormones) by feeding the results from previous actions into the system, and thereby adjusting the outcome of future actions [17].

The idea that animals respond to perturbations in an automatic and coordinated way originated from mechanics with the invention of self-regulatory devices. The study of these self-regulatory products has been around for a long time, but really took off in the late 18th century. At this time the steam engine, which was regulated by corrective feedback, was developed and later improved by James Watt. Then in the 19th century, James Clerk Maxwell built on his work and published a mathematical analysis that explained the principles of self-regulatory devices [17, 27]. This eventually became the foundation to which control theory is built upon, and is defined as a feedback-regulated system that controls its behaviour without being directed by external factors [17]. Two important papers, published in 1943, found that the mathematical principles of control

theory can be used to explain the self-regulatory behaviour in living organisms [28, 29]. One of the authors was Norbert Wiener, which later introduced the term "cybernetics" as the science of communications and self-regulated control in both machines and animals [17, 30].

With the development of cybernetics "integral control", which was introduced in the beginning of the 20th century as a way to regulate industrial processes, was applied in the study of living organisms in order to achieve homeostasis [31, 32]. Integral control is a control-engineering method that involves system analysis and control theory (see Ch. 2.3). Upon external perturbations it is able to keep a controlled variable, say A, preciesly and robustly at its set-point by feeding the integrated error back into the perturbation-independent process. This is due to the compensatory actions of the manipulated variable [1, 2, 33, 34], which is here called E. Different kinetic requirements of integral control can be used in physiological processes to achieve homeostasis, and among them are zero-order kinetics in the removal of E [7], antithetic or dual-E control [35, 36], and a mixture of autocatalytic synthesis of E and first-order kinetics in the removal of E [37].

1.5 Background and frequency compensations

Retinal light adaptation, according to the literature, involves compensating backgrounds [3, 8, 38, 39]. We therefore became interested in understanding the underlying feedback mechanisms of this phenomenon. As such, we created controllers that (mainly) incorporate integral control in terms of zero-order kinetics. Also incorporating a type of feedback, here termed "coherent feedback", will enable these controllers to compensate for step-wise perturbations (i.e., frequency) at different but constant backgrounds. The term "coherent feedback" was introduced by Lloyd and others [5, 6]. Since the feedback, which can compensate for backgrounds is similar to Lloyd's coherent feedback definition [6], we adopted this term. A variant of coherent feedback is "incoherent feedback". In this case controllers can still compensate for step-wise perturbations, which is here termed "frequency compensation", without having the ability to adapt to different backgrounds.

1.6 Layout of the thesis

Since the work of this thesis is to study the photoadaptation of light in the retina, photoadaptation is the first topic that is introduced. Light that enters the eye hits the photoreceptors in the outer part of the retina. This initiates a phototransduction cascade that activates the subsequent bipolar and ganglion cells, in which the latter cell's axons come together to form the optic nerve that enters the central nervous system for further image processing [3, 8, 40, 41].

This thesis deals with three types of controllers that correspond to the behaviours of different retinal cells. First, a set of eight single-layered (also called one-layered) basic negative feedback motifs will be provided. These controllers respond to different but constant light increments with decreasing amplitudes, where some of them show faster resetting times in anology to the resetting kinetics seen in vertebrate photoreceptors [8, 42, 43]. Their ability to reset at their pre-perturbation levels are due to the incorporation of a basic integral controller [7].

Retinal ganglion cells are known to oscillate, as well as having partial frequency compensations [39]. We therefore created two-layered frequency compensated oscillators in order to represent these cells. These controllers are subjected to step-wise perturbations at different but constant background illuminations, which test their adaptation to frequency and light, respectively. Coherent or incoherent feedback are included into the controllers and enable them to show frequency compensation. Those with coherent feedback also manage to compensate backgrounds.

Lastly, retinal light adaptation (RLA) models will be introduced as a way to study the cellular interactions in the whole retina. These controllers have three feedback layers that correspond to different retinal cells. The first layer represents one of the photoreceptor models, which sends an inhibitory signal to a hypothetical bipolar cell in the second layer. The bipolar cell then feeds a signal to the third and final layer, which is represented by a frequency compensated ganglion cell. It is the feedback organization in the ganglion cell layer that regulates retinal background compensation.

Part of my work, regarding the eight negative feedback motfis, has been published in PLOS ONE (see Appendix C). A manusscript has also been submitted to PLOSE ONE (see Appendix D), which deals with some of my results of the frequency compensated oscillators. This manusscript was under review at the time this thesis was submitted.

Chapter 2

Materials and Methods

2.1 Computational methods

Computations were made by using the Fortran subroutine LSODE (https://computing.llnl.gov/projects/odepack), and the graphical outputs were generated with Gnuplot (www.gnuplot.info). These plots, as well as other figures, were annotated with Adobe Illustrator (https://www.adobe.com/). The time derivative of different variables are indicated by the dot notation, and rate constants are given in arbitary units (a.u.) with the notation k_i (where i=1,2,3...). The number i does not depend on the type of kinetic conditions (i.e., Michaelis constants, turnover number, inhibition constants, or activation constants). Computations have been made more accessible to the general public by converting some of the Fortran results to python (see Appendix A) and MATLAB scripts (see Appendix B).

2.2 Types of chemical negative feedbacks

There are eight basic single (one-layered) negative feedback loops (Fig. 2.1), which are analyzed with respect to an applied step and constant but different backgrounds. These controllers divide equally into inflow and outflow controllers, and are able to keep a controlled variable A robustly at its set-point. In particular, the controlled variable A is back-regulated to its set-point after step-perturbations are applied. A is compensated by compensatory fluxes provided by the manipulated variable E, which either stimulates the increase or reduction of A, depending on whether the feedback motif is an inflow or outflow controller, respectively [1]. Step-wise perturbations were used because integral controllers, in general, are known to fully compensate them [44].

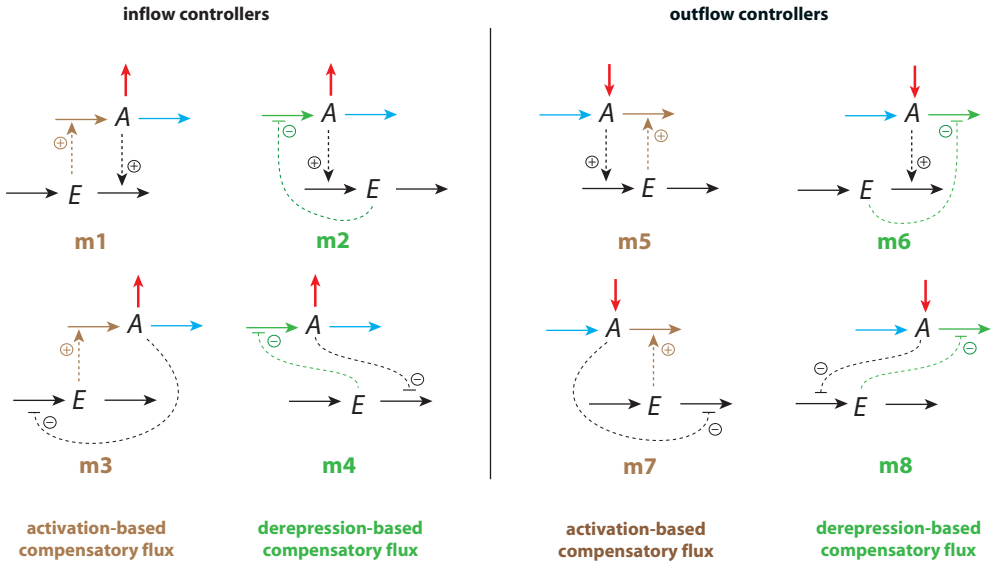

FIGURE 2.1: Controller motifs m1-m8. Step-perturbations and constant background reactions are indicated by red and blue arrows, respectively. Solid lines indicate chemical reactions. Dashed lines represent signaling events, in which activation-based compensatory fluxes are indicated by a brown color and derepression-based compensatory fluxes by a green color. Plus and minus signs represent, respectively, activation and inhibition. Integral control is incoporated by zero-order kinetics. Figure was taken from Ref. [1] with permisssion.

In the inflow controllers, m1-m4, step-perturbations (red arrows) and constant background reactions (blue arrows) are applied such that A is reduced, and it is increased back to its set-point either by an activation-based compensatory flux (controllers m1 and m3) that directly stimulates the production of A or by a derepression-based compensatory flux (controllers m2 and m4) in which the synthesis of A is inhibited by a negative feedback.

In controllers m5-m8, which are outflow controllers, the opposite occurs and A is increased when step-perturbations (red arrows) and backgrounds (blue arrows) are applied. The activation-based compensatory flux (controllers m5 and m7) reduces A back to its set-point by directly activating the breakdown of A, whereas the derepression-based compensatory flux (controllers m6 and m8) inhibits the breakdown of A through negative feedback [1].

Details about each of these controllers can be found in Ch. 3.2, along with their response kinetics to changes in illumination. These controllers incoporate integral control by zero-order kinetics (see next chapter). However, an additional m2 controller that incorporates integral control by autocatalysis, will also be provided.

2.3 Integral control

As mentioned, integral control is a control-engineering concept that keeps a controlled variable (A) precisely and robustly at its set-point (A_{set}), which is accomplished by feeding the integrated error back into the perturbation-independent process. We will use outflow controller m5 (Fig. 2.2a) to illustrate how integral control (Fig. 2.2b) can be incorporated into this controller motif by zero-order kinetics.

Inflow perturbations (by k_1 and k_3) in m5 (panel a) will temporarily increase the level of A to above A_{set}, which means that more E is activated through the rate constant k_5. The compensatory actions of E (with k_6 and k_7) then contribute to a higher removal of A (through k_4) and, as a result, the controller shows robust perfect adaptation of A. This is due to the incoporation of integral control as zero-order Michaelis Menten (MM) kinetics in the removal of E. The MM parameters V_{max} and K_m are represented by k_6 and k_7, respectively.

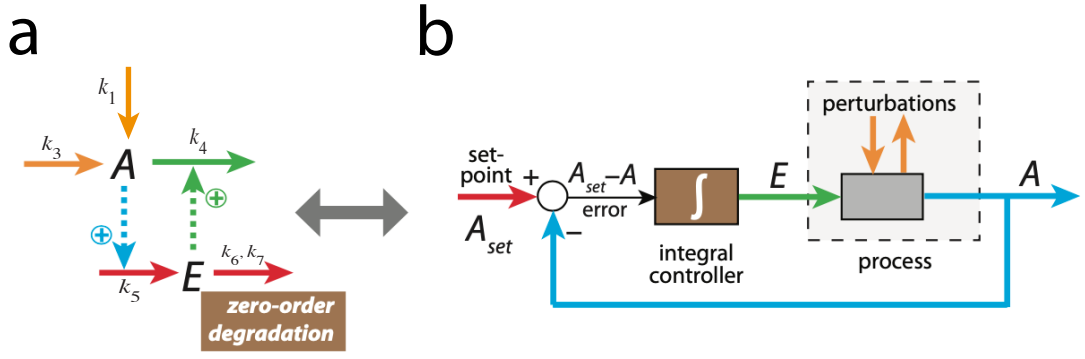

FIGURE 2.2: Integral control in terms of zero-order kinetics. Figure was redrawn from Ref. [2], Fig. 1. a) Controller motif m5 from Fig. 2.1 is shown together with rate constants k_i (where i=1, 2, 3...). The negative feedback loop shows robust perfect adaptation of A due to removing E by zero-order kinetics. For explanation, see text. b) Typical flow chart of integral control. Uncontrollable perturbations (orange arrows) add or remove the controlled variable A. The difference between A and the set-point A_{set}, A_{set}-A, is measured and integrated over time (brown "integral controller" box). This gives the concentration of the manipulated variable E (green line) that is necessary to bring A back to A_{set} through a negative feedback loop (blue line). The colors in panel b correspond to those in panel a.

In panel b this is illustrated in terms of an integral controller scheme. Environmental perturbations (orange arrows) remove the concentration of A in comparison to A_{set}. This difference or error, ϵ=A_{set}−A, is integrated over time (brown "integral controller" box) and yields the concentration of E (green line). This new level of E feeds into the process (grey box) that generates A and brings A back to its set-point through a negative feedback loop (blue line) [45].

The time derivative of the controlled variable ($\dot{A}$) can be determined by subtracting the sum of outflow perturbations k_{pert}^{inflow} (arrows pointing away from A) from the sum of inflow perturbations k_{pert}^{inflow} (arrows pointing towards A) that remove and add A, respectively. These perturbations also need to be multiplied with the species that (may) have influenced the inflow or outflow of A (i.e. A or E):

$$\dot{A} = k_{pert}^{inflow} - k_{pert}^{outflow} = (k_1 + k_3) - (k_2 + k_4 \cdot E) \cdot A \tag{2.1}$$

where A and E both affect the outflow perturbations.

A similar process is done for the time derivative of the manipulated variable ($\dot{E}$). However, the removal of E occurs by zero-order MM kinetics due to the application of integral control:

$$\dot{E} = k_{pert}^{inflow} - k_{pert}^{outflow} = k_5 \cdot A - \frac{k_6 \cdot E}{k_7 + E} \tag{2.2}$$

where the inflow and outflow perturbations are affected by A and E, respectively.

By incorporating this type of integral control one assumes that $k_7 \ll E_{ss}$ (ss: steady state) and, as such, that $E/(k_7+E) \approx 1$. Finally, the set-point A_{set} can be determined together with the steady state assumption, i.e. $\dot{E}=0$:

$$\dot{E} = k_5 \cdot A - \frac{k_6 \cdot E}{k_7 + E} \approx k_5 \cdot A - k_6 = -k_5 \underbrace{\left(\underbrace{\frac{k_6}{k_5}}_{A_{set}} - A \right)}_{error} \tag{2.3}$$

where E is proportional to the integrated error.

Chapter 3

Results

3.1 Photoadaptation in the retina

This section provides information about photoadaptation in the retina, i.e., how retinal cells adapt to changes in illumination. Incoming light goes through the optical components of the eye before it is focused onto the retinal surface. The light then travels through the retinal layers and towards the photoreceptors' outer segments. These segments contain light-sensitive photopigments that change configuration in response to light, which initiates a phototransduction cascade [3, 8, 40, 41]. This cascade of events will be explained, along with the basic types of retinal cells and their interactions within the retinal layers.

3.1.1 Phototransduction cascade

Phototransduction is the process of converting photons from light into electrical signals or potentials across the cell membrane of photoreceptors. Rods and cones contain light-sensitive photopigments of rhodopsin and photopsin, respectively, which are located in membraneous disks of their outer segments. These pigments change configuration in response to light, and are responsible for initiating the phototransduction cascade. This series of events will be explained by using rods as an example. However, a similar process occurs in cones when photopsin is hit with light instead of rhodopsin.

Rhodopsin consists of the light-absorbing chromophore and vitamin-A derivative retinal and one or several types of the protein opsin, with each opsin absorbing light at a particular wavelength. An incoming photon of light is absorbed by retinal and, as a result, breaks a double carbon-bond that changes the configuration of 11-cis retinal into All-trans retinal. This triggers a cascade of events in which opsin first leaves retinal

to activate the intracellular messenger transducin. Transducin then activates phosphodiesterase (PDE) that is responsible for hydrolyzing the nucleotide cyclic guanosine monophosphate (cGMP). The role of cGMP is to gate or control the amount of cations (Ca^{2+} and Na^{+}) that flow into the membrane channels of the photoreceptor's outer segment. This influx of ions is opposed by the efflux of cations (K^{+}) in potassium-selective channels of the photoreceptor's inner segment. A decreased concentration of cGMP means that there is less cGMP to bind to the membraneous channels. The channels of the outer segment therefore start to close when illumination is increased.

The increased concentration of cGMP in the dark, however, allows for a higher influx of cations through the cGMP-gated channels. This inward current of ions contributes more than the efflux of K^{+} ions in the inner segment. Photoreceptors are therefore depolarized in the dark with a membrane potential of about -40 mV, and have a high neurotransmitter release of glutamate at the synapse. In light, however, the decreased concentration of cGMP yields a lower influx of positive ions. The membrane potential therefore starts to hyperpolarize, i.e., it becomes more negative until it reaches a saturation around -65 mV. Hyperpolarized photoreceptors release less glutamate due to the fewer channels that are open. Photoreceptors show graded membrane potentials and not action potentials.

How much the phototransduction cascade is amplified varies with the level of illumination. The amplification process stops by bringing the activated molecules back to their inactive states. The first step is when rhodopsin kinase phosphorylates the activated rhodopsin, which allows the protein arrestin to bind to rhodopsin. This stops the latter molecule from activating transducin and, as a consequence, the rest of the phototransduction cascade. Lastly, rhodopsin is regenerated by a complex process involving the retinoid cycle [3, 8, 40, 41].

3.1.1.1 Intracellular feedback loops in photoreceptors

The phototransduction cascade is said to be regulated by an overlay of three negative feedback loops, which is illustrated in Fig. 3.1. cGMP first activates the inflow of Ca^{2+} ions through cyclic nucleotide-gated (CNG) channels of the outer segment (outlined in purple). Ca^{2+} ions then regulate cGMP and itself by three feedback loops. In feedback loop 1 (outlined in red) Ca^{2+} ions inhibit guanylate cyclase (GC), which synthesizes cGMP. cGMP is also regulated in feedback loop 2, where Ca^{2+} ions activate the breakdown of cGMP through transducin and PDE. Feedback loop 3 (outlined in yellow) is activated when the concentration of Ca^{2+} ions become high. In this loop calcium inhibits its own influx of ions through the CNG-channels, which is necessary

to avoid cytotoxic concentrations of Ca^{2+} ions. Lastly, K^+ ions are pumped out of the cell through potassium-dependent sodium-calcium exchangers (NCKX) of the inner segment. This has a negative effect on calcium's contribution on the membrane potential [1].

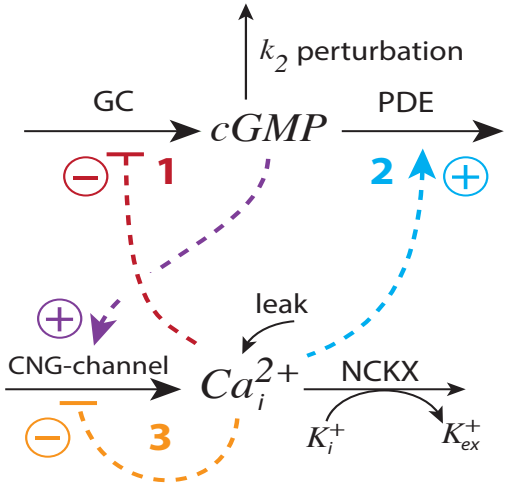

FIGURE 3.1: Regulation of photoadaptation by an overlay of three negative feedback loops. Lower and higher levels of light intensities, represented by the perturbation k_2, increase or decrease the concentration of cGMP in the photoreceptors, respectively. cGMP activates the inflow of calcium ions (outlined in purple). These ions further affect cGMP by inhibiting the synthesis of GC in feedback loop 1, and by activating the breakdown of cGMP by PDE in feedback loop 2. In feedback loop 3 Ca^{2+} ions inhibit their own transport through the CNG-channels in order to avoid cytotoxicity. Finally, their ions, along with potassium (K^+) ions, are pumped out of the cell by NCKX-channels of the outer segment. Also, there is a constant leak of Ca^{2+} out of the endoplasmic reticulum indicated by the term "leak". Figure was redrawn from Ref. [1], Fig. 18.

3.1.2 Interactions within the retinal layers

Five basic types of cells are distributed throughout the ten retinal layers, which is illustrated in Fig. 3.2. One of these is the light-sensitive photoreceptor, which is made of an an outer segment, inner segment, and a synaptic terminal. There are two types of photoreceptors, rods and cones, and their outer segments have stacks of membraneous disks containing the photopigments rhodopsin and photopsin, respectively. Rods have free-floating disks whereas cones have disks that are connected to the plasma membrane. Another difference structurally is that the outer segment of rods are long and cylindrical whereas the ones for cones are shorter and more tapered. Rods are sensitive to light and operate under dim-light conditions. However, as the light increases rods stop functioning and cones take over. The cones are less sensitive to light but can operate at a wide range of the visual spectrum [3, 8, 40, 41]. In the human retina there are about 100 million

rods, and they are typically found throughout the periphery of the retina. There are way less cones, about 5 millions, and most of them are found in the fovea. The fovea only contains cones and has high visual acuity [8, 38].

The base of the photoreceptors are connected to the outermost retinal pigmented epithelium layer (PE) **(layer 1)**, which is a thin and single layer of epithelial cells that are connected through tight junctions. There are no blood vessels in the retina and the choroid below the PE therefore supplies the retina with necessary nutrients, water, and molecules. The RPE therefore functions as a barrier between the blood and nutrient supply from the choroid to the retina. PE also prevents scattering of light by absorbing photons through its pigmented molecules of melanin, as well as to recycle photopigments. The outer segment of the photoreceptors, which are partially submerged in the PE, constitues the photoreceptor layer (PRL) **(layer 2)**. The inner segment of photoreceptors stretches over both the outer limiting membrane (OLM) **(layer 3)** and outer nuclear layer (ONL) **(layer 4)**.

Upon light exposure the photoreceptor experiences a graded membrane potential and releases glutamate at its synaptic terminal in the outer plexiform layer (OPL) **(layer 5)**. As previously mentioned, the photoreceptor cell becomes depolarized in the dark and releases much glutamate. With increasing illumination the cell becomes hyperpolarized and releases less glutamate. In the same outer plexiform layer a downstream bipolar cell receives the signal, as well as a horizontal cell. A bipolar cell has its central body in the inner nuclear layer (INL) **(layer 6)** with a synaptic terminal on both sides. There are two main types of bipolar cells. These are the on-center and off-center bipolar cells, in which the center or annulus of the receptive field, respectively, is excited by a spot of light. Off-center bipolar cells have ionotropic AMPA kainate receptors that open Ca^{2+}-channels in response to glutamate. Thus, when an off-center bipolar cell reacts to a depolarized photoreceptor it receives many glutamates. This means that there is a higher influx of Ca^{2+} ions, which also makes the bipolar cell depolarized. The opposite occurs when the off-center bipolar cell responds to a hyperpolarized photoreceptor that releases less glutamate, and the cell becomes hyperpolarized. The other main type of bipolar cell, on-center bipolar cell, has the metabotropic glutamate receptor 6 (mGluR6), which instead closes Ca^{2+}-channels in response to glutamate. This means that on-center bipolar cells that receive synaptic inputs from depolarized and hyperpolarized photoreceptors become, respectively, hyperpolarized and depolarized.

After the bipolar cell has experienced a graded membrane potential, either in terms of depolarization or hyperpolarization, it relases glutamate onto the downstream ganglion cell in the inner plexiform layer (IPL) **(layer 7)**. The neurotransmitter is also released

onto amacrine cells in the same layer. Ganglion cells also follow the on-center and off-center pathways, and there are both on-center and off-center ganglion cells. The ganglion cell axons are located in the ganglion cell layer (GCL) **(layer 8)** and come together in the nerve fiber layer (NFL) **(layer 9)** to form the optic nerve that enters the central nervous system. Ganglion cells instead show action potentials and generate spikes in response to light, which is due to the longer travelling distance of the signal. Lastly, there is an inner limiting membrane (ILM) **(layer 10)** next to the NFL.

As mentioned, there are also horizontal and amacrine cells in the retina. The horizontal and amacrine cells receive glutamate from the synaptic terminals of photoreceptors and bipolar cells, respectively. Horizontal cells inhibit the photoreceptors by releasing GABA onto their synaptic terminals. They also span laterally over a wide region in the outer plexiform layer to aid in the signaling between photoreceptors and bipolar cells. Amacrine cells instead send inhibitory feedback to the bipolar cells in terms of GABA.

In addition to the five basic types of retinal cells there are interplexiform cells that stabilize the outer and inner plexiform layers. There are also glial cells, i.e. muller cells, astrocytes, and microglica, distributed throughout the retina [3, 8, 40, 41].

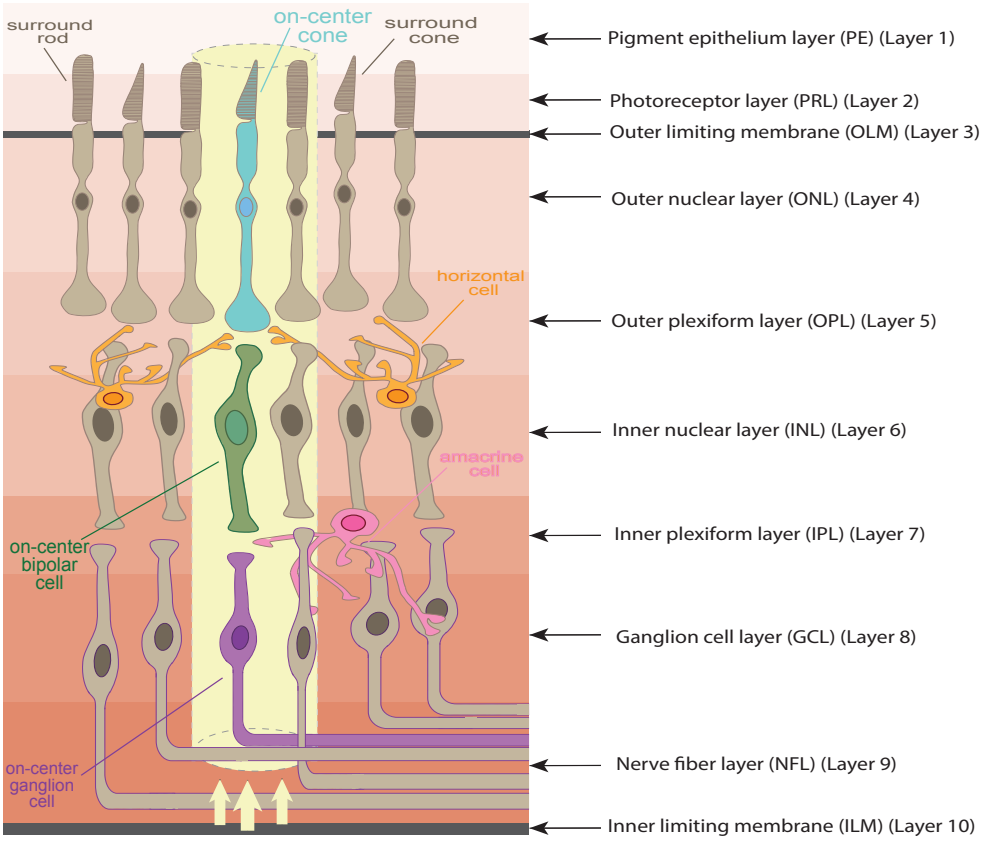

FIGURE 3.2: Cellular interactions within the retina. This figure illustrates the retinal interactions that occur when a spot of light (indicated by yellow arrows) excites the center (indicated by yellow "cylinder") of the receptive field. An on-center cone (colored blue) is first hit with light. Neurotransmitter is then released from its synaptic terminal and onto the on-center bipolar cell (colored green) and horizontal cells (colored orange). An on-center ganglion cell (colored purple) and amacrine cell (colored pink) then receives this signal. Ganglion cell axons come together in the nerve fiber layer to create the otic nerve that enters the central nervous system. Cells outside of the center (yellow "cylinder") are in the annulus of the receptive field. Each of the ten retinal layers has a distinctive name (indicated by horizontal arrows) and background color. Figure was redrawn from Ref. [3], Fig. 11.5 and Fig. 11.21.

3.2 One-layered controller motifs m1-m8

In the following chapter we are looking at how the single-negative feedback motifs (from Fig. 2.1) are influenced by a step-wise perturbation at constant but different backgrounds. All controllers incorporate integral control by zero-order kinetics. This enable them to keep the controlled variable A under robust homeostatic control by the manipulated variable E, where the compensatory fluxes of E are either based on activation or derepression. As mentioned, Fig. 3.1 illustrates how the phototransduction cascade is regulated by an overlay of three negative feedback loops. In fact, the m1-m8 controllers represent a simplified version of this figure with two negative feedbacks (feedback loop 3 is absent), where cGMP and Ca^{2+} are represented by A and E, respectively. Feedback loops 1 and 2 manage to keep cGMP homeostatically regulated as long as the levels of GC and PDE (represented by their respective k_i-values) are high enough [1]. The single-negative (or one-layered) feedback motifs are therefore meant to represent the retinal photoreceptor.

3.2.1 Controllers with activation-based compensatory fluxes

This subsection contains the results for inflow controllers m1 and m3, as well as the outflow controllers m5 and m7. All motifs have activation-based compensatory fluxes. These fluxes oppose the change in A, caused by a step-wise perturbation and constant but different background, and eventually direct A back to its set-point A_{set} in order to maintain homeostasis.

Controller m1

Regarding the inflow controller m1 in Fig. 3.3a, a step-perturbation k_2 (red arrow) and constant background k_4 (blue arrow) are applied in such a way that A is temporarily reduced. The change in A is compensated by the activation-based compensatory flux $j_3{=}k_3{\cdot}E$, directed by E, which increases the level of A by directly activating the synthesis of A.

The rate constants of A and E are, respectively:

$$\dot{A} = k_3{\cdot}E - (k_2 + k_4){\cdot}A \tag{3.1}$$

$$\dot{E} = k_5 - A\left(\frac{k_6{\cdot}E}{k_7{+}E}\right) \tag{3.2}$$

Integral control is incorporated by a zero-order degredation of E with the assumption that $k_7{\ll}E_{ss}$, which means that $E/(k_7{+}E) \approx 1$. Together with the steady state approximation (i.e. $\dot{E}{=}0$) the set-point A_{set} can be determined:

$$\dot{E} = 0 \;\Rightarrow\; k_5 = k_6{\cdot}A_{ss} \;\Rightarrow\; A_{set}{=}A_{ss}{=}\left(\frac{k_5}{k_6}\right) \tag{3.3}$$

Rearranging the previous equation also shows that E is proportional to the integrated error ($\epsilon{=}A_{set}{-}A$):

$$\dot{E} = k_6(\underbrace{\frac{k_5}{k_6}}_{A_{set}} - A) = k_6{\cdot}\epsilon \;\Rightarrow\; E(t) = k_6\int_0^t \epsilon(t'){\cdot}dt' \tag{3.4}$$

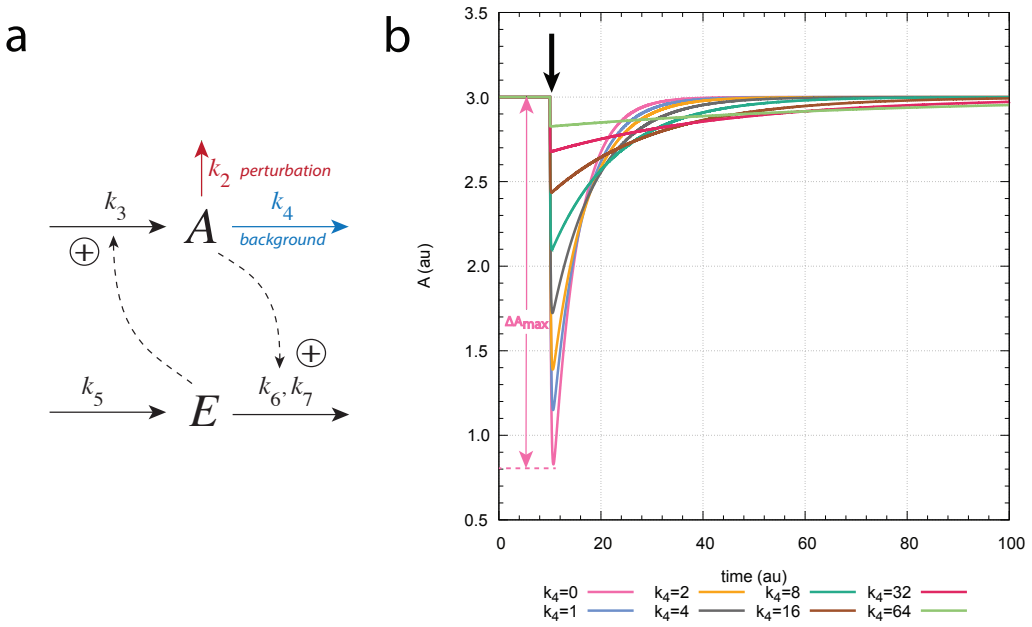

FIGURE 3.3: Resetting kinetics of controller motif m1. (a) Reaction scheme with integral control incoporated as a zero-order Michaelis-Menten (MM) type degredation of E. The MM parameters V_{max} and K_m are represented by k_6 and k_7, respectively. k_2 is a perturbation (red arrow) and k_4 represents a background reaction (blue arrow). Solid arrows represent chemical reactions. Dashed lines indicate signaling events, where activation is represented by a plus sign. Figure was redrawn from Ref. [1], Fig. 3. (b) Response kinetics of the m1 controller (in a.u.) at a step-wise perturbation k_2 (indicated by vertical arrow) from phase 1 (k_2=1.0) to phase 2 (k_2=5.0) at time t=10 with different but constant backgrounds k_4 from 0→64 (k_4 variable, phases 1 and 2). The concentration of A is plotted as a function of time. Controller m1 shows a successive decrease in the maximum excursion of A, ΔA_{max}, along with a slower resetting time for A. ΔA_{max} for k_4=0 is indicated. Other rate constants (phases 1 and 2): k_3=1.0, k_5=3.0, k_6=1.0, k_7=1×10^{-6}. Initial concentrations of A: A_0=3.0 (k_4 from 0→64). Initial concentrations of E: E_0=3.0 (k_4=0); E_0=6.0 (k_4=1); E_0=9.0 (k_4=2); E_0=15.0 (k_4=4); E_0=27.0 (k_4=8); E_0=51.0 (k_4=16); E_0=99.0 (k_4=32); E_0=195.0 (k_4=64). See Appendix A and B for python and MATLAB scripts, respectively.

The response kinetics of controller m1 can be seen in Fig. 3.3b, where the concentration of A is followed as a function of time. A k_2-step from 1→5 is applied at time t=10 and the background k_4 is increased from 0→64. As is typical for controllers based on activated compensatory fluxes, the ΔA_{max} decreases with increasing background and the response period increases. However, the controller is clearly able to correct for the deviations and defends its set-point A_{set}=3.0.

Controller m3

The m3 controller in Fig. 3.4a is exposed to a step-perturbation k_2 (red arrow) and constant background k_4 (blue arrow) that (temporarily) reduce the concentration of A, and in which A is increased back to its set-point A_{set} by an activation-based compensatory flux $j_3{=}k_3{\cdot}E$.

The rate equations of A and E become, respectively:

$$\dot{A} = k_3{\cdot}E - (k_2 + k_4){\cdot}A \tag{3.5}$$

$$\dot{E} = \frac{k_5 k_8}{k_8{+}A} - \frac{k_6{\cdot}E}{k_7{+}E} \tag{3.6}$$

As for the m1 controller (Fig. 3.3a), integral control is assumed to follow zero-order kinetics in the removal of E ($k_7 \ll E_{ss}$), and, together with the steady state assumption, the set-point A_{set} is given by:

$$\dot{E}{=}0 \;\Rightarrow\; \frac{k_5 k_8}{k_8{+}A_{ss}} = k_6 \;\Rightarrow\; A_{ss}{=}A_{set}{=}k_8\left(\frac{k_5}{k_6} - 1\right) \tag{3.7}$$

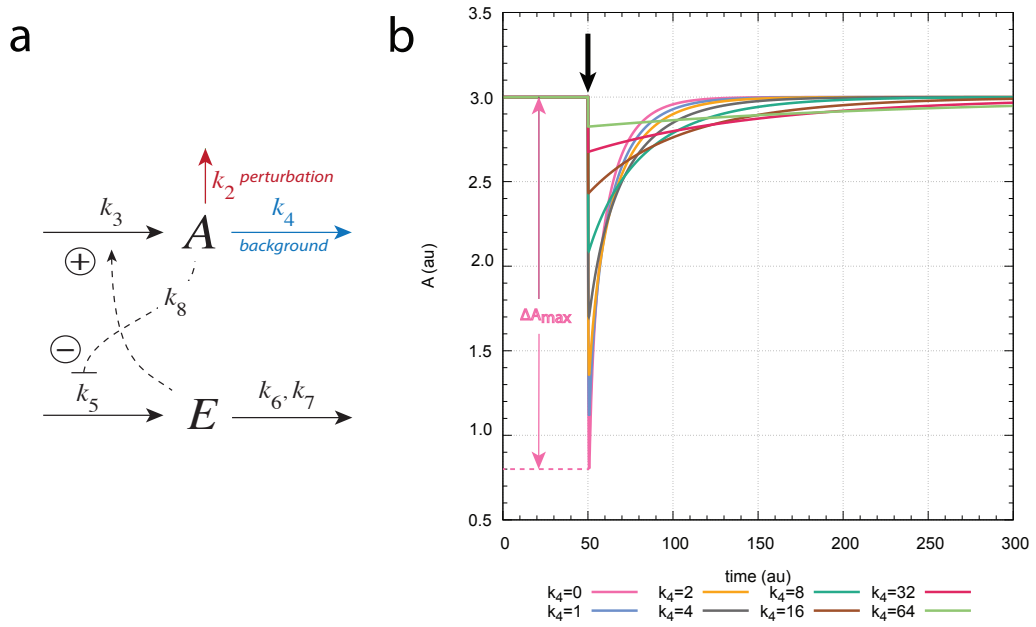

FIGURE 3.4: Resetting kinetics of controller motif m3. (a) Reaction scheme with integral control incoporated as a zero-order Michaelis-Menten (MM) type degredation of E. The MM parameters V_{max} and K_m are represented by k_6 and k_7, respectively. k_2 is a perturbation (red arrow) and k_4 represents a background reaction (blue arrow). Solid lines represent chemical reactions. Dashed lines indicate signaling events, where activation is represented by a plus sign and inhibition by a minus sign. Figure was redrawn from Ref. [1], Fig. S1 (S1 Text). (b) Response kinetics of the m3 controller (in a.u.) at a step-wise change k_2 (vertical arrow) from phase 1 (k_2=1.0) to phase 2 (k_2 = 5.0) at time t=50 with different but constant background reactions k_4 from 0→64 (k_4 variable, phases 1 and 2). The concentration of A is plotted as a function of time. Similarily to the m1 controller (Fig. 3.3b), m3 shows a successive decrease in the maximum excursion of A, ΔA_{max}, along with a slower resetting time for A. ΔA_{max} for k_4=0 is indicated. Other rate constants (phases 1 and 2): k_3=1.0, k_5=31.0, k_6=1.0, k_7=1×10^{-6}, k_8=0.1. Initial concentrations of A: A_0=3.0 (k_4 from 0→64). Initial concentrations of E: E_0=3.0 (k_4=0); E_0=6.0 (k_4=1); E_0=9.0 (k_4=2); E_0=15.0 (k_4=4); E_0=27.0 (k_4=8); E_0=51.0 (k_4=16); E_0=99.0 (k_4=32); E_0=195.0 (k_4=64). See Appendix A and B for python and MATLAB scripts, respectively.

The resetting kinetics of m3 (Fig. 3.4b), in response to a step-wise perturbation k_2 from 1→5 at time t=50 with a constant background k_4 from 0→64, is similar to the m1 controller's (Fig. 3.3b) decreased ΔA_{max} excursion and increased period length. Despite showing a somewhat longer resetting time, possibly caused by the inhibition of E, m3 is able to maintain A_{set}=3.0.

Controller m5

Controller m5 (Fig. 3.5a), which is an outflow controller, is exposed to an inflow step-perturbation k_1 (red arrow) that temporarily incresases the concentration of A to above A_{set}. The perturbation-induced change is opposed by the compensatory flux $j_3{=}k_4{\cdot}E{\cdot}A$ that directly activates the breakdown of A. This behaviour is also balanced by a constant background inflow k_3 (blue arrow), as well by A activating the synthesis of E.

The rate equations of A and E become, respectively:

$$\dot{A} = k_1 + k_3 - k_4 \cdot E \cdot A \tag{3.8}$$

$$\dot{E} = k_5 \cdot A - \frac{k_6 \cdot E}{k_7 + E} \tag{3.9}$$

Determining the set-point A_{set} ($k_7 \ll E_{ss}$):

$$\dot{E}{=}0 \;\Rightarrow\; k_5 \cdot A_{ss}{=}k_6 \;\Rightarrow\; A_{ss}{=}A_{set}{=}\frac{k_6}{k_5} \tag{3.10}$$

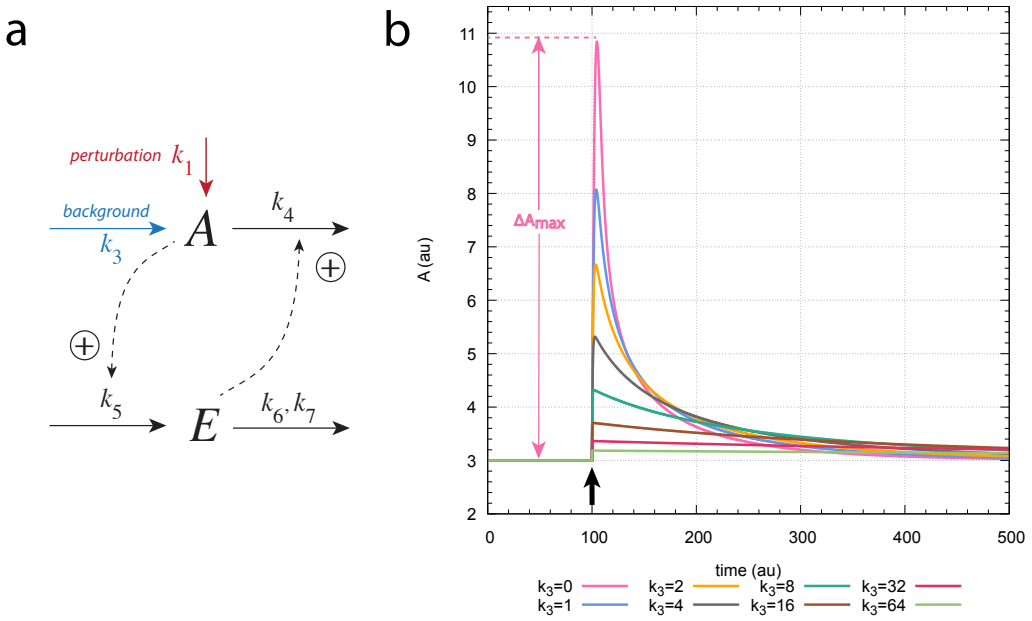

FIGURE 3.5: Resetting kinetics of controller motif m5. (a) Reaction scheme with integral control incoporated as a zero-order Michaelis-Menten (MM) type degredation of E. The MM parameters V_{max} and K_m are represented by k_6 and k_7, respectively. k_1 is a perturbation (red arrow) and k_3 represents a background reaction (blue arrow). Solid lines represent chemical reactions. Dashed lines indicate signaling events, where activation is represented by a plus sign. Figure was redrawn from Ref. [1], Fig. S3 (S1 Text). (b) Response kinetics of the m5 controller (in a.u.) at a step-wise perturbation k_1 (indidcated by vertical arrow) from phase 1 (k_1=1.0) to phase 2 (k_1 = 5.0) at time t=100 with different but constant background reactions k_3 from 0→64 (k_3 variable, phases 1 and 2). The concentration of A is plotted as a function of time. m5 shows a successive decrease of the maximum excursion in A, ΔA_{max}, along with a longer resetting time for A. ΔA_{max} for k_3=0 is indicated. Other rate constants (phases 1 and 2): k_4=0.005, k_5=1.0, k_6=3.0, k_7=1×10^{-6}. Initial concentrations of A: A_0=3.0 (k_3 from 0→64). Initial concentrations of E: E_0=66.667 (k_3=0); E_0=133.33 (k_3=1); E_0=200.0 (k_3=2); E_0=333.33 (k_3=4); E_0=600.0 (k_3=8); E_0=1133.33 (k_3=16); E_0=2200.0 (k_3=32); E_0=4333.33 (k_3=64). See Appendix A and B for python and MATLAB scripts, respectively.

The response kinetics of A in controller m5, as a function of time, can be seen in Fig. 3.5b, with A_{set}=3.0 and constant background k_3 varying from 0 to 64. The step-perturbation k_1 goes from 1→5 at time t=100. m5 shows a decreased ΔA_{max} and a longer resetting period as the background k_3 increases.

Controller m7

The outflow controller m7 (Fig. 3.6a) has an activation-based compensatory flux $j_4{=}k_4{\cdot}A{\cdot}E$ that opposes the inflow of A caused by the step-perturbation k_1 (red arrow) and constant background k_3 (blue arrow).

Determining the rate equations of A and E, respectively:

$$\dot{A} = k_1 + k_3 - k_4{\cdot}A{\cdot}E \tag{3.11}$$

$$\dot{E} = k_5 - \left(\frac{k_6{\cdot}E}{k_7{+}E}\right) \cdot \left(\frac{k_8}{k_8{+}A}\right) \tag{3.12}$$

The set-point A_{set} is given by:

$$\dot{E} = 0 \;\Rightarrow\; k_5 = \frac{k_6 k_8}{(k_8{+}A_{ss})} \;\Rightarrow\; A_{set}{=}A_{ss}{=}k_8\left(\frac{k_6}{k_5}{-}1\right) \tag{3.13}$$

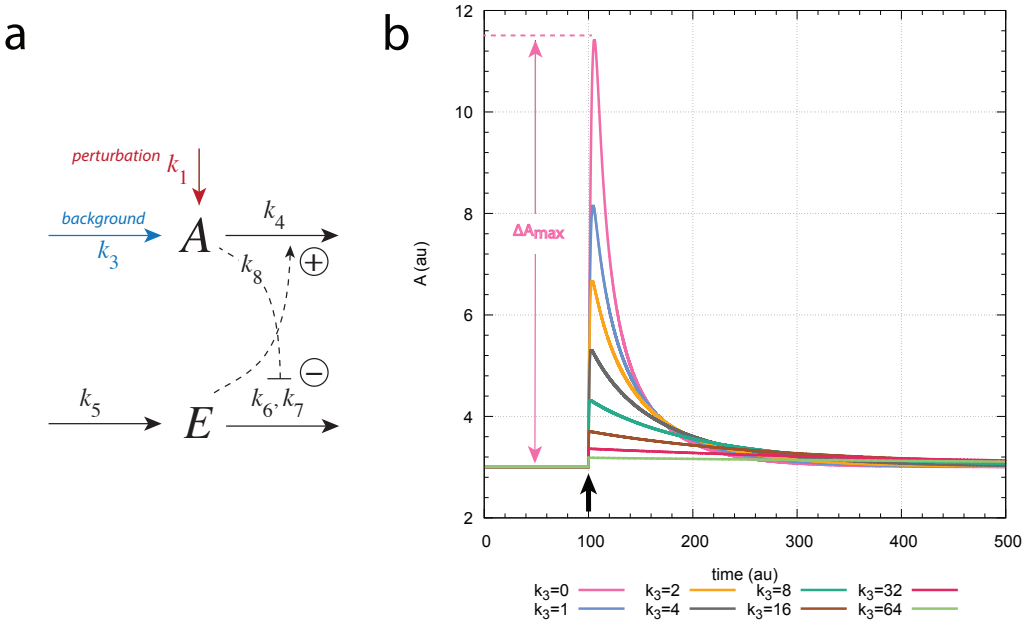

FIGURE 3.6: Resetting kinetics of controller motif m7. (a) Reaction scheme with integral control incoporated as a zero-order Michaelis-Menten (MM) type degredation of E. The MM parameters V_{max} and K_m are represented by k_6 and k_7, respectively. k_1 is a perturbation (red arrow) and k_3 represents a background reaction (blue arrow). Solid lines represent chemical reactions. Dashed lines indicate signaling events, where activation is represented by a plus sign and inhibition by a minus sign. Figure was redrawn from Ref. [1], Fig. 5. (b) Response kinetics of the m7 controller (in a.u.) at a step-wise perturbation k_1 (indicated by vertical arrow) from phase 1 (k_1=1.0) to phase 2 (k_1 = 5.0) at time t=100 with different but constant backgrounds k_3 from 0→64 (k_3 variable, phases 1 and 2). The concentration of A is plotted as a function of time. m7 shows a successive decrease of the maximum excursion, ΔA_{max}, along with a longer resetting time for A. ΔA_{max} for k_3=0 is indicated. Other rate constants (phases 1 and 2, in au): k_4=0.003, k_5=1.0, k_6=31.0, k_7=1×10^{-6}, k_8=0.1. Initial concentrations of A: A_0=3.0 (k_3 from 0→64). Initial concentrations of E: E_0=11.11 (k_3=0); E_0=22.22 (k_3=1); E_0=33.33 (k_3=2); E_0=55.55 (k_3=4); E_0=99.99 (k_3=8); E_0=188.89 (k_3=16); E_0=366.67 (k_3=32); E_0=722.22 (k_3=64). See Appendix A and B for python and MATLAB scripts, respectively.

The response kinetics of m7, as a function of time, in Fig. 3.6 (panel b) shows a decreased ΔA_{max} and longer response period with increasing backgrounds k_3 from 0→64 at time t=100. It has the same set-point A_{set}=3.0 as the other controllers, and is subjected to a step-perturbation k_1 from 1→5. The response kinetics of m7 is very similar to m5 (see Fig. 3.5b).

3.2.2 Controllers with derepression-based compensatory fluxes

In this subsection the results for inflow controllers m2 and m4 and outflow controllers m6 and m8 are described. In these controllers the concentration of A is homeostatically regulated upon a step-wise perturbation and constant but different background, where the compensatory actions of E are based on derepression. There is also provided a m2 controller which incorporates integral control by autocatalysis.

Controller m2

Inflow controller m2 (Fig. 3.7a) has a derepression-based compensatory flux $j_3{=}k_3k_8/(k_8{+}E)$ that opposes the outflow of A caused by the step-perturbation k_2 (red arrow) and constant but different background k_4. When A is decreased by k_2 there is less A to activate E, which means that A gradually returns to its set-point since there is less E to inhibit the synthesis of A.

Determining the rate equations of A and E, respectively:

$$\dot{A} = \frac{k_3k_8}{k_8{+}E} - (k_2 + k_4){\cdot}A \tag{3.14}$$

$$\dot{E} = k_5{\cdot}A - \frac{k_6{\cdot}E}{k_7{+}E} \tag{3.15}$$

Assuming integral control by zero-order kinetics (i.e. $E/(k_7{+}E){\approx}1$) and that $\dot{E}{=}0$ (steady state approximation), the set-point A_{set} is given by:

$$\dot{E}{=}0 \;\Rightarrow\; k_5 \cdot A_{ss}{=}k_6 \;\Rightarrow\; A_{ss}{=}A_{set}{=}\frac{k_6}{k_5} \tag{3.16}$$

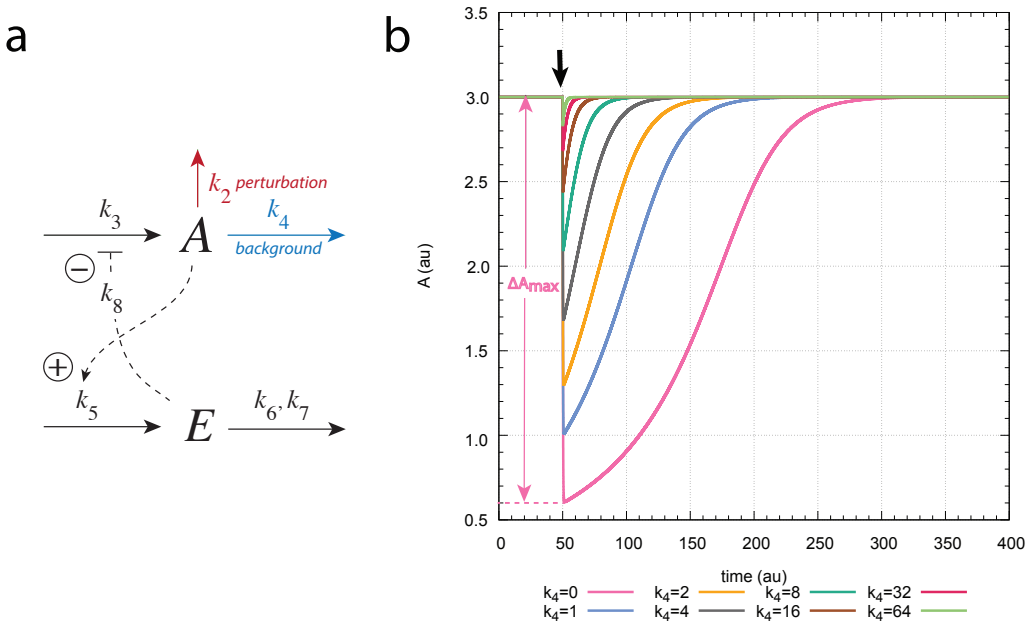

FIGURE 3.7: Response kinetics of controller motif m2. (a) Reaction scheme with integral control incoporated as a zero-order Michaelis-Menten (MM) type degredation of E. The MM parameters V_{max} and K_m are represented by k_6 and k_7, respectively. k_2 is a perturbation (red arrow) and k_4 (blue arrow) represents a background reaction. Solid lines represent chemical reactions. Dashed lines indicate signaling events, where activation is represented by a plus sign and inhibition by a minus sign. Figure was redrawn from Ref. [1], Fig. 7. (b) Response kinetics of the m2 controller (in a.u.) at a step-wise perturbation k_2 (indicated by vertical arrow) from phase 1 (k_2=1.0) to phase 2 (k_2 = 5.0) at time t=50 with different but constant backgrounds k_4 from 0→64 (k_4 variable, phases 1 and 2). The concentration of A is plotted as a function of time. m2 shows a successive decrease of the maximum excursion of A, ΔA_{max}, along with a shorter resetting period. ΔA_{max} is indicated for k_4=0. Other rate constants (phases 1 and 2, in au): k_3=1×10^4, k_5=1.0, k_6=3.0, k_7=1×10^{-6}, k_8=0.1. Initial concentrations of A: A_0=3.0 (k_4 from 0→64). Initial concentrations of E: E_0=333.15 (k_4=0); E_0=166.57 (k_4=1); E_0=111.01 (k_4=2); E_0=66.57 (k_4=4); E_0=36.94 (k_4=8); E_0=19.51 (k_4=16); E_0=10.00 (k_4=32); E_0=5.03 (k_4=64). See Appendix A and B for python and MATLAB scripts, respectively.

The m2 controller (Fig. 3.7 b) is able to maintain A_{set}=3.0 when being subjected to a step-perturbation k_2 from 1→5 at time t=50. Compared to the controllers with activation-based compensatory fluxes (see Ch. 3.2.1), the m2 controller also shows a successive decrease of ΔA_{max} but a shorter response time with increasing backgrounds k_4 from 0→64.

Autocatalytic m2 controller

Inflow and autocatalytic m2 controller (Fig. 3.8a) has a derepression-based compensatory flux j_3=$k_3k_8/(k_8$+$E)$ that opposes the outflow of A caused by the step-perturbation k_2 (red arrow) and constant but different background reaction k_4 (blue arrow). An outflow of A causes less E to inhibit the synthesis of A, which means that A gradually returns to its set-point. What is different from this controller, compared to the m2 controller with integral incorporated as zero-order kinetics (Fig. 3.7a), is that E also activates its own synthesis.

The rate equations of A and E are, respectively:

$$\dot{A} = \frac{k_3 \cdot k_8}{k_8 + E} + k_1 - (k_2 + k_4) \cdot A \tag{3.17}$$

$$\dot{E} = k_5 \cdot A \cdot E - k_6 \cdot E \tag{3.18}$$

The set-point A_{set} is:

$$\dot{E}{=}0 \;\; \Rightarrow \;\; k_5 \cdot A_{ss} \cdot E_{ss} {=} k_6 \cdot E_{ss} \;\; \Rightarrow \;\; A_{ss} {=} A_{set} {=} \frac{k_6}{k_5} \tag{3.19}$$

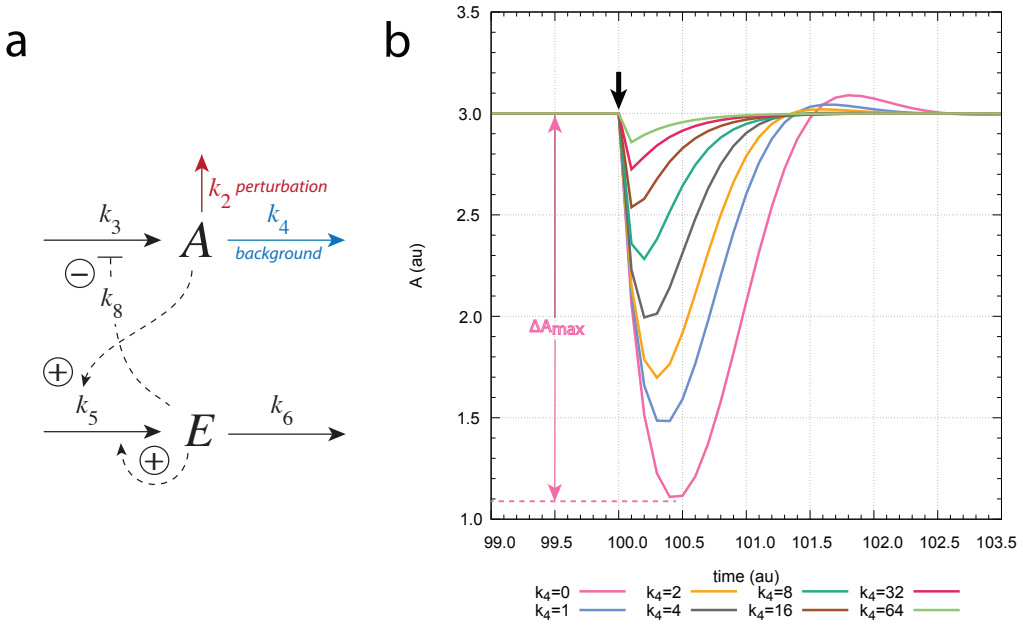

FIGURE 3.8: Response kinetics of autocatalytic m2 controller motif. (a) Reaction scheme with integral control incorporated by autocatalysis. k_2 is a perturbation (red arrow) and k_4 (blue arrow) represents a constant background reaction. Solid lines represent chemical reactions. Dashed lines indicate signaling events, where activation is represented by a plus sign and inhibition by a minus sign. Figure was redrawn from Ref. [1], Fig. 7. (b) Response kinetics of the autocatalytic m2 controller (in a.u.) at a step-wise perturbation k_2 (indicated by a vertical arrow) from phase 1 (k_2=1.0) to phase 2 (k_2 = 5.0) at time t=100 with different but constant backgrounds k_4 from 0→64 (k_4 variable, phases 1 and 2). The concentration of A is plotted as a function of time. The controller shows a successive decrease of the maximum excursion of A, ΔA_{max}, along with a shorter resetting period. Notice the much faster resetting time compared to m2 in Fig. 3.7b. ΔA_{max} is indicated for k_4=0. Other rate constants (phases 1 and 2): k_3=1×10^{+4}, k_5=1.0, k_6=3.0, k_8=1×10^{-1}. Initial concentrations of A: A_0=3.0 (k_4 from 0→64). Initial concentrations of E: E_0=333.23 (k_4=0); E_0=166.57 (k_4=1); E_0=111.01 (k_4=2); E_0=66.57 (k_4=4); E_0=36.94 (k_4=8); E_0=19.51 (k_4=16); E_0=10.00 (k_4=32); E_0=5.03 (k_4=64). See Appendix A for python script.

The autocatalytic m2 controller (Fig. 3.8 b) shows a successive decrease of ΔA_{max} and shorter response time with increasing background k_4 from 0→64. The controller is subjected to a step-perturbation k_2 from 1→5 at time t=50 and is able to maintain its set-point A_{set}=3.0. However, notice the much faster resetting time compared to the m2 controller with integral control incorporated by zero-order kinetics (Fig. 3.7b). At a constant background k_4=0, for instance, the resetting time for the autocatalytic m2 controller is about 100 times faster than for the m2 controller.

Controller m4

Inflow controller m4 (Fig. 3.9a) has a derepression-based compensatory flux $j_3{=}k_3k_8/(k_8{+}E)$ (with inhibitory constant k_8) that counteracts the decrease of A caused by the step-perturbation k_2 (red arrow) and constant but different background k_4. There is another inhibition term (with k_9) where A inhibits the breakdown of E.

The rate equations of A and E become, respectively:

$$\dot{A} = k_2{\cdot}A - k_4{\cdot}A + \frac{k_3k_8}{k_8{+}E} \tag{3.20}$$

$$\dot{E} = k_5 - \left(\frac{k_6{\cdot}E}{k_7{+}E}\right) \cdot \left(\frac{k_9}{k_9{+}A}\right) \tag{3.21}$$

Using the assumptions that $E/(k_7{+}E){\approx}1)$ and $\dot{E}{=}0$, the set-point A_{set} becomes:

$$\dot{E}{=}0 \;\Rightarrow\; \frac{k_6k_9}{k_9{+}A_{ss}} = k_5 \;\Rightarrow\; A_{ss}{=}A_{set}{=}k_9\left(\frac{k_6}{k_5} - 1\right) \tag{3.22}$$

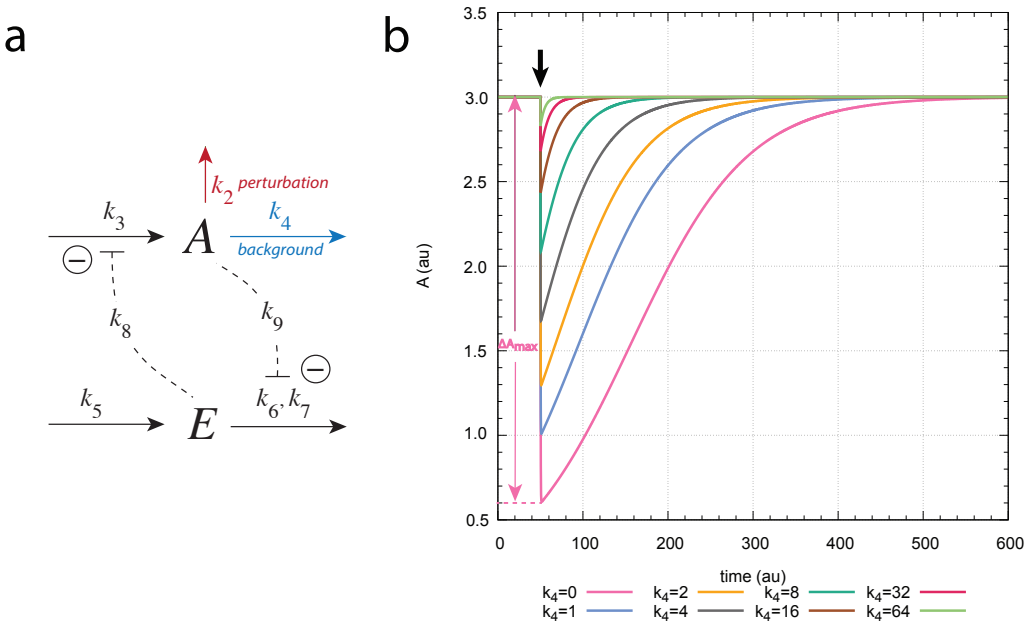

FIGURE 3.9: Response kinetics of controller motif m4. (a) Reaction scheme with integral control incoporated as a zero-order Michaelis-Menten (MM) type degredation of E. The MM parameters V_{max} and K_m are represented by k_6 and k_7, respectively. k_2 is a perturbation (red arrow) and k_4 (blue arrow) represents a background reaction. Solid lines represent chemical reactions. Dashed lines indicate signaling events, where inhibition is represented by a minus sign. Figure was redrawn from Ref. [1], Fig. S1 (S2 Text). (b) Response kinetics of the m4 controller (in a.u.) at a step-wise perturbation k_2 (indicated by a vertical arrow) from phase 1 (k_2=1.0) to phase 2 (k_2 = 5.0) at time t=50 with different but constant backgrounds k_4 from 0→64 (k_4 variable, phases 1 and 2). The concentration of A is plotted as a function of time. m4 shows a successive decrease of the maximum excursion of A, ΔA_{max}, along with a shorter resetting period. ΔA_{max} is indicated for k_4=0. Other rate constants (phases 1 and 2): k_3=1×10^4, k_5=1.0, k_6=31.0, k_7=1×10^{-6}, k_8=0.1, k_9=0.1. Initial concentrations of A: A_0=3.0 (k_4 from 0→64). Initial concentrations of E: E_0=333.18 (k_4=0); E_0=166.57 (k_4=1); E_0=111.01 (k_4=2); E_0=66.57 (k_4=4); E_0=36.94 (k_4=8); E_0=19.51 (k_4=16); E_0=10.00 (k_4=32); E_0=5.03 (k_4=64). See Appendix A and B for python and MATLAB scripts, respectively.

The resetting kinetics of m4 (Fig. 3.9b) shows a successive decrease of ΔA_{max} and decreased resetting time as the background k_4 increases from 0→64 at a step-perturbation k_2 from 1→5 at time t=50. Controller m4 behaves very similar to m2 (Fig. 3.7b) with the exception that m2 has a shorter resetting time.

Controller m6

Controller m6 (Fig. 3.10a) has a derepression-based compensatory flux $j_4{=}k_4k_8{\cdot}A/(k8{+}E)$ (with inhibitory constant k_8) that opposes the inflow of A. The inflow of A is due to a step-perturbation k_1 (red arrow) and constant but different background k_3 (blue arrow).

Determining the rate equations of A and E, respectively:

$$\dot{A} = k_1 + k_3 - \left(\frac{k_4{\cdot}k_8}{k_8{+}E}\right){\cdot}A \tag{3.23}$$

$$\dot{E} = k_5 - \left(\frac{k_6{\cdot}E}{k_7{+}E}\right){\cdot}A \tag{3.24}$$

The set-point A_{set} is given by:

$$\dot{E}{=}0 \;\Rightarrow\; k_5 - k_6{\cdot}A_{ss} = 0 \;\Rightarrow\; A_{ss}{=}A_{set}{=}\frac{k_5}{k_6} \tag{3.25}$$

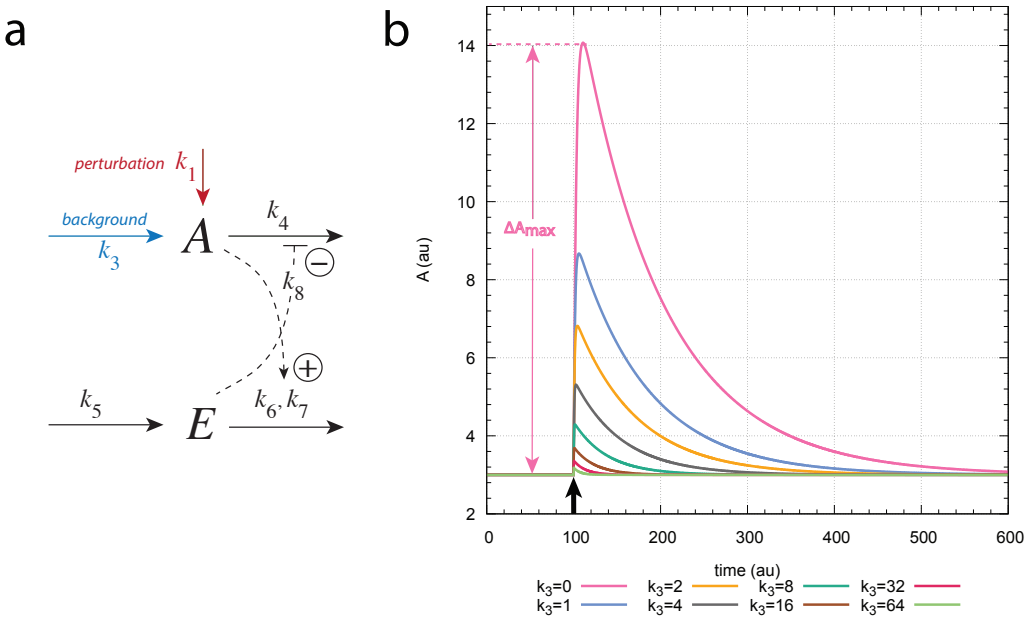

FIGURE 3.10: Resetting kinetics of controller motif m6. (a) Reaction scheme with integral control incoporated as a zero-order Michaelis-Menten (MM) type degredation of E. The MM parameters V_{max} and K_m are represented by k_6 and k_7, respectively. k_1 is a perturbation (red arrow) and k_3 (blue arrow) represents a background reaction. Solid lines represent chemical reactions. Dashed lines indicate signaling events, where activation is represented by a plus sign and inhibition by a minus sign. Figure was redrawn from Ref. [1], Fig. S3 (S2 Text). (b) Response kinetics of the m6 controller (in a.u.) at a step-wise perturbation k_1 (indicated by vertical arrow) from phase 1 (k_1=1.0) to phase 2 (k_1 = 5.0) at time t=100 with different but constant backgrounds k_3 from 0→64 (k_3 variable, phases 1 and 2). The concentration of A is plotted as a function of time. m6 shows a successive decrease of the maximum excursion of A, ΔA_{max}, along with a shorter resetting period. ΔA_{max} is indicated for k_3=0. Other rate constants (phases 1 and 2): k_4=1×10^4, k_5=6.0, k_6=2.0, k_7=1×10^{-6}, k_8=0.1. Initial concentrations of A: A_0=3.0 (k_3 from 0→64). Initial concentrations of E: E_0=2999.81 (k_3=0); E_0=1499.90 (k_3=1); E_0=999.90 (k_3=2); E_0=599.90 (k_3=4); E_0=333.23 (k_3=8); E_0=176.37 (k_3=16); E_0=90.81 (k_3=32); E_0=46.05 (k_3=64). See Appendix A and B for python and MATLAB scripts, respectively.

Outflow controller m6 in Fig. 3.10b shows a successive decrease of both ΔA_{max} and the resetting period when the step-perturbation k_1 is increased from 1→5 at time t=100, while having a constant but different background inflow k_3 from 0→64. The controller is able to defend its set-point A_{set}=3.0.

Controller m8

Fig. 3.11a shows an outflow controller m8 with a compensatory flux j_4=k_4·k_9·A/(k_9+E) (with k_9) that opposes the increase of A when a step-perturbation k_1 (red arrow) is applied at a constant background inflow k_3 (blue arrow). A inhibits the synthesis of E through the inhibitory constant k_8.

The rate equations of A and E become, respectively:

$$\dot{A} = k_1 + k_3 - k_4 \cdot A \cdot \left(\frac{k_9}{k_9 + E} \right) \tag{3.26}$$

$$\dot{E} = k_5 \cdot \left(\frac{k_8}{k_8 + A} \right) - \frac{k_6 \cdot E}{k_7 + E} \tag{3.27}$$

The set-point A_{set} is given by:

$$\dot{E}=0 \;\Rightarrow\; k_5 \cdot \left(\frac{k_8}{k_8 + A_{ss}} \right) = k_6 \;\Rightarrow\; A_{set}=A_{ss}=k_8 \left(\frac{k_5}{k_6} - 1 \right) \tag{3.28}$$

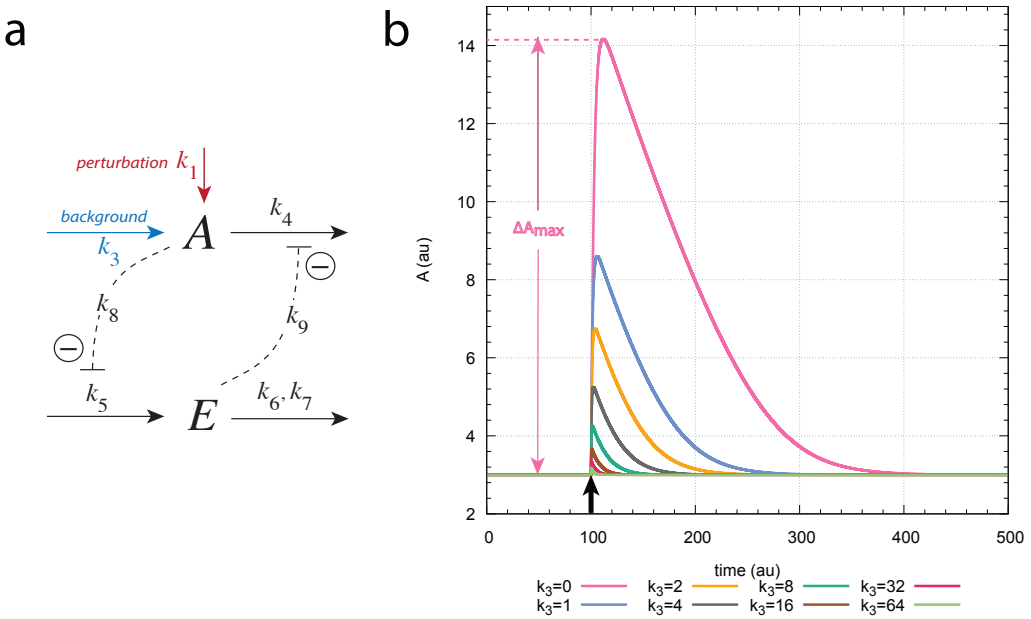

FIGURE 3.11: Resetting kinetics of controller motif m8. (a) Reaction scheme with integral control incoporated as a zero-order Michaelis-Menten (MM) type degredation of E. The MM parameters V_{max} and K_m are represented by k_6 and k_7, respectively. k_1 is a perturbation (red arrow) and k_3 (blue arrow) represents a background reaction. Solind lines represent chemical reactions. Dashed lines indicate signaling events, where inhibition is represented by a minus sign. Figure was redrawn from Ref. [1], Fig. 10. (b) Response kinetics of the m8 controller (in a.u.) at a step-wise perturbation k_1 (indicated by the vertical arrow) from phase 1 (k_1=1.0) to phase 2 (k_1 = 5.0) at time t=100 with different but constant backgrounds k_3 from 0→64 (k_3 variable, phases 1 and 2). The concentration of A is plotted as a function of time. m8 shows a successive decrease of the maximum excursion of A, ΔA_{max}, along with a shorter resetting period. ΔA_{max} is indicated for k_3=0. Other rate constants (phases 1 and 2, in au): k_4=1×10^4, k_5=620.0, k_6=20.0, k_7=1×10^{-6}, k_8=0.1, k_9=0.1. Initial concentrations of A: A_0=3.0 (k_3 from 0→64). Initial concentrations of E: E_0=2998.35 (k_3=0); E_0=1499.91 (k_3=1); E_0=999.90 (k_3=2); E_0=599.90 (k_3=4); E_0=333.23 (k_3=8); E_0=176.37 (k_3=16); E_0=90.81 (k_3=32); E_0=46.05 (k_3=64). See Appendix A and B for python and MATLAB scripts, respectively.

The resetting kinetics in m8 (Fig. 3.11b) shows a decreased ΔA_{max} excursion, along with a shorter resetting time. The controller is subjected to a step-perturbation k_1 from 1→5 at time t=100, and a constant but different background k_3 from 0→64. This controller behaves similarly to m6 (Fig. 3.10b), with the exception that m8 has a slightly faster resetting period.

3.3 Two-layered frequency compensated oscillators

Retinal ganglion cells are known to oscillate, as well as having partial frequency compensations [39]. We created frequency compensated oscillators in order to represent these retinal cells. These controllers have a central feedback layer that is based on motif m1-m8 (Fig. 2.1), in which the time average vaule of A (Eq. 3.29) is kept homeostatically stable by the manipulated variable E. Upon step-perturbations and constant background reactions the oscillator goes from $<A>$ to its set-point A_{set}.

$$<A>(t) = \frac{1}{t}\int_0^t A{\cdot}dt \tag{3.29}$$

In these controllers there is a second feedback layer that keeps the the time average concentration of E (of the central layer) (Eq. 3.30) robustly at a certain set-point. This is due to the outer layer having two additional controller species, I_1 and I_2, which act directly or indirectly on A. In addition to maintaining E-homeostasis, I_1 and I_2 ensure frequency homeostasis.

$$<E>(t) = \frac{1}{t}\int_0^t E{\cdot}dt \tag{3.30}$$

It has previously been shown that these two-layered layered oscillators show robust frequency homeostasis [2]. However, the oscillators also show background compensation when I_1 and I_2 feed directly or "coherently" back to A (see Ch. 3.3.1), i.e., the controller responds to a step-perturbation independent of the level of an applied constant background. This type of feedback was termed "coherent feedback" in analogy to a similar feedback mechanism used in quantum control theory and optics. Background compensations are not seen when I_1 and I_2 feed into the process that generates A by so-called "incoherent feedback" (see Ch. 3.3.2) [5, 6].

3.3.1 Frequency compensated oscillator with coherent feedback

In this section we are looking at a frequency compensated oscillator (Fig. 3.12a) that incorporates integral control in terms of coherent feedback (Fig. 3.12b) [5, 6], which allows the controller to neutralize backgrounds (Fig. 3.15).

It is structured into two negative feedback layers (Fig. 3.12a), in which one of them constitutes the m2-based (Fig. 3.7) central A-e-E-A loop (colored green). This basic derepression-based m2 scheme has an additional intermediate e that turns the central oscillator into a limit-cycle oscillator [2]. The central oscillator is an inflow controller and can therefore only (in theory) compensate for outflow perturbations [46]. Thus, when there is an outflow of A due to a step-wise perturbation k_2 (colored red) and constant backgrounds k_{10} (colored blue), the compensatory actions of E ($j_3{=}k_3{\cdot}k_5/(k_5{+}E)$) keeps the average concentration of A, $<A>$, homeostatically stable at A_{set}.

In the other feedback layer (colored orange) the average concentration of E, $<E>$, is instead kept under robust homeostatic control. This is made possible by the controller species I_1 and I_2 that function as outflow or inflow controllers of A, respectively. In fact, it is the control of $<E>$ by I_1 and I_2 that allow for the oscillator's frequency homeostasis [2]. Since the integral controller species I_1 and I_2 feed directly or coherently [5, 6] back to A (see Fig. 3.12b), the controller shows robust background compensation.

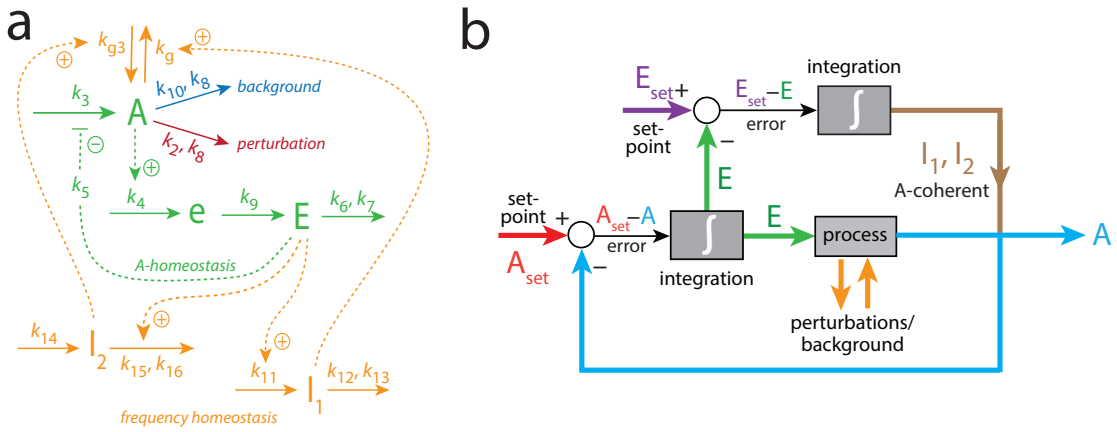

FIGURE 3.12: Example of an oscillator with frequency control and coherent feedback, i.e., with background compensation. Figure was redrawn from Ref. [4], Fig. 4. a) Reaction scheme of oscillator with two negative feedback layers, in which the central A-e-E-A loop is based on derepression-based motif m2 (Fig. 3.7a). Solid arrows represent chemical reactions. Dashed lines indicate signaling events, where activation is represented by a plus sign and inhibition by a minus sign. b) Integral control scheme with coherent feedback, where I_1 and I_2 feed directly back to A. Coherent feedback, which is a term used in quantum control theory and optics [5, 6], yields an additional control of E via A by I_1 and I_2. In particular, uncontrollable perturbations (orange arrows) add or remove A. The difference or error between the controlled variable and its set-point (A_{set}-A) is measured and integrated over time (lower grey "integration box"). This gives the necessary E-concentration (horizontal green line) for maintaining A under robust homeostatic control. A difference from the basic integral controller (Fig. 2.2b), is that the outpout of E (vertical green line) is also used as input in a second control system. Here, the error between E and E_{set} is measured and integrated over time (upper grey "integration box"). This gives the I_1- and I_2-concentrations (brown line) to be fed directly or coherently back to A through a negative feedback loop (blue line) in order to maintain $E_{set^{I1}}$ and $E_{set^{I2}}$, respectively.

The rate equations of A, e, E, I_1, and I_2, respectively, are given by:

$$\dot{A} = k_{g3}{\cdot}I_2 + \frac{k_3{\cdot}k_5}{k_5{+}E} - \frac{k_g{\cdot}A{\cdot}I_1}{k_{17}{+}A} - \underbrace{\frac{k_2{\cdot}A}{k_8{+}A}}_{\text{perturbation}} - \underbrace{\frac{k_{10}{\cdot}A}{k_8{+}A}}_{\text{background}} \tag{3.31}$$

$$\dot{e} = k_4{\cdot}A - k_9{\cdot}e \tag{3.32}$$

$$\dot{E} = k_9{\cdot}e - \frac{k_6{\cdot}E}{k_7 + E} \tag{3.33}$$

$$\dot{I}_1 = k_{11}{\cdot}E - \frac{k_{12}{\cdot}I_1}{k_{13} + I_1} \tag{3.34}$$

$$\dot{I}_2 = k_{14} - \left(\frac{k_{15}{\cdot}I_2}{k_{16}+I_2}\right){\cdot}E \tag{3.35}$$

Integral control, in the central layer, is enabled by zero-order kinetics in the removal of E (i.e. $E/(k_7{+}E){\approx}1$), which is necessary for achieving robust perfect adapation of $<A>$. Given the steady state (ss) approximation (i.e., $\dot{E}{=}\dot{e}{=}0$) the set-point A_{set} can be determined:

$$k_4{\cdot}<A_{ss}> = k_9{\cdot}<e_{ss}> = k_6 \cdot \underbrace{\left(\frac{E_{ss}}{k_7{+}E_{ss}}\right)}_{\approx 1\,(\text{zero}-\text{order})} \;\Rightarrow\; <A_{ss}>{=}A_{set}{=}\frac{k_6}{k_4} \tag{3.36}$$

where the oscillating system goes from $<A_{ss}>$ to A_{set} when oscillatory and A to A_{set} when non-oscillatory [2].

The controller variables I_1 and I_2 (in the outer feedback layer) are assumed to be degraded by zero-order kinetics. I_1 and I_2 function, respectively, as outflow and inflow controllers with respect to $<E>$ when oscillatory and E while non-oscillatory [2]. When considering the steady state (ss) approximation (i.e., $E{=}0$) the manipulated variable's set-points, $E_{set}^{I_1}$ and $E_{set}^{I_2}$, with regards to, respectively, I_1 and I_2 become:

$$k_{11}{\cdot}<E_{ss}> = k_{12} \cdot \underbrace{\left(\frac{I_{1,ss}}{k_{13}{+}I_{1,ss}}\right)}_{\approx 1\,(\text{zero}-\text{order})} \;\Rightarrow\; <E_{ss}>{=}E_{set}^{I_1}{=}\frac{k_{12}}{k_{11}} \tag{3.37}$$

$$k_{14} = k_{15}{\cdot}<E_{ss}> \underbrace{\left(\frac{I_{2,ss}}{k_{16}{+}I_{2,ss}}\right)}_{\approx 1\,(\text{zero}-\text{order})} \;\Rightarrow\; <E_{ss}>{=}E_{set}^{I_2}{=}\frac{k_{14}}{k_{15}} \tag{3.38}$$

Since I_1 is an outflow controller it becomes active when $<E>$ is higher than $E_{set}^{I_1}$. The opposite occurs for the inflow controller I_2, which operates whenever $<E>$ is lower than $E_{set}^{I_2}$. Due to wind-up [2] the concentration of $E_{set}^{I_2}$ should be lower than $E_{set}^{I_1}$.

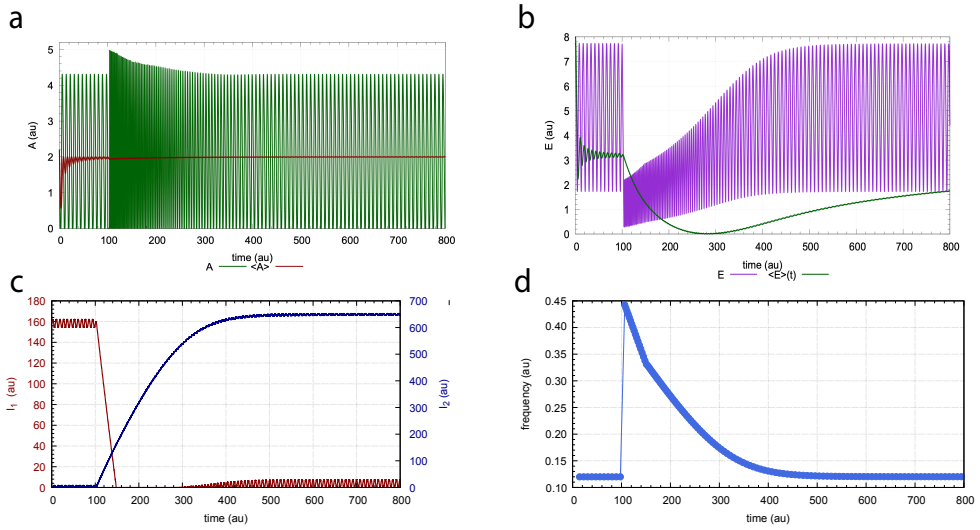

FIGURE 3.13: Frequency compensation of the feedback scheme in Fig. 3.12a at a constant background k_{10}=0. The controller is tested at a step-perturbation k_2 from 1→9 at time t=100. Panels a and b show the resetting kinetics of A and E as a function of time, as well as their average concentrations $<A>$ and $<E>$, respectively. Panel c shows the contributions of the controller species I_1 and I_2 over time. In panel d the frequency, or inverse of the period length, is plotted as a function of time. Notice the oscillator's frequency homeostasis. Other rate constants (phases 1 and 2, in a.u.): k_4=k_{11}=k_{15}=1.0, k_5=0.1, k_6=2.0, k_7=k_8=k_{13}=k_{16}=1×10^{-6}, k_9=20.0, k_{12}=5.0, k_{14}=4.99, k_g=k_{g3}=1×10^{-2}. Initial concentrations of A, E, e, I_1, and I_2 (in au), respectively: 2.2084, 7.7021, 1.1354×10^{-1}, 1.5773×10^{2}, and 4.3563. See Appendix A for python scripts.

Fig. 3.13 shows the oscillator's behaviour to a step-wise perturbation k_2 from 1.0 (phase 1) to 9.0 (phase 2) at time t=100, while having a constant background outflow k_{10}=0. Panels a and b show the oscillations of A and E, respectively, over time. They also show their respective average concentrations, $<A>$ and $<E>$, which are homeostatically regulated by the compensatory actions of I_1 and I_2 in panel c. If I_1 and I_2 were absent, i.e., no control of $<E>$ via A by I_1 and I_2, then E would be the only regulator of $<A>$. In panel d the frequency, or inverse of the period length, is plotted as a function of time. The frequency clearly resets to its pre-perturbation level after some time.

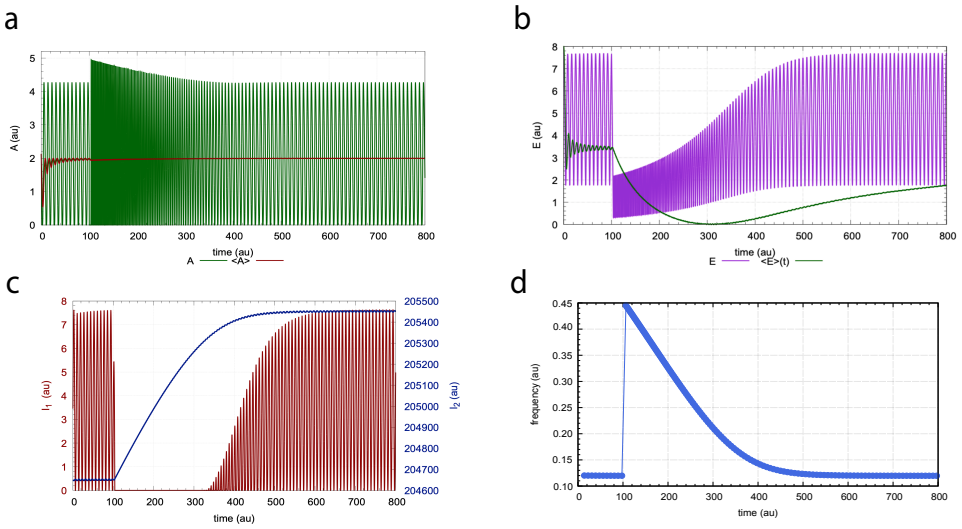

FIGURE 3.14: Frequency compensation of the feedback scheme in Fig. 3.12a at a constant background k_{10}=2048. The controller is tested at a step-perturbation k_2 from 1→9 at time t=100. Panels a and b show the resetting kinetics of A and E as a function of time, as well as their average concentrations $<A>$ and $<E>$, respectively. Panel c shows the contributions of the controller species I_1 and I_2 over time. In panel d the frequency, or inverse of the period length, is plotted as a function of time. Notice the oscillator's frequency homeostasis. Other rate constants (phases 1 and 2, in a.u.) as in Fig. 3.13. Initial concentrations of A, E, e, I_1, and I_2 (in au), respectively: 2.1377, 7.6720, 1.0996×10^{-1}, 1.1354×10^{-1}, 3.4304, and 2.0465×10^{5}. See Appendix A for python scripts.

The same k_2-step is applied in Fig. 3.14 at k_{10}=2048. Based on the feedback scheme in Fig. 3.12a the larger background will result in a higher removal of A. This is clearly compensated for in panel a by a large increase in the inflow controller I_2, as well as a reduction in the outflow controller I_1 (panel c). I_1 and I_2 continue to maintain the set-points for A and E in panels a and b, respectively. Frequency homeostasis (panel d) is also observed at this k_{10}-value. In fact, the same sensitivity is shown for the maximum frequency, indicating that the oscillator shows frequency compensation independent of the applied background.

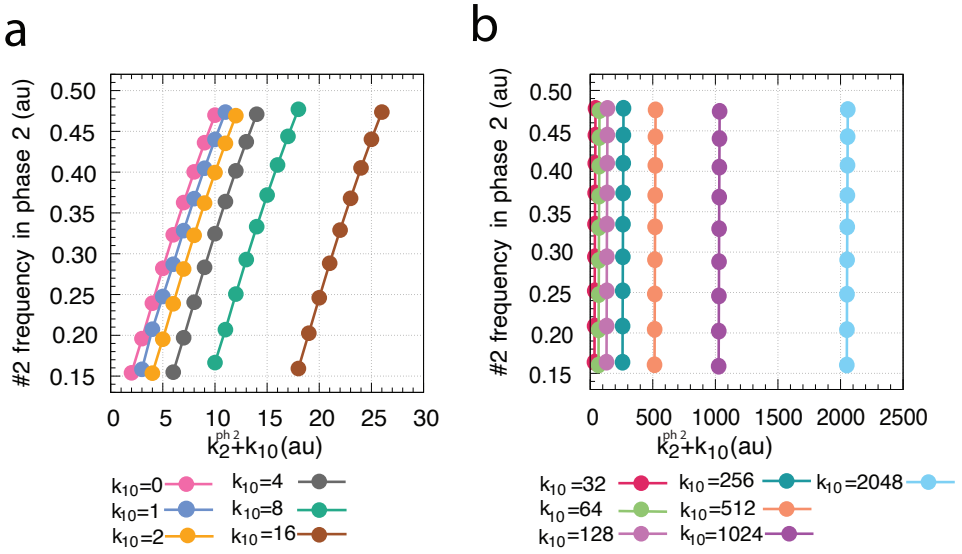

FIGURE 3.15: Frequency and background compensations of the oscillator from Fig. 3.12a. The figure shows the number 2 frequency (in phase 2) as a function of $k_2^{ph2}+k_{10}$. Frequency adaptation of the controller (in a.u.) at a step-wise perturbation from phase 1 (k_2=1.0) to phase 2 (k_2 variable, k_2 from 2→10) with constant background perturbations k_{10} from 0→16 in panel a and 32→2048 in panel b (k_{10} variable, phases 1 and 2). The total perturbations (k_2+k_{10}) induce parallel lines, which show frequency adaptation. Other rate constants (phases 1 and 2, in a.u.) as in Fig. 3.13. Initial concentrations of A, E, e, I_1, and I_2 (in a.u.), respectively: A_0=0.3780, E_0=2.4784, e_0=1.5993×10^{-2}, $I_{1,0}$=4.5727×10^2, $I_{2,0}$=2.9817×10^2 (k_{10} from 0→128); A_0=0.9866, E_0=7.3508, e_0=5.2447×10^{-2}, $I_{1,0}$=5.8243, $I_{2,0}$=2.5447×10^4 (k_{10}=256); A_0=8.3872×10^{-4}, E_0=4.8793, e_0=3.9572×10^{-5}, $I_{1,0}$=7.6544, $I_{2,0}$=5.1046×10^4 (k_{10}=512); A_0=1.7657, E_0=7.6866, e_0=9.1430×10^{-2}, $I_{1,0}$=4.2379, $I_{2,0}$=1.0225×10^5 (k_{10}=1024); A_0=2.1377, E_0=7.6720, e_0=1.0996×10^{-1}, $I_{1,0}$=3.4304, $I_{2,0}$=2.0465×10^5 (k_{10}=2048).

In Fig. 3.15 the frequency of A is plotted as a function of $k_2^{ph2}+k_{10}$, where the oscillator's response to a step-wise perturbation from k_2=1.0 (phase 1) to k_2=2→10 in phase 2 (with increments of one) is shown. This is repeated at lower backgrounds from 0→16 in panel a and higher k_{10} values from 32→2048 in panel b. Notice how the total perturbations (k_2+k_{10}) induce parallel lines, i.e., the oscillator is capable of eliminating backgrounds. Thus, the frequency compensated oscillator with coherent feedback shows robust background compensation.

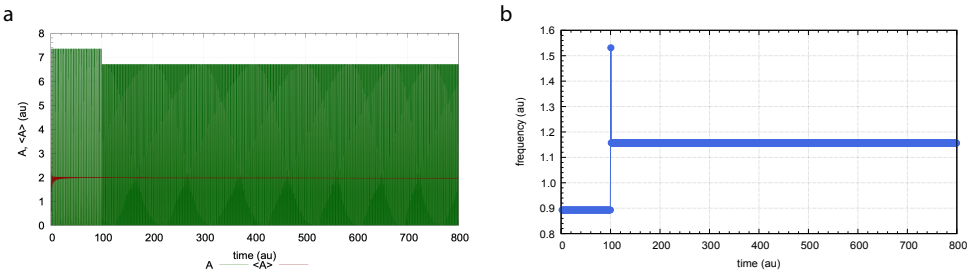

FIGURE 3.16: Frequency response of the feedback scheme in Fig. 3.12a when eliminating I_1 and I_2. The controller is tested at a step-perturbation k_2 from 1→9 at time t=100 and a constant background k_{10}=32. Panel a shows the response of A as a function of time, as well as the average concentration $<A>$. Notice how the frequency in panel b increases from phase 1 to 2, i.e. the oscillator does not show frequency adaptation. Other rate constants (phases 1 and 2, in a.u.): k_4=1.0, k_5=0.1, k_6=2.0, k_7=k_8=1×10^{-6}, k_9=20.0. Initial concentrations of A, and E (in a.u.), respectively: 4.7695 and 9.1501×10^{-1}

The necessesity of I_1 and I_2 in ensuring frequency homeostasis was tested by eliminating their effects in Fig. 3.12a, i.e., by setting I_1 and I_2 to zero. The results can be seen in Fig. 3.16, in which the oscillator was subjected to a step-perturbation k_2 from 1→9 at time t=100 and background k_{10}=32. Panel a shows the oscillations of A over time, where its average concentration remains the same ($<A>$=2.0) due to the compensatory actions of E. However, in panel b the controller becomes sensitive to k_2-steps and does no longer show frequency homeostasis. This indicates that I_1 and I_2 are necessary in ensuring the oscillator's frequency compensation.

3.3.2 Frequency compensated oscillator with incoherent feedback

This section deals with a two-layered frequency compensated oscillator (Fig. 3.17a), where integral control is incorporated by incoherent feedback (Fig. 3.17b) [5, 6]. A feedback mechanism like this does not enable the controller to eliminate backgrounds (Fig. 3.20).

The controller in Fig. 3.17a is a frequency compensated oscillator with incoherent feedback [5, 6], where the central a-A-E-a feedback loop (colored green) is based on motif m2 (Fig. 3.7). This controller uses an intermediate a in front of A to turn the central oscillator into a limit-cycle oscillator [2]. There is an outflow of A when a step-perturbation k_2 (colored red) and background reaction k_{10} (colored blue) are applied. Since the central oscillator is an inflow controller it will compensate for the ouflow perturbations [46], in which the compensatory fluxes of E (j_3=$k_3 \cdot k_5/(k_5+E)$) keep the average concentration of A, $<A>$, under robust homeostatic control.

An outer feedback layer (colored orange), with controller species I_1 and I_2, keep the average concentration of E, $<E>$, homeostatically regulated. The outflow controller I_1 and inflow controller I_2 are also responsible for enabling the oscillator's frequency homeostasis [2]. This oscillator does not show background compensation since I_1 and I_2 feed incoherently (Fig. 3.17b) [5, 6] back to A in the central oscillator.

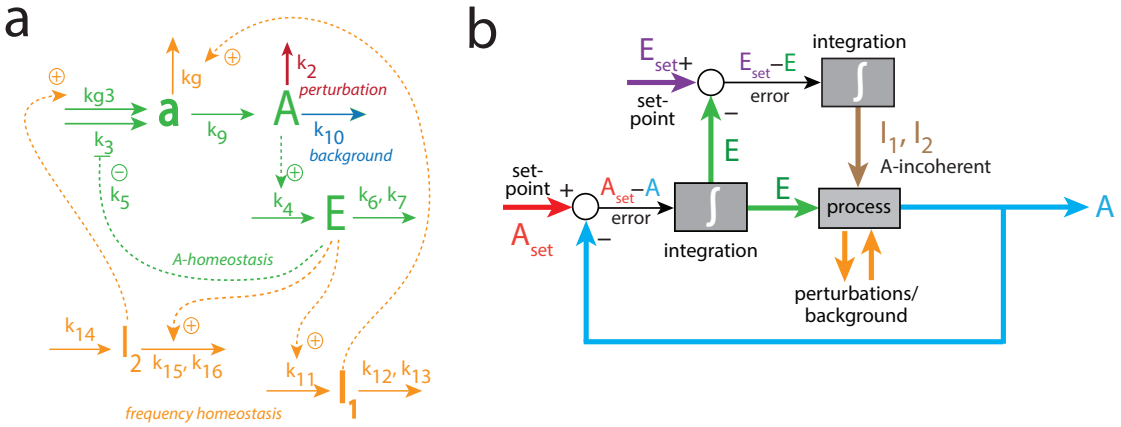

FIGURE 3.17: Example of an oscillator with frequency control and incoherent feedback, i.e., no background compensation. Figure was redrawn from Ref. [4], Fig. 15. a) Reaction scheme of oscillator with two negative feedback layers, in which the central A-E-a-A loop is based on derepression-based motif m2 (Fig. 3.7a). Solid arrows represent chemical reactions. Dashed lines indicate signaling events, where activation is represented by a plus sign and inhibition by a minus sign. b) Integral control scheme with incoherent feedback, where I_1 and I_2 feed back to A through the precursor a. Incoherent feedback, which is a term used in quantum control theory and optics [5, 6], yields an additional control of E via A by I_1 and I_2. In particular, uncontrollable perturbations (orange arrows) add or remove A. The difference or error between the controlled variable and its set-point (A_{set}-A) is measured and integrated over time (lower grey "integration box"). This gives the necessary E-concentration (horizontal green line) for maintaining A under robust homeostatic control. A difference from the basic integral controller (Fig. 2.2b), is that the outpout of E (vertical green line) is also used as input in a second control system. Here, the error between E and E_{set} is measured and integrated over time (upper grey "integration box"). This gives the I_1- and I_2-concentrations (brown line) to be fed incoherently back to A, i.e., into the process that generates A, in order to maintain $E_{set^{I1}}$ and $E_{set^{I2}}$, respectively.

The rate equations of A, a, E, I_1, and I_2 are, respectively:

$$\dot{A} = (k_2 + k_{10}) \cdot A + k_9 \cdot a \tag{3.39}$$

$$\dot{a} = \frac{(k_3 + k_{g3} \cdot I_2) \cdot k_5}{k_5 + E} - (k_9 + k_g \cdot I_1) \cdot a \tag{3.40}$$

$$\dot{E} = k_4 \cdot A - \frac{k_6 \cdot E}{k_7 + E} \tag{3.41}$$

$$\dot{I}_1 = k_{11} \cdot E - \frac{k_{12} \cdot I_1}{k_{13} + I_1} \tag{3.42}$$

$$\dot{I}_2 = k_{14} - \left(\frac{k_{15}{\cdot}I_2}{k_{16}+I_2}\right){\cdot}E \tag{3.43}$$

Integral control is implemented as a zero-order removal of E (i.e. $E/(k_7{+}E){\approx}1$) in the central A-E-a-E loop, where the set-point A_{set} is determined together with the steady state (ss) approximation:

$$k_4{\cdot}{<}A_{ss}{>} = k_6 \cdot \underbrace{\left(\frac{E_{ss}}{k_7{+}E_{ss}}\right)}_{\approx 1\,(\text{zero}-\text{order})} \;\Rightarrow\; {<}A_{ss}{>}{=}A_{set}{=}\frac{k_6}{k_4} \tag{3.44}$$

in which $<A_{ss}>$ goes to A_{set} when oscillatory and A goes to A_{set} when non-oscillatory [2].

In the outer feedback layer I_1 and I_2 are also assumed to follow zero-order kinetics in their removal, which assumes that $k_{13}{\ll}I_{1,ss}$ and $k_{16}{\ll}I_{1,ss}$, respectively. As such, the set-points for the manipulated variable, $E^{I_1}_{set}$ and $E^{I_2}_{set}$, can be determined together with the steady state (ss) approximation:

$$k_{11}{\cdot}{<}E_{ss}{>} = k_{12} \cdot \underbrace{\left(\frac{I_{1,ss}}{k_{13}{+}I_{1,ss}}\right)}_{\approx 1\,(\text{zero}-\text{order})} \;\Rightarrow\; {<}E_{ss}{>}{=}E^{I_1}_{set}{=}\frac{k_{12}}{k_{11}} \tag{3.45}$$

$$k_{14} = k_{15}{\cdot}{<}E_{ss}{>}\underbrace{\left(\frac{I_{2,ss}}{k_{16}{+}I_{2,ss}}\right)}_{\approx 1\,(\text{zero}-\text{order})} \;\Rightarrow\; {<}E_{ss}{>}{=}E^{I_2}_{set}{=}\frac{k_{14}}{k_{15}} \tag{3.46}$$

Since I_1 works as an outflow controller it becomes active whenever $<E>$ is above $E^{I_1}_{set}$, whereas the inflow controller I_2 becomes operative when $<E>$ is below $E^{I_2}_{set}$ [2].

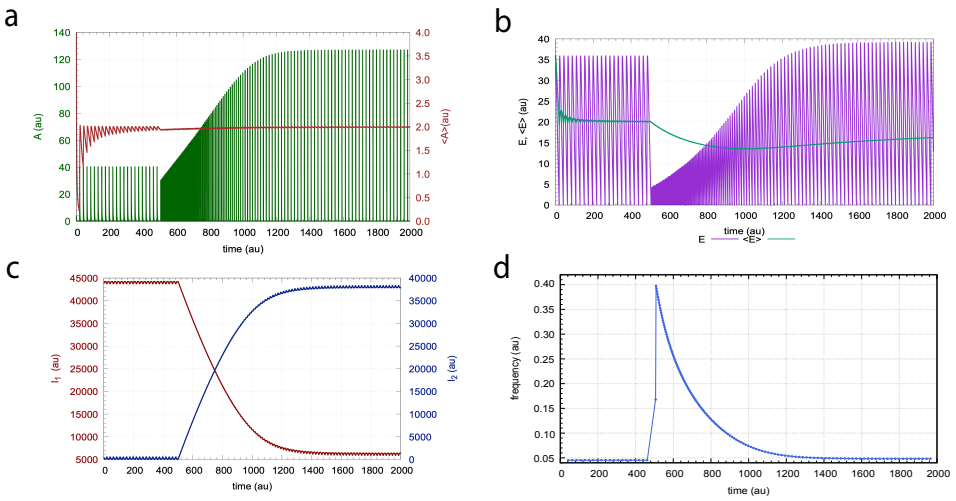

FIGURE 3.18: Frequency compensation of the feedback scheme in Fig. 3.17a at a constant background k_{10}=0. The controller is tested at a step-perturbation k_2 from 1→9 at time t=500. Panels a and b show the resetting kinetics of A and E as a function of time, as well as their average concentrations $<A>$ and $<E>$, respectively. Panel c shows the contributions of the controller species I_1 and I_2 over time. In panel d the frequency, or inverse of the period length, is plotted as a function of time. Notice the oscillator's frequency homeostasis. Other rate constants (phases 1 and 2, in a.u.): k_3=1×10^6, k_4=1.0, k_5=k_7=k_{13}=k_{16}=1×10^{-6}, k_6=k_9=2.0, k_{11}=k_{15}=5.0, k_{12}=100, k_{14}=99.99, k_g=1×10^{-3}, k_{g3}=1.0×10^2. Initial concentrations of A, E, a, I_1, and I_2 (in a.u.), respectively: 4.0427, 35.257, 6.4860×10^{-4} , 4.3800×10^4, and 4.5757×10^2. See Appendix A for python scripts.

The oscillator's behaviour in response to outflow perturbations k_2 and k_{10} can be seen in Fig. 3.18. A step-wise perturbation k_2 from 1.0 (phase 1) to 9.0 (phase 2) at time t=500 and a background k_{10}=0 are applied. Panel a shows the oscillations of A as a function of time, along with its average concentration $<A>$=2.0. The average concentration of A is kept robustly at A_{set} by the compensatory actions of E (panel b). I_1 and I_2 in panel c are responsible for maintaining the manipulated variable's average concentration $<E>$ (panel b). In panel d the frequency, or inverse of the period length, is plotted as a function of time. This controller clearly shows frequency homeostasis.

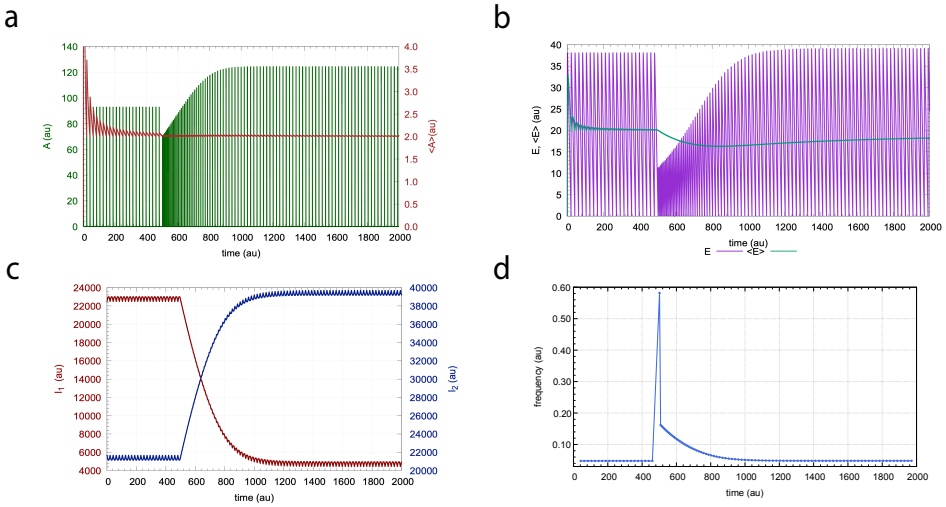

FIGURE 3.19: Frequency compensation of the feedback scheme in Fig. 3.17a at a constant background k_{10}=2. The controller is tested at a step-perturbation k_2 from 1→9 at time t=500. Panels a and b show the resetting kinetics of A and E as a function of time, as well as their average concentrations $<A>$ and $<E>$, respectively. Panel c shows the contributions of the controller species I_1 and I_2. In panel d the frequency, or inverse of the period length, is plotted as a function of time. Notice the oscillator's frequency homeostasis. Other rate constants (phases 1 and 2, in a.u.) as in Fig. 3.18. Initial concentrations of A, E, a, I_1, and I_2 (in a.u.), respectively: 1.4906×10^{-1}, 1.6789×10^{-1}, 5.6795×10^{-1}, 2.2515×10^{4}, and 2.1643×10^{4}. See Appendix A for python scripts.

Fig. 3.19 shows the results from the same k_2-step at k_{10}=2. I_1 and I_2 (panel c) still keep $<A>$ (panel a) and $<E>$ (panel b) homeostatically regulated. They also ensure frequency homeostasis (panel d) but the maximum frequency for this background has increased. Thus, the controller does not show the same sensitivity to the maximum frequency at different backgrounds.

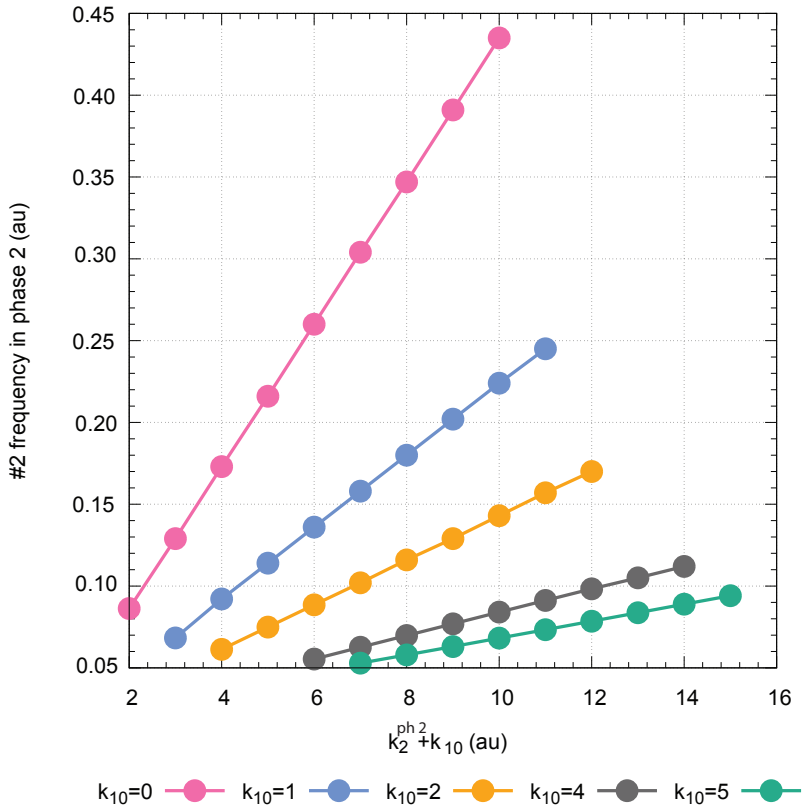

FIGURE 3.20: Frequency compensated oscillator without background compensation from Fig. 3.17a. The figure shows the number 2 frequency (in phase 2) as a function of $k_2^{ph2}+k_{10}$. Frequency adaptation of the oscillator (in a.u.) at a step-wise perturbation from phase 1 (k_2=1.0) to phase 2 (k_2 variable, k_2 from 2→10) with constant background perturbations k_{10} from 0→5 (k_{10} variable, phases 1 and 2). Notice how the gradient of the straight lines decreases with increasing k_{10} values. Other rate constants (phases 1 and 2, in a.u.) as in Fig. 3.18. Initial concentrations of A, E, a, I_1, and I_2 (in a.u.), respectively: A=3.7479×10^{-3}, E=9.8732, a=2.2113×10^{-3}, I_1=4.4299×10^4, I_2=1.2833×10^2 (k_{10}=0); A=2.5176×10^{-3}, E=28.864, a=2.4152×10^{-3}, I_1=3.2608×10^4, I_2=1.1810×10^4 (k_{10}=1); A=3.6061×10^{-1}, E=37.282, a=3.6550×10^{-3}, I_1=2.3614×10^4, I_2=2.0794×10^4 (k_{10}=2); A=6.7083×10^{-3}, E=17.367, a=1.7148×10^{-2}, I_1=1.3637×10^4, I_2=3.0761×10^4 (k_{10}=4); A=6.1278×10^{-3}, E=22.250, a=1.8648×10^{-2}, I_1=1.0208×10^4, I_2=3.4180×10^4 (k_{10}=5).

In Fig. 3.20 the frequency of A as is plotted as a function of $k_2^{ph2}+k_{10}$. A step-perturbation from k_2=1.0 (phase 1) to k_2=2→10 in phase 2 (with increments of one) is applied, along with a constant background reaction k_{10} from 0→5. Notice how the frequency of the oscillator (with incoherent feedback) decreases with increasing k_{10}-values. This means that the controller lacks the ability to robustly compensate backgrounds. Also, the oscillator breaks down and stops functioning at k_{10} values higher than 5.5.

3.3.3 Oscillator with frequency independence

Finally, the necessity of I_1 and I_2 in ensuring frequency and background compensations are tested, which is done by excluding the second feedback layer in a limit-cycle m5-based oscillator (Fig. 3.21a). A basic integral controller (Fig. 3.21b) is incorporated into this single negative feedback layer. This oscillator shows frequency independence and no background compensation (Fig. 3.24).

The controller in Fig. 3.21a is a quasi-harmonic oscillator based on the inflow controller m5 (Fig. 3.5) and shows frequency independence. The difference from m5 is that this oscillator has an additional intermediate e that turns it into a limit-cycle oscillator [2]. When applying a step-perturbation k_{15} (colored red) and background reaction k_{14} (colored blue) there is an inflow of A, which is opposed by the compensatory fluxes of E (j_3=k_2·k_3/(k_3+E)) in order to keep A robustly at its set-point. The basic integral controller (Fig. 3.21b) is incoporated into the oscillator since there is no control of <E> by I_1 and I_2.

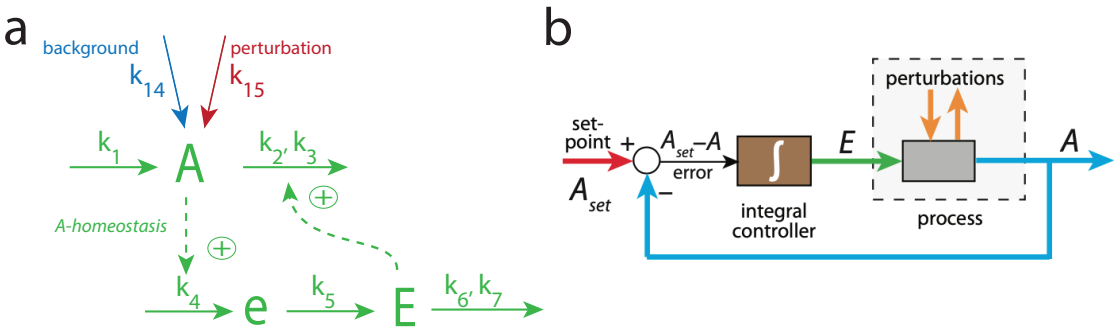

FIGURE 3.21: Controller scheme of the frequency independent oscillator. (a) Controller motif with integral control incoporated as a zero-order Michaelis-Menten (MM) type degredation of E. The MM parameters V_{max} and K_m are represented by k_6 and k_7, respectively. k_{15} is a perturbation and k_{14} represents a background reaction. Solid arrows represent chemical reactions. Dashed lines indicate signaling events, where activation is represented by a plus sign. (b) Basic integral controller that is incorporated into the oscillator. Uncontrollable perturbations (orange arrows) add or remove A. The difference or error between the controlled variable and its set-point (A_{set}-A) is measured and integrated over time (brown "integral controller box"). This gives the necessary E-concentration (green line) for maintaining A under robust homeostatic control. Figure was redrawn from Ref. [7], Fig. 1.

The rate equations of A, e, and E are, respectively:

$$\dot{A} = k_1 - \left(\frac{k_2 \cdot A}{k_3 + A}\right) \cdot E \tag{3.47}$$

$$\dot{e} = k_4 \cdot A - k_5 \cdot e \tag{3.48}$$

$$\dot{E} = k_5 \cdot e - \frac{k_6 \cdot E}{k_7 + E} \tag{3.49}$$

where for simplicity's sake k_1=k_1+k_{14}+k_{15}.

Assuming steady state (ss) and zero-order degredation of E gives the following set-point A_{set}:

$$k_4 \cdot <A_{ss}> = k_5 \cdot <e_{ss}> = k_6 \cdot \underbrace{\left(\frac{E_{ss}}{k_7 + E_{ss}}\right)}_{\approx 1\,(\text{zero}-\text{order})} \quad \Rightarrow \quad <A_{ss}> = A_{set} = \frac{k_6}{k_4} \tag{3.50}$$

where $<A_{ss}>$ goes to A_{set} when oscillatory whereas A goes to A_{set} when non-oscillatory [2].

Determining the harmonic set-point

Since this is a quasi-harmonic oscillator the harmonic set-point can also be determined. First, by assuming steady state (i.e. $\dot{A} = 0$) the following expression is obtained:

$$\dot{A}{=}k_1 - k_2{\cdot}\ E \tag{3.51}$$

Taking the time derivative once more gives the expression of $\ddot{A}$:

$$\ddot{A}{=} - k_2{\cdot}\dot{E} = -k_2{\cdot}k_5{\cdot}e - k_6 = k_4{\cdot}A - k_6 \tag{3.52}$$

Rearranging Eq. 3.52 gives the harmonic set-point:

$$\frac{\ddot{A}}{\omega^2} + A = \langle A_{set} \rangle \tag{3.53}$$

where $\omega = k_2 \cdot k_4$.

The notation of Eq. 3.53 is:

$$A(t) = A_0{\cdot}sin{\cdot}(\omega{\cdot}t + \gamma) + A_{set} \tag{3.54}$$

where $\omega = \frac{2{\cdot}\pi}{P}$ and P is the period length.

Taking the time derivative of Eq. 3.54 gives:

$$\dot{A}(t){=}\omega{\cdot}A_0{\cdot}cos{\cdot}(\omega{\cdot}t + \gamma) \tag{3.55}$$

and by taking the time derivative of Eq. 3.56 one gets:

$$\ddot{A}(t){=} - \omega^2{\cdot}A_0{\cdot}sin{\cdot}(\omega{\cdot}t + \gamma) \tag{3.56}$$

Then by rearranging the equations one gets the expression for the harmonic set-point:

$$\frac{\ddot{A}(t)}{\omega^2} = -A_0{\cdot}sin{\cdot}(\omega{\cdot}t + \gamma) + A_0{\cdot}sin{\cdot}(\omega{\cdot}t + \gamma) + \langle A_{set} \rangle = \langle A_{set} \rangle \tag{3.57}$$

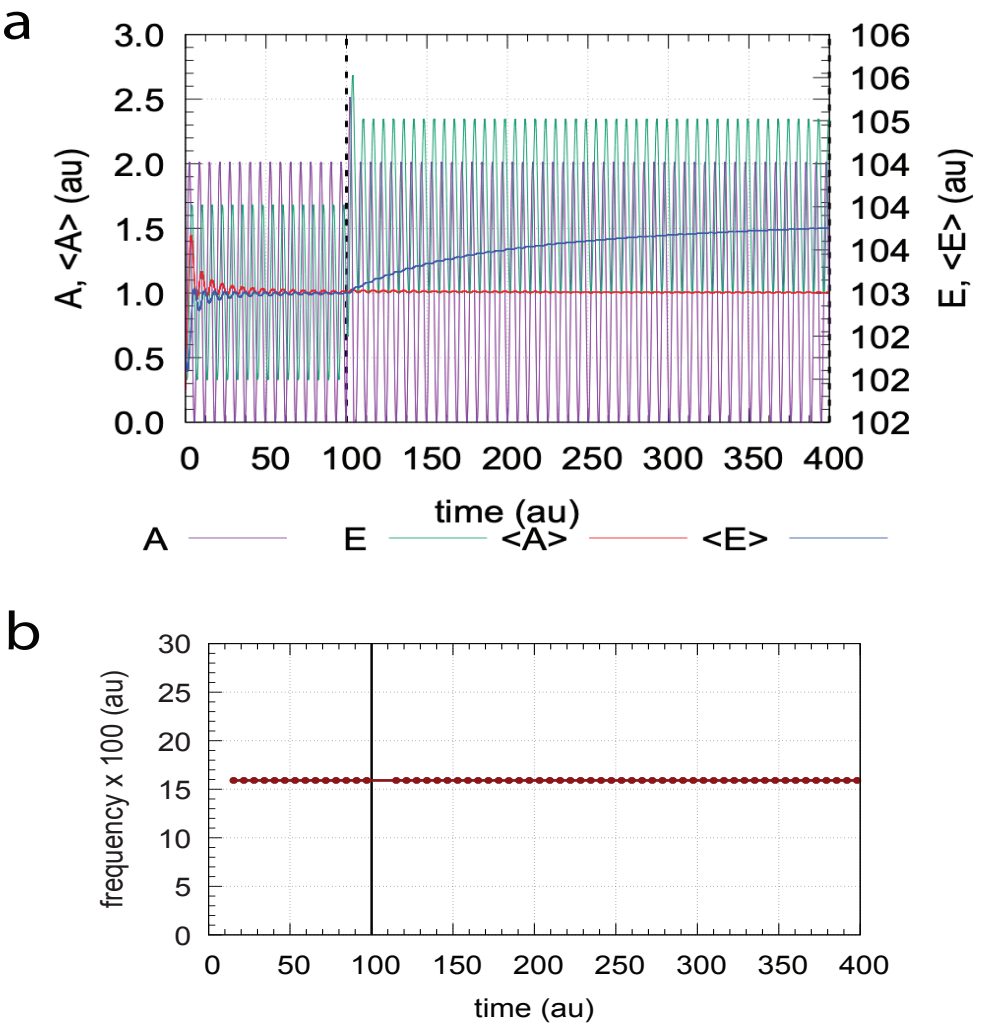

FIGURE 3.22: Response kinetics of the feedback scheme in Fig. 3.21a at a constant background k_{14}=2. The controller is tested at a step-perturbation k_{15} from 1→2 at time t=100. The resetting kinetics (in a.u.) of A and E are shown as a function of time, as well as their average concentrations $<A>$ and $<E>$, respectively (panel a). Panel b shows the frequency (x 100) as a function of time (a.u.). Notice the frequency indepence of the controller. Other rate constants (phases 1 and 2, in a.u.): k_1=k_5=100, k_2=k_4=k_6=1.0, k_3=k_7=1×10^{-6}. Initial concentrations of A, E, and e (in au), respectively: 2.4708×10^{-1}, 1.0235×10^{2}, 2.4065×10^{-3}. See Appendix A for python scripts.

The oscillator's response to inflow perturbations k_{14} and k_{15} are shown in Fig. 3.22. In addition to a constant background k_{14}=2 the controller is subjected to a k_{15}-step from 1.0 (phase 1) to 2.0 (phase 2) at time t=100. Panel a shows the oscillations of A and E over time, as well as their respective average concentrations $<A>$ and $<E>$. There is a homeostatic control of $<A>$=1.0 by E. However, since this oscillator has a single negative feedback layer there is no additional control of $<E>$ by I_1 and I_2. The lack of I_1 and I_2 becomes even more apparent in panel b, where the oscillator shows complete frequency independence.

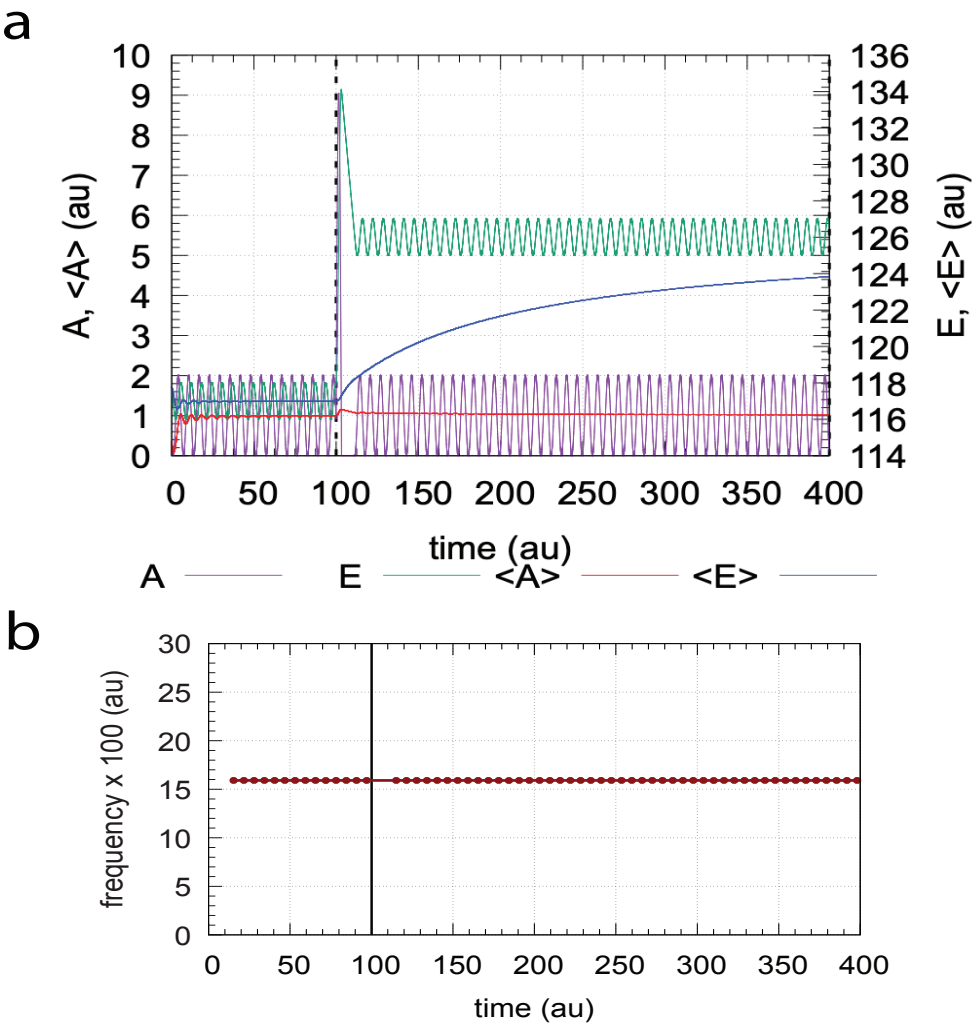

FIGURE 3.23: Response kinetics of the feedback scheme in Fig. 3.21a at a constant background k_{14}=16. The controller is tested at a step-perturbation k_{15} from 1→10 at time t=100. The resetting kinetics (in a.u.) of A and E are shown as a function of time, as well as their respective average concentrations $<A>$ and $<E>$. Panel b shows the frequency (x 100) as a function of time (a.u.). Notice the frequency independence of the controller. Other rate constants (phases 1 and 2, in a.u.) as in Fig. 3.22. Initial concentrations of A, E, and e (in a.u.), respectively: 3.6316×10^{-1}, 1.1780×10^{2}, 3.7122×10^{-3}. See Appendix A for python scripts.

Fig. 3.23 shows instead the results of a step-wise perturbation k_{15} from 1.0 (phase 1) to 10.0 (phase 2) at k_{14}=16. The set-point of $<A>$=1.0 (panel a) remains the same. Panel b still shows frequency independence. In fact, the frequency value is exactly the same for this background.

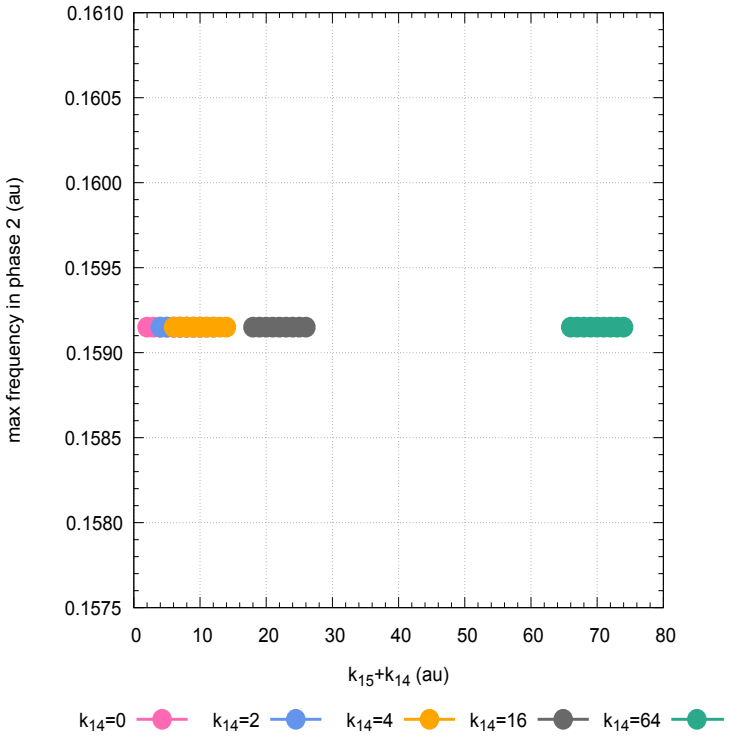

FIGURE 3.24: Oscillator from Fig. 3.21a with frequency independence. The figure shows the maximum frequency (in phase 2) as a function of k_{15}^{ph2}+k_{14}. The controller is applied a step-wise perturbation from phase 1 (k_{15}=1.0) to phase 2 (k_{15} variable, k_{15} from 2→10) with constant background perturbations k_{14} from 0→64 (k_{14} variable, phases 1 and 2). The controller shows frequency independence. Other rate constants (phases 1 and 2, in a.u.): k_1=k_5=1×10^2, k_2=k_4=k_6=1.0, k_3=k_7=1×10^{-6}. Initial concentrations of A, e, and E (in a.u.), respectively: A_0=1.6912, e_0=1.6838×10^{-2}, E_0=1.0027×10^2, I_{1_0}=4.4299×10^4, I_{2_0}=1.2833×10^2 (k_{14} from 0→64).

In Fig. 3.24 the maximum frequency of A is plotted as a function of k_{15}^{ph2}+k_{14}. The oscillator is subjected to a step-perturbation k_{15}=1.0 (phase 1) to k_{15}=2→10 in phase 2 (with increments of one) is applied, along with a constant background reaction from k_{14}=0→64. The frequency value of the oscillator remains completley flat at different backgrounds. There is no frequency compensation due to the lack of an outer feedback layer with I_1 and I_2.

3.4 Three-layered retinal light adaptation (RLA) models

This section provides a set of three-layered retinal light adaptation (RLA) models, where each negative feedback layer corresponds to a different retinal cell. Exposing these controllers to a step-perturbation and constant but different backgrounds allow us to examine their response to frequency and light, respectively.

The retinal interactions are illustrated in Fig. 3.25. In fact, this is a simplified version of the retinal structure shown in (Fig. 3.2). Here, light (indicated by yellow arrows) travels through the center (and not the annulus) of the receptive field. This excites the on-center cone (colored blue) in the first feedbak layer, which are represented by the m1-m8 controllers (Fig. 2.1). In this layer the controlled variable A is homeostatically regulated due to the compensatory actions of the manipulated variable E. A hypothetical on-center bipolar cell (colored green) then receives an inhibitory signal from E. This determines the concentration of A_{pp} in the subsequent on-center ganglion cell (colored purple), which is represented by a frequency compensated oscillator (see Ch. 3.3).

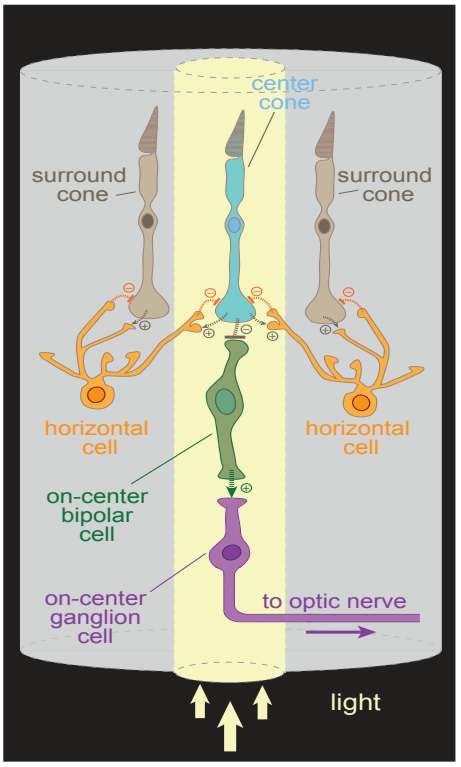

FIGURE 3.25: Cellular interactions within the retinal layers. This figure is a simplified version of the retinal structure shown in (Fig. 3.2). Here, light (indicated yellow arrows) travels through the center (and not the annulus) of the receptive field. This excites the on-center cone (colored blue) in the first feedbak layer, in which an inhibitory signal is received by the on-center bipolar cell (colored green) of the second layer. A subsequent on-center ganglion cell (colored purple) then receives a signal from the bipolar cell, before ganglion cell axons come together to form the optic nerve that enters the central nervous system. Horizontal cell (colored orange) interactions are also indicated in the figure.

A_{pp} is the controlled variable in the ganglion cell and its time average concentration, $<A_{pp}>(t)$, is homeostatically regulated by the manipulated variable E_{pp}.

$$<A_{pp}>(t) = \frac{1}{t}\int_0^t A{\cdot}dt \tag{3.58}$$

There is an additional control of E_{pp} or its time average concentration, $<E_{pp}>(t)$, by the controller species I_1 and I_2.

$$<E_{pp}>(t) = \frac{1}{t}\int_0^t E{\cdot}dt \tag{3.59}$$

I_1 and I_2 also ensure frequency control of the oscillator. In fact, it has been shown that these two-layered oscillators enable robust frequency homeostasis [2]. The controller variables I_1 and I_2 feed back to A_{pp} directly by coherent feedback or incoherently [5, 6] into the process that generates A_{pp}.

3.4.1 Background compensated RLA controller dominated by I_2

This section provides a RLA controller (Fig. 3.26a) capable of eliminating backgrounds (Fig. 3.29). This is due to the coherent feedback of I_1 and I_2 [5, 6] in the frequency compensated ganglion cell.

The RLA controller, shown in Fig. 3.26a, is structured into three negative feedback layers. Each layer represents a retinal cell and their interactions are illustrated in panel b. The first photoreceptor layer, with an on-center cone (colored blue), constitutes the derepression-based inflow controller m2 (Fig. 3.7). There is an outflow of A due to a step-perturbation k_2 (colored red) and a background k_4 (colored blue). A is maintained under robust homeostatic control by the compensatory actions of E ($j_3{=}k_3k_8/(k_8{+}E)$). E further sends inhibitory information to the on-center bipolar cell (colored green), which further activates the removal of A_{pp} in the on-center ganglion cell (colored purple). This third and final layer is represented by a frequency compensated oscillator (see Ch. 3.3). Thus, I_1 and I_2 also ensure E_{pp}- and frequency-homeostasis in this oscillator, as well as background compensation due to their coherent feedback back to A_{pp} [5, 6].

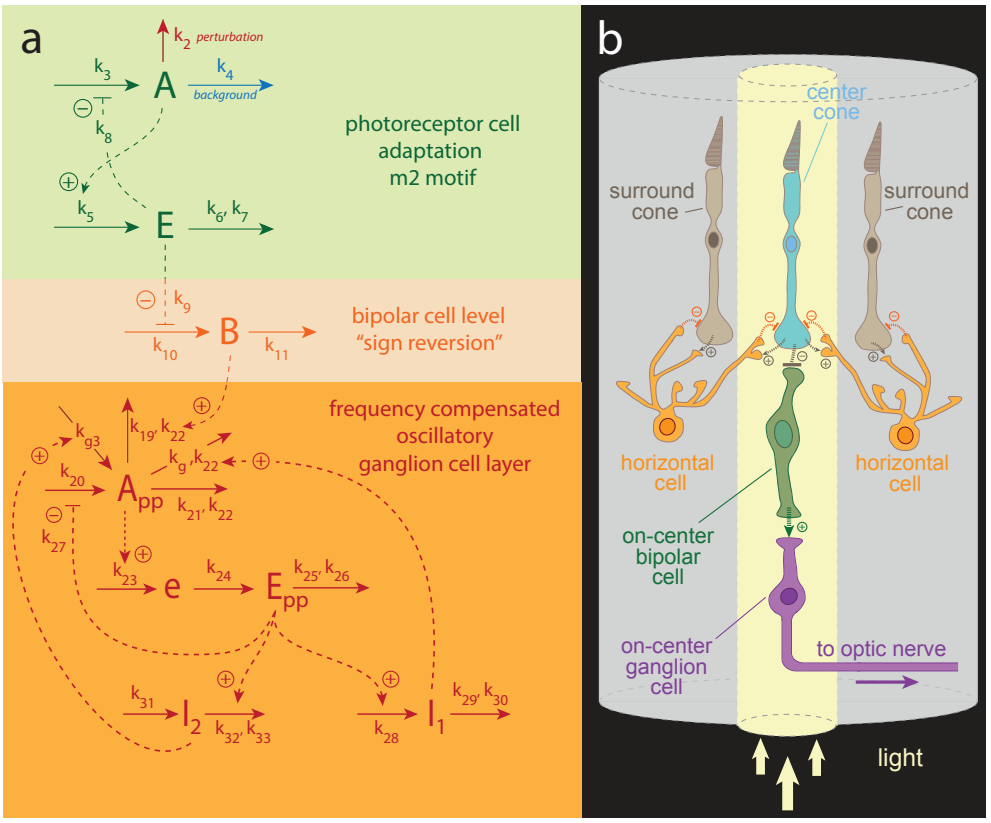

FIGURE 3.26: Retinal light adaptation (RLA) model with frequency control at the ganglion cell level. a) Simple RLA controller with three layers of negative feedback. The first negative feedback layer constitutes the m2 motif (Fig. 3.7), in which integral control is incoporated as a zero-order Michaelis-Menten (MM) type degredation of E. This allows for robust perfect adaptation of A. The controller is subjected to outflow perturbations k_2 and k_4. Inhbitory information from E is sent to the bipolar cell in the second layer, and B further activates the removal of A_{pp} in the ganglion cell layer. A_{pp} is homeostatically controlled by E_{pp}. I_1 and I_2 ensure E_{pp}- and frequency-homeostasis of the oscillator. I_1 and I_2 feed coherently [5, 6] back to A_{pp}, which enable the controller to neutralize backgrounds. Solid arrows represent chemical reactions. Dashed lines indicate signaling events, where activation is represented by a plus sign and inhibition by a minus sign. b) Cellular interactions within the retinal layers. This figure is a simplified version of the retinal structure shown in (Fig. 3.2). Here, light (yellow arrows) travels through the center (and not the annulus) of the receptive field. This excites the on-center cone (colored blue) in the first feedbak layer, in which an inhibitory signal is received by the on-center bipolar cell (colored green) of the second layer. A subsequent on-center ganglion cell (colored purple) then receives a signal from the bipolar cell, before ganglion cell axons come together to form the optic nerve that enters the central nervous system. Horizontal cell interactions are also indicated in the figure. Figure was redrawn from Fig. 11.21, Ref. [3].

The rate equations of A and E in the photoreceptor layer become, respectively:

$$\dot{A} = \frac{k_3 \cdot k_8}{k_8 + E} - (k_2 + k_4) \cdot A \tag{3.60}$$

$$\dot{E} = k_5 \cdot A - \frac{k_6 \cdot E}{k_7 + E} \tag{3.61}$$

The rate equation of B in the bipolar cell layer is:

$$\dot{B} = \frac{k_{10} \cdot k_9}{k_9 + E} - k_{11} \cdot B \tag{3.62}$$

The rate equations of A_{pp}, e, E_{pp}, I_1, and I_2 in the ganglion cell layer are, respectively:

$$\dot{A_{pp}} = k_{g3} \cdot I_2 + \frac{k_{20} \cdot k_{27}}{k_{27} + E_{pp}} - \left(\frac{k_g \cdot A_{pp}}{k_{22+A_{pp}}} \right) \cdot I_1 - \frac{k_{21} \cdot A_{pp}}{k_{22} + A_{pp}} - \left(\frac{k_{19} \cdot A_{pp}}{k_{22} + A_{pp}} \right) \cdot B \tag{3.63}$$

$$\dot{e} = k_{23} \cdot A_{pp} - k_{24} \cdot e \tag{3.64}$$

$$\dot{E_{pp}} = k_{24} \cdot e - \frac{k_{25} \cdot E_{pp}}{k_{26} + E_{pp}} \tag{3.65}$$

$$\dot{I}_1 = k_{28} \cdot E_{pp} - \frac{k_{29} \cdot I_1}{k_{30} + I_1} \tag{3.66}$$

$$\dot{I}_2 = k_{31} - \left(\frac{k_{32} \cdot I_2}{k_{33} + I_2} \right) \cdot E_{pp} \tag{3.67}$$

E is assumed to be removed by zero-order MM-kinetics in the photoreceptor layer. Together with the steady state approximation (i.e. $\dot{E}$=0) the set-point A_{set} can be determined:

$$k_5 \cdot A_{ss} = k_6 \;\; \Rightarrow \;\; A_{ss} = A_{set} = \frac{k_6}{k_5} \tag{3.68}$$

The same assumptions are made with regards to the set-point $A_{pp,set}$ in the ganglion cell layer:

$$k_{23} \cdot <A_{pp,ss}> = k_{24} \cdot <e_{ss}> \underbrace{\left(\frac{E_{pp,ss}}{k_{26} + E_{pp,ss}} \right)}_{\approx 1 \,(\text{zero-order})} \cdot k_{25} \;\; \Rightarrow \;\; <A_{pp,ss}> = A_{pp,set} = \frac{k_{25}}{k_{23}} \tag{3.69}$$

E_{pp} has two set-points, $E_{set}^{I_1}$ and $E_{set}^{I_2}$, depending on whether it interacts with I_1 or I_2, respectively:

$$k_{28}\cdot<E_{pp,ss}> = \underbrace{\left(\frac{I_{1,ss}}{k_{30}+I_{1,ss}}\right)}_{\approx 1\,(\text{zero}-\text{order})}\cdot k_{29} \;\Rightarrow\; <E_{pp,ss}> = E_{pp,set}^{I_1} = \frac{k_{29}}{k_{28}} \tag{3.70}$$

$$k_{31} = \underbrace{\left(\frac{I_{2,ss}}{k_{33}+I_{2,ss}}\right)}_{\approx 1\,(\text{zero}-\text{order})}\cdot k_{29}\cdot<E_{pp,ss}> \;\Rightarrow\; <E_{pp,ss}> = E_{pp,set}^{I_2} = \frac{k_{31}}{k_{32}} \tag{3.71}$$

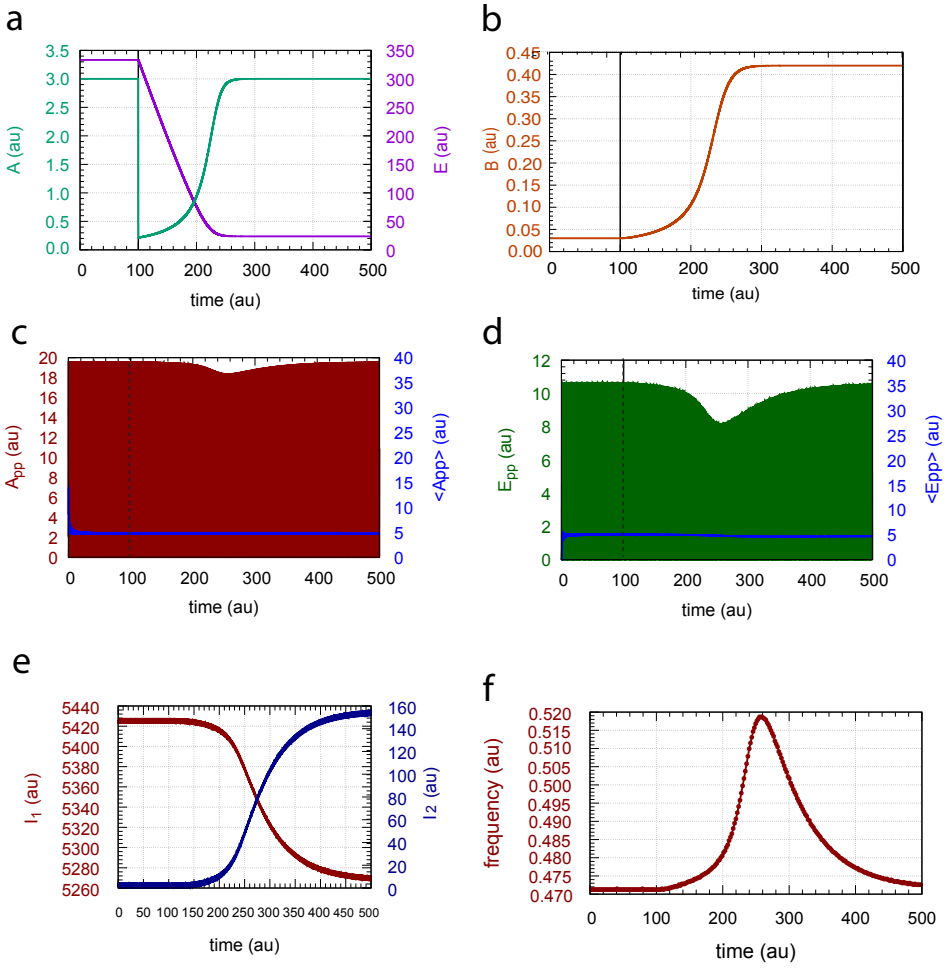

FIGURE 3.27: Response kinetics of the RLA controller from Fig. 3.26a with background k_4=0. The controller is tested at a step-perturbation k_2 from 1.0 (phase 1) to 20.0 (phase 2) at time t=100. Panel a shows the resetting kinetics of A and E as a function of time. Panel b shows the increase in B over time. The resetting kinetics of A_{pp} and E_{pp} are shown in panel c and d, respectively, along with their respective average concentrations $<A_{pp}>$ and $<E_{pp}>$. Panel e shows the contributions of the controller species I_1 and I_2 over time. In panel d the frequency, or inverse of the period length, is plotted as a function of time. Notice the controller's frequency homeostasis. Other rate constants (phases 1 and 2, in a.u.): k_3=1×10^4, k_5=k_{21}=k_{28}=k_{32}=1.0, k_6=3.0, k_7=k_{22}=k_{26}=1×10^{-3}, k_8=k_9=k_{10}=k_{11}=k_{27}=0.1, k_{19}=8.0, k_{20}=100.0, k_{23}=16.0, k_{24}=0.5, k_{25}=80, k_{29}=5.0, k_{30}=k_{33}=1×10^{-6}, k_{31}=4.99, k_g=k_{g3}=1×10^{-2}. Initial concentrations of A, E, B, A_{pp}, e, E_{pp}, I_1, and I_2 (in a.u.), respectively: 3.0000, 3.3323×10^2, 3.0000×10^{-2}, 3.9304, 1.0647×10^2, 1.9892×10^{-3}, 5.4263×10^3, 9.7850×10^{-1}.

Fig. 3.27 shows the RLA controller's response to a step-wise perturbation k_2 from 1.0 (phase 1) to 14.0 (phase 2) at time t=100 at a constant background outflow k_4=0. In panel a the concentration of A and E are plotted as a function of time. The outflow of A is opposed by the compensatory actions of E, which back-regulates A to A_{set}. An increase in B from phase 1 to 2 (panel b) is observed due to the outflow of E. This results in an outflow of A_{pp} and E_{pp} in panel c and d, respectively. Both A_{pp} and E_{pp} are

kept under robust homeostatic control by I_1 and I_2 (panel e). In panel f the frequency is plotted as a function of time. The frequency clearly resets at its pre-perturbation level after some time, which is caused by the control of E_{pp} by I_1 and I_2.

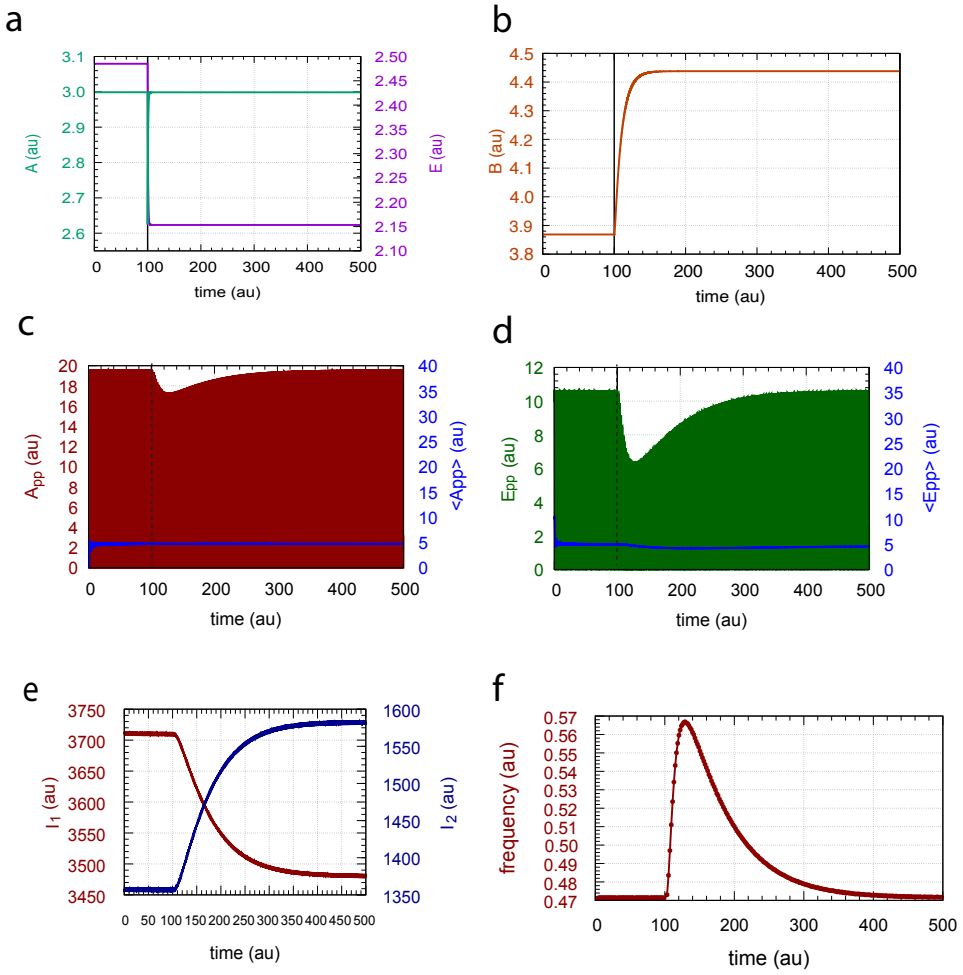

FIGURE 3.28: Response kinetics of the RLA controller from Fig. 3.26a with background k_4=128. The controller is tested at a step-perturbation k_2 from 1.0 (phase 1) to 20.0 (phase 2) at time t=100. Panel a shows the resetting kinetics of A and E as a function of time. Panel b shows the increase in B over time. The resetting kinetics of A_{pp} and E_{pp} are shown in panel c and d, respectively, along with their respective average concentrations $<A_{pp}>$ and $<E_{pp}>$. Panel e shows the contributions of the controller species I_1 and I_2 over time. In panel d the frequency, or inverse of the period length, is plotted as a function of time. Notice the controller's frequency homeostasis. Other rate constants (phases 1 and 2, in a.u.) as in Fig. 3.27. Initial concentrations of A, E, B, A_{pp}, e, E_{pp}, I_1, and I_2 (in a.u.), respectively: 2.9988, 2.4850, 3.8684, 2.6784×10^{-4}, 1.7625×10^{2}, 9.8798, 3.7092×10^{3}, 1.3583×10^{3}.

Fig. 3.28 shows instead the results of a step-perturbation k_2 from 1.0 (phase 1) to 20.0 (phase 2) at k_4=128. The resetting kinetics of A is much faster due to the higher outflow of E (panel a). This further increases the concentration of B in panel b, which results in a larger outflow of A_{pp} and E_{pp} in panel c and d, respectively. At this higher k_4-value

A_{pp} and E_{pp} are still homeostatically regulated. The higher background is compensated for by I_1 and I_2 (panel e), in which the inflow controller I_2 seems to contribute a lot. Although the maximum frequency has increased in panel f (due to the higher k_2-step), frequency compensation is still seen.

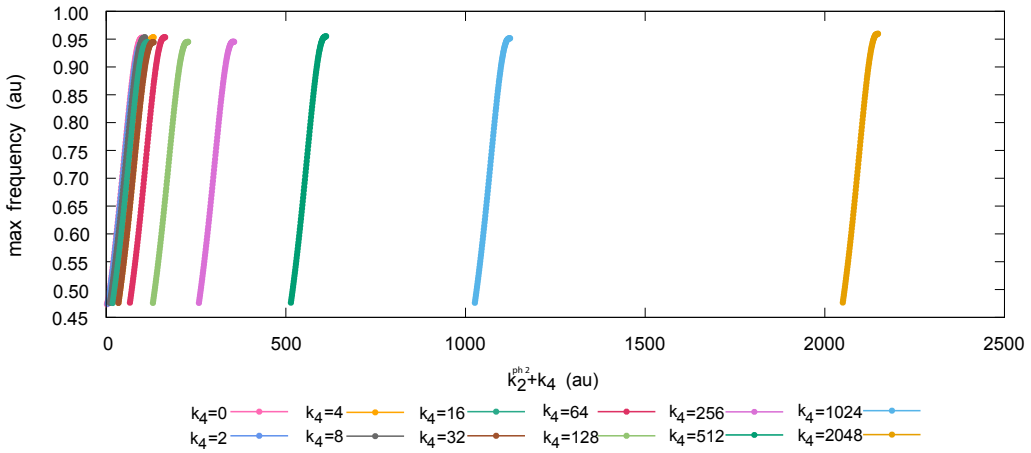

FIGURE 3.29: Frequency and background compensations of the RLA controller from Fig. 3.26a. The figure shows the maximum frequency (in phase 2) as a function of $k_2^{ph2}+k_4$. The controller is applied step-wise perturbation from k_2=1.0 (phase 1) to k_2=2→100 in phase 2 (with increments of one) with constant background perturbation k_4 from 0→2048 (k_4 variable, phases 1 and 2). The controller shows robust background and frequency compensations. Other rate constants (phases 1 and 2, in a.u.) as in Fig. 3.27. Initial concentrations of A, E, B, A_{pp}, e, E_{pp}, I_1, and I_2 (in a.u.), respectively: 3.0000, 3.3323×10^{2}, 3.0000×10^{-2}, 3.9304, 1.0647×10^{2}, 1.9892×10^{-3}, 5.4263×10^{3}, 9.7850×10^{-1} (k_4=0); 3.0000, 1.1101×10^{2}, 9.0000×10^{-2}, 9.7940, 2.0076×10^{2}, 3.2180, 5.3753×10^{3}, 3.9409 (k_4=2); 3.0000, 1.0001×10^{1}, 9.9000×10^{-1}, 1.8289×10^{1}, 1.4873×10^{2}, 1.2631×10^{-2}, 2.9836×10^{4}, 2.5182×10^{4} (k_4=4); 3.0000, 3.6937×10^{1}, 2.7000×10^{-1}, 4.4809, 1.0678×10^{2}, 2.0061×10^{-3}, 3.0351×10^{4}, 2.5117×10^{4} (k_4=8); 3.0000, 1.9508×10^{1}, 5.1000×10^{-1}, 2.7090×10^{-5}, 1.4408×10^{2}, 9.8073, 5.0887×10^{3}, 4.6678×10^{1} (k_4=16); 3.0000, 1.0001×10^{1}, 9.9000×10^{-1}, 5.6417×10^{-5}, 1.3432×10^{2}, 8.3457, 4.8472×10^{3}, 1.8810×10^{2} (k_4=32); 3.0000, 5.0282, 1.9500, 4.8072×10^{-3}, 1.8646×10^{2}, 8.6693, 2.9876×10^{4}, 2.5992×10^{4} (k_4=64); 2.9988, 2.4850, 3.8684, 2.6784×10^{-4}, 1.7625×10^{2}, 9.8798, 3.7092×10^{3}, 1.3583×10^{3} (k_4=128); 3.0000, 1.1970, 7.7100, 5.1717×10^{-4}, 1.5576×10^{2}, 1.0597×10^{1}, 2.0078×10^{3}, 2.7276×10^{3} (k_4=256); 3.0000, 5.4977×10^{-1}, 1.5390×10^{1}, 5.7915×10^{-3}, 1.7878×10^{2}, 9.6191, 2.4551×10^{4}, 3.1417×10^{4} (k_4=512); 3.0000, 2.2520×10^{-1}, 3.0750×10^{1}, 1.9292×10^{1}, 1.5661×10^{2}, 2.9704×10^{-2}, 3.4338×10^{2}, 1.9497×10^{4} (k_4=1024); 3.0000, 6.2684×10^{-2}, 6.1469×10^{1}, 8.4807×10^{-1}, 1.9810×10^{2}, 6.6854, 5.5685×10^{3}, 4.9299×10^{4} (k_4=2048).

Fig. 3.29 shows the maximum frequency of A_{pp} over total outflow perturbations (k_2+k_4). A step-perturbation k_2=1.0 (phase 1) to k_2=2→100 in phase 2 (with increments of one) is applied, along with a constant background reaction k_4 of 0→2048. The controller shows parallell sigmodial curves at different but constant background reactions, i.e., the oscillator is able to compensate backgrounds.

3.4.2 RLA controller without background compensation

This section provides a RLA controller (Fig. 3.30a) that lacks the ability to compensate backgrounds (Fig. 3.33), which is a result of eliminating I_1 and I_2 from the ganglion cell layer.

A three-layered RLA controller without frequency control is shown in In Fig. 3.30a. The negative feedback layers represent different retinal cells, in which their cellular interactions are illustrated in panel b. The first layer constitutes the photoreceptor cell, with an on-center cone (colored blue), and is based on the autocatalytic m2 controller (Fig. 3.8). An outflow of A is observed when a step-perturbation k_2 (colored red) and background k_4 (colored blue) are active. This is opposed by the compensatory fluxes of E (j_3=k_3·k_8/(k_8+E)), which is responsible for keeping A under robust homeostatic control. E further sends an inhibitory signal to B in the on-center bipolar cell (colored green) layer, which then activates the removal of A_{pp} in the on-center ganglion cell (colored purple) layer. Since I_1 and I_2 are absent in the (oscillatory) ganglion cell, there is no additional control of A_{pp} by I_1 and I_2 nor is there frequency compensation.

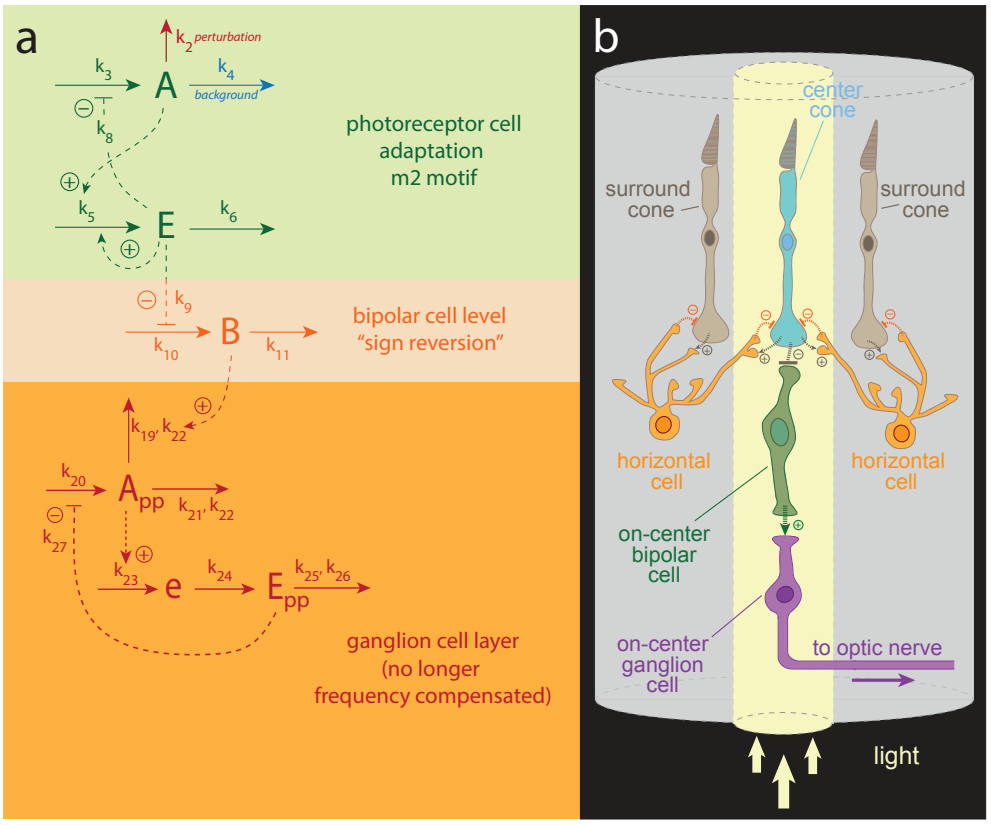

FIGURE 3.30: Retinal light adaptation (RLA) model without frequency control at the ganglion cell level. a) Simple RLA controller with three layers of negative feedback. The first negative feedback layer constitutes the autocatalytic m2 controller (Fig. 3.8). This allows for robust perfect adaptation of A. The controller is subjected to outflow perturbations k_2 and k_4. Inhbitory information from E is sent to the bipolar cell in the second layer, and B further activates the removal of A_{pp} in the ganglion cell layer. A_{pp} is homeostatically controlled by E_{pp}. Solid arrows represent chemical reactions. Dashed lines indicate signaling events, where activation is represented by a plus sign and inhibition by a minus sign. b) Cellular interactions within the retinal layers. This figure is a simplified version of the retinal structure shown in (Fig. 3.2). Here, light (yellow arrows) travels through the center (and not the annulus) of the receptive field. This excites the on-cecnter cone (colored blue) in the first feedbak layer, in which an inhibitory signal is received by the on-center bipolar cell (colored green) of the second layer. A subsequent on-center ganglion cell (colored purple) then receives a signal from the bipolar cell, before ganglion cell axons come together to form the optic nerve that enters the central nervous system. Horizontal cell interactions are also indicated in the figure. Figure was redrawn from Fig. 11.21, Ref. [3].

The rate equations of A and E in the photoreceptor layer become, respectively:

$$\dot{A} = \frac{k_3 \cdot k_8}{k_8 + E} - (k_2 + k_4) \cdot A \tag{3.72}$$

$$\dot{E} = k_5 \cdot A \cdot E - k_6 \cdot E \tag{3.73}$$

The rate equation of B in the bipolar cell layer is:

$$\dot{B} = k_{10} \cdot E - k_{11} \cdot B \tag{3.74}$$

Rate equations of A_{pp}, e, and E_{pp} in the ganglion cell layer are, respectively:

$$\dot{A_{pp}} = \frac{k_{20} \cdot k_{27}}{k_{27} + E_{pp}} - \left(\frac{k_{19} \cdot A_{pp}}{k_{22+A_{pp}}} \right) \cdot B - \frac{k_{21} \cdot A_{pp}}{k_{22} + A_{pp}} \tag{3.75}$$

$$\dot{e} = k_{23} \cdot A_{pp} - k_{24} \cdot e \tag{3.76}$$

$$\dot{E_{pp}} = k_{24} \cdot e - \frac{k_{25} \cdot E_{pp}}{k_{26} + E_{pp}} \tag{3.77}$$

Integral control is assumed to follow an autocatalytic removal of E. Together with the steady state (ss) approximation (i.e. $\dot{E}$=0) the set-point A_{set} in the photoreceptor layer can be determined:

$$k_5 \cdot A_{ss} \cdot E_{ss} = k_6 \cdot E_{ss} \;\; \Rightarrow \;\; A_{ss} = A_{set} = \frac{k_6}{k_5} \tag{3.78}$$

By considering the same assumptions for the ganglion cell layer, the set-point $A_{pp,set}$ becomes:

$$k_{23} \cdot <A_{pp,ss}> = k_{24} \cdot <e_{ss}> \underbrace{\left(\frac{E_{pp,ss}}{k_{26} + E_{pp,ss}} \right)}_{\approx 1 \,(\text{zero-order})} \cdot k_{25} \;\; \Rightarrow \;\; <A_{pp,ss}> = A_{pp,set} = \frac{k_{25}}{k_{23}} \tag{3.79}$$

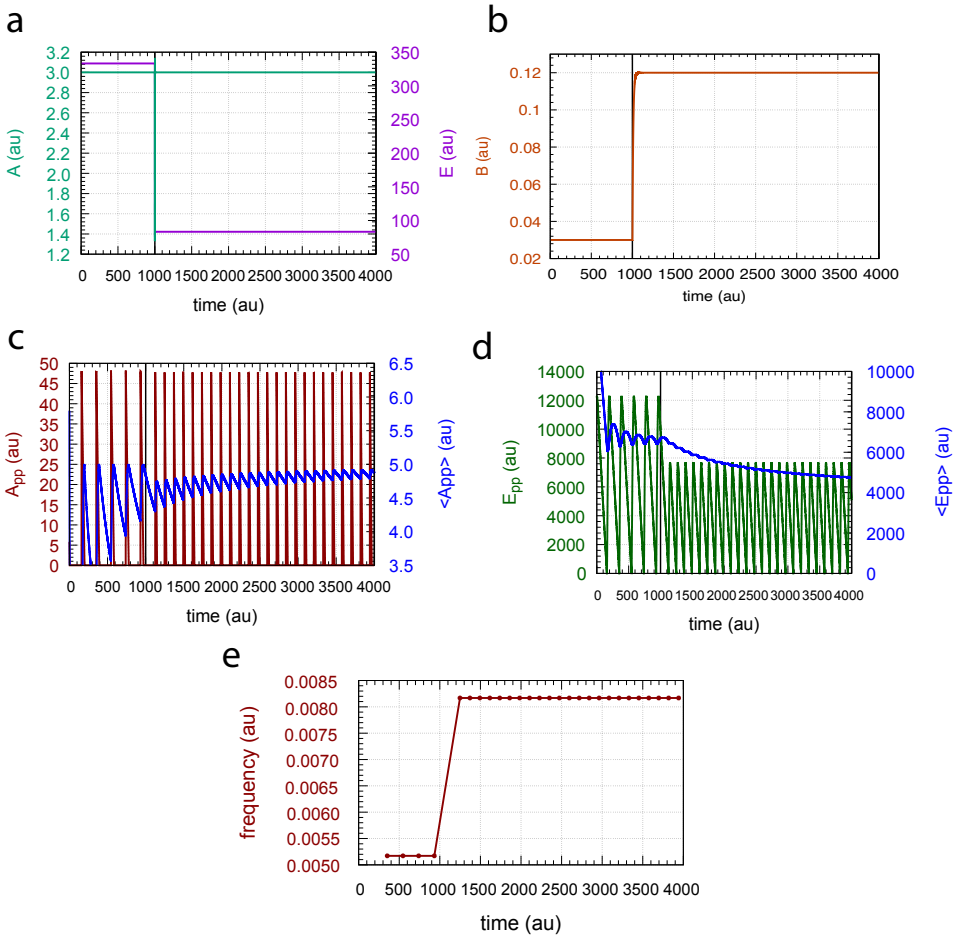

FIGURE 3.31: Response kinetics of the RLA controller from Fig. 3.30a with background k_4=0. The controller is tested at a step-perturbation k_2 from 1.0 (phase 1) to 4.0 (phase 2) at time t=1000. Panel a shows the resetting kinetics of A and E as a function of time. Panel b shows the increase in B over time. The resetting kinetics of A_{pp} is shown in panel c, along with its average concentration $<A_{pp}>$. Panel d shows the response kinetics of E_{pp} as a function of time together with its average concentration $<E_{pp}>$. In panel d the frequency, or inverse of the period length, is plotted as a function of time. Notice the controller's inability to produce frequency homeostais. Other rate constants (phases 1 and 2, in a.u.): k_3=1×10^4, k_5=k_{21}=1.0, k_6=3.0, k_8=k_9=k_{11}=k_{27}=0.1, k_{10}=10, k_{19}=8.0, k_{20}=100, k_{22}=k_{26}=1×10^{-3}, k_{23}=16.0, k_{24}=0.5, k_{25}=80.0. Initial concentrations of A, E, B, A_{pp}, e, and E_{pp} (in a.u.), respectively: 3.0000, 3.3323×10^2, 3.0000×10^{-2}, 5.8034, 2.6501×10^2, 1.2184×10^4.

Fig. 3.31 shows the controller's response to a step-wise perturbation k_2 from 1.0 (phase 1) to 4.0 (phase 2) at time t=1000, while having a constant background outflow k_4=0. Panel a shows the response of A and E over time. The outflow of A is quickly brought back to its set-point by the compensatory actions of E, which decreases from phase 1 to 2 due to the outflow perturbations. There is therefore more B in panel b to activate the removal of A_{pp} in panel c. However, the compensatory actions of E_{pp} brings A_{pp} back to its set-point. This RLA controller does not show E_{pp}- (panel d) or frequency-homeostasis (panel e) due to the lack of I_1 and I_2.

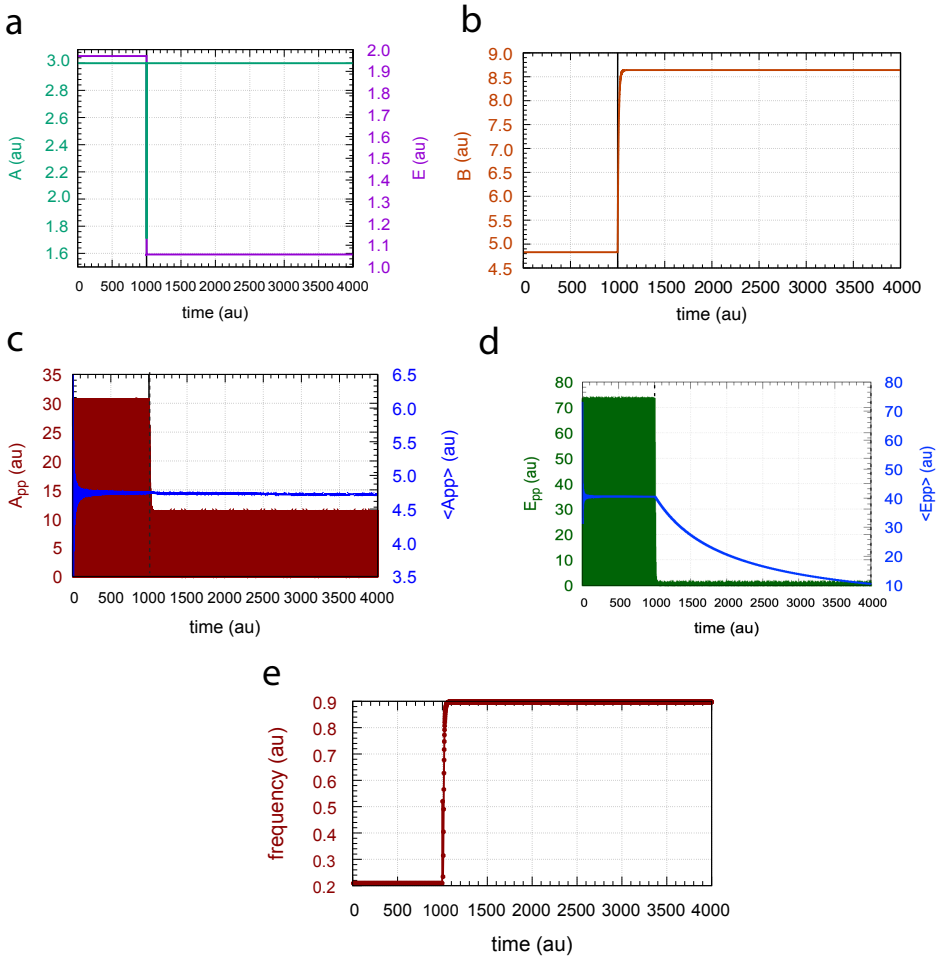

FIGURE 3.32: Response kinetics of the RLA controller from Fig. 3.30a with background k_4=160. The controller is tested at a step-perturbation k_2 from 1.0 (phase 1) to 128.0 (phase 2) at time t=1000. Panel a shows the resetting kinetics of A and E as a function of time. Panel b shows the increase in B over time. The resetting kinetics of A_{pp} is shown in panel c, along with its average concentration $<A_{pp}>$. Panel d shows the response kinetics of E_{pp} as a function of time together with its average concentration $<E_{pp}>$. In panel d the frequency, or inverse of the period length, is plotted as a function of time. Notice the controller's inability to produce frequency homeostais. Other rate constants (phases 1 and 2, in a.u.) as in Fig. 3.31. Initial concentrations of A, E, B, A_{pp}, e, and E_{pp} (in a.u.), respectively: 3.0000, 1.9704, 4.8300, 3.4535×10^{-6}, 1.4768×10^{2}, 7.3201×10^{1}.

Fig. 3.32 shows instead the results of a step-wise perturbation k_2 from 1.0 (phase 1) to 128 (phase 2) at time t=1000 at k_4=160. At this background the concentration of B (panel b) is much higher, which is due to outflow perturbations reducing the concentration of E (panel a). The controller is still able to keep $<A>$ (panel c) homeostatically regulated. However, due to the lack of I_1 and I_2 there is no regulation of $<E>$ (panel d) or the frequency (panel e).

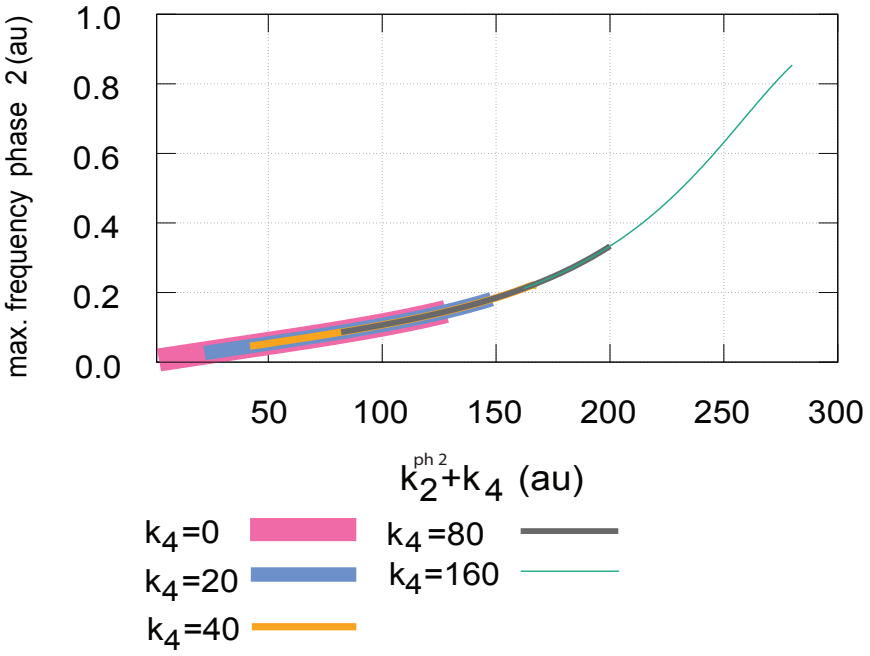

FIGURE 3.33: Frequency adaptation of the RLA controller from Fig. 3.30a. The figure shows the maxmimum frequency (in phase 2) as a function of $k_2^{ph2}+k_4$. The controller is applied a step-wise perturbation from k_2=1.0 (phase 1) to k_2=2→128 in phase 2 (with increments of one) with constant background perturbation k_4 from 0→160 (k_4 variable, phases 1 and 2). The controller does not show frequency nor background compensation. Other rate constants (phases 1 and 2, in a.u.) as in Fig. 3.31. Initial concentrations of A, E, B, A_{pp}, e, and E_{pp} (in a.u.), respectively: 3.0000, 3.3323×10^{2}, 3.0000×10^{-2}, 5.8034, 2.6501×10^{2}, 1.2184×10^{4} (k_4=0); 3.0000, 3.3323×10^{2}, 3.0000×10^{-2}, 5.8034, 2.6501×10^{2}, 1.2184×10^{4} (k_4=20); 3.0000, 3.3323×10^{2}, 3.0000×10^{-2}, 5.8034, 2.6501×10^{2}, 1.2184×10^{4} (k_4=40); 3.0000, 4.0152, 2.4300, 1.4076×10^{-6}, 3.5068×10^{2}, 3.4797×10^{2} (k_4=80); 3.0000, 1.9704, 4.8300, 1.9703×10^{3}, 3.4535×10^{-6}, 1.4768×10^{2}, 7.3201×10^{1} (k_4=160).

The maximum frequency of A_{pp} is plotted as a function of total outflow perturbations (k_2+k_4) in Fig. 3.33. The controller is subjected to a step-perturbation from k_2=1.0 (phase 1) to k_2=2→128 in phase 2 (with increments of one), along with a constant background reaction k_4 from 0→160. Although there is some type of relationship in terms of overlapping and continuous curves with increasing backgrounds, the controller does not possess the ability to neutralize backgrounds.

3.4.3 Background compensated RLA controller dominated by I_1

This section provides a second type of RLA controller (Fig. 3.34a) that can neutralize backgrounds (Fig. 3.37), which is also here caused by coherent feedback [5, 6] in the frequency compensated ganglion cell.

The RLA controller in Fig. 3.34a is structured into three negative feedback layers. Each layer corresponds to different retinal cells, in which their cellular interactions are illustrated in panel b. The first photoreceptor layer, with an on-center cone (colored blue), represents the derepression-based inflow controller m2 (Fig. 3.7). An outflow of A (caused by step-perturbation k_2 (colored red) and background k_4 (colored blue)) is opposed by E ($j_3 = k_3 \cdot k_8/(k_8+E)$). E then sends inhibitory information to B in the second layer, which represents an on-center bipolar cell (colored green). B further activates the inflow of A_{pp} in the on-center ganglion cell (colored purple) layer, which is represented by a frequency compensated oscillator (see Ch. 3.3). This third and final layer therefore includes the inflow controller I_1 and outflow controller I_2. I_1 and I_2 ensure E_{pp}- and frequency-homeostasis, and their coherent feedback [5, 6] leads to background compensation.

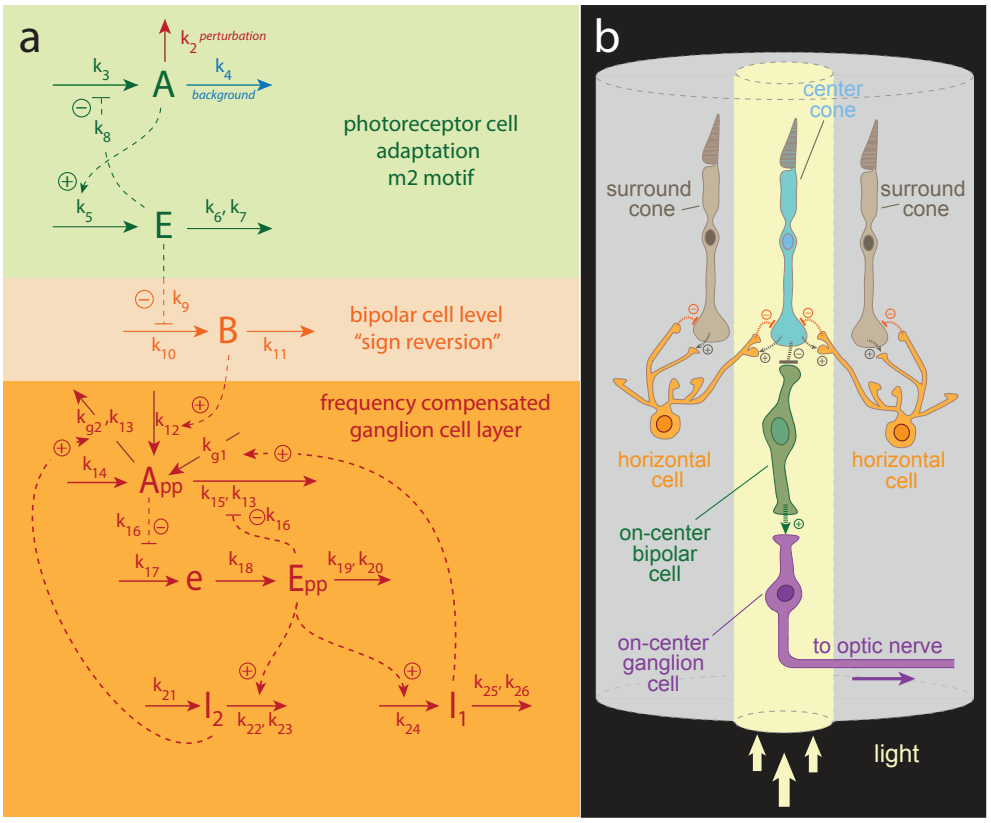

FIGURE 3.34: Retinal light adaptation (RLA) model with frequency control at the ganglion cell level. a) Simple RLA controller with three layers of negative feedback. The first negative feedback layer constitutes the m2 motif (Fig. 3.7), in which integral control is incoporated as a zero-order Michaelis-Menten (MM) type degredation of E. This allows for robust perfect adaptation of A. The controller is subjected to outflow perturbations k_2 and k_4. Inhbitory information from E is sent to the bipolar cell in the second layer, and B further activates the inflow of A_{pp} in the ganglion cell layer. A_{pp} is homeostatically controlled by E_{pp}. I_1 and I_2 ensure E_{pp}- and frequency-homeostasis of the oscillator. I_1 and I_2 feed coherently [5, 6] back to A_{pp}, which enable the controller to neutralize backgrounds. Solid arrows represent chemical reactions. Dashed lines indicate signaling events, where activation is represented by a plus sign and inhibition by a minus sign. b) Cellular interactions within the retinal layers. This figure is a simplified version of the retinal structure shown in (Fig. 3.2). Here, light (yellow arrows) travels through the center (and not the annulus) of the receptive field. This excites the on-center cone (colored blue) in the first feedbak layer, in which an inhibitory signal is received by the on-center bipolar cell (colored green) of the second layer. A subsequent on-center ganglion cell (colored purple) then receives a signal from the bipolar cell, before ganglion cell axons come together to form the optic nerve that enters the central nervous system. Horizontal cell interactions are also indicated in the figure. Figure was redrawn from Fig. 11.21, Ref. [3].

The rate equations of A and E in the photoreceptor cell are, respectively:

$$\dot{A} = \frac{k_3 \cdot k_8}{k_8 + E} - (k_2 + k_4) \cdot A \tag{3.80}$$

$$\dot{E} = k_5 \cdot A - \frac{k_6 \cdot E}{k_7 + E} \tag{3.81}$$

The rate equation of B in the bipolar cell layer is given by:

$$\dot{B} = \frac{k_{10} \cdot k_9}{k_9 + E} - k_{11} \cdot B \tag{3.82}$$

Rate equations of A_{pp}, e, E_{pp}, I_1, and I_2 in the ganglion cell layer are, respectively:

$$\dot{A_{pp}} = k_{14} + k_{g1} \cdot I_1 + k_{12} \cdot B - \left(\frac{k_{g2} \cdot A_{pp}}{k_{13} + A_{pp}} \right) \cdot I_2 - \left(\frac{k_{15} \cdot A_{pp}}{k_{13} + A_{pp}} \right) \cdot \left(\frac{k_{16}}{k_{16} + E_{pp}} \right) \tag{3.83}$$

$$\dot{e} = \frac{k_{17} \cdot k_{16}}{k_{16} + A_{pp}} \tag{3.84}$$

$$\dot{E_{pp}} = k_{18} \cdot e - \frac{k_{19} \cdot E_{pp}}{k_{20} + E_{pp}} \tag{3.85}$$

$$\dot{I}_1 = k_{24} \cdot E_{pp} - \frac{k_{25} \cdot I_1}{k_{26} + I_1} \tag{3.86}$$

$$\dot{I}_2 = k_{21} - \left(\frac{k_{22} \cdot I_2}{k_{23} + I_2} \right) \cdot E_{pp} \tag{3.87}$$

Assuming zero-order degredation of E and steady state (ss) gives A_{set} in the photoreceptor layer:

$$k_5 \cdot A_{ss} = k_6 \;\; \Rightarrow \;\; A_{ss} = A_{set} = \frac{k_6}{k_5} \tag{3.88}$$

The same assumptions are made with regards to $A_{pp,set}$ in the ganglion cell layer:

$$\frac{k_{17} \cdot k_{16}}{k_{16} \cdot <A_{pp,ss}>} = k_{19} = \; \Rightarrow \;\; <A_{pp,ss}> = A_{pp,set} = \left(\frac{k_{17}}{k_{19}} - 1 \right) \cdot k_{16} \tag{3.89}$$

The set-points for E_{pp} when affected by I_1 and I_2 are, respectively, given by:

$$k_{24}\cdot<E_{pp,ss}> = \underbrace{\left(\frac{I_{1,ss}}{k_{26}+I_{1,ss}}\right)}_{\approx 1\,(\text{zero}-\text{order})}\cdot k_{25} \quad \Rightarrow \quad <E_{pp,ss}> = E^{I_1}_{pp,set} = \frac{k_{25}}{k_{24}} \tag{3.90}$$

$$k_{21} = \underbrace{\left(\frac{I_{2,ss}}{k_{23}+I_{2,ss}}\right)}_{\approx 1\,(\text{zero}-\text{order})}\cdot k_{22}\cdot<E_{pp,ss}> \quad \Rightarrow \quad <E_{pp,ss}> = E^{I_2}_{pp,set} = \frac{k_{21}}{k_{22}} \tag{3.91}$$

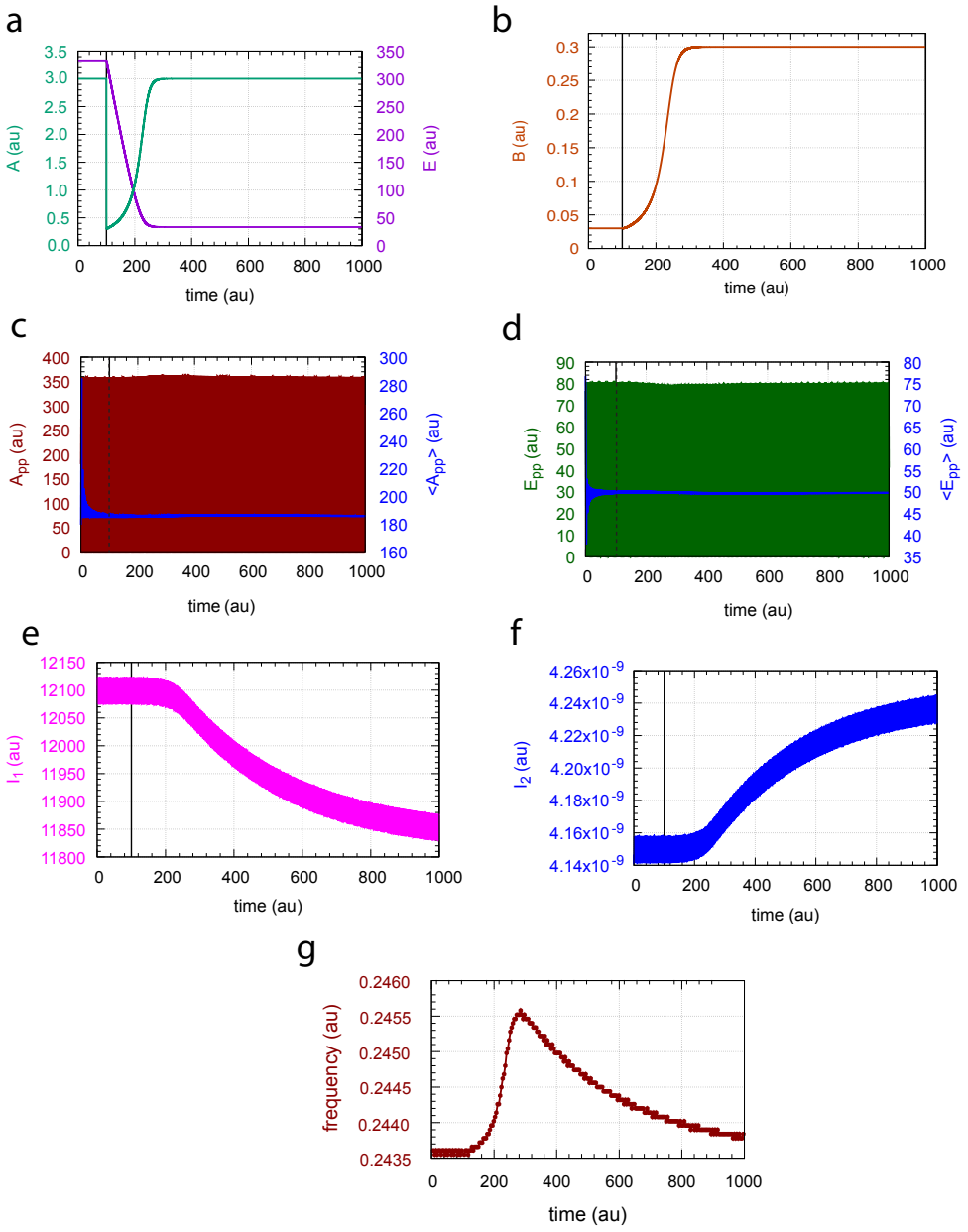

FIGURE 3.35: Response kinetics of the RLA controller from Fig. 3.34 with background k_4=0. The controller is tested at a step-perturbation k_2 from 1.0 (phase 1) to 10.0 (phase 2) at time t=100. Panel a shows the resetting kinetics of A and E as a function of time. Panel b shows the increase in B over time. The resetting kinetics of A_{pp} and E_{pp} are shown in panel c and d, respectively, along with their respective average concentrations $<A_{pp}>$ and $<E_{pp}>$. Panel e and f show the contributions of the controller species I_1 and I_2, respectively, over time. In panel g the frequency, or inverse of the period length, is plotted as a function of time. Notice the controller's frequency homeostasis. Other rate constants (phases 1 and 2, in a.u,): k_3=k_{15}=1×10^4, k_5=k_{18}=k_{22}=k_{24}=1.0, k_6=3.0, k_7=1×10^{-3}, k_8=k_9=k_{11}=k_{16}=0.1, k_{10}=k_{12}=10.0, k_{13}=k_{20}=k_{23}=k_{26}=1×10^{-6}, k_{14}=0.0, k_{17}=1×10^3, k_{19}=k_{21}=k_{25}=50, k_{g1}=k_{g2}=1×10^{-2}. Initial concentrations of A, E, B, A_{pp}, e, E_{pp}, I_1, and I_2 (in a.u.), respectively: 3.0000, 3.3323×10^2, 3.0000×10^{-2}, 1.7893×10^2, 3.3126×10^1, 7.6836×10^1, 1.2108×10^4, 4.1468×10^{-9}.

Fig. 3.35 shows the RLA controller's response to a step-wise perturbation k_2 from 1.0 (phase 1) to 10.0 (phase 2) at time t=100, while having a constant background outflow k_4=0. The outflow of A is compensated by E in panel a, where the variables are plotted as a function of time. The concentration B over time (panel b) increases from phase 1 to 2. B further activates the inflow of A_{pp} in panel c, in which its average concentration $<A_{pp}>$ is kept robustly at its set-point by an outflow of E_{pp} (panel d). $<E_{pp}>$ is instead homeostatically regulated by I_1 and I_2 in panels e and f, respectively. Finally, the ability of I_1 and I_2 in ensuring frequency homeostasis can be seen in panel f.

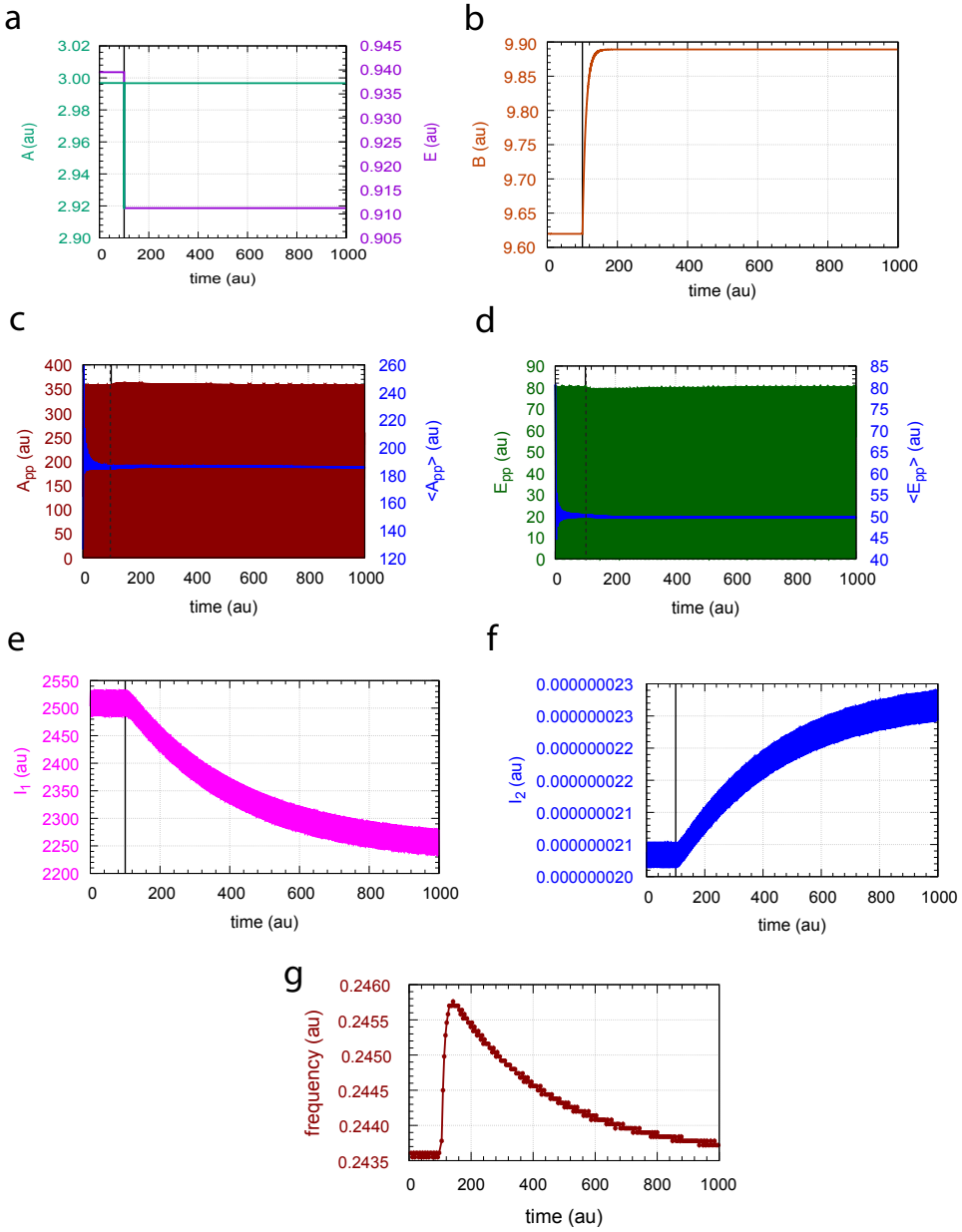

FIGURE 3.36: Response kinetics of the RLA controller from Fig. 3.34 with background k_4=320. The controller is tested at a step-perturbation k_2 from 1.0 (phase 1) to 10.0 (phase 2) at time t=100. Panel a shows the resetting kinetics of A and E as a function of time. Panel b shows the increase in B over time. The resetting kinetics of A_{pp} and E_{pp} are shown in panel c and d, respectively, along with their respective average concentrations $<A_{pp}>$ and $<E_{pp}>$. Panel e and f show the contributions of the controller species I_1 and I_2, respectively, over time. In panel g the frequency, or inverse of the period length, is plotted as a function of time. Notice the controller's frequency homeostasis. Other rate constants (phases 1 and 2, in au) as in Fig. 3.35. Initial concentrations of A, E, B, A_{pp}, e, E_{pp}, I_1, and I_2 (in au), respectively: 2.9968E, 9.3953×10^{-1}, 9.6198, 1.2536×10^{2}, 5.3802×10^{1}, 8.0468×10^{1}, 2.5032×10^{3}, 2.0381×10^{-8}.

Fig. 3.36 shows the results of the same k_2-step at k_4=320. At this higher k_4-value the resetting kinetics of A is much faster since there is less E to inhibit the synthesis of A. A higher concentration of B is observed in panel b. The controller still manages to maintain $<A_{pp}>$ (panel c) and $<E_{pp}>$ (panel d) under robust homeostatic control. This is due to the compensatory actions of I_1 and I_2 in panels e and f, respectively, where a particular large change is observed for the inflow controller I_1. Although panel g shows a different sensitivity to the maximum frequency, the frequency resets to its pre-perturbation level after some time.

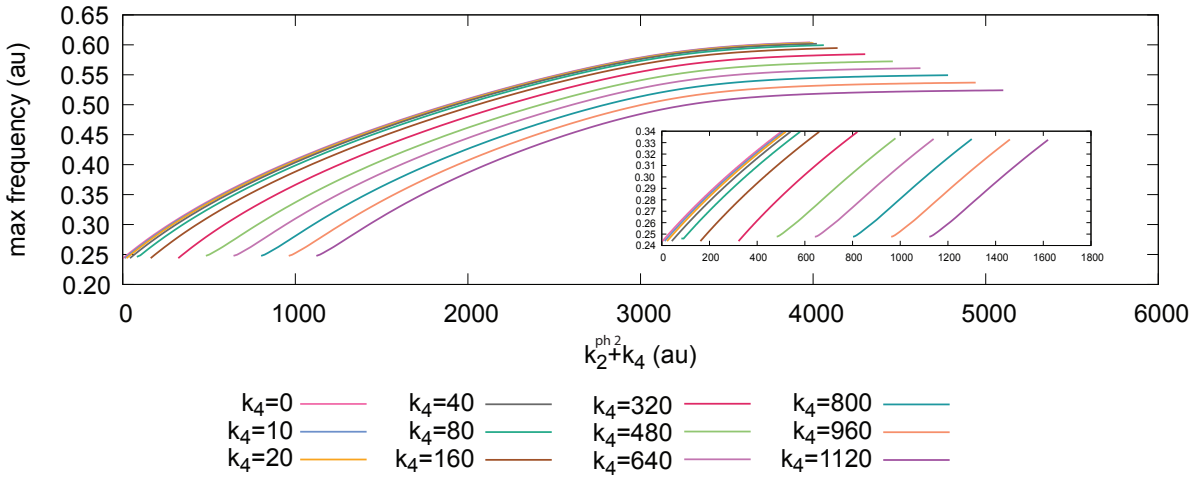

FIGURE 3.37: Frequency and background compensations of the RLA from Fig. 3.34. The figure shows the maximum frequency (in phase 2) as a function of $k_2^{ph2}+k_4$. The controller is tested at a step-perturbation from k_2=1.0 (phase 1) to k_2=2→100 in phase 2 (with increments of one) with constant backgrounds k_4 from 0→1120 (k_4 variable, phases 1 and 2). The oscillator shows parallell curves at different backgrounds. Notice, in the lower left corner, that the controller becomes oscillatory at higher backgrounds. Other rate constants (phases 1 and 2, in a.u.) as in Fig. 3.35. Initial concentrations of A, E, B, A_{pp}, e, E_{pp}, I_1, and I_2 (in a.u.), respectively: 3.0000, 3.3323×10^{2}, 3.0000×10^{-2}, 1.7893×10^{2}, 3.3126×10^{1}, 7.6836×10^{1}, 1.2108×10^{4}, 4.1468×10^{-9} (k_4=0); 2.9999, 3.0204×10^{1}, 3.2999×10^{-1}, 2.6012×10^{1}, 1.3489×10^{2}, 4.4650×10^{1}, 1.1775×10^{4}, 4.2642×10^{-9} (k_4=10); 2.9998, 1.5774×10^{1}, 6.2996×10^{-1}, 3.0816×10^{2}, 9.8665, 3.8609×10^{1}, 1.1520×10^{4}, 4.3592×10^{-9} (k_4=20); 2.9996, 8.0311, 1.2298, 1.0126×10^{2}, 6.6940×10^{1}, 7.8222×10^{1}, 1.0887×10^{4}, 4.6140×10^{-9} (k_4=40); 2.9993, 4.0163, 2.4294, 2.3534×10^{2}, 1.9783×10^{1}, 6.4162×10^{1}, 9.7192×10^{3}, 5.1710×10^{-9} (k_4=80); 2.9985, 1.9714, 4.8276, 2.2409×10^{2}, 2.1944×10^{1}, 6.7249×10^{1}, 7.3194×10^{3}, 6.8781×10^{-9} (k_4=160); 2.9968, 9.3953×10^{-1}, 9.6198, 1.2536×10^{2}, 5.3802×10^{1}, 8.0468×10^{1}, 2.5032×10^{3}, 2.0381×10^{-8} (k_4=320); 2.9950, 5.9417×10^{-1}, 1.4406×10^{1}, 2.3875×10^{2}, 1.9448×10^{1}, 6.3218×10^{1}, 9.2579×10^{1}, 2.2308×10^{3} (k_4=480); 2.9929, 4.2126×10^{-1}, 1.9184×10^{1}, 2.9206×10^{2}, 1.1643×10^{1}, 4.5278×10^{1}, 9.5719×10^{1}, 7.0601×10^{3} (k_4=640); 2.9906, 3.1746×10^{-1}, 2.3955×10^{1}, 3.2501×10^{2}, 8.3990, 3.1632×10^{1}, 9.1661×10^{1}, 1.1794×10^{4} (k_4=800); 2.9880, 2.4826×10^{-1}, 2.8714×10^{1}, 3.5602×10^{2}, 5.6819, 1.4126×10^{1}, 8.0765×10^{1}, 1.6554×10^{4} (k_4=960); 2.9850, 1.9885×10^{-1}, 3.3462×10^{1}, 3.3942×10^{-8}, 3.5223×10^{1}, 2.3835×10^{-6}, 6.4296×10^{1}, 2.1294×10^{4} (k_4=1120).

Fig. 3.37 shows the maximum frequency of A_{pp} over total outflow perturbations (k_2+k_4). A step-perturbation from k_2=1.0 (phase 1) to k_2=2→100 in phase 2 (with increments of one) is applied, along with a constant background reaction k_4 from 0→1120. This controller shows parallell curves with increasing backgrounds, indicating that the oscillator is background compensated. An interesting observation is that the controller becomes oscillatory at higher backgrounds starting from k_4=320. This is illustrated in the smaller figure in the lower right corner.

Chapter 4

Discussion

4.1 Derepression-based fluxes induce "photoreceptor" resetting kinetics

All one-layered (single-layered) controller motifs m1-m8 (Fig. 2.1) were subjected to a step-perturbation at constant but different backgrounds, in which their response amplitude decreased monotonically with increasing background. The homeostatic controllers divided (equally) into two classes based on whether the compensatory flux was based on activation or derepression.

Controllers with derepression-based compensatory fluxes showed a faster response time with increasing background. This type of response, i.e., decreased sensitivity but accelerated response kinetics, is analogous to the derepression kinetics seen in vertebrate photoreceptors (rods and cones) that respond to light [8, 42, 43]. This is illustrated by the voltage response of a Macaque monkey's rod cell in in Fig. 4.1, where the photoreceptor cell has been subjected to flashes of 10 ms at different but constant intensities of light. An increase in background gives also here a decreased sensitivity and shorter resetting time.

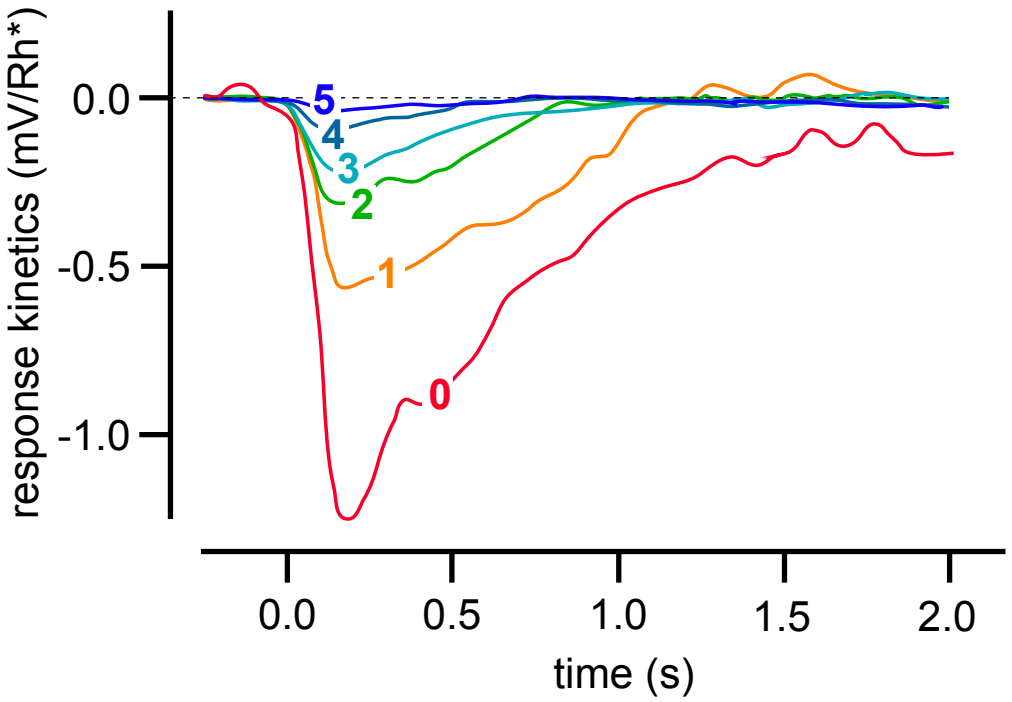

FIGURE 4.1: Photoadaptation of a Macaqaue monkey's rod cell. The rod cell was subjected to flashes of 10 ms at different but constant intensities of light. Notice the decreased sensitivity but accelerated response kinetics at increasing backgrounds. Background light intensities (in photons $\mu m^{-2}s^{-1}$): **0**, 0; **1**, 3.1; **2**, 12; **3**, 41; **4**, 84; **5**, 162. Figure was redrawn from Ref. [8], Fig. 22-19c.

The time for the activation-based controllers to reach steady state, however, increased with increasing backgrounds. A prolonged response time like this could possibly have a negative effect in physiological systems. For instanse, blood glucose is homeostatically regulated by two major feedbak loops involving insulin and glucagon. Insulin and glucagon are secreted from the pancreas when blood sugar levels are, respectively, high and low. Continuous high levels of blood sugar ("glucose overload") [47, 48] could possibly result in a slower resetting of the insulin-based feedback loop. Slower resetting times may be one of the causes for insulin resistanse and early diabetes. This topic would, of course, need further investigation.

4.2 Coherent feedback yields background compensated oscillators

In order for the oscillators to show **frequency compensation** there must be two layers of negative feedback, in which I_1 and I_2 keep $<E>$ homeostatically regulated. The controller species function as either inflow or outflow controllers. A change in the controlled variable A, however, is mainly compensated by the inflow controller. Thus, an outflow or inflow of A results in, respectively, a large increase or decrease in the inflow controller. Inflow controllers, on the other hand, show a much smaller change in response to background changes. It would therefore be interesting to test if the oscillators possess frequency homeostasis without the integral outflow controllers.

Frequency control in ganglion cells [39] are not, to the best of our knowledge, particularly discussed in the litterature. An interesting topic of study would therefore be whether ganglion cells possess this trait or not. One can also wonder if there are other retinal cells (i.e., amacrine cells) that induce this type of behaviour or if it arises by intracellular interactions within the ganglion cell. Based on results from the frequency compensated controllers the ganglion cell would need two additional controller species to obtain frequency homeostasis.

For the oscillators to also have **background compensation**, I_1 and I_2 must feed directly or coherently to the controlled variable A in the central layer. This type of feedback was termed coherent feedback in analogy to a similar concept used in quantum control theory and optics [5, 6]. To conclude, oscillators with coherent feedback shows automatic frequency control and maintain the response profile in a perturbation. The outer layer can also feed into the process that generates A by incoherent feedback. These oscillators still show frequency compensation but lose their ability to compensate for backgrounds. Loss of background compensation is also seen in the single negative feedback controllers. We are not aware of any biological examples where "robust background compensation" is seen. This ability to compensate backgrounds, however, could possibly be of interest in synthetic biology.

4.3 Retinal background compensation regulated at the ganglion cell level

The three-layered RLA controllers, representing the retina as a whole, consisted of a photoreceptor, bipolar, and ganglion cell. There needs to be a frequency compensated ganglion cell in order for the retinal controller to show frequency homeostasis. A change in the controlled variable A_{pp} in the ganglion cell layer is mainly regulated by the compensatory actions of the integral inflow controller. Thus, a bipolar cell that activates the outflow or inflow of A_{pp} causes, respectively, a large increase or decrease of the integral inflow controller. For the RLA controllers to also be background compensated the ganglion cell layer must incorporate coherent feedback, in which I_1 and I_2 feed directly or coherently back to the controlled variable A_{pp}. To conclude, it is the feedback organization in the ganglion cell that decides whether the frequency shows background compensation.

4.4 Are retinal cells capable of compensating backgrounds?

A hallmark in retinal light adaptation, according to Ref. [8], is that ganglion cells have some form of background compensating mechanisms. This statement was based on the response of a cat's ganglion cell (Fig. 4.2) towards a test spot of light in the receptive field center, while being under the influence of constant but different background luminances. This resulted in a sigmoidal curve, where the response profile remained stable at different intensities of light.

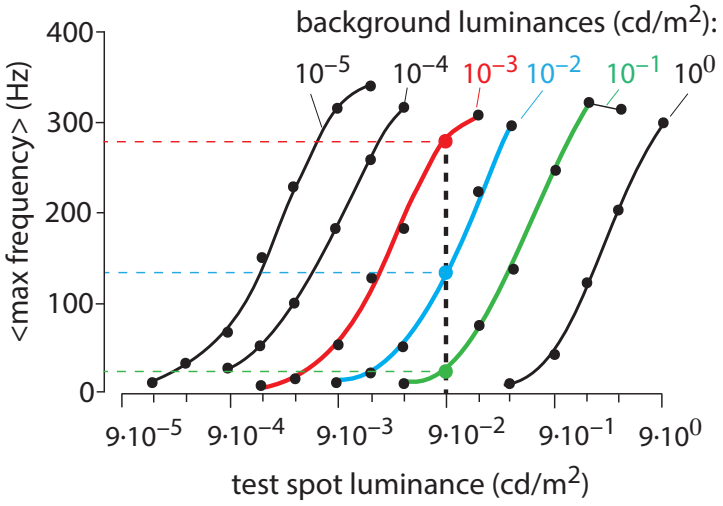

FIGURE 4.2: Light adaptation of a cat's on-center ganglion cell. Average maximum frequency (Hz) is plotted as a function of test spot luminance (cd/m^2) at background illuminations (from $9{\cdot}10^{-5}$ to $9{\cdot}10^{-0}$ cd/m^2). A vertical dashed line indicates a test spot luminance of $9{\cdot}10^{-2}$ cd/m^2. Notice how the mean maximum frequency decreases as the background illumination increases from the red ($9{\cdot}10^{-3}$ cd/m^2) towards the green curve ($9{\cdot}10^{-1}$ cd/m^2). Figure was redrawn from Ref. [8], Fig. 8.

We therefore became interested in understanding the underlying mechanisms of background compensation. "Background compensation" was defined by us as a negative feedback system that has a compensatory mechanism, in which the response to a perturbation remains unchanged with regards to different but constant background levels. This definition of background compensation, however, is not in agreement with the results of Fig. 4.2. For instance, for the red, blue and green curves, which represent three different backgrounds, the average maximum frequency (Hz) decreases with increasing background at a test spot luminance of $9{\cdot}10^{-2}$ cd/m^2 (indicated by a vertical dashed line). This type of adaptation can also be shown for the non-background compensated photoreceptor cell in Fig. 4.1.

In order to show this we need to use the Hill-type Michaelis-Menten equation:

$$V = \frac{V_{max} I^{\alpha}}{I^{\alpha}+\sigma^{\alpha}} \tag{4.1}$$

where V is the response amplitude of retinal cells, and I represents the light perturbation.

The cooperativity α is 1.0 and 0.7-0.8, respectively, for photoreceptor and ganglion cells. For bipolar and sustained ganglion cells α=1.2−1.4. The α-value of transient ganglion cells, however, is approximately 3.4 [8].

Since the photoreceptor is represented by α=1.0, the above equation becomes:

$$V = \frac{V_{max} I}{I+\sigma} \tag{4.2}$$

This equation describes the response amplitude V_1 of a single pigment system when there is a background I_0 and a perturbation I_1 [49]. However, as the cooperativity increases from α to α_1=$\alpha + I_0$ it is described in the following way:

At a constant background I_0 Eq 4.2 becomes:

$$V_0 = \frac{V_{max} I_0}{I_0+\sigma} \tag{4.3}$$

When a light perturbation I_1 is applied in addition to I_0 the total response amplitude yields:

$$V_1 + V_0 = \frac{V_{max}(I_0+I_1)}{I_0+I_1+\sigma} \tag{4.4}$$

Finally, by subtracting Eq 4.3 from Eq 4.4 the following expression is obtained for the reponse amplitude V_1:

$$\begin{aligned} V_1 &= V_{max}\left[\frac{(I_0+I_1)}{I_0+I_1+\sigma} - \frac{I_0}{I_0+\sigma}\right] = V_{max}\left[\frac{(I_0+I_1)\cdot(I_0+\sigma) - I_0\cdot(I_0+I_1+\sigma)}{(I_0+I_1+\sigma)\cdot(I_0+\sigma)}\right] \\ &= V_{max}\left[\frac{I_1\cdot\sigma}{(I_0+I_1+\sigma)\cdot(I_0+\sigma)}\right] = \frac{V_{max}\cdot\sigma}{I_0+\sigma}\left(\frac{I_1}{I_0+I_1+\sigma}\right) \\ &= V_{max,1}\left(\frac{I_1}{I_1+\sigma_1}\right) \end{aligned} \tag{4.5}$$

In Fig 4.3 Eq 4.2 has been plotted for six different values of α, which represent different backgrounds. V_{max} was, for the sake of simplicity, set to one. In panel a and d both

axes are, respectively, linear and logarithmic. Panel b has a logarithmic ordinate and linear abscissa wheras panel c has a logarithmic abscissa and linear ordinate.

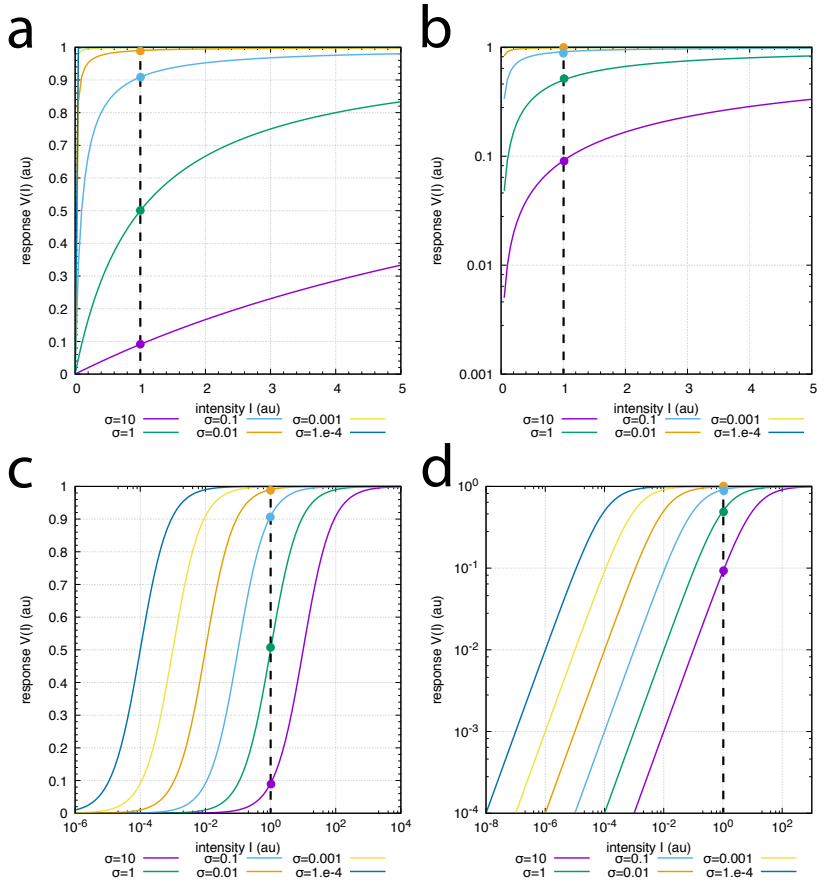

FIGURE 4.3: Photoreceptors' adaptation to light in terms of the Michaelis-Menten equation. Eq 4.2 has been plotted for six different values of α. V_{max}=1. The dashed vertical line shows how V decreases from the orange towards the purple curve as background illumination increases. In panel a and d both axes are, respectively, linear and logarithmic. Panel b has a logarithmic ordinate and linear abscissa wheras panel c has a logarithmic abscissa and linear ordinate.

The results of the photoreceptor in Fig 4.3c are similar to the response of the ganglion cell in Fig. 4.2. Although the photoreceptor cell lacks background compensation (Fig. 4.1), the parallel curve-shifts in panels c and d can be misleading in thinking that they do. As was the case for the ganglion cell (Fig. 4.2), the photoreceptor cell also shows a decrease in frequency when the background changes from the orange to the purple curve (indicated by a dashed vertical line). This could indicate that parallel curves (in log-plots) with decreasing frequencies are not sufficient to decide whether retinal cells possess background compensation mechanisms or not.

Kleinschmidt and Dowling [50] showed the light response of a gecko photoreceptor in a log-log plot. This also gave parallel lines independent of the applied background illumination. They concluded that the response profile's lateral shifts were due to adaptation

mechanisms in the photoreceptor.

To conclude, although background compensation mechanisms cannot be excluded, semi- or double-logarithmic plots with parallel lines are not sufficient in concluding with background compensation.

Appendix A

Python scripts

A.1 Python scripts for m1-m8 controllers

This section provides python scripts for each of the m1-m8 controllers' (Fig. 2.1) response kinetics. The m1 controller will be used as an example. The other python scripts are run in a similar way.

m1 controller

Two python scripts regarding the m1 controller, "m1.py" (Fig. A.1) and "plot_m1_A_merged.py" (Fig. A.2), must be inside the current working folder, as well as two additional folders called "A-data" and "plots". "m1.py" must be run before "plot_m1_A_merged.py".

"m1.py" containes the controller's information (rate constants, step-perturbations, initial concentrations, rate equations, etc.) in order to generate the response amplitude of A at different backgrounds k_4. An example of this script at k_4=64 is given in Fig. A.1. Running this script generates "k_4=64.txt" (inside "A-data") and "m1plot_k4=64.pdf" (inside "plots") containing the response amplitude. This script should also be run k_4=0, 1, 2, 4, 8, 16, 32, 64.

For instance, if we wanted to generate the response amplitude for k_4=0 the following changes must be made:

- Change the background k_4 (line 15) from 64 to 0.
- Change the initial concentrations of A and E at k_4=64 (line 29) to the ones for k_4=0 (Fig. 3.3b).
- Change "...k_4=64.txt" to "...k_4=0.txt" (line 43).
- Change "...m1plot_k4=64.pdf" to "...m1plot_k4=0" (line 53).

This will instead generate "k_4=0.txt" and "m1plot_k4=0.pdf", where the latter is shown in the upper right corner of Fig. A.1.

```
1  import numpy as np
2  import matplotlib.pyplot as plt
3  from scipy.integrate import odeint
4  import csv
5
6  p1k2 = 1 #k2 during phase 1
7  p2k2 = 5 #k2 during phase 2
8
9  ##################### defenition of model ################
10 def model(x,t, vark2):                                    #
11     #parameters:                                          #
12     k1 = 0                                               #
13     k2 = vark2 #perturbation                             #
14     k3 = 1                                               #
15     k4 = 64      #background, make changes               #
16     k5 = 3                                               #
17     k6 = 1                                               #
18     k7 = 10**-6                                          #
19                                                          #
20     A = x[0]                                             #
21     E = x[1]                                             #
22                                                          #
23     dAdt = k1 - ((k2+k4)*A) + (k3*E) #rate eq for A      #
24     dEdt = k5 -((k6*E)/(k7+E))*A     #rate eq for E      #
25                                                          #
26     return [dAdt, dEdt]                                  #
27 ############################################################
28
29 x0 = [3.0,195.0] # initial concentrations (A0, E0)
30 t1=np.linspace(0,10,1000)    #phase 1 time array
31 t2=np.linspace(10,100,9000) #phase 2 time array
32 t = np.concatenate((t1,t2)) #total time array, phase 1 + phase 2
33
34 #solve model for phases 1 and 2
35 y = odeint(model, x0, t1, args=(p1k2,)) #solve for phase 1
36 x1 = y[-1]     #get last element of array y
37 print (y[-1])  #print last element of array y
38 y = np.concatenate((y, odeint(model, x1, t2, args=(p2k2,)))) #solve for phase 2, and concatenat with pahse
39
40 A = y[:,0] # A-array
41 E = y[:,1] # E-array
42
43 with open("./A-data/k4=64.txt", 'w', newline='') as file: #creates 'k4=x.txt' file, insert k4 value
44     writer = csv.writer(file)
45     writer.writerows([A]) #write A-data as a comma-separated-values (csv) file
46
47 plt.plot(t,A,label = 'A')
48 plt.xlabel("time (au)")
49 plt.ylabel("A (au)")
50 plt.grid()
51 plt.xlim(0.0,100)
52 plt.ylim(0.5,3.5)
53 plt.savefig("plots/m1plot_k4=64.pdf") #make changes wrt k4 in file name
54 plt.show()
```

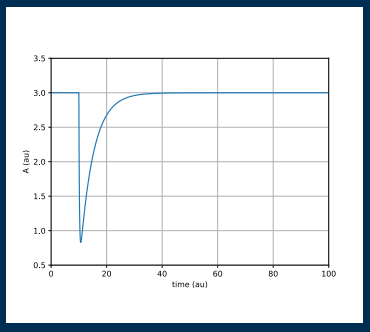

FIGURE A.1: Python script for generating m1's response amplitude of A at background k_4=64. Making some changes (see above) gives the response amplitude for k_4=0 (see upper right corner). Run this script at k_4=0, 1, 2, 4, 8, 16, 32, 64. Insert the corresponding initial concentrations of A and E from Fig. 3.3b.

Finally, the response amplitudes for different k_4-values can be merged together by running "plot_m1_A_merged.py" (Fig. A.2). This creates "A_plots_merged.pdf" (inside "plots"), and shows the resetting kinetics of m1 from Fig. 3.3b. This can be seen in the upper right corner of Fig. A.2.

```python
import matplotlib.pyplot as plt
import numpy as np

y1= np.loadtxt('./A-data/k4=0.txt', delimiter=',', unpack=True)
y2= np.loadtxt('./A-data/k4=1.txt', delimiter=',', unpack=True)
y3= np.loadtxt('./A-data/k4=2.txt', delimiter=',', unpack=True)
y4= np.loadtxt('./A-data/k4=4.txt', delimiter=',', unpack=True)
y5= np.loadtxt('./A-data/k4=8.txt', delimiter=',', unpack=True)
y6= np.loadtxt('./A-data/k4=16.txt', delimiter=',', unpack=True)
y7= np.loadtxt('./A-data/k4=32.txt', delimiter=',', unpack=True)
y8= np.loadtxt('./A-data/k4=64.txt', delimiter=',', unpack=True)

t1=np.linspace(0,10,1000)    #phase 1 time array
t2=np.linspace(10,100,9000) #phase 2 time array
t = np.concatenate((t1,t2)) #total time array, phase 1 + phase 2

# plt.plot(t,y1,t,y2,t,y3,t,y4,t,y5,t,y6,t,y7,t,y8)
plt.plot(t,y1,label="$k_4$=0")
plt.plot(t,y2,label="$k_4$=1")
plt.plot(t,y3,label="$k_4$=2")
plt.plot(t,y4,label="$k_4$=4")
plt.plot(t,y5,label="$k_4$=8")
plt.plot(t,y6,label="$k_4$=16")
plt.plot(t,y7,label="$k_4$=32")
plt.plot(t,y8,label="$k_4$=64")
plt.grid()
plt.legend(loc='lower right')
plt.title('merged A-profiles, $k_2$=1--->5 & $k_4$=0,1,2,4,..64')
plt.xlabel('time (au)')
plt.ylabel('A (au)')
plt.xlim(0.0,100)
plt.ylim(0.5,3.5)
plt.savefig("./plots/A_plots_merged.pdf")
plt.show()
```

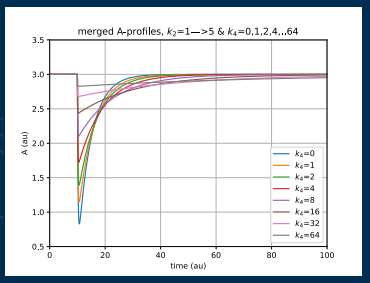

FIGURE A.2: Python script for generating m1's resetting kinetics (see upper right corner) from Fig. 3.3b. Run this script after producing the response amplitudes for k_4=0, 1, 2, 4, 8, 16, 32, 64 (Fig. A.1)

.

m2 controller

```python
import numpy as np
import matplotlib.pyplot as plt
from scipy.integrate import odeint
import csv

p1k2 = 1 #k2 during phase 1
p2k2 = 5 #k2 during phase 2

#################### defenition of model ################
def model(x,t, vark2):                                  #
    #parameters:                                        #
    k1 = 0                                              #
    k2 = vark2 #perturbation                            #
    k3 = 1                                              #
    k4 = 64     #background, make changes               #
    k5 = 3                                              #
    k6 = 1                                              #
    k7 = 10**-6                                         #
                                                        #
    A = x[0]                                            #
    E = x[1]                                            #
                                                        #
    dAdt = k1 - ((k2+k4)*A) + (k3*E) #rate eq for A     #
    dEdt = k5 -((k6*E)/(k7+E))*A     #rate eq for E     #
                                                        #
    return [dAdt, dEdt]                                 #
#########################################################

x0 = [3.0,195.0] # initial concentrations (A0, E0)
t1=np.linspace(0,10,1000)   #phase 1 time array
t2=np.linspace(10,100,9000) #phase 2 time array
t = np.concatenate((t1,t2)) #total time array, phase 1 + phase 2

#solve model for phases 1 and 2
y = odeint(model, x0, t1, args=(p1k2,)) #solve for phase 1
x1 = y[-1]      #get last element of array y
print (y[-1])  #print last element of array y
y = np.concatenate((y, odeint(model, x1, t2, args=(p2k2,)))) #solve for phase 2, and concatenat with pahse

A = y[:,0] # A-array
E = y[:,1] # E-array

with open("./A-data/k4=64.txt", 'w', newline='') as file: #creates 'k4=x.txt' file, insert k4 value
    writer = csv.writer(file)
    writer.writerows([A]) #write A-data as a comma-separated-values (csv) file

plt.plot(t,A,label = 'A')
plt.xlabel("time (au)")
plt.ylabel("A (au)")
plt.grid()
plt.xlim(0.0,100)
plt.ylim(0.5,3.5)
plt.savefig("plots/m1plot_k4=64.pdf") #make changes wrt k4 in file name
plt.show()
```

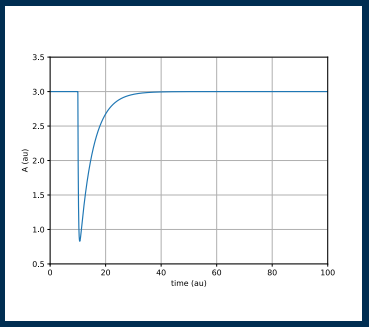

FIGURE A.3: Python script for generating m2's response amplitude of A at background k_4=64. Making some changes (see above) gives the response amplitude for k_4=2 (see upper right corner). Run this script at k_4=0, 1, 2, 4, 8, 16, 32, 64. Insert the corresponding initial concentrations of A and E from Fig. 3.7b.

```python
import matplotlib.pyplot as plt
import numpy as np

y1= np.loadtxt('./A-data/k4=0.txt', delimiter=',', unpack=True)
y2= np.loadtxt('./A-data/k4=1.txt', delimiter=',', unpack=True)
y3= np.loadtxt('./A-data/k4=2.txt', delimiter=',', unpack=True)
y4= np.loadtxt('./A-data/k4=4.txt', delimiter=',', unpack=True)
y5= np.loadtxt('./A-data/k4=8.txt', delimiter=',', unpack=True)
y6= np.loadtxt('./A-data/k4=16.txt', delimiter=',', unpack=True)
y7= np.loadtxt('./A-data/k4=32.txt', delimiter=',', unpack=True)
y8= np.loadtxt('./A-data/k4=64.txt', delimiter=',', unpack=True)

t1=np.linspace(0,10,1000)   #phase 1 time array
t2=np.linspace(10,100,9000) #phase 2 time array
t = np.concatenate((t1,t2)) #total time array, phase 1 + phase 2

# plt.plot(t,y1,t,y2,t,y3,t,y4,t,y5,t,y6,t,y7,t,y8)
plt.plot(t,y1,label="$k_4$=0")
plt.plot(t,y2,label="$k_4$=1")
plt.plot(t,y3,label="$k_4$=2")
plt.plot(t,y4,label="$k_4$=4")
plt.plot(t,y5,label="$k_4$=8")
plt.plot(t,y6,label="$k_4$=16")
plt.plot(t,y7,label="$k_4$=32")
plt.plot(t,y8,label="$k_4$=64")
plt.grid()
plt.legend(loc='lower right')
plt.title('merged A-profiles, $k_2$=1--->5 & $k_4$=0,1,2,4,..64')
plt.xlabel('time (au)')
plt.ylabel('A (au)')
plt.xlim(0.0,100)
plt.ylim(0.5,3.5)
plt.savefig("./plots/A_plots_merged.pdf")
plt.show()
```

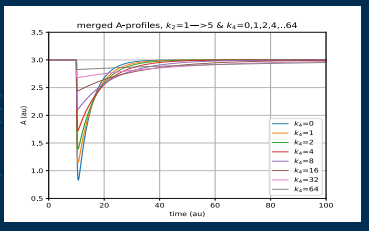

FIGURE A.4: Python script for generating m2's resetting kinetics (see upper right corner) from Fig. 3.7b. Run this script after having producing the response ampltidues for k_4=0, 1, 2, 4, 8, 16, 32, 64 (Fig. A.3)

autocatalytic m2 controller

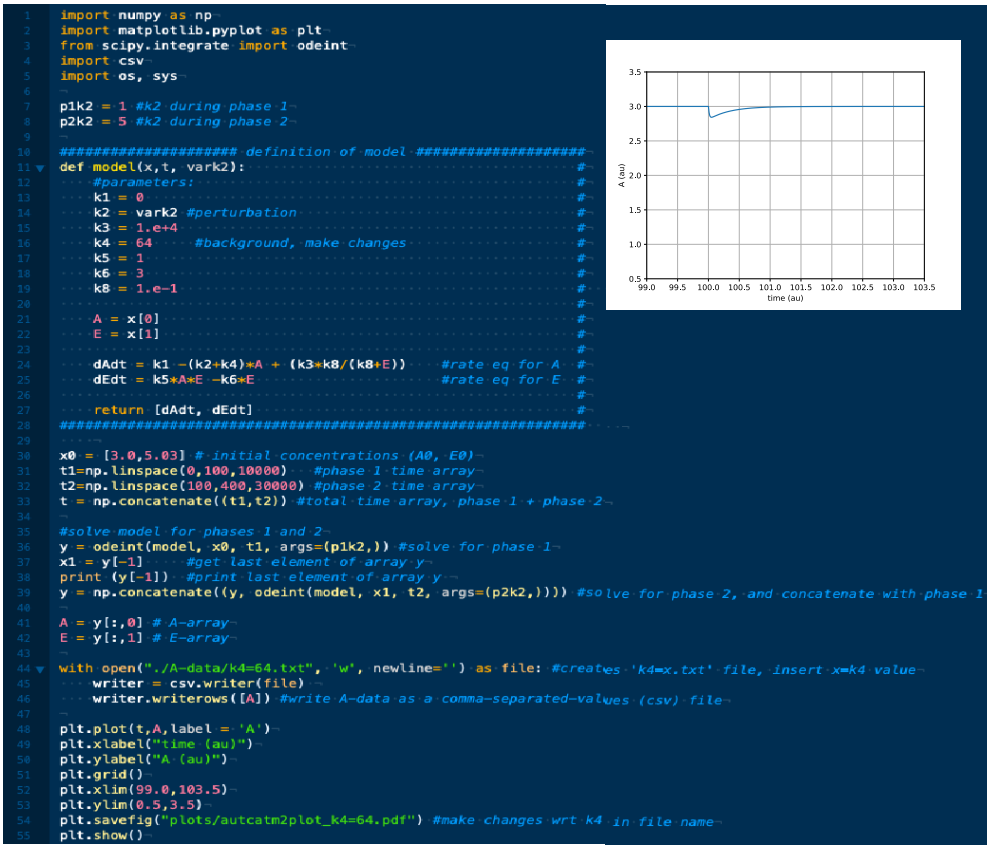

```
import numpy as np
import matplotlib.pyplot as plt
from scipy.integrate import odeint
import csv
import os, sys

p1k2 = 1 #k2 during phase 1
p2k2 = 5 #k2 during phase 2

#################### definition of model ####################
def model(x,t, vark2):                                      #
    #parameters:                                            #
    k1 = 0                                                  #
    k2 = vark2 #perturbation                                #
    k3 = 1.e+4                                              #
    k4 = 64      #background, make changes                  #
    k5 = 1                                                  #
    k6 = 3                                                  #
    k8 = 1.e-1                                              #
                                                            #
    A = x[0]                                                #
    E = x[1]                                                #
                                                            #
    dAdt = k1 -(k2+k4)*A + (k3*k8/(k8+E))     #rate eq for A #
    dEdt = k5*A*E -k6*E                       #rate eq for E #
                                                            #
    return [dAdt, dEdt]                                     #
############################################################

x0 = [3.0,5.03] # initial concentrations (A0, E0)
t1=np.linspace(0,100,10000)    #phase 1 time array
t2=np.linspace(100,400,30000) #phase 2 time array
t = np.concatenate((t1,t2)) #total time array, phase 1 + phase 2

#solve model for phases 1 and 2
y = odeint(model, x0, t1, args=(p1k2,)) #solve for phase 1
x1 = y[-1]     #get last element of array y
print (y[-1])  #print last element of array y
y = np.concatenate((y, odeint(model, x1, t2, args=(p2k2,)))) #solve for phase 2, and concatenate with phase 1

A = y[:,0] # A-array
E = y[:,1] # E-array

with open("./A-data/k4=64.txt", 'w', newline='') as file: #creates 'k4=x.txt' file, insert x=k4 value
    writer = csv.writer(file)
    writer.writerows([A]) #write A-data as a comma-separated-values (csv) file

plt.plot(t,A,label = 'A')
plt.xlabel("time (au)")
plt.ylabel("A (au)")
plt.grid()
plt.xlim(99.0,103.5)
plt.ylim(0.5,3.5)
plt.savefig("plots/autcatm2plot_k4=64.pdf") #make changes wrt k4 in file name
plt.show()
```

FIGURE A.5: Python script for generating autocatalytic m2's response amplitude of A at background k_4=64 (see upper right corner). By making some changes (see above), run this script at k_4=0, 1, 2, 4, 8, 16, 32, 64. Insert the corresponding initial concentrations of A and E from Fig. 3.8b.

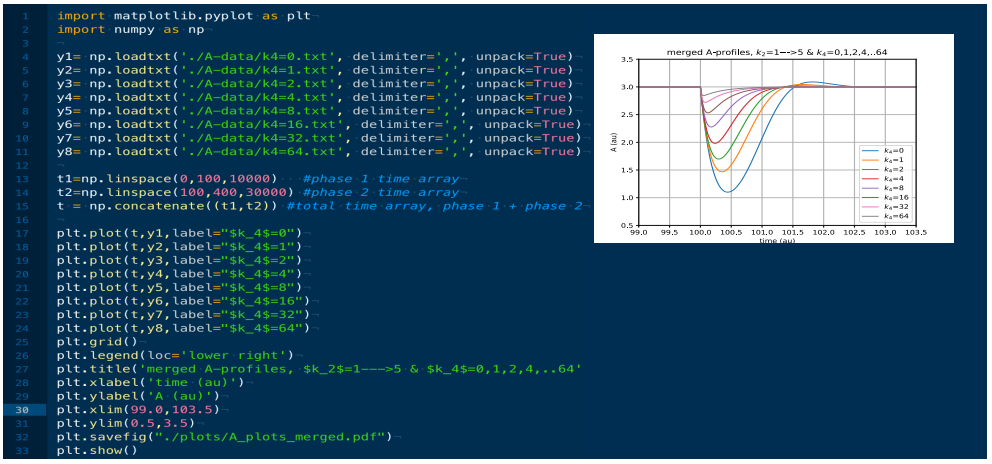

```
import matplotlib.pyplot as plt
import numpy as np

y1= np.loadtxt('./A-data/k4=0.txt', delimiter=',', unpack=True)
y2= np.loadtxt('./A-data/k4=1.txt', delimiter=',', unpack=True)
y3= np.loadtxt('./A-data/k4=2.txt', delimiter=',', unpack=True)
y4= np.loadtxt('./A-data/k4=4.txt', delimiter=',', unpack=True)
y5= np.loadtxt('./A-data/k4=8.txt', delimiter=',', unpack=True)
y6= np.loadtxt('./A-data/k4=16.txt', delimiter=',', unpack=True)
y7= np.loadtxt('./A-data/k4=32.txt', delimiter=',', unpack=True)
y8= np.loadtxt('./A-data/k4=64.txt', delimiter=',', unpack=True)

t1=np.linspace(0,100,10000)    #phase 1 time array
t2=np.linspace(100,400,30000) #phase 2 time array
t = np.concatenate((t1,t2)) #total time array, phase 1 + phase 2

plt.plot(t,y1,label="$k_4$=0")
plt.plot(t,y2,label="$k_4$=1")
plt.plot(t,y3,label="$k_4$=2")
plt.plot(t,y4,label="$k_4$=4")
plt.plot(t,y5,label="$k_4$=8")
plt.plot(t,y6,label="$k_4$=16")
plt.plot(t,y7,label="$k_4$=32")
plt.plot(t,y8,label="$k_4$=64")
plt.grid()
plt.legend(loc='lower right')
plt.title('merged A-profiles, $k_2$=1--->5 & $k_4$=0,1,2,4,..64'
plt.xlabel('time (au)')
plt.ylabel('A (au)')
plt.xlim(99.0,103.5)
plt.ylim(0.5,3.5)
plt.savefig("./plots/A_plots_merged.pdf")
plt.show()
```

FIGURE A.6: Python script for generating autocatalytic m2's resetting kinetics (see upper right corner) from Fig. 3.8b. Run this script after producing the response amplitudes for k_4=0, 1, 2, 4, 8, 16, 32, 64 (Fig. A.5)

m3 controller

```python
import numpy as np
import matplotlib.pyplot as plt
from scipy.integrate import odeint
import csv

p1k2 = 1 #k2 during phase 1
p2k2 = 5 #k2 during phase 2

#################### defenition of model ##################
def model(x,t, vark2):                                    #
    #parameters:                                          #
    k1 = 0                                                #
    k2 = vark2 #perturbation                              #
    k3 = 1                                                #
    k4 = 64     #background, make changes                 #
    k5 = 31                                               #
    k6 = 1                                                #
    k7 = 1.e-6                                            #
    k8 = 0.1                                              #
    A = x[0]                                              #
    E = x[1]                                              #
                                                          #
    dAdt = k1 - ((k2+k4)*A) + (k3*E)      #rate eq for A  #
    dEdt = k5*k8/(k8+A) -((k6*E)/(k7+E))  #rate eq for E  #
                                                          #
    return [dAdt, dEdt]                                   #
###########################################################

x0 = [3.0,195.0] # initial concentrations (A0, E0)
t1=np.linspace(0,50,1000)    #phase 1 time array
t2=np.linspace(50,300,9000) #phase 2 time array
t = np.concatenate((t1,t2)) #total time array, phase 1 + phase 2

#solve model for phases 1 and 2
y = odeint(model, x0, t1, args=(p1k2,)) #solve for phase 1
x1 = y[-1]      #get last element of array y
print (y[-1])   #print last element of array y
y = np.concatenate((y, odeint(model, x1, t2, args=(p2k2,)))) #solve for phase 2, and concatenate with phase 1

A = y[:,0] # A-array
E = y[:,1] # E-array

with open("./A-data/k4=64.txt", 'w', newline='') as file: #creates 'k4=x.txt' file, insert k4 value
    writer = csv.writer(file)
    writer.writerows([A]) #write A-data as a comma-separated-values (csv) file

plt.plot(t,A,label = 'A')
plt.xlabel("time (au)")
plt.ylabel("A (au)")
plt.grid()
plt.xlim(0.0,300)
plt.ylim(0.5,3.5)
plt.savefig("plots/m3plot_k4=64.pdf") #make changes wrt k4 in file name
plt.show()
```

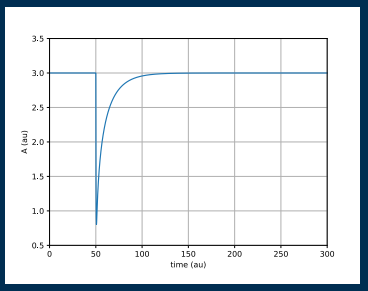

FIGURE A.7: Python script for generating m3's response amplitude of A at background k_4=64. Making some changes (see above) gives the response amplitude for k_4=0 (see upper right corner). Run this script at k_4=0, 1, 2, 4, 8, 16, 32, 64. Insert the corresponding initial concentrations of A and E from Fig. 3.4b.

```python
import matplotlib.pyplot as plt
import numpy as np

y1= np.loadtxt('./A-data/k4=0.txt', delimiter=',', unpack=True)
y2= np.loadtxt('./A-data/k4=1.txt', delimiter=',', unpack=True)
y3= np.loadtxt('./A-data/k4=2.txt', delimiter=',', unpack=True)
y4= np.loadtxt('./A-data/k4=4.txt', delimiter=',', unpack=True)
y5= np.loadtxt('./A-data/k4=8.txt', delimiter=',', unpack=True)
y6= np.loadtxt('./A-data/k4=16.txt', delimiter=',', unpack=True)
y7= np.loadtxt('./A-data/k4=32.txt', delimiter=',', unpack=True)
y8= np.loadtxt('./A-data/k4=64.txt', delimiter=',', unpack=True)

t1=np.linspace(0,50,1000)    #phase 1 time array
t2=np.linspace(50,300,9000) #phase 2 time array
t = np.concatenate((t1,t2)) #total time array, phase 1 + phase 2

# plt.plot(t,y1,t,y2,t,y3,t,y4,t,y5,t,y6,t,y7,t,y8)
plt.plot(t,y1,label="$k_4$=0")
plt.plot(t,y2,label="$k_4$=1")
plt.plot(t,y3,label="$k_4$=2")
plt.plot(t,y4,label="$k_4$=4")
plt.plot(t,y5,label="$k_4$=8")
plt.plot(t,y6,label="$k_4$=16")
plt.plot(t,y7,label="$k_4$=32")
plt.plot(t,y8,label="$k_4$=64")

plt.grid()
plt.legend(loc='lower right')
plt.title('merged A-profiles, $k_2$=1--->5 & $k_4$=0,1,2,4,..64')
plt.xlabel('time (au)')
plt.ylabel('A (au)')
plt.xlim(0.0,300)
plt.ylim(0.5,3.5)
plt.savefig("./plots/A_plots_merged.pdf")
plt.show()
```

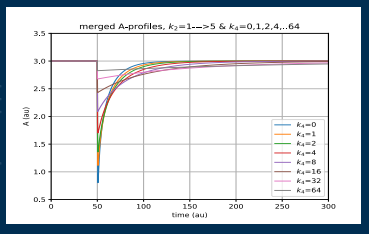

FIGURE A.8: Python script for generating m3's resetting kinetics (see upper right corner) from Fig. 3.4b. Run this script after producing the response amplitudes for k_4=0, 1, 2, 4, 8, 16, 32, 64 (Fig. A.7)

m4 controller

```python
import numpy as np
import matplotlib.pyplot as plt
from scipy.integrate import odeint
import csv
import os, sys

p1k2 = 1 #k2 during phase 1
p2k2 = 5 #k2 during phase 2

#################### definition of model ##################
def model(x,t, vark2):                                    #
    #parameters:                                          #
    k1 = 0                                                #
    k2 = vark2 #perturbation                              #
    k3 = 1.e+4                                            #
    k4 = 64      #background, make changes                #
    k5 = 1                                                #
    k6 = 31                                               #
    k7 = 1.e-6                                            #
    k8 = 0.1                                              #
    k9 = 0.1                                              #
                                                          #
    A = x[0]                                              #
    E = x[1]                                              #
                                                          #
    dAdt = k1 -(k2+k4)*A + (k3*k8/(k8+E))     #rate eq for A  #
    dEdt = k5 -((k6*E)/(k7+E))*(k9/(k9+A))    #rate eq for E  #
                                                          #
    return [dAdt, dEdt]                                   #
###########################################################

x0 = [3.0,5.03] # initial concentrations (A0, E0)
t1=np.linspace(0,50,10000)   #phase 1 time array
t2=np.linspace(50,600,50000) #phase 2 time array
t = np.concatenate((t1,t2)) #total time array, phase 1 + phase 2

#solve model for phases 1 and 2
y = odeint(model, x0, t1, args=(p1k2,)) #solve for phase 1
x1 = y[-1]      #get last element of array y
print (y[-1])   #print last element of array y
y = np.concatenate((y, odeint(model, x1, t2, args=(p2k2,)))) #solve for phase 2
                                                             #and concatenate with phase 1

A = y[:,0] # A-array
E = y[:,1] # E-array

with open("./A-data/k4=64.txt", 'w', newline='') as file: #creates 'k4=x.txt' file
                                                          #insert x=k4 value
    writer = csv.writer(file)
    writer.writerows([A]) #write A-data as a comma-separated-values (csv) file

plt.plot(t,A,label = 'A')
plt.xlabel("time (au)")
plt.ylabel("A (au)")
plt.grid()
plt.xlim(0.0,600)
plt.ylim(0.5,3.5)
plt.savefig("plots/m4plot_k4=64.pdf") #make changes wrt k4 in file name
plt.show()
```

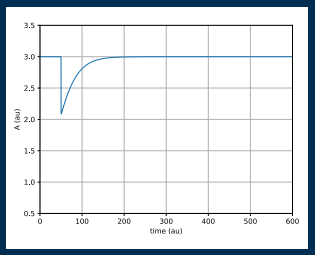

FIGURE A.9: Python script for generating m4's response amplitude of A at background k_4=64. Making some changes (see above) gives the response amplitude for k_4=8 (see upper right corner). Run this script at k_4=0, 1, 2, 4, 8, 16, 32, 64. Insert the corresponding initial concentrations of A and E from Fig. 3.9b.

```python
import matplotlib.pyplot as plt
import numpy as np

y1= np.loadtxt('./A-data/k4=0.txt', delimiter=',', unpack=True)
y2= np.loadtxt('./A-data/k4=1.txt', delimiter=',', unpack=True)
y3= np.loadtxt('./A-data/k4=2.txt', delimiter=',', unpack=True)
y4= np.loadtxt('./A-data/k4=4.txt', delimiter=',', unpack=True)
y5= np.loadtxt('./A-data/k4=8.txt', delimiter=',', unpack=True)
y6= np.loadtxt('./A-data/k4=16.txt', delimiter=',', unpack=True)
y7= np.loadtxt('./A-data/k4=32.txt', delimiter=',', unpack=True)
y8= np.loadtxt('./A-data/k4=64.txt', delimiter=',', unpack=True)

t1=np.linspace(0,50,10000)   #phase 1 time array
t2=np.linspace(50,600,50000) #phase 2 time array
t = np.concatenate((t1,t2)) #total time array, phase 1 + phase 2

plt.plot(t,y1,label="$k_4$=0")
plt.plot(t,y2,label="$k_4$=1")
plt.plot(t,y3,label="$k_4$=2")
plt.plot(t,y4,label="$k_4$=4")
plt.plot(t,y5,label="$k_4$=8")
plt.plot(t,y6,label="$k_4$=16")
plt.plot(t,y7,label="$k_4$=32")
plt.plot(t,y8,label="$k_4$=64")
plt.grid()
plt.legend(loc='lower right')
plt.title('merged A-profiles, $k_2$=1--->5 & $k_4$=0,1,2,4,..64')
plt.xlabel('time (au)')
plt.ylabel('A (au)')
plt.xlim(0.0,600)
plt.ylim(0.5,3.5)
plt.savefig("./plots/A_plots_merged.pdf")
plt.show()
```

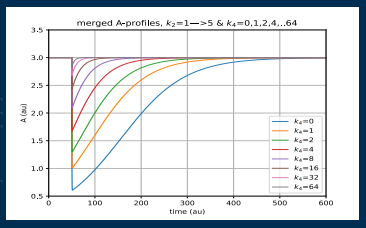

FIGURE A.10: Python script for generating m4's resetting kinetics (see upper right corner) from Fig. 3.9b. Run this script after producing the response amplitudes for k_4=0, 1, 2, 4, 8, 16, 32, 64 (Fig. A.9)

m5 controller

```python
import numpy as np
import matplotlib.pyplot as plt
from scipy.integrate import odeint
import csv

p1k1 = 1 #k1 during phase 1
p2k1 = 5 #k1 during phase 2

#################### definition of model ###################
def model(x,t, vark1):                                      #
    #parameters:                                            #
    k1 = vark1 #perturbation                                #
    k2 = 0                                                  #
    k3 = 64    #background, make changes                    #
    k4 = 0.005                                              #
    k5 = 1                                                  #
    k6 = 3                                                  #
    k7 = 1.e-6                                              #
                                                            #
    A = x[0]                                                #
    E = x[1]                                                #
                                                            #
    dAdt = k1 + k3 -(k2+k4*E)*A      #rate eq for A         #
    dEdt = k5*A -k6*E/(k7+E)         #rate eq for E         #
                                                            #
    return [dAdt, dEdt]                                     #
############################################################

x0 = [3.0,4333.33] # initial concentrations (A0, E0)
t1=np.linspace(0,100,10000)   #phase 1 time array
t2=np.linspace(100,500,40000) #phase 2 time array
t = np.concatenate((t1,t2)) #total time array, phase 1 + phase 2

#solve model for phases 1 and 2
y = odeint(model, x0, t1, args=(p1k1,)) #solve for phase 1
x1 = y[-1]      #get last element of array y
print (y[-1])   #print last element of array y
y = np.concatenate((y, odeint(model, x1, t2, args=(p2k1,)))) #solve for phase 2, and concatenate with phase 1

A = y[:,0] # A-array
E = y[:,1] # E-array

with open("./A-data/k3=64.txt", 'w', newline='') as file: #creates 'k3=x.txt' file, insert x=k3 value
    writer = csv.writer(file)
    writer.writerows([A]) #write A-data as a comma-separated-values (csv) file

plt.plot(t,A,label = 'A')
plt.xlabel("time (au)")
plt.ylabel("A (au)")
plt.grid()
plt.xlim(0.0,500)
plt.ylim(2,11)
plt.savefig("plots/m5plot_k3=64.pdf") #saves plot
plt.show()
```

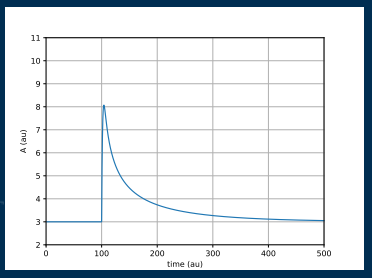

FIGURE A.11: Python script for generating m5's response amplitude of A at background k_3=64. Making some changes (see above) gives the response amplitude for k_3=1 (see upper right corner). Run this script at k_3=0, 1, 2, 4, 8, 16, 32, 64. Insert the corresponding initial concentrations of A and E from Fig. 3.5b.

```python
import matplotlib.pyplot as plt
import numpy as np

y1= np.loadtxt('./A-data/k3=0.txt', delimiter=',', unpack=True)
y2= np.loadtxt('./A-data/k3=1.txt', delimiter=',', unpack=True)
y3= np.loadtxt('./A-data/k3=2.txt', delimiter=',', unpack=True)
y4= np.loadtxt('./A-data/k3=4.txt', delimiter=',', unpack=True)
y5= np.loadtxt('./A-data/k3=8.txt', delimiter=',', unpack=True)
y6= np.loadtxt('./A-data/k3=16.txt', delimiter=',', unpack=True)
y7= np.loadtxt('./A-data/k3=32.txt', delimiter=',', unpack=True)
y8= np.loadtxt('./A-data/k3=64.txt', delimiter=',', unpack=True)

t1=np.linspace(0,100,10000)   #phase 1 time array
t2=np.linspace(100,500,40000) #phase 2 time array
t = np.concatenate((t1,t2)) #total time array, phase 1 + phase 2

plt.plot(t,y1,label="$k_3$=0")
plt.plot(t,y2,label="$k_3$=1")
plt.plot(t,y3,label="$k_3$=2")
plt.plot(t,y4,label="$k_3$=4")
plt.plot(t,y5,label="$k_3$=8")
plt.plot(t,y6,label="$k_3$=16")
plt.plot(t,y7,label="$k_3$=32")
plt.plot(t,y8,label="$k_3$=64")

plt.grid()
plt.legend(loc='upper right')
plt.title('merged A-profiles, $k_1$=1--->5 & $k_3$=0,1,2,4,8..64')
plt.xlabel('time (au)')
plt.ylabel('A (au)')
plt.xlim(0.0,500)
plt.ylim(2,11)
plt.savefig("./plots/A_plots_merged.pdf")
plt.show()
```

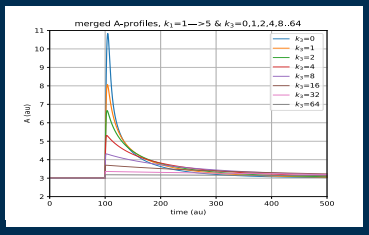

FIGURE A.12: Python script for generating m5's resetting kinetics (see upper right corner) from Fig. 3.5b. Run this script after producing the response amplitudes for k_5=0, 1, 2, 4, 8, 16, 32, 64 (Fig. A.11)

m6 controller

```python
import numpy as np
import matplotlib.pyplot as plt
from scipy.integrate import odeint
import csv

p1k1 = 1 #k1 during phase 1
p2k1 = 5 #k1 during phase 2

#################### definition of model ##################
def model(x,t, vark1):                                    #
    #parameters:                                          #
    k1 = vark1 #perturbation                              #
    k2 = 0                                                #
    k3 = 64  #background, make changes                    #
    k4 = 1.e+4                                            #
    k5 = 6                                                #
    k6 = 2                                                #
    k7 = 1.e-6                                            #
    k8 = 0.1                                              #
                                                          #
    A = x[0]                                              #
    E = x[1]                                              #
                                                          #
    dAdt = k1+k3-k2*A-k4*k8*A/(k8+E)     #rate eq for A   #
    dEdt = k5-k6*A*E/(k7+E)              #rate eq for E   #
                                                          #
    return [dAdt, dEdt]                                   #
###########################################################

x0 = [3.0,46.05] # initial concentrations (A0, E0)
t1=np.linspace(0,100,10000)    #phase 1 time array
t2=np.linspace(100,600,40000) #phase 2 time array
t = np.concatenate((t1,t2)) #total time array, phase 1 + phase 2

#solve model for phases 1 and 2
y = odeint(model, x0, t1, args=(p1k1,)) #solve for phase 1
x1 = y[-1]      #get last element of array y
print (y[-1])   #print last element of array y
y = np.concatenate((y, odeint(model, x1, t2, args=(p2k1,)))) #solve for phase 2, and concatenate with phase 1

A = y[:,0] # A-array
E = y[:,1] # E-array

with open("./A-data/k3=64.txt", 'w', newline='') as file: #creates 'k3=x.txt' file, insert x=k3 value
    writer = csv.writer(file)
    writer.writerows([A]) #write A-data as a comma-separated-values (csv) file

plt.plot(t,A,label = 'A')
plt.xlabel("time (au)")
plt.ylabel("A (au)")
plt.grid()
plt.xlim(0.0,600)
plt.ylim(2,15)
plt.savefig("plots/m6plot_k3=64.pdf") #saves plot
plt.show()
```

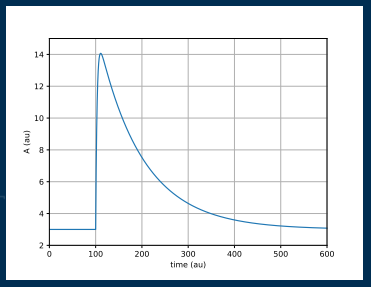

FIGURE A.13: Python script for generating m6's response amplitude of A at background k_3=64. Making some changes (see above) gives the response amplitude for k_3=0 (see upper right corner). Run this script at k_3=0, 1, 2, 4, 8, 16, 32, 64. Insert the corresponding initial concentrations of A and E from Fig. 3.10b.

```python
import matplotlib.pyplot as plt
import numpy as np

y1= np.loadtxt('./A-data/k3=0.txt', delimiter=',', unpack=True)
y2= np.loadtxt('./A-data/k3=1.txt', delimiter=',', unpack=True)
y3= np.loadtxt('./A-data/k3=2.txt', delimiter=',', unpack=True)
y4= np.loadtxt('./A-data/k3=4.txt', delimiter=',', unpack=True)
y5= np.loadtxt('./A-data/k3=8.txt', delimiter=',', unpack=True)
y6= np.loadtxt('./A-data/k3=16.txt', delimiter=',', unpack=True)
y7= np.loadtxt('./A-data/k3=32.txt', delimiter=',', unpack=True)
y8= np.loadtxt('./A-data/k3=64.txt', delimiter=',', unpack=True)

t1=np.linspace(0,100,10000)    #phase 1 time array
t2=np.linspace(100,600,40000) #phase 2 time array
t = np.concatenate((t1,t2)) #total time array, phase 1 + phase 2

plt.plot(t,y1,label="$k_3$=0")
plt.plot(t,y2,label="$k_3$=1")
plt.plot(t,y3,label="$k_3$=2")
plt.plot(t,y4,label="$k_3$=4")
plt.plot(t,y5,label="$k_3$=8")
plt.plot(t,y6,label="$k_3$=16")
plt.plot(t,y7,label="$k_3$=32")
plt.plot(t,y8,label="$k_3$=64")

plt.grid()
plt.legend(loc='upper right')
plt.title('merged A-profiles, $k_1$=1--->5 & $k_3$=0,1,2,4,8..64')
plt.xlabel('time (au)')
plt.ylabel('A (au)')
plt.xlim(0.0,600)
plt.ylim(2,15)
plt.savefig("./plots/A_plots_merged.pdf")
plt.show()
```

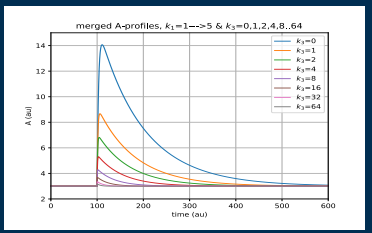

FIGURE A.14: Python script for generating m6's resetting kinetics (see upper right corner) from Fig. 3.10b. Run this script after producing the response amplitudes for k_6=0, 1, 2, 4, 8, 16, 32, 64 (Fig. A.13)

m7 controller

```python
import numpy as np
import matplotlib.pyplot as plt
from scipy.integrate import odeint
import csv

p1k1 = 1 #k1 during phase 1
p2k1 = 5 #k1 during phase 2

#################### definition of model ###################
def model(x,t, vark1):                                      #
    #parameters:                                            #
    k1 = vark1 #perturbation                                #
    k2 = 0                                                  #
    k3 = 64     #background, make changes                   #
    k4 = 0.03                                               #
    k5 = 1                                                  #
    k6 = 31                                                 #
    k7 = 1.e-6                                              #
    k8 = 0.1                                                #
                                                            #
    A = x[0]                                                #
    E = x[1]                                                #
                                                            #
    dAdt = k1 + k3 -k2*A -k4*A*E          #rate eq for A    #
    dEdt = k5 -((k6*E)/(k7+E))*(k8/(k8+A))   #rate eq for E #
                                                            #
    return [dAdt, dEdt]                                     #
############################################################

x0 = [3.0,722.22] # initial concentrations (A0, E0)
t1=np.linspace(0,100,10000)   #phase 1 time array
t2=np.linspace(100,500,40000) #phase 2 time array
t = np.concatenate((t1,t2)) #total time array, phase 1 + phase 2

#solve model for phases 1 and 2
y = odeint(model, x0, t1, args=(p1k1,)) #solve for phase 1
x1 = y[-1]      #get last element of array y
print (y[-1])   #print last element of array y
y = np.concatenate((y, odeint(model, x1, t2, args=(p2k1,)))) #solve for phase 2, and concatenate with phase 1

A = y[:,0] # A-array
E = y[:,1] # E-array

with open("./A-data/k3=64.txt", 'w', newline='') as file: #creates 'k3=x.txt' file, insert x=k3 value
    writer = csv.writer(file)
    writer.writerows([A]) #write A-data as a comma-separated-values (csv) file

plt.plot(t,A,label = 'A')
plt.xlabel("time (au)")
plt.ylabel("A (au)")
plt.grid()
plt.xlim(0.0,500)
plt.ylim(2,12)
plt.savefig("plots/m7plot_k3=64.pdf") #saves plot
plt.show()
```

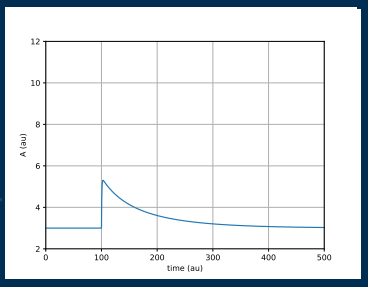

FIGURE A.15: Python script for generating m7's response amplitude of A at background k_3=64. Making some changes (see above) gives the response amplitude for k_3=4 (see upper right corner). Run this script at k_3=0, 1, 2, 4, 8, 16, 32, 64. Insert the corresponding initial concentrations of A and E from Fig. 3.6b.

```python
import matplotlib.pyplot as plt
import numpy as np

y1= np.loadtxt('./A-data/k3=0.txt', delimiter=',', unpack=True)
y2= np.loadtxt('./A-data/k3=1.txt', delimiter=',', unpack=True)
y3= np.loadtxt('./A-data/k3=2.txt', delimiter=',', unpack=True)
y4= np.loadtxt('./A-data/k3=4.txt', delimiter=',', unpack=True)
y5= np.loadtxt('./A-data/k3=8.txt', delimiter=',', unpack=True)
y6= np.loadtxt('./A-data/k3=16.txt', delimiter=',', unpack=True)
y7= np.loadtxt('./A-data/k3=32.txt', delimiter=',', unpack=True)
y8= np.loadtxt('./A-data/k3=64.txt', delimiter=',', unpack=True)

t1=np.linspace(0,100,10000)   #phase 1 time array
t2=np.linspace(100,500,40000) #phase 2 time array
t = np.concatenate((t1,t2)) #total time array, phase 1 + phase 2

plt.plot(t,y1,label="$k_3$=0")
plt.plot(t,y2,label="$k_3$=1")
plt.plot(t,y3,label="$k_3$=2")
plt.plot(t,y4,label="$k_3$=4")
plt.plot(t,y5,label="$k_3$=8")
plt.plot(t,y6,label="$k_3$=16")
plt.plot(t,y7,label="$k_3$=32")
plt.plot(t,y8,label="$k_3$=64")

plt.grid()
plt.legend(loc='right')
plt.title('merged A-profiles, $k_1$=1--->5 & $k_3$=0,1,2,4,8..64')
plt.xlabel('time (au)')
plt.ylabel('A (au)')
plt.xlim(0.0,500)
plt.ylim(2,12)
plt.savefig("./plots/A_plots_merged.pdf")
plt.show()
```

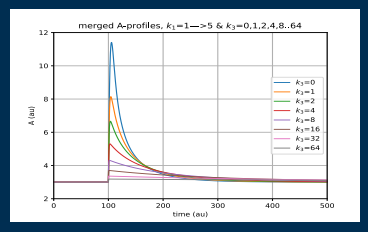

FIGURE A.16: Python script for generating m7's resetting kinetics (see upper right corner) from Fig. 3.6b. Run this script after producing the response amplitudes for k_7=0, 1, 2, 4, 8, 16, 32, 64 (Fig. A.15)

m8 controller

```python
import numpy as np
import matplotlib.pyplot as plt
from scipy.integrate import odeint
import csv

p1k1 = 1 #k1 during phase 1
p2k1 = 5 #k1 during phase 2

#################### definition of model ##################
def model(x,t, vark1):                                    #
    #parameters:                                          #
    k1 = vark1 #perturbation                              #
    k2 = 0                                                #
    k3 = 64    #background, make changes                  #
    k4 = 1.e4                                             #
    k5 = 620                                              #
    k6 = 20                                               #
    k7 = 1.e-6                                            #
    k8 = 0.1                                              #
    k9 = 0.1                                              #
                                                          #
    A = x[0]                                              #
    E = x[1]                                              #
                                                          #
    dAdt = k1 + k3 -k2*A -k4*A*k9/(k9+E)          #rate eq for A  #
    dEdt = k5*(k8/(k8+A))-k6*E/(k7+E)             #rate eq for E  #
                                                          #
    return [dAdt, dEdt]                                   #
###########################################################

x0 = [3.0,46.05] # initial concentrations (A0, E0)
t1=np.linspace(0,100,10000)   #phase 1 time array
t2=np.linspace(100,500,40000) #phase 2 time array
t = np.concatenate((t1,t2)) #total time array, phase 1 + phase 2


#solve model for phases 1 and 2
y = odeint(model, x0, t1, args=(p1k1,)) #solve for phase 1
x1 = y[-1]    #get last element of array y
print (y[-1])  #print last element of array y
y = np.concatenate((y, odeint(model, x1, t2, args=(p2k1,)))) #solve for phase 2, and concatenate with phase 1

A = y[:,0] # A-array
E = y[:,1] # E-array

with open("./A-data/k3=64.txt", 'w', newline='') as file: #creates 'k3=x.txt' file, insert x=k3 value
    writer = csv.writer(file)
    writer.writerows([A]) #write A-data as a comma-separated-values (csv) file

plt.plot(t,A,label = 'A')
plt.xlabel("time (au)")
plt.ylabel("A (au)")
plt.grid()
plt.xlim(0.0,500)
plt.ylim(1,15)
plt.savefig("plots/m8plot_k3=64.pdf") #saves plot
plt.show()
```

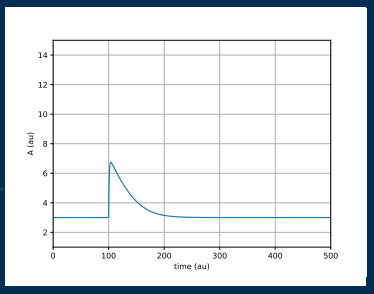

FIGURE A.17: Python script for generating m8's response amplitude of A at background k_3=64. Making some changes (see above) gives the response amplitude for k_3=2 (see upper right corner). Run this script at k_3=0, 1, 2, 4, 8, 16, 32, 64. Insert the corresponding initial concentrations of A and E from Fig. 3.11b.

```python
import matplotlib.pyplot as plt
import numpy as np

y1= np.loadtxt('./A-data/k3=0.txt', delimiter=',', unpack=True)
y2= np.loadtxt('./A-data/k3=1.txt', delimiter=',', unpack=True)
y3= np.loadtxt('./A-data/k3=2.txt', delimiter=',', unpack=True)
y4= np.loadtxt('./A-data/k3=4.txt', delimiter=',', unpack=True)
y5= np.loadtxt('./A-data/k3=8.txt', delimiter=',', unpack=True)
y6= np.loadtxt('./A-data/k3=16.txt', delimiter=',', unpack=True)
y7= np.loadtxt('./A-data/k3=32.txt', delimiter=',', unpack=True)
y8= np.loadtxt('./A-data/k3=64.txt', delimiter=',', unpack=True)

t1=np.linspace(0,100,10000)   #phase 1 time array
t2=np.linspace(100,500,40000) #phase 2 time array
t = np.concatenate((t1,t2)) #total time array, phase 1 + phase 2

plt.plot(t,y1,label="$k_3$=0")
plt.plot(t,y2,label="$k_3$=1")
plt.plot(t,y3,label="$k_3$=2")
plt.plot(t,y4,label="$k_3$=4")
plt.plot(t,y5,label="$k_3$=8")
plt.plot(t,y6,label="$k_3$=16")
plt.plot(t,y7,label="$k_3$=32")
plt.plot(t,y8,label="$k_3$=64")

plt.grid()
plt.legend(loc='right')
plt.title('merged A-profiles, $k_1$=1--->5 & $k_3$=0,1,2,4,8..64')
plt.xlabel('time (au)')
plt.ylabel('A (au)')
plt.xlim(0.0,500)
plt.ylim(1,15)
plt.savefig("./plots/A_plots_merged.pdf")
plt.show()
```

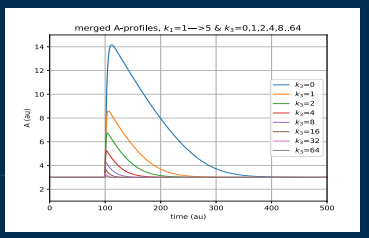

FIGURE A.18: Python script for generating m8's resetting kinetics (see upper right corner) from Fig. 3.11b. Run this script after producing the response amplitudes for k_8=0, 1, 2, 4, 8, 16, 32, 64 (Fig. A.17)

A.2 Python scripts for frequency compensated controllers

Frequency compensated oscillator with coherent feedback at k_{10}=0

This section containes python scripts for the frequency compensated oscillator with coherent feedback from Fig. 3.13. A background k_{10}=0 and step-wise perturbation k_2 from 1→9 at time t=100 are applied. A and E are plotted as a function of time in Fig. A.19 and Fig. A.20, respectively. Frequency is plotted as a function of time in Fig. A.21, and I_1 and I_2 are shown as a function of time in Fig. A.22.

```python
import numpy as np
import matplotlib.pyplot as plt
from scipy.integrate import odeint
import csv
import os, sys

p1k2 = 1 #k2 during phase 1
p2k2 = 10 #k2 during phase 2

################################definition of model#####################################################################
def model(x,t,vark2):  #,vark2
    #parameters/constants:
    k1 = 0
    k2 = vark2 #perturbation
    k3 = 100
    k4 = 1
    k5 = 0.1
    k6 = 2
    k7 = 10**-6
    k8 = 10**-6
    k9 = 20
    k10 = 0 # background, make changes
    k11 = 1
    k12 = 5
    k13 = 10**-6
    k14 = 4.99
    k15 = 1
    k16 = 10**-6
    k17 = 10**-6
    kg = 10**-2
    kg3 = 10**-2

    # assign each ODE to a vector element:
    A = x[0]
    E = x[1]
    EI = x[2] # e intermediate
    I1 = x[3]
    I2 = x[4]

    #define each ODE:
    dAdt=k1+(k3*k5)/(k5+E)-(k2*A/(k8+A))-(k10*A/(k8+A))-(kg*A*I1/(k17+A))+(kg3*I2) #rate equation for A
    dEdt=k9*EI-k6*E/(k7+E) # rate equation for E
    dEIdt=k4*A-k9*EI # rate equation for e
    dI1dt=k11*E-k12*I1/(k13+I1) # rate equation for I1
    dI2dt=k14-k15*E*I2/(k16+I2) # rate equation for I2

    return [dAdt, dEdt, dEIdt, dI1dt, dI2dt]
##########################################################################################################################

x0 = [2.2084,7.7021,1.1354e-1,1.5773e2,4.3563] # initial concentrations (A0, E0, EI0, I10, I20)

# declare a time vector (time window):
t1=np.linspace(0,100,10000)   #phase 1 time array
t2=np.linspace(100,800,30000) #phase 2 time array
t = np.concatenate((t1,t2)) #total time array, phase 1 + phase 2

#solve model for phases 1 and 2
y = odeint(model, x0, t1, args=(p1k2,)) #solve for phase 1
x1 = y[-1]    #get last element of array y
# print (y[-1])   #print last element of array y
y = np.concatenate((y, odeint(model, x1, t2, args=(p2k2,)))) #solve for phase 2 and concatenate with phase 1

A = y[:,0] # A-array
E = y[:,1] # E-array
EI = y[:,2] # e-array
I1 = y[:,3] # I1-array
I2 = y[:,4] # I2-array

#plot the results:
plt.plot(t,A,label = 'A', color='green')
plt.xlabel("time (au)")
plt.ylabel("A (au)", color='green')
plt.grid()
plt.xlim(0.0,800)
plt.ylim(0.0,5.3)
plt.savefig("plots/A-time-plot_k10=0.pdf") #make changes wrt k10 in file name
plt.show()
```

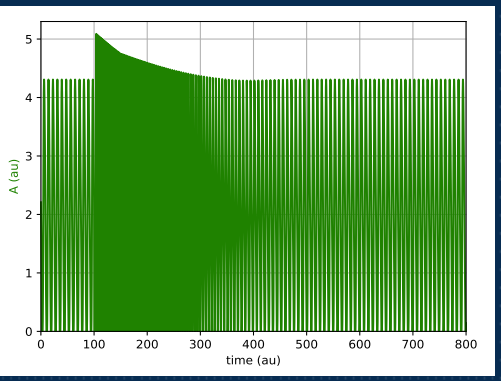

FIGURE A.19: Frequency compensated oscillator with coherent feedback at k_{10}=0 and k_2 from 1→9. A is plotted as a function of time.

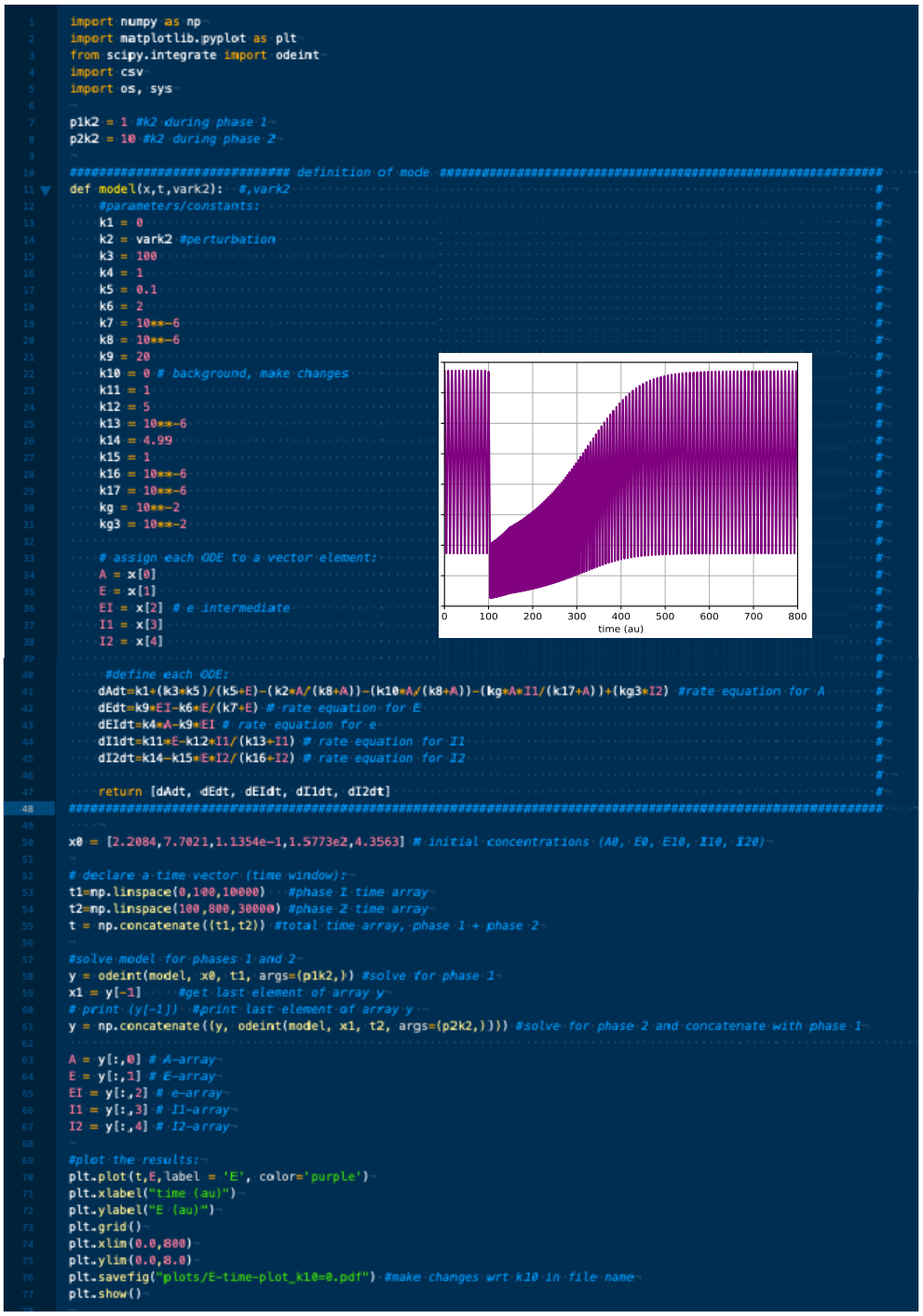


```python
import numpy as np
import matplotlib.pyplot as plt
from scipy.integrate import odeint
import csv
import os, sys

p1k2 = 1 #k2 during phase 1
p2k2 = 10 #k2 during phase 2

############################## definition of mode ##########################################################
def model(x,t,vark2):  #,vark2
    #parameters/constants:
    k1 = 0
    k2 = vark2 #perturbation
    k3 = 100
    k4 = 1
    k5 = 0.1
    k6 = 2
    k7 = 10**-6
    k8 = 10**-6
    k9 = 20
    k10 = 0 # background, make changes
    k11 = 1
    k12 = 5
    k13 = 10**-6
    k14 = 4.99
    k15 = 1
    k16 = 10**-6
    k17 = 10**-6
    kg = 10**-2
    kg3 = 10**-2

    # assign each ODE to a vector element:
    A = x[0]
    E = x[1]
    EI = x[2] # e intermediate
    I1 = x[3]
    I2 = x[4]

    #define each ODE:
    dAdt=k1+(k3*k5)/(k5+E)-(k2*A/(k8+A))-(k10*A/(k8+A))-(kg*A*I1/(k17+A))+(kg3*I2) #rate equation for A
    dEdt=k9*EI-k6*E/(k7+E) # rate equation for E
    dEIdt=k4*A-k9*EI # rate equation for e
    dI1dt=k11*E-k12*I1/(k13+I1) # rate equation for I1
    dI2dt=k14-k15*E+I2/(k16+I2) # rate equation for I2

    return [dAdt, dEdt, dEIdt, dI1dt, dI2dt]
############################################################################################################

x0 = [2.2084,7.7021,1.1354e-1,1.5773e2,4.3563] # initial concentrations (A0, E0, E10, I10, I20)

# declare a time vector (time window):
t1=np.linspace(0,100,10000)  #phase 1 time array
t2=np.linspace(100,800,30000) #phase 2 time array
t = np.concatenate((t1,t2)) #total time array, phase 1 + phase 2

#solve model for phases 1 and 2
y = odeint(model, x0, t1, args=(p1k2,)) #solve for phase 1
x1 = y[-1]     #get last element of array y
# print (y[-1])  #print last element of array y
y = np.concatenate((y, odeint(model, x1, t2, args=(p2k2,)))) #solve for phase 2 and concatenate with phase 1

A = y[:,0] # A-array
E = y[:,1] # E-array
EI = y[:,2] # e-array
I1 = y[:,3] # I1-array
I2 = y[:,4] # I2-array

#plot the results:
plt.plot(t,E,label = 'E', color='purple')
plt.xlabel("time (au)")
plt.ylabel("E (au)")
plt.grid()
plt.xlim(0.0,800)
plt.ylim(0.0,8.0)
plt.savefig("plots/E-time-plot_k10=0.pdf") #make changes wrt k10 in file name
plt.show()
```

FIGURE A.20: Frequency compensated oscillator with coherent feedback at k_{10}=0 and k_2 from 1→9. E is plotted as a function of time.

```python
import numpy as np
import matplotlib.pyplot as plt
from scipy.integrate import odeint
import csv
import os, sys

p1k2 = 1 #k2 during phase 1
p2k2 = 10 #k2 during phase 2

############################## definition of model ##########################################################
def model(x,t,vark2):  #,vark2
    #parameters/constants:
    k1 = 0
    k2 = vark2 #perturbation
    k3 = 100
    k4 = 1
    k5 = 0.1
    k6 = 2
    k7 = 10**-6
    k8 = 10**-6
    k9 = 20
    k10 = 0 # background, make changes
    k11 = 1
    k12 = 5
    k13 = 10**-6
    k14 = 4.99
    k15 = 1
    k16 = 10**-6
    k17 = 10**-6
    kg = 10**-2
    kg3 = 10**-2

    # assign each ODE to a vector element:
    A = x[0]
    E = x[1]
    EI = x[2] # e intermediate
    I1 = x[3]
    I2 = x[4]

    #define each ODE:
    dAdt=k1+(k3*k5)/(k5+E)-(k2+A/(k8+A))-(k10*A/(k8+A))-(kg+A*I1/(k17+A))+(kg3*I2) #rate equation for A
    dEdt=k9*EI-k6*E/(k7+E) # rate equation for E
    dEIdt=k4*A-k9*EI # rate equation for e
    dI1dt=k11*E-k12*I1/(k13+I1) # rate equation for I1
    dI2dt=k14-k15*E*I2/(k16+I2) # rate equation for I2

    return [dAdt, dEdt, dEIdt, dI1dt, dI2dt]
##############################################################################################################

x0 = [2.2084,7.7021,1.1354e-1,1.5773e2,4.3563] # initial concentrations (A0, E0, E10, I10, I20)

# declare a time vector (time window):
t1=np.linspace(0,100,10000)  #phase 1 time array
t2=np.linspace(100,800,30000) #phase 2 time array
t = np.concatenate((t1,t2)) #total time array, phase 1 + phase 2

#solve model for phases 1 and 2
y = odeint(model, x0, t1, args=(p1k2,)) #solve for phase 1
x1 = y[-1]   #get last element of array y
# print (y[-1])  #print last element of array y
y = np.concatenate((y, odeint(model, x1, t2, args=(p2k2,)))) #solve for phase 2 and concatenate with phase 1

A = y[:,0] # A-array
E = y[:,1] # E-array
EI = y[:,2] # e-array
I1 = y[:,3] # I1-array
I2 = y[:,4] # I2-array

tmax=[]
freq=[]
per=[]
tfreq=[]
i=1
while(i>=1) and (i<=len(A)-2):
    if(A[i-1]<=A[i]) and (A[i]>=A[i+1]): #get Amax values
        tmax.append(t[i])                #get tmax values
    i=i+1

j=1
while(j>=1) and (j<=len(tmax)-1):
    period=tmax[j]-tmax[j-1]
    if(period>0):
        frequency=1/period
        if(frequency<0.5):
            per.append(period)
            freq.append(frequency)
            tfreq.append(tmax[j])
    j=j+1

#plot the frequency against time:
plt.plot(tfreq,freq,label = 'frequency', color='blue')
plt.xlabel("time (au)")
plt.ylabel("frequency (au)")
plt.grid()
plt.xlim(0,800)
plt.ylim(0.1,0.5)
plt.savefig("plots/freq-time-plot_k10=0.pdf") # make changes wrt k10 in file name
plt.show()
```

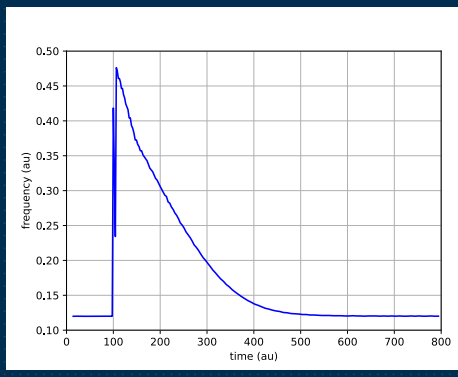

FIGURE A.21: Frequency compensated oscillator with coherent feedback at k_{10}=0 and k_2 from 1→9. Frequency is plotted as a function of time.

```python
import numpy as np
import matplotlib.pyplot as plt
from scipy.integrate import odeint
import csv
import os, sys

p1k2 = 1 #k2 during phase 1
p2k2 = 10 #k2 during phase 2

##############################definition of model##########################################################
def model(x,t,vark2):  #,vark2
    #parameters/constants:
    k1 = 0
    k2 = vark2 #perturbation
    k3 = 100
    k4 = 1
    k5 = 0.1
    k6 = 2
    k7 = 10**-6
    k8 = 10**-6
    k9 = 20
    k10 = 0 # background, make changes
    k11 = 1
    k12 = 5
    k13 = 10**-6
    k14 = 4.99
    k15 = 1
    k16 = 10**-6
    k17 = 10**-6
    kg = 10**-2
    kg3 = 10**-2

    # assign each ODE to a vector element:
    A = x[0]
    E = x[1]
    EI = x[2] # e intermediate
    I1 = x[3]
    I2 = x[4]

    #define each ODE:
    dAdt=k1+(k3*k5)/(k5+E)-(k2*A/(k8+A))-(k10*A/(k8+A))-(kg*A*I1/(k17+A))+(kg3*I2) #rate equation for A
    dEdt=k9*EI-k6*E/(k7+E) # rate equation for E
    dEIdt=k4*A-k9*EI # rate equation for e
    dI1dt=k11*E-k12*I1/(k13+I1) # rate equation for I1
    dI2dt=k14-k15*E*I2/(k16+I2) # rate equation for I2

    return [dAdt, dEdt, dEIdt, dI1dt, dI2dt]
##############################################################################################################

x0 = [2.2084,7.7021,1.1354e-1,1.5773e2,4.3563] # initial concentrations (A0, E0, EI0, I10, I20)

# declare a time vector (time window):
t1=np.linspace(0,100,10000)  #phase 1 time array
t2=np.linspace(100,800,30000) #phase 2 time array
t = np.concatenate((t1,t2)) #total time array, phase 1 + phase 2

#solve model for phases 1 and 2
y = odeint(model, x0, t1, args=(p1k2,)) #solve for phase 1
x1 = y[-1]    #get last element of array y
# print (y[-1])  #print last element of array y
y = np.concatenate((y, odeint(model, x1, t2, args=(p2k2,)))) #solve for phase 2 and concatenate with phase 1

A = y[:,0] # A-array
E = y[:,1] # E-array
EI = y[:,2] # e-array
I1 = y[:,3] # I1-array
I2 = y[:,4] # I2-array

#Creating a plot with both I1 (y1-axis) and I2 (y2-axis)
fig, ax = plt.subplots()
ax2 = ax.twinx()
ax.plot(t, I1, color ='red')
ax2.plot(t, I2, color ='blue')
ax.set_xlabel('time (au)')
ax.set_ylabel("$I_1$ (au)", color ='red')
ax2.set_ylabel("$I_2$ (au)", color = 'blue')
plt.grid()
plt.xlim(0.0,800)
plt.savefig("plots/I12-time-plot_k10=0.pdf") #make changes wrt k10 in file name
plt.show()
```

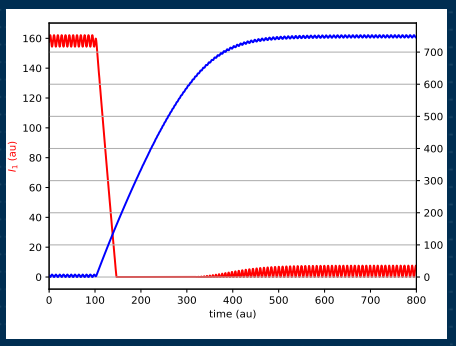

FIGURE A.22: Frequency compensated oscillator with coherent feedback at k_{10}=0 and k_2 from 1→9. I_1 and I_2 are plotted as a function of time.

Frequency compensated oscillator with coherent feedback at k_{10}=2048

This section containes python scripts for the frequency compensated oscillator with coherent feedback from Fig. 3.14. A background k_{10}=2048 and step-wise perturbation k_2 from 1→9 at time t=100 are applied. A and E are plotted as a function of time in Fig. A.23 and Fig. A.24, respectively. Frequency is plotted as a function of time in Fig. A.25, and I_1 and I_2 are shown as a function of time in Fig. A.26.

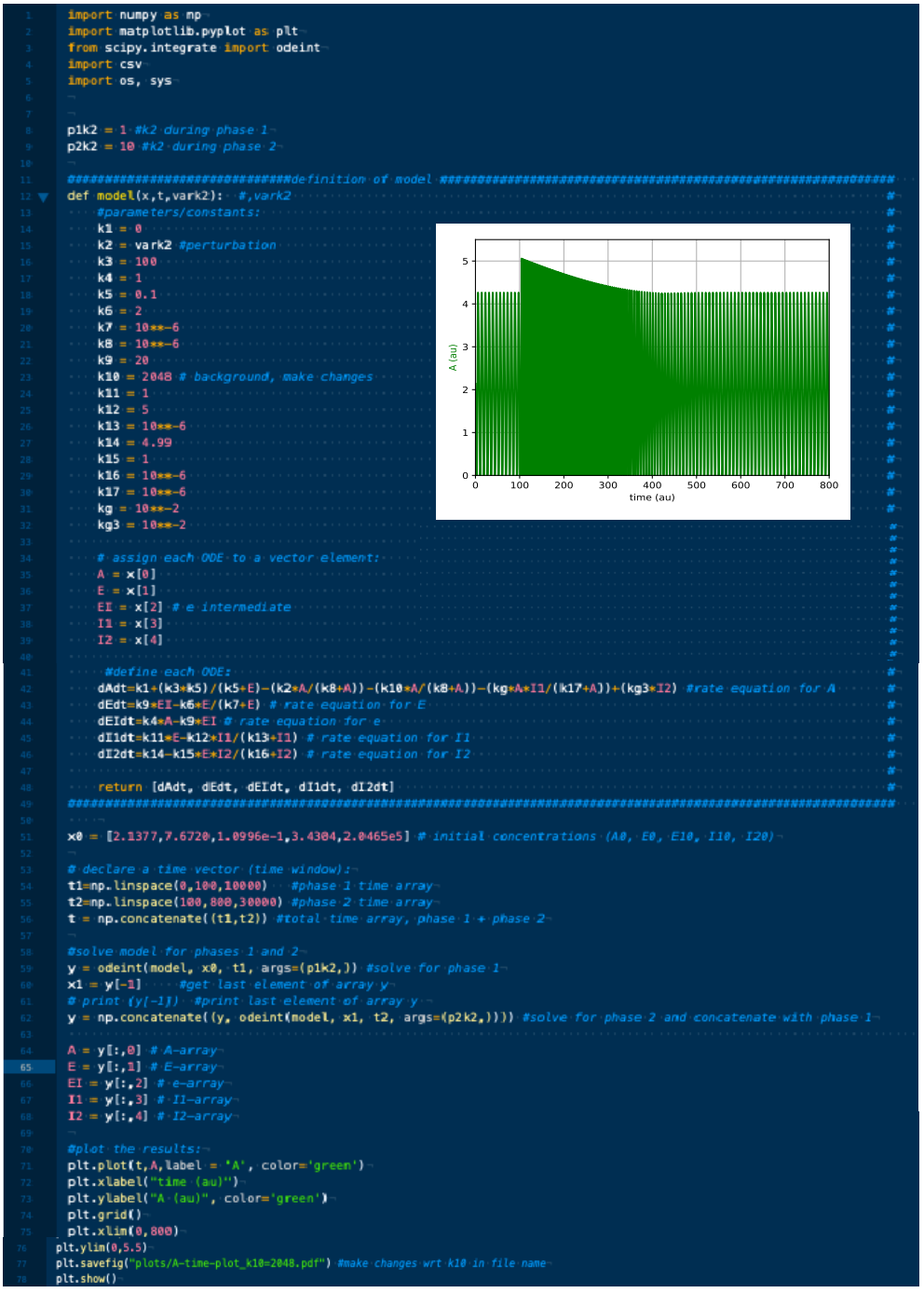

FIGURE A.23: Frequency compensated oscillator with coherent feedback at k_{10}=2048 and k_2 from 1→9. A is plotted as a function of time.

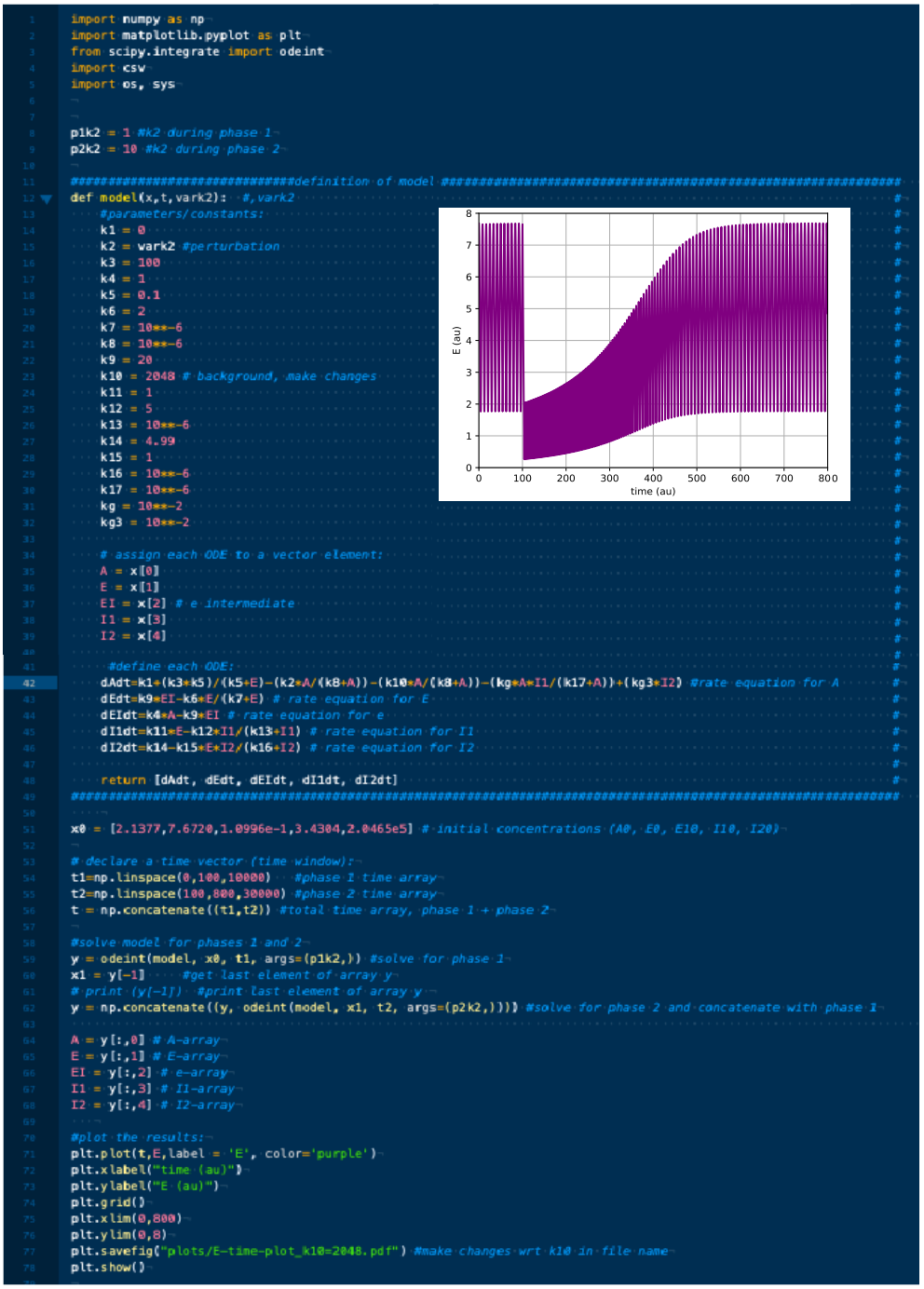


```python
import numpy as np
import matplotlib.pyplot as plt
from scipy.integrate import odeint
import csw
import os, sys


p1k2 = 1 #k2 during phase 1
p2k2 = 10 #k2 during phase 2

################################definition of model ###########################################################
def model(x,t,wark2):  #,wark2
    #parameters/constants:
    k1 = 0
    k2 = wark2 #perturbation
    k3 = 100
    k4 = 1
    k5 = 0.1
    k6 = 2
    k7 = 10**-6
    k8 = 10**-6
    k9 = 20
    k10 = 2048 # background, make changes
    k11 = 1
    k12 = 5
    k13 = 10**-6
    k14 = 4.99
    k15 = 1
    k16 = 10**-6
    k17 = 10**-6
    kg = 10**-2
    kg3 = 10**-2

    # assign each ODE to a vector element:
    A = x[0]
    E = x[1]
    EI = x[2] # e intermediate
    I1 = x[3]
    I2 = x[4]

    #define each ODE:
    dAdt=k1+(k3*k5)/(k5+E)-(k2*A/(k8+A))-(k10*A/(k8+A))-(kg*A*I1/(k17+A))+(kg3*I2) #rate equation for A
    dEdt=k9*EI-k6*E/(k7+E) # rate equation for E
    dEIdt=k4*A-k9*EI # rate equation for e
    dI1dt=k11*E-k12*I1/(k13+I1) # rate equation for I1
    dI2dt=k14-k15*E*I2/(k16+I2) # rate equation for I2

    return [dAdt, dEdt, dEIdt, dI1dt, dI2dt]
###############################################################################################################

x0 = [2.1377,7.6720,1.0996e-1,3.4304,2.0465e5] # initial concentrations (A0, E0, EI0, I10, I20)

# declare a time vector (time window):
t1=np.linspace(0,100,10000)   #phase 1 time array
t2=np.linspace(100,800,30000) #phase 2 time array
t = np.concatenate((t1,t2)) #total time array, phase 1 + phase 2

#solve model for phases 1 and 2
y = odeint(model, x0, t1, args=(p1k2,)) #solve for phase 1
x1 = y[-1]    #get last element of array y
# print (y[-1])  #print last element of array y
y = np.concatenate((y, odeint(model, x1, t2, args=(p2k2,)))) #solve for phase 2 and concatenate with phase 1

A = y[:,0] # A-array
E = y[:,1] # E-array
EI = y[:,2] # e-array
I1 = y[:,3] # I1-array
I2 = y[:,4] # I2-array

#plot the results:
plt.plot(t,E,label = 'E', color='purple')
plt.xlabel("time (au)")
plt.ylabel("E (au)")
plt.grid()
plt.xlim(0,800)
plt.ylim(0,8)
plt.savefig("plots/E-time-plot_k10=2048.pdf") #make changes wrt k10 in file name
plt.show()
```

FIGURE A.24: Frequency compensated oscillator with coherent feedback at k_{10}=2048 and k_2 from 1→9. E is plotted as a function of time.

```python
import numpy as np
import matplotlib.pyplot as plt
from scipy.integrate import odeint
import csv
import os, sys


p1k2 = 1 #k2 during phase 1
p2k2 = 10 #k2 during phase 2

##############################definition of model ##########################################################################
def model(x,t,vark2):  #,vark2                                                                                          #
    #parameters/constants:                                                                                              #
    k1 = 0                                                                                                              #
    k2 = vark2 #perturbation                                                                                            #
    k3 = 100                                                                                                            #
    k4 = 1                                                                                                              #
    k5 = 0.1                                                                                                            #
    k6 = 2                                                                                                              #
    k7 = 10**-6                                                                                                         #
    k8 = 10**-6                                                                                                         #
    k9 = 20                                                                                                             #
    k10 = 2048 # background, make changes                                                                               #
    k11 = 1                                                                                                             #
    k12 = 5                                                                                                             #
    k13 = 10**-6                                                                                                        #
    k14 = 4.99                                                                                                          #
    k15 = 1                                                                                                             #
    k16 = 10**-6                                                                                                        #
    k17 = 10**-6                                                                                                        #
    kg = 10**-2                                                                                                         #
    kg3 = 10**-2                                                                                                        #
                                                                                                                        #
    # assign each ODE to a vector element:                                                                              #
    A = x[0]                                                                                                            #
    E = x[1]                                                                                                            #
    EI = x[2] # e intermediate                                                                                          #
    I1 = x[3]                                                                                                           #
    I2 = x[4]                                                                                                           #
                                                                                                                        #
    #define each ODE:                                                                                                 #
    dAdt=k1+(k3*k5)/(k5+E)-(k2*A/(k8+A))-(k10*A/(k8+A))-(kg*A*I1/(k17+A))+(kg3*I2) #rate equation for A                  #
    dEdt=k9*EI-k6*E/(k7+E) # rate equation for E                                                                        #
    dEIdt=k4*A-k9*EI # rate equation for e                                                                              #
    dI1dt=k11*E-k12*I1/(k13+I1) # rate equation for I1                                                                  #
    dI2dt=k14-k15*E*I2/(k16+I2) # rate equation for I2                                                                  #
                                                                                                                        #
    return [dAdt, dEdt, dEIdt, dI1dt, dI2dt]                                                                            #
################################################################################################################################

x0 = [2.1377,7.6720,1.0996e-1,3.4304,2.0465e5] # initial concentrations (A0, E0, E10, I10, I20)

# declare a time vector (time window):
t1=np.linspace(0,100,10000)   #phase 1 time array
t2=np.linspace(100,800,30000) #phase 2 time array
t = np.concatenate((t1,t2)) #total time array, phase 1 + phase 2

#solve model for phases 1 and 2
y = odeint(model, x0, t1, args=(p1k2,)) #solve for phase 1
x1 = y[-1]     #get last element of array y
# print (y[-1]) #print last element of array y
y = np.concatenate((y, odeint(model, x1, t2, args=(p2k2,)))) #solve for phase 2 and concatenate with phase 1

A = y[:,0] # A-array
E = y[:,1] # E-array
EI = y[:,2] # e-array
I1 = y[:,3] # I1-array
I2 = y[:,4] # I2-array

tmax=[]
freq=[]
per=[]
tfreq=[]
i=1
while(i>=1) and (i<=len(A)-2):
    if(A[i-1]<=A[i]) and (A[i]>=A[i+1]): #get Amax values
        tmax.append(t[i])                #get tmax values
    i=i+1

j=1
while(j>=1) and (j<=len(tmax)-1):
    period=tmax[j]-tmax[j-1]
    if(period>0):
        frequency=1/period
        if(frequency<0.5):
            per.append(period)
            freq.append(frequency)
            tfreq.append(tmax[j])
    j=j+1

#plot the frequency against time:
plt.plot(tfreq,freq,label = 'frequency', color='blue')
plt.xlabel("time (au)")
plt.ylabel("frequency (au)")
plt.grid()
plt.xlim(0,800)
plt.ylim(0.1,0.5)
plt.savefig("plots/freq-time-plot_k10=2048.pdf") # make changes wrt k10 in file name
plt.show()
```

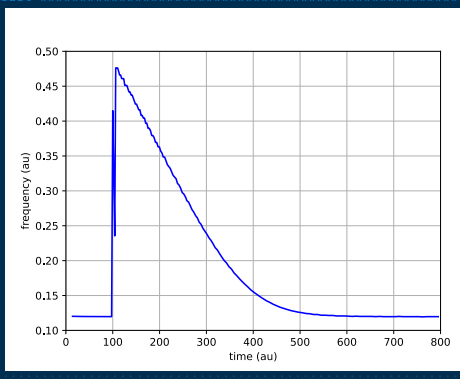

FIGURE A.25: Frequency compensated oscillator with coherent feedback at k_{10}=2048 and k_2 from 1→9. Frequency is plotted as a function of time.

```python
import numpy as np
import matplotlib.pyplot as plt
from scipy.integrate import odeint
import csv
import os, sys


p1k2 = 1 #k2 during phase 1
p2k2 = 10 #k2 during phase 2

#################################definition of model ##########################################################
def model(x,t,vark2):  #,vark2
    #parameters/constants:
    k1 = 0
    k2 = vark2 #perturbation
    k3 = 100
    k4 = 1
    k5 = 0.1
    k6 = 2
    k7 = 10**-6
    k8 = 10**-6
    k9 = 20
    k10 = 2048 # background, make changes
    k11 = 1
    k12 = 5
    k13 = 10**-6
    k14 = 4.99
    k15 = 1
    k16 = 10**-6
    k17 = 10**-6
    kg = 10**-2
    kg3 = 10**-2

    # assign each ODE to a vector element:
    A = x[0]
    E = x[1]
    EI = x[2] # e-intermediate
    I1 = x[3]
    I2 = x[4]

    #define each ODE:
    dAdt=k1+(k3*k5)/(k5+E)-(k2*A/(k8+A))-(k10*A/(k8+A))-(kg*A*I1/(k17+A))+(kg3*I2) #rate equation for A
    dEdt=k9*EI-k6*E/(k7+E) # rate equation for E
    dEIdt=k4*A-k9*EI # rate equation for e
    dI1dt=k11+E-k12*I1/(k13+I1) # rate equation for I1
    dI2dt=k14-k15*E*I2/(k16+I2) # rate equation for I2

    return [dAdt, dEdt, dEIdt, dI1dt, dI2dt]
###############################################################################################################

x0 = [2.1377,7.6720,1.0996e-1,3.4304,2.0465e5] # initial concentrations (A0, E0, EI0, I10, I20)

# declare a time vector (time window):
t1=np.linspace(0,100,10000)  #phase 1 time array
t2=np.linspace(100,800,30000) #phase 2 time array
t = np.concatenate((t1,t2)) #total time array, phase 1 + phase 2

#solve model for phases 1 and 2
y = odeint(model, x0, t1, args=(p1k2,)) #solve for phase 1
x1 = y[-1]      #get last element of array y
# print (y[-1])  #print last element of array y
y = np.concatenate((y, odeint(model, x1, t2, args=(p2k2,)))) #solve for phase 2 and concatenate with phase 1

A = y[:,0] # A-array
E = y[:,1] # E-array
EI = y[:,2] # e-array
I1 = y[:,3] # I1-array
I2 = y[:,4] # I2-array

#Creating a plot with both I1 (y1-axis) and I2 (y2-axis)
fig, ax = plt.subplots()
ax2 = ax.twinx()
ax.plot(t, I1, color ='red')
ax2.plot(t, I2, color ='blue')
ax.set_xlabel('time (au)')
ax.set_ylabel("$I_1$ (au)", color ='red')
ax2.set_ylabel("$I_2$ (au)", color = 'blue')
ax2.set_ylim(204600,205600)
ax.set_ylim(0,8)
plt.xlim(0,800)
plt.grid()
plt.savefig("plots/I12-time-plot_k10=2048.pdf") #make changes wrt k10 in file name
plt.show()
```

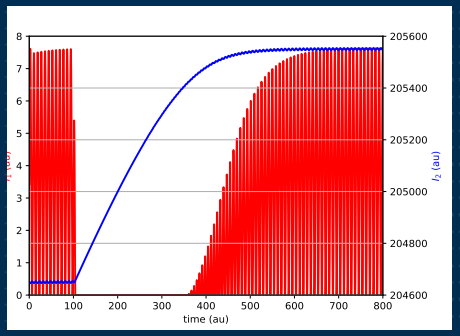

FIGURE A.26: Frequency compensated oscillator with coherent feedback at k_{10}=2048 and k_2 from 1→9. I_1 and I_2 are plotted as a function of time.

Frequency compensated oscillator with incoherent feedback at k_{10}=0

This section containes python scripts for the frequency compensated oscillator with incoherent feedback from Fig. 3.18. A background k_{10}=0 and step-wise perturbation k_2 from 1→9 at time t=500 are applied. A and E are plotted as a function of time in Fig. A.27 and Fig. A.28, respectively. Frequency is plotted as a function of time in Fig. A.29, and I_1 and I_2 are shown as a function of time in Fig. A.30.

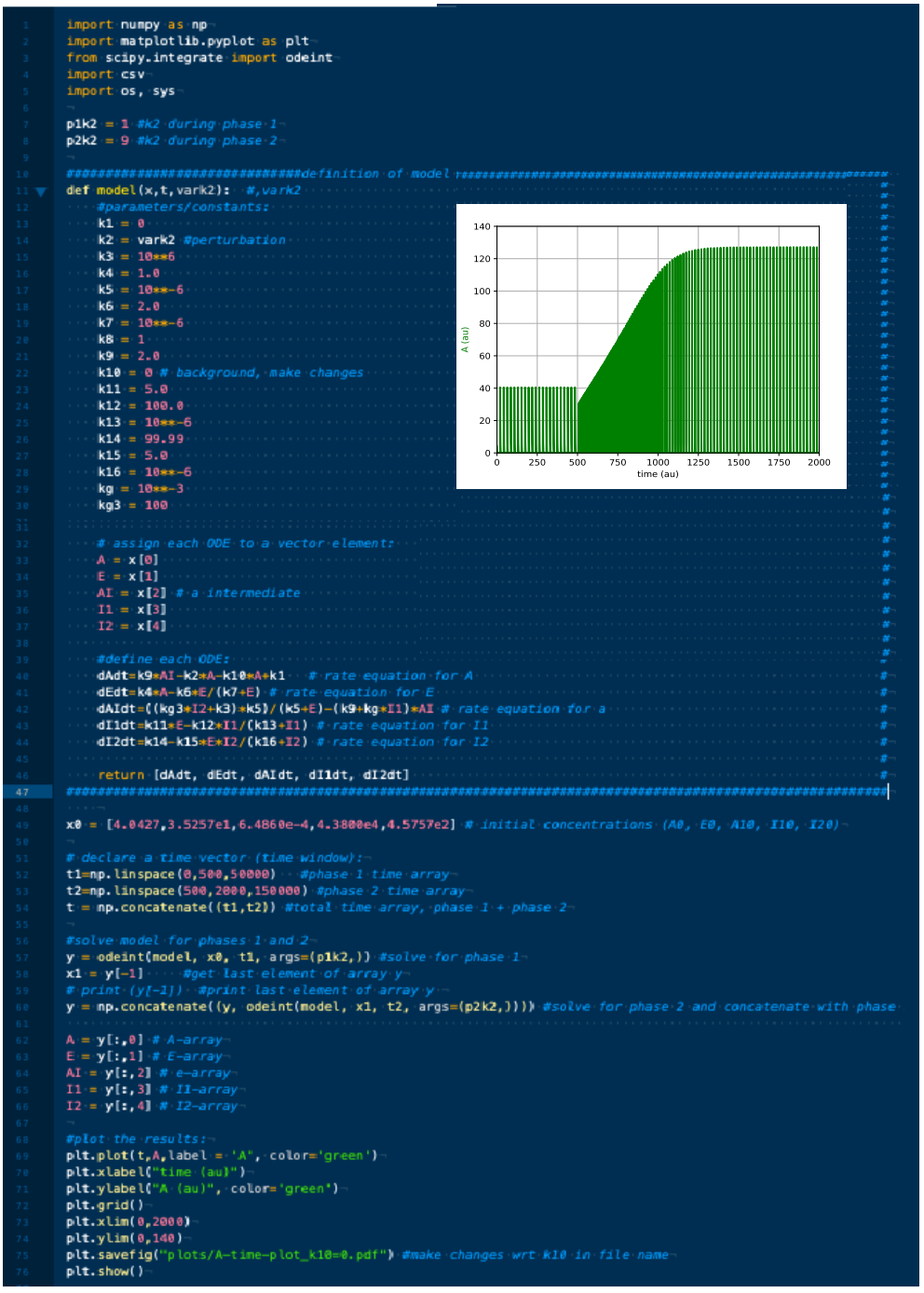

FIGURE A.27: Frequency compensated oscillator with incoherent feedback at k_{10}=0 and k_2 from 1→9. A is plotted as a function of time.

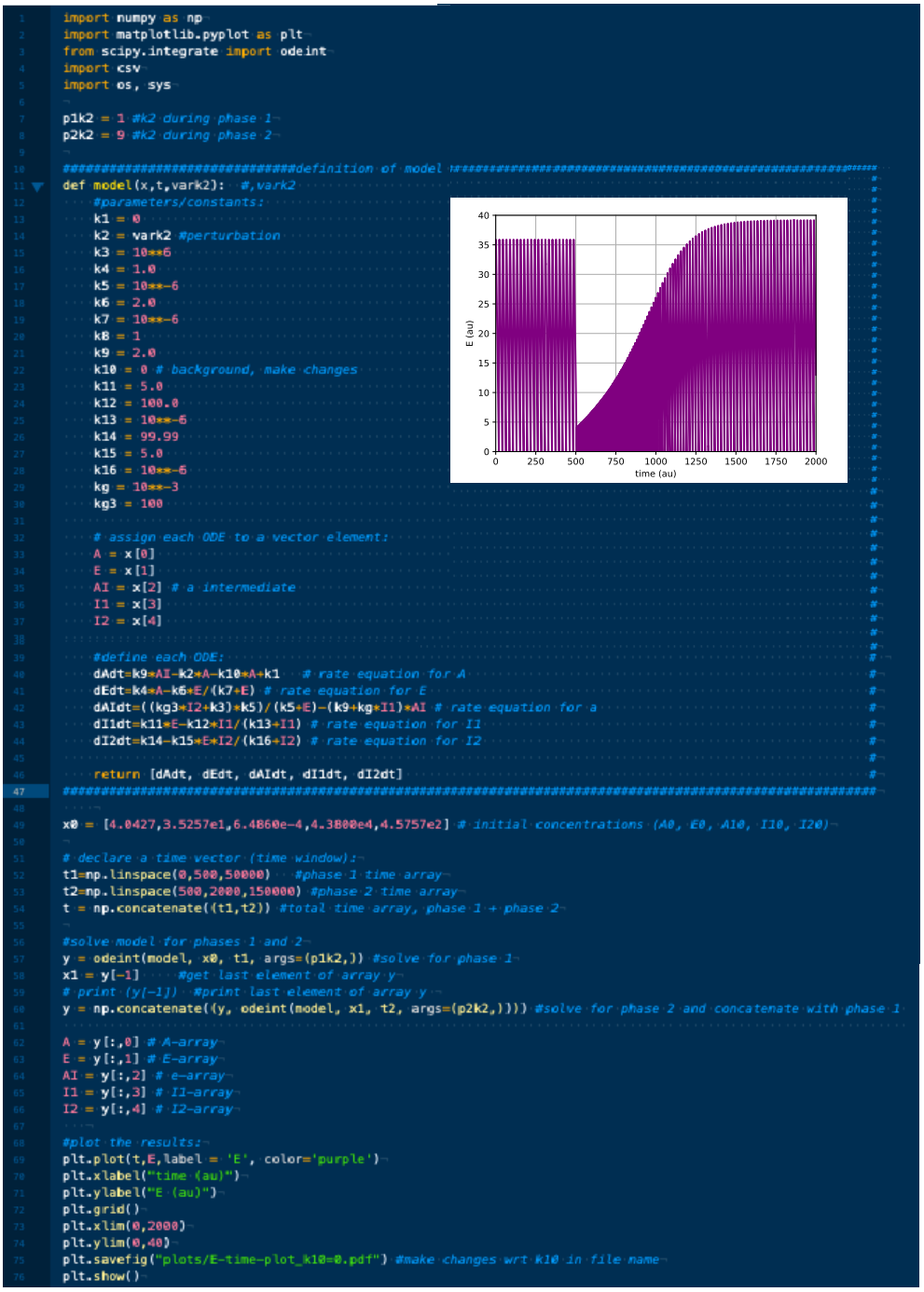


```python
import numpy as np
import matplotlib.pyplot as plt
from scipy.integrate import odeint
import csv
import os, sys

p1k2 = 1 #k2 during phase 1
p2k2 = 9 #k2 during phase 2

##############################definition of model ##########################################################
def model(x,t,vark2):  #,vark2
    #parameters/constants:
    k1 = 0
    k2 = vark2 #perturbation
    k3 = 10**6
    k4 = 1.0
    k5 = 10**-6
    k6 = 2.0
    k7 = 10**-6
    k8 = 1
    k9 = 2.0
    k10 = 0 # background, make changes
    k11 = 5.0
    k12 = 100.0
    k13 = 10**-6
    k14 = 99.99
    k15 = 5.0
    k16 = 10**-6
    kg = 10**-3
    kg3 = 100

    # assign each ODE to a vector element:
    A = x[0]
    E = x[1]
    AI = x[2] # a intermediate
    I1 = x[3]
    I2 = x[4]

    #define each ODE:
    dAdt=k9*AI-k2*A-k10*A+k1   # rate equation for A
    dEdt=k4*A-k6*E/(k7+E) # rate equation for E
    dAIdt=((kg3*I2+k3)*k5)/(k5+E)-(k9+kg*I1)*AI # rate equation for a
    dI1dt=k11*E-k12*I1/(k13+I1) # rate equation for I1
    dI2dt=k14-k15*E*I2/(k16+I2) # rate equation for I2

    return [dAdt, dEdt, dAIdt, dI1dt, dI2dt]
###############################################################################################################

x0 = [4.0427,3.5257e1,6.4860e-4,4.3800e4,4.5757e2] # initial concentrations (A0, E0, AI0, I10, I20)

# declare a time vector (time window):
t1=np.linspace(0,500,50000)   #phase 1 time array
t2=np.linspace(500,2000,150000) #phase 2 time array
t = np.concatenate((t1,t2)) #total time array, phase 1 + phase 2

#solve model for phases 1 and 2
y = odeint(model, x0, t1, args=(p1k2,)) #solve for phase 1
x1 = y[-1]    #get last element of array y
# print (y[-1])  #print last element of array y
y = np.concatenate((y, odeint(model, x1, t2, args=(p2k2,)))) #solve for phase 2 and concatenate with phase 1

A = y[:,0] # A-array
E = y[:,1] # E-array
AI = y[:,2] # e-array
I1 = y[:,3] # I1-array
I2 = y[:,4] # I2-array

#plot the results:
plt.plot(t,E,label = 'E', color='purple')
plt.xlabel("time (au)")
plt.ylabel("E (au)")
plt.grid()
plt.xlim(0,2000)
plt.ylim(0,40)
plt.savefig("plots/E-time-plot_k10=0.pdf") #make changes wrt k10 in file name
plt.show()
```

FIGURE A.28: Frequency compensated oscillator with incoherent feedback at k_{10}=0 and k_2 from 1→9. E is plotted as a function of time.

```python
import numpy as np
import matplotlib.pyplot as plt
from scipy.integrate import odeint
import csv
import os, sys

p1k2 = 1 #k2 during phase 1
p2k2 = 9 #k2 during phase 2

##############################definition of model ##########################################################################
def model(x,t,vark2):  #,vark2
    #parameters/constants:
    k1 = 0
    k2 = vark2 #perturbation
    k3 = 10**6
    k4 = 1.0
    k5 = 10**-6
    k6 = 2.0
    k7 = 10**-6
    k8 = 1
    k9 = 2.0
    k10 = 0 # background, make changes
    k11 = 5.0
    k12 = 100.0
    k13 = 10**-6
    k14 = 99.99
    k15 = 5.0
    k16 = 10**-6
    kg = 10**-3
    kg3 = 100

    # assign each ODE to a vector element:
    A = x[0]
    E = x[1]
    AI = x[2] # a intermediate
    I1 = x[3]
    I2 = x[4]

    #define each ODE:
    dAdt=k9*AI-k2*A-k10*A+k1   # rate equation for A
    dEdt=k4*A-k6*E/(k7+E) # rate equation for E
    dAIdt=((kg3+I2+k3)*k5)/(k5+E)-(k9+kg+I1)*AI # rate equation for a
    dI1dt=k11*E-k12*I1/(k13+I1) # rate equation for I1
    dI2dt=k14-k15*E*I2/(k16+I2) # rate equation for I2

    return [dAdt, dEdt, dAIdt, dI1dt, dI2dt]
##################################################################################################################################

x0 = [4.0427,3.5257e1,6.4860e-4,4.3800e4,4.5757e2] # initial concentrations (A0, E0, A10, I10, I20)


# declare a time vector (time window):
t1=np.linspace(0,500,50000)   #phase 1 time array
t2=np.linspace(500,2000,150000) #phase 2 time array
t = np.concatenate((t1,t2)) #total time array, phase 1 + phase 2

#solve model for phases 1 and 2
y = odeint(model, x0, t1, args=(p1k2,)) #solve for phase 1
x1 = y[-1]    #get last element of array y
# print (y[-1])  #print last element of array y
y = np.concatenate((y, odeint(model, x1, t2, args=(p2k2,)))) #solve for phase 2 and concatenate with phase 1

A = y[:,0] # A-array
E = y[:,1] # E-array
AI = y[:,2] # e-array
I1 = y[:,3] # I1-array
I2 = y[:,4] # I2-array

tmax=[]
freq=[]
per=[]
tfreq=[]
i=1
while(i>=1) and (i<=len(A)-2):
    if(A[i-1]<=A[i]) and (A[i]>=A[i+1]): #get Amax values
        tmax.append(t[i])                #get tmax values
    i=i+1

j=1
while(j>=1) and (j<=len(tmax)-1):
    period=tmax[j]-tmax[j-1]
    if(period>0):
        frequency=1/period
        if(frequency<0.5):
            per.append(period)
            freq.append(frequency)
            tfreq.append(tmax[j])
    j=j+1

#plot the frequency against time:
plt.plot(tfreq,freq,label = 'frequency', color='blue')
plt.xlabel("time (au)")
plt.ylabel("frequency (au)")
plt.grid()
plt.xlim(0,2000)
plt.ylim(0.03,0.43)
plt.savefig("plots/freq-time-plot_k10=0.pdf") # make changes wrt k10 in file name
plt.show()
```

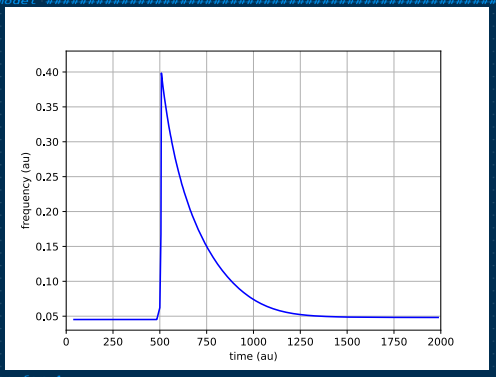

FIGURE A.29: Frequency compensated oscillator with incoherent feedback at k_{10}=0 and k_2 from 1→9. Frequency is plotted as a function of time.

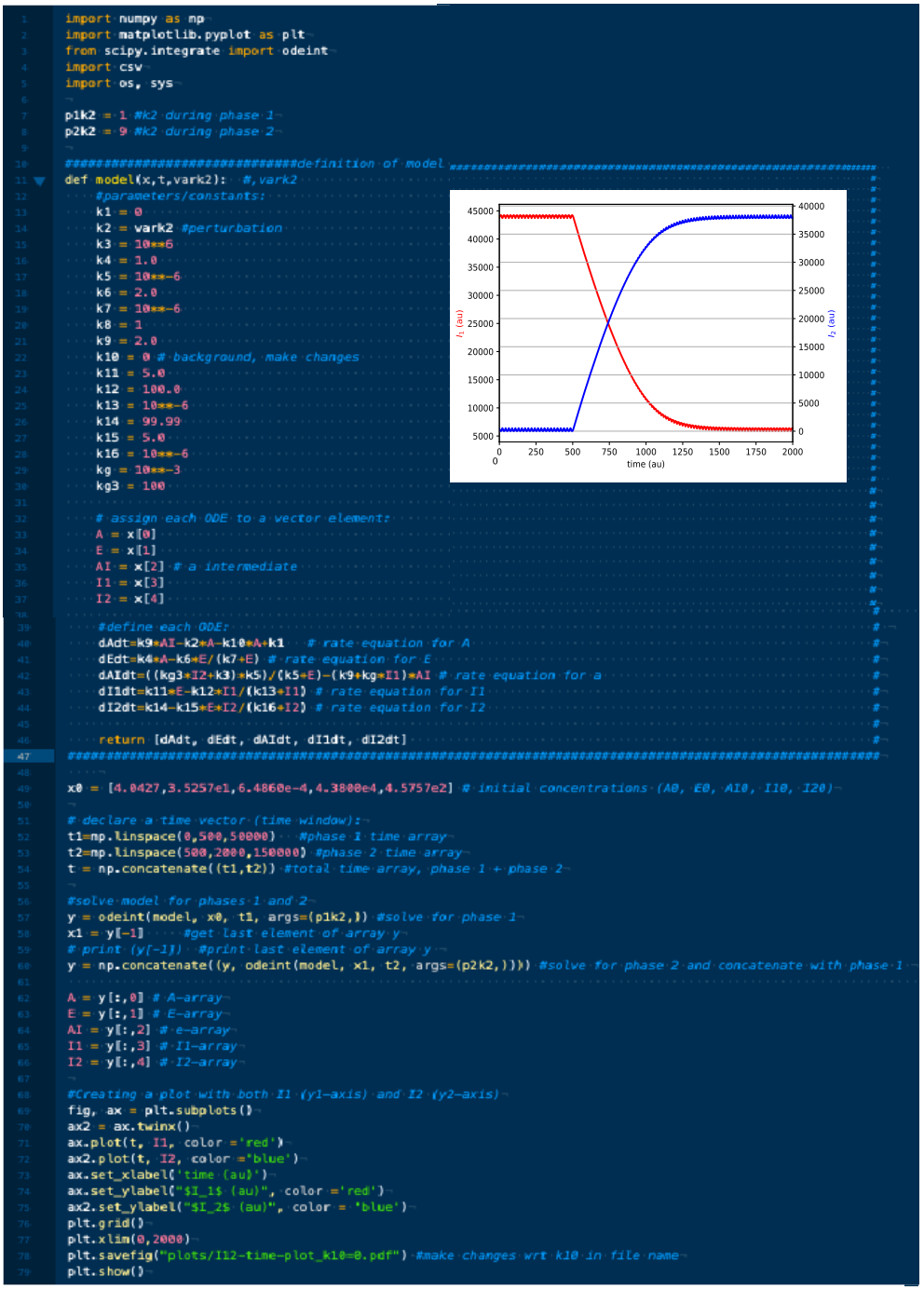

FIGURE A.30: Frequency compensated oscillator with incoherent feedback at k_{10}=0 and k_2 from 1→9. I_1 and I_2 are plotted as a function of time.

Frequency compensated oscillator with incoherent feedback at k_{10}=2

This section containes python scripts for the frequency compensated oscillator with incoherent feedback from Fig. 3.19. A background k_{10}=2 and step-wise perturbation k_2 from 1→9 at time t=500 are applied. A and E are plotted as a function of time in Fig. A.31 and Fig. A.32, respectively. Frequency is plotted as a function of time in Fig. A.33, and I_1 and I_2 are shown as a function of time in Fig. A.34.

```python
import numpy as np
import matplotlib.pyplot as plt
from scipy.integrate import odeint
import csv
import os, sys

p1k2 = 1 #k2 during phase 1
p2k2 = 9 #k2 during phase 2

##############################definition of model##########################################################
def model(x,t,vark2):  #,vark2
    #parameters/constants:
    k1 = 0
    k2 = vark2 #perturbation
    k3 = 10**6
    k4 = 1.0
    k5 = 10**-6
    k6 = 2.0
    k7 = 10**-6
    k8 = 1
    k9 = 2.0
    k10 = 2 # background, make changes
    k11 = 5.0
    k12 = 100.0
    k13 = 10**-6
    k14 = 99.99
    k15 = 5.0
    k16 = 10**-6
    kg = 10**-3
    kg3 = 100

    # assign each ODE to a vector element:
    A = x[0]
    E = x[1]
    AI = x[2] # a intermediate
    I1 = x[3]
    I2 = x[4]

    #define each ODE:
    dAdt=k9*AI-k2*A-k10*A+k1   # rate equation for A
    dEdt=k4*A-k6*E/(k7+E) # rate equation for E
    dAIdt=((kg3*I2+k3)*k5)/(k5+E)-(k9+kg*I1)*AI # rate equation for a
    dI1dt=k11*E-k12*I1/(k13+I1) # rate equation for I1
    dI2dt=k14-k15*E*I2/(k16+I2) # rate equation for I2

    return [dAdt, dEdt, dAIdt, dI1dt, dI2dt]
##########################################################################################################

x0 = [1.4906e-1,1.6789e-1,5.6795e-1,2.2515e4,2.1643e4] # initial concentrations (A0, E0, AI0, I10, I20)

# declare a time vector (time window):
t1=np.linspace(0,500,50000)   #phase 1 time array
t2=np.linspace(500,2000,150000) #phase 2 time array
t = np.concatenate((t1,t2)) #total time array, phase 1 + phase 2

#solve model for phases 1 and 2
y = odeint(model, x0, t1, args=(p1k2,)) #solve for phase 1
x1 = y[-1]      #get last element of array y
# print (y[-1])  #print last element of array y
y = np.concatenate((y, odeint(model, x1, t2, args=(p2k2,)))) #solve for phase 2 and concatenate with phase 1

A = y[:,0] # A-array
E = y[:,1] # E-array
AI = y[:,2] # e-array
I1 = y[:,3] # I1-array
I2 = y[:,4] # I2-array

#plot the results:
plt.plot(t,A,label = 'A', color='green')
plt.xlabel("time (au)")
plt.ylabel("A (au)", color="green")
plt.grid()
plt.xlim(0,2000)
plt.ylim(0,140)
plt.savefig("plots/A-time-plot_k10=2.pdf") #make changes wrt k10 in file name
plt.show()
```

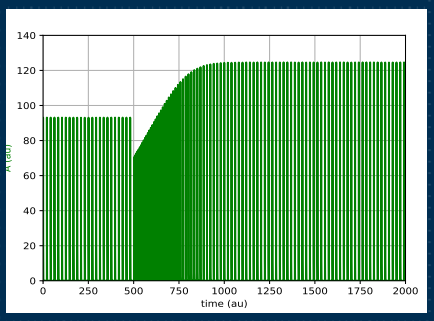

FIGURE A.31: Frequency compensated oscillator with incoherent feedback at k_{10}=2 and k_2 from 1→9. A is plotted as a function of time.

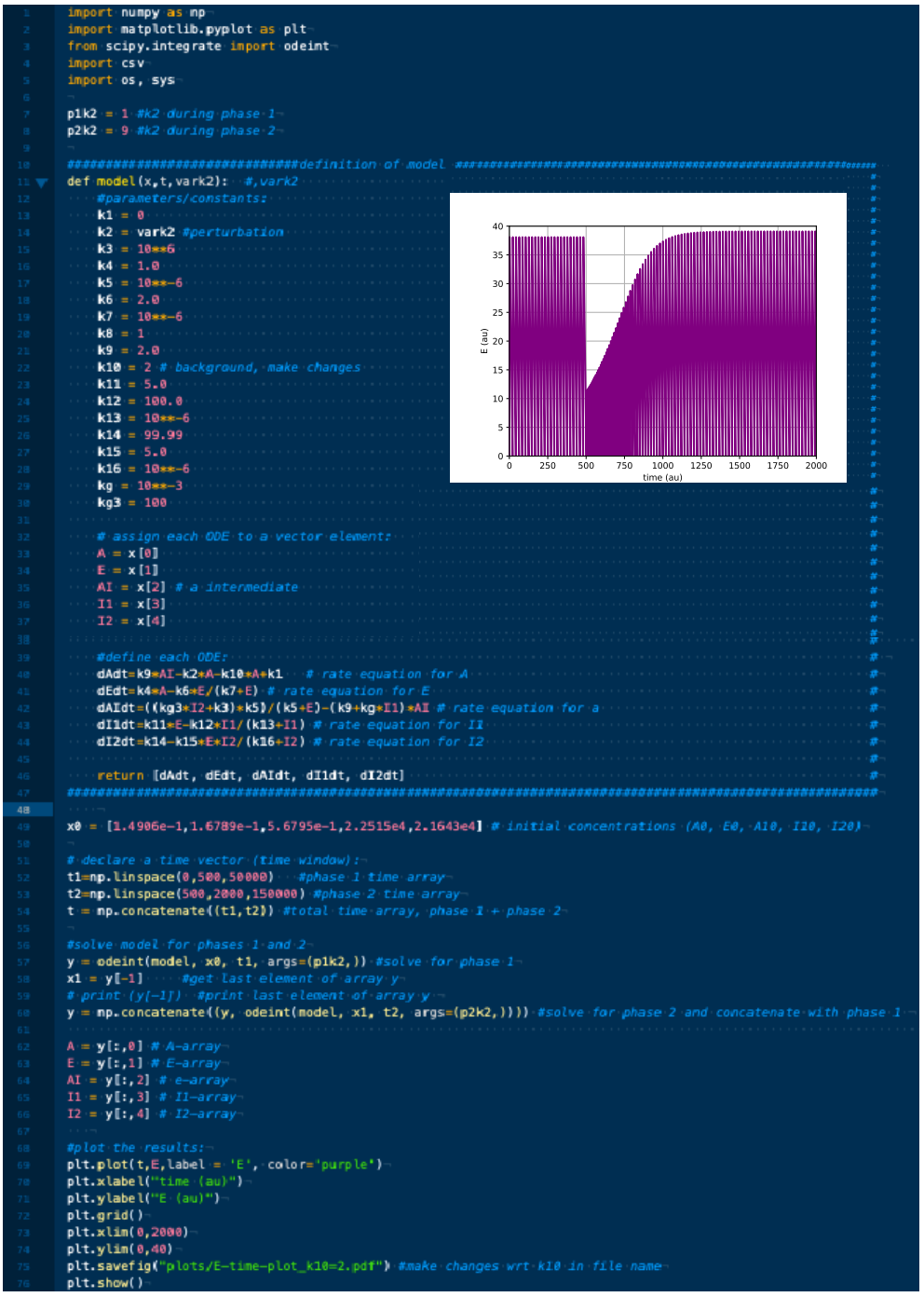


```python
import numpy as np
import matplotlib.pyplot as plt
from scipy.integrate import odeint
import csv
import os, sys

p1k2 = 1 #k2 during phase 1
p2k2 = 9 #k2 during phase 2

##############################definition of model ##########################################################
def model(x,t,vark2):  #,vark2
    #parameters/constants:
    k1 = 0
    k2 = vark2 #perturbation
    k3 = 10**6
    k4 = 1.0
    k5 = 10**-6
    k6 = 2.0
    k7 = 10**-6
    k8 = 1
    k9 = 2.0
    k10 = 2 # background, make changes
    k11 = 5.0
    k12 = 100.0
    k13 = 10**-6
    k14 = 99.99
    k15 = 5.0
    k16 = 10**-6
    kg = 10**-3
    kg3 = 100

    # assign each ODE to a vector element:
    A = x[0]
    E = x[1]
    AI = x[2] # a intermediate
    I1 = x[3]
    I2 = x[4]

    #define each ODE:
    dAdt=k9*AI-k2*A-k10*A+k1   # rate equation for A
    dEdt=k4*A-k6*E/(k7+E) # rate equation for E
    dAIdt=((kg3*I2+k3)*k5)/(k5+E)-(k9+kg*I1)*AI # rate equation for a
    dI1dt=k11*E-k12*I1/(k13+I1) # rate equation for I1
    dI2dt=k14-k15*E*I2/(k16+I2) # rate equation for I2

    return [dAdt, dEdt, dAIdt, dI1dt, dI2dt]
##############################################################################################################

x0 = [1.4906e-1,1.6789e-1,5.6795e-1,2.2515e4,2.1643e4] # initial concentrations (A0, E0, A10, I10, I20)

# declare a time vector (time window):
t1=np.linspace(0,500,50000)   #phase 1 time array
t2=np.linspace(500,2000,150000) #phase 2 time array
t = np.concatenate((t1,t2)) #total time array, phase 1 + phase 2

#solve model for phases 1 and 2
y = odeint(model, x0, t1, args=(p1k2,)) #solve for phase 1
x1 = y[-1]    #get last element of array y
# print (y[-1])  #print last element of array y
y = np.concatenate((y, odeint(model, x1, t2, args=(p2k2,)))) #solve for phase 2 and concatenate with phase 1

A = y[:,0] # A-array
E = y[:,1] # E-array
AI = y[:,2] # e-array
I1 = y[:,3] # I1-array
I2 = y[:,4] # I2-array

#plot the results:
plt.plot(t,E,label = 'E', color='purple')
plt.xlabel("time (au)")
plt.ylabel("E (au)")
plt.grid()
plt.xlim(0,2000)
plt.ylim(0,40)
plt.savefig("plots/E-time-plot_k10=2.pdf") #make changes wrt k10 in file name
plt.show()
```

FIGURE A.32: Frequency compensated oscillator with incoherent feedback at k_{10}=2 and k_2 from 1→9. E is plotted as a function of time.

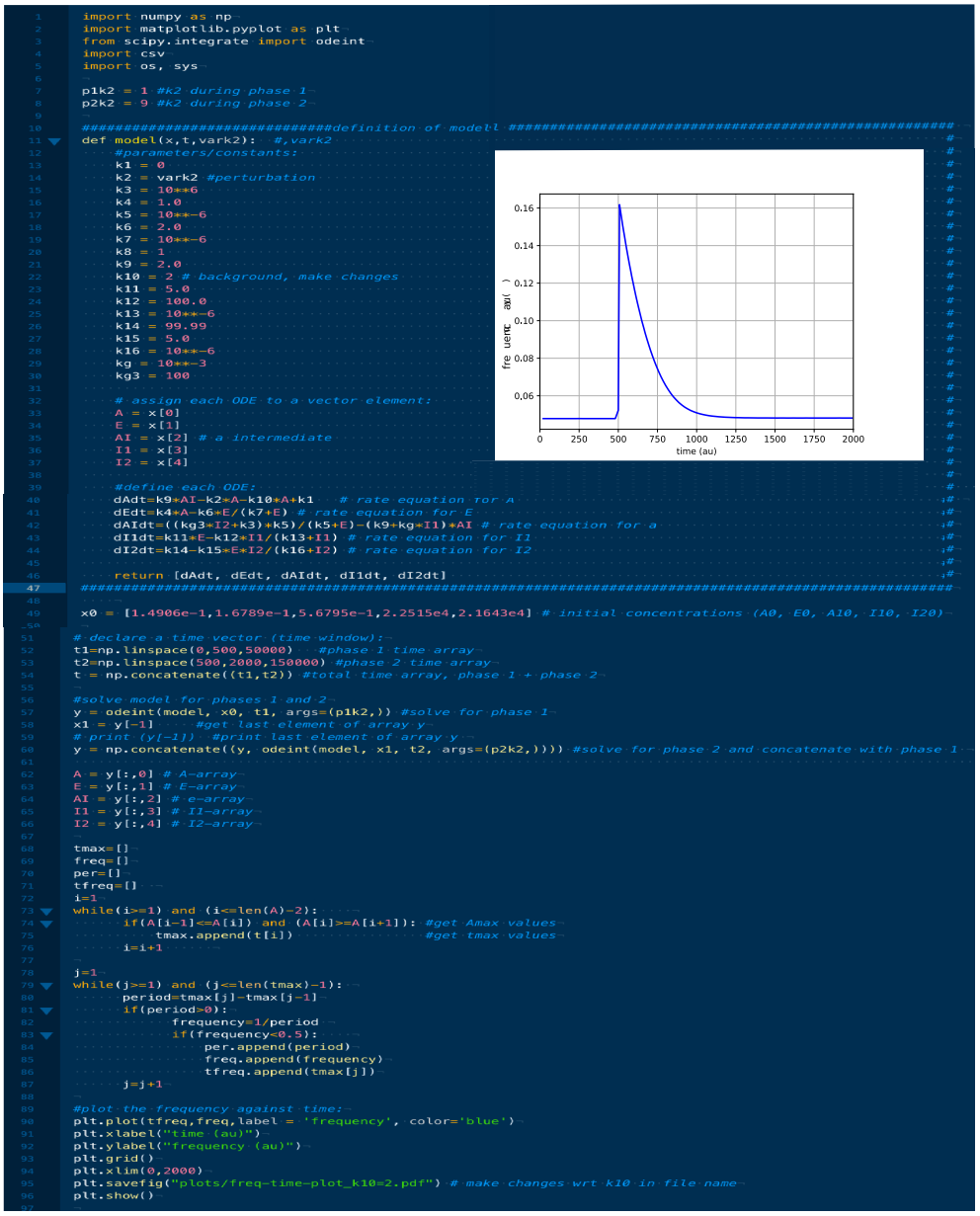

FIGURE A.33: Frequency compensated oscillator with incoherent feedback at k_{10}=2 and k_2 from 1→9. Frequency is plotted as a function of time.

```python
import numpy as np
import matplotlib.pyplot as plt
from scipy.integrate import odeint
import csv
import os, sys

p1k2 = 1 #k2 during phase 1
p2k2 = 9 #k2 during phase 2

################################definition of model ##################################################
def model(x,t,vark2):  #,vark2
    #parameters/constants:
    k1 = 0
    k2 = vark2 #perturbation
    k3 = 10**6
    k4 = 1.0
    k5 = 10**-6
    k6 = 2.0
    k7 = 10**-6
    k8 = 1
    k9 = 2.0
    k10 = 2 # background, make changes
    k11 = 5.0
    k12 = 100.0
    k13 = 10**-6
    k14 = 99.99
    k15 = 5.0
    k16 = 10**-6
    kg = 10**-3
    kg3 = 100

    # assign each ODE to a vector element:
    A = x[0]
    E = x[1]
    AI = x[2] # a intermediate
    I1 = x[3]
    I2 = x[4]

    #define each ODE:
    dAdt=k9*AI-k2*A-k10*A+k1   # rate equation for A
    dEdt=k4*A-k6*E/(k7+E) # rate equation for E
    dAIdt=((kg3*I2+k3)*k5)/(k5+E)-(k9+kg*I1)*AI # rate equation for a
    dI1dt=k11*E-k12*I1/(k13+I1) # rate equation for I1
    dI2dt=k14-k15*E*I2/(k16+I2) # rate equation for I2

    return [dAdt, dEdt, dAIdt, dI1dt, dI2dt]
#########################################################################################################

x0 = [1.4906e-1,1.6789e-1,5.6795e-1,2.2515e4,2.1643e4] # initial concentrations (A0, E0, AI0, I10, I20)

# declare a time vector (time window):
t1=np.linspace(0,500,50000)   #phase 1 time array
t2=np.linspace(500,2000,150000) #phase 2 time array
t = np.concatenate((t1,t2)) #total time array, phase 1 + phase 2

#solve model for phases 1 and 2
y = odeint(model, x0, t1, args=(p1k2,)) #solve for phase 1
x1 = y[-1]    #get last element of array y
# print (y[-1])  #print last element of array y
y = np.concatenate((y, odeint(model, x1, t2, args=(p2k2,)))) #solve for phase 2 and concatenate with phase 1

A = y[:,0] # A-array
E = y[:,1] # E-array
AI = y[:,2] # e-array
I1 = y[:,3] # I1-array
I2 = y[:,4] # I2-array

#Creating a plot with both I1 (y1-axis) and I2 (y2-axis)
fig, ax = plt.subplots()
ax2 = ax.twinx()
ax.plot(t, I1, color ='red')
ax2.plot(t, I2, color ='blue')
ax.set_xlabel('time (au)')
ax.set_ylabel("$I_1$ (au)", color ='red')
ax2.set_ylabel("$I_2$ (au)", color = 'blue')
plt.grid()
plt.xlim(0,2000)
plt.savefig("plots/I12-time-plot_k10=2.pdf") #make changes wrt k10 in file name
plt.show()
```

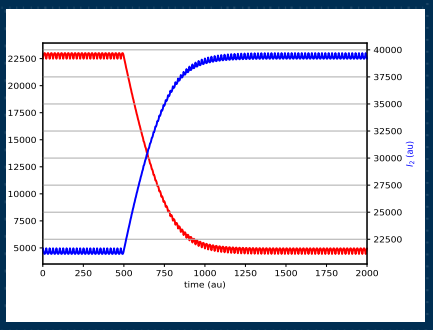

FIGURE A.34: Frequency compensated oscillator with incoherent feedback at k_{10}=2 and k_2 from 1→9. I_1 and I_2 are plotted as a function of time.

Oscillator with frequency independence at k_{14}=2

This section containes python scripts for the frequency independent oscillator from Fig. 3.22. A background k_{14}=2 and step-wise perturbation k_{15} from 1→2 at time t=100 are applied. A and E are plotted as a function of time in Fig. A.35 and Fig. A.36, respectively.

```python
import numpy as np
import matplotlib.pyplot as plt
from scipy.integrate import odeint
import csv
import os, sys

p1k15 = 1 #k15 during phase 1
p2k15 = 2 #k15 during phase 2

##############################definition of model##########################################
def model(x,t,vark15):  #,vark15
    #parameters/constants:
    k1 = 100
    k2 = 1
    k3 = 10**-6
    k4 = 1.0
    k5 = 100
    k6 = 1
    k7 = 10**-6
    k14 = 2 # background, make changes
    k15 = vark15 # perturbation

    # assign each ODE to a vector element:
    A = x[0]
    E = x[1]
    EI = x[2] # e intermediate

    #define each ODE:
    dAdt=k1+k14+k15-(k2*A*E/(k3+A))   # rate equation for A
    dEdt=k5*EI-(k6*E)/(k7+E) # rate equation for E
    dEIdt=k4*A-k5*EI # rate equation for e

    return [dAdt, dEdt, dEIdt]
##########################################################################################

x0 = [2.4708e-1,1.0235e2,2.4065e-3] # initial concentrations (A0, E0, E10)

# declare a time vector (time window):
t1=np.linspace(0,100,10000)   #phase 1 time array
t2=np.linspace(100,400,30000) #phase 2 time array
t = np.concatenate((t1,t2)) #total time array, phase 1 + phase 2

#solve model for phases 1 and 2
y = odeint(model, x0, t1, args=(p1k15,)) #solve for phase 1
x1 = y[-1]      #get last element of array y
# print (y[-1])  #print last element of array y
y = np.concatenate((y, odeint(model, x1, t2, args=(p2k15,)))) #solve for phase 2 and concatenate with phase 1

A = y[:,0] # A-array
E = y[:,1] # E-array
EI = y[:,2] # e-array

#plot the results:
plt.plot(t,A,label = 'A', color='green')
plt.xlabel("time (au)")
plt.ylabel("A (au)", color='green')
plt.grid()
plt.xlim(0,400)
plt.ylim(0,2.6)
plt.savefig("plots/A-time-plot_k14=2.pdf") #make changes wrt k14 in file name
plt.show()
```

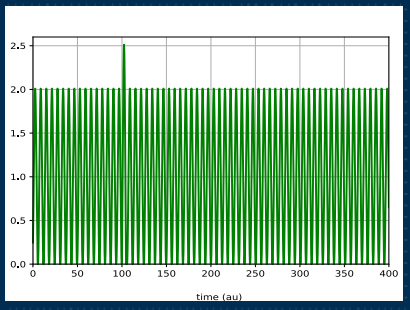

FIGURE A.35: Frequency independent oscillator at k_{14}=0 and k_{15} from 1→2. A is plotted as a function of time.

```python
import numpy as np
import matplotlib.pyplot as plt
from scipy.integrate import odeint
import csv
import os, sys

p1k15 = 1 #k15 during phase 1
p2k15 = 2 #k15 during phase 2

################################definition of model ##########################################
def model(x,t,vark15):  #,vark15
    #parameters/constants:
    k1 = 100
    k2 = 1
    k3 = 10**-6
    k4 = 1.0
    k5 = 100
    k6 = 1
    k7 = 10**-6
    k14 = 2 # background, make changes
    k15 = vark15 # perturbation

    # assign each ODE to a vector element:
    A = x[0]
    E = x[1]
    EI = x[2] # e intermediate

    #define each ODE:
    dAdt=k1+k14+k15-(k2*A*E/(k3+A))   # rate equation for A
    dEdt=k5*EI-(k6*E)/(k7+E) # rate equation for E
    dEIdt=k4*A-k5*EI # rate equation for e

    return [dAdt, dEdt, dEIdt]
###############################################################################################

x0 = [2.4708e-1,1.0235e2,2.4065e-3] # initial concentrations (A0, E0, EI0)

# declare a time vector (time window):
t1=np.linspace(0,100,10000)   #phase 1 time array
t2=np.linspace(100,400,30000) #phase 2 time array
t = np.concatenate((t1,t2)) #total time array, phase 1 + phase 2

#solve model for phases 1 and 2
y = odeint(model, x0, t1, args=(p1k15,)) #solve for phase 1
x1 = y[-1]    #get last element of array y
# print (y[-1])  #print last element of array y
y = np.concatenate((y, odeint(model, x1, t2, args=(p2k15,)))) #solve for phase 2 and concatenate with phase 1

A = y[:,0] # A-array
E = y[:,1] # E-array
EI = y[:,2] # e-array

#plot the results:
plt.plot(t,E,label = 'E', color='purple')
plt.xlabel("time (au)")
plt.ylabel("E (au)")
plt.grid()
plt.xlim(0,400)
plt.ylim(102,106)
plt.savefig("plots/E-time-plot_k14=2.pdf") #make changes wrt k14 in file name
plt.show()
```

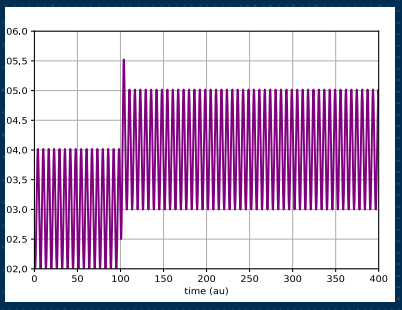

FIGURE A.36: Frequency independent oscillator at k_{14}=0 and k_{15} from 1→2. E is plotted as a function of time.

Oscillator with frequency independence at k_{14}=16

This section containes python scripts for the frequency independent oscillator from Fig. 3.23. A background k_{14}=16 and step-wise perturbation k_{15} from 1→10 at time t=100 are applied. A and E are plotted as a function of time in Fig. A.37 and Fig. A.38, respectively.

```python
import numpy as np
import matplotlib.pyplot as plt
from scipy.integrate import odeint
import csv
import os, sys

p1k15 = 1 #k15 during phase 1
p2k15 = 10 #k15 during phase 2

##############################definition of model##################################################
def model(x,t,vark15):  #,vark15
    #parameters/constants:
    k1 = 100
    k2 = 1
    k3 = 10**-6
    k4 = 1.0
    k5 = 100
    k6 = 1
    k7 = 10**-6
    k14 = 16 # background, make changes
    k15 = vark15 # perturbation

    # assign each ODE to a vector element:
    A = x[0]
    E = x[1]
    EI = x[2] # e intermediate

    #define each ODE:
    dAdt=k1+k14+k15-(k2*A*E/(k3+A))  # rate equation for A
    dEdt=k5*EI-(k6*E)/(k7+E) # rate equation for E
    dEIdt=k4*A-k5*EI # rate equation for e

    return [dAdt, dEdt, dEIdt]
###################################################################################################

x0 = [3.6316e-1,1.1780e2,3.7122e-3] # initial concentrations (A0, E0, EI0)

# declare a time vector (time window):
t1=np.linspace(0,100,10000)   #phase 1 time array
t2=np.linspace(100,400,30000) #phase 2 time array
t = np.concatenate((t1,t2)) #total time array, phase 1 + phase 2

#solve model for phases 1 and 2
y = odeint(model, x0, t1, args=(p1k15,)) #solve for phase 1
x1 = y[-1]    #get last element of array y
# print (y[-1])  #print last element of array y
y = np.concatenate((y, odeint(model, x1, t2, args=(p2k15,)))) #solve for phase 2 and concatenate with phase 1

A = y[:,0] # A-array
E = y[:,1] # E-array
EI = y[:,2] # e-array

#plot the results:
plt.plot(t,A,label = 'A', color='green')
plt.xlabel("time (au)")
plt.ylabel("A (au)", color='green')
plt.grid()
plt.xlim(0,400)
plt.ylim(0,9.5)
plt.savefig("plots/A-time-plot_k14=16.pdf") #make changes wrt k14 in file name
plt.show()
```

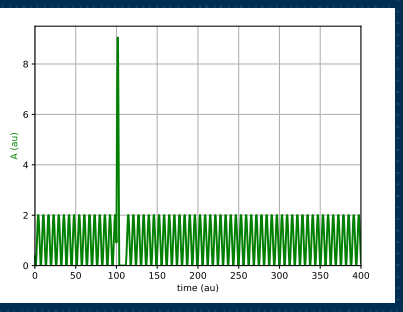

FIGURE A.37: Frequency independent oscillator at k_{15}=2 and k_2 from 1→2. A is plotted as a function of time.

```python
import numpy as np
import matplotlib.pyplot as plt
from scipy.integrate import odeint
import csv
import os, sys

p1k15 = 1 #k15 during phase 1
p2k15 = 10 #k15 during phase 2

##############################definition of model ##################################################
def model(x,t,vark15):  #,vark15
    #parameters/constants:
    k1 = 100
    k2 = 1
    k3 = 10**-6
    k4 = 1.0
    k5 = 100
    k6 = 1
    k7 = 10**-6
    k14 = 16 # background, make changes
    k15 = vark15 # perturbation

    # assign each ODE to a vector element:
    A = x[0]
    E = x[1]
    EI = x[2] # e intermediate

    #define each ODE:                                                                              #
    dAdt=k1+k14+k15-(k2*A*E/(k3+A))   # rate equation for A                                        #
    dEdt=k5*EI-(k6*E)/(k7+E) # rate equation for E                                                 #
    dEIdt=k4*A-k5*EI # rate equation for e                                                         #
                                                                                                   #
    return [dAdt, dEdt, dEIdt]                                                                     #
#####################################################################################################

x0 = [3.6316e-1,1.1780e2,3.7122e-3] # initial concentrations (A0, E0, EI0)

# declare a time vector (time window):
t1=np.linspace(0,100,10000)   #phase 1 time array
t2=np.linspace(100,400,30000) #phase 2 time array
t = np.concatenate((t1,t2)) #total time array, phase 1 + phase 2

#solve model for phases 1 and 2
y = odeint(model, x0, t1, args=(p1k15,)) #solve for phase 1
x1 = y[-1]      #get last element of array y
# print (y[-1])  #print last element of array y
y = np.concatenate((y, odeint(model, x1, t2, args=(p2k15,)))) #solve for phase 2 and concatenate with phase 1

A = y[:,0] # A-array
E = y[:,1] # E-array
EI = y[:,2] # e-array

#plot the results:
plt.plot(t,E,label = 'E', color='purple')
plt.xlabel("time (au)")
plt.ylabel("E (au)")
plt.grid()
plt.xlim(0,400)
plt.savefig("plots/E-time-plot_k14=16.pdf") #make changes wrt k14 in file name
plt.show()
```

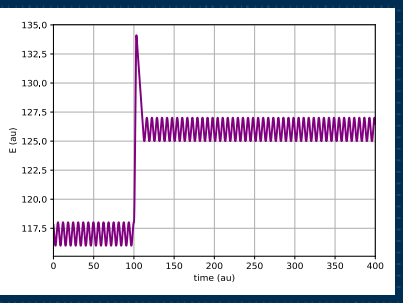

FIGURE A.38: Oscillator with frequency independence. E is plotted as a function of time.

Appendix B

MATLAB scripts

B.1 MATLAB scripts for m1-m8 controllers

This section provides MATLAB scripts for each of the m1-m8 controllers' (Fig. 2.1) response kinetics. The m1 controller will be used as an example. The other MATLAB scripts are run in a similar way.

m1 controller

Three MATLAB scripts regarding the m1 controller, "m1.m", "run_m1.m", and "A_merged _data.m", must be inside the current working folder, as well as an additional folder called "output" that has three subfolders named "A-data", "t-data" and "figures". "m1.m" containes the rate equations of m1. The response amplitude of A at a particular background k_4 can be seen by running "run_m1.m". These scripts incorporate different k_4 values from the one used in Fig. 3.3b but they generate the same type of resetting kinetics.

Panel a in Fig. B.1 shows "run_m1.m" at k_4=128. Running this script generates "k_4=128.txt" (inside "A-data" and "t-data"). Together with "m1.py" (panel b) the resulting response amplitude (panel c) can be seen in "A_k4=128.pdf" (inside "figures"). This script can be run at different backgrounds by changing the k_4 value in panel a, and inserting the corresponding initial concentrations of A and E.

a

```
% matlab calculation of m1
clear all
warning('off','all')

% define matlab rate constant vector k; k(i),ith element in k;
% from fortran rate constants Ki;

% fortran <=> matlab (motif 1)
%-------------------------------
% K1=0.0    <=> k(1)
% K2=1.0    <=> k(2) step-perturbation:
%                  1 (phase 1, t<10)--> 5 (phase 2, t>=10)
% K3=1.0    <=> k(3) rate constant for compensatory flux
% K4        <=> k(4) background, variable
% K5=3.0    <=> k(5) defines set-point
% K6=1.0    <=> k(6) defines set-point
% KM=1.e-6  <=> k(7) KM or k7 to get zero-order removal of E

%vector of rate constant values:
 %   k1 k2 k3  k4  k5  k6   k7
 k =[0  1  1   128   3.0 1.0 1.e-6];

%  total simulation time
T=[0 200.00];

%  assignments motif 1 zero-order controller:
%  y(1) <-> A
%  y(2) <-> E

%  initial concentrations:
y0=[3.0 387.0];

% options for numerical integration
options = odeset('RelTol',1.0e-4,'absTol',1e-7,'MaxStep',0.01);
% Solve model
[T, Y]=ode23s(@m1,T,y0,options,k);

[minValue, minIndex] = min(Y(:,1));
 Amax=3-minValue;
 mkdir ./output/A-data
 mkdir ./output/t-data
 mkdir ./output/figures

 Adata = fopen('./output/A-data/k4=128.txt','w');
 fprintf(Adata,'%f\n',Y(:,1));

 tdata = fopen('./output/t-data/k4=128.txt','w');
 fprintf(tdata,'%f\n',T);

figure % make a figure
plot(T,Y(:,1),'LineWidth',2.0);
xlabel('time (au)');
ylabel('A (au)');
grid on;
str1=sprintf('k_4=128, ΔAmax= %.4f \n ', Amax);
title(str1,'FontSize',16);
exportgraphics(figure(1), './output/figures/A_k4=128.pdf');
```

b

```
function dy=m1(T,y,k);

dy=zeros(2,1);

%  assignments motif 1 controller (Fig. 4):
%  y(1) <-> A
%  y(2) <-> E


%k2 step increase from t>= 10.0:
if T >= 10.00
    k(2)=5.0;
end


dy(1)=k(1)-(k(2)+k(4))*y(1)+k(3)*y(2);
dy(2)=k(5)-y(1)*((k(6)*y(2))/(k(7)+y(2)));
```

c

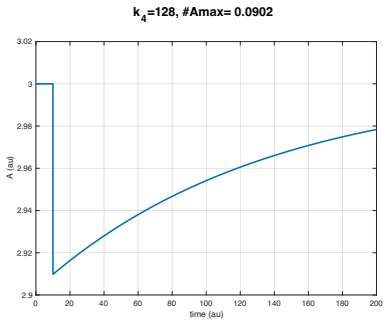

FIGURE B.1: MATLAB scripts for generating m1's response amplitude of A at background k_4=128. Run the script in panel a in order to generate the response amplitude of A in panel c. This can be run at different backgrounds by changing the k_4 value in panel a, and inserting the corresponding initial concentrations of A and E. Panel b contains the rate equations.

Response amplitudes for different k_4-values (k_4=0, 1, 2, 4, 8, 16, 32, 64, 128) can be merged together by running "A_merged_data.m" (Fig. B.2a). This creates "A_merged.pdf" (inside "figures"), and shows similar resetting kinetics (panel b) as in Fig. 3.3b.

a

```
% opens and reads files in 'A-data' and 't-data' directories
% and plots an overlay of all A-data/A-profiles as a function
% of time.

formatSpec = '%f'; %format specifier

%assign FileIDs/FileHandles for files:
Adata0 = fopen('./output/A-data/k4=0.txt','r');
tdata0 = fopen('./output/t-data/k4=0.txt','r');

Adata1 = fopen('./output/A-data/k4=1.txt','r');
tdata1 = fopen('./output/t-data/k4=1.txt','r');

Adata2 = fopen('./output/A-data/k4=2.txt','r');
tdata2 = fopen('./output/t-data/k4=2.txt','r');

Adata4 = fopen('./output/A-data/k4=4.txt','r');
tdata4 = fopen('./output/t-data/k4=4.txt','r');

Adata8 = fopen('./output/A-data/k4=8.txt','r');
tdata8 = fopen('./output/t-data/k4=8.txt','r');

Adata16 = fopen('./output/A-data/k4=16.txt','r');
tdata16 = fopen('./output/t-data/k4=16.txt','r');

Adata32 = fopen('./output/A-data/k4=32.txt','r');
tdata32 = fopen('./output/t-data/k4=32.txt','r');

Adata64 = fopen('./output/A-data/k4=64.txt','r');
tdata64 = fopen('./output/t-data/k4=64.txt','r');

Adata128 = fopen('./output/A-data/k4=128.txt','r');
tdata128 = fopen('./output/t-data/k4=128.txt','r');

%read files, both A and t values:
A0 = fscanf(Adata0,formatSpec);
t0 = fscanf(tdata0,formatSpec);

A1 = fscanf(Adata1,formatSpec);
t1 = fscanf(tdata1,formatSpec);

A2 = fscanf(Adata2,formatSpec);
t2 = fscanf(tdata2,formatSpec);

A4 = fscanf(Adata4,formatSpec);
t4 = fscanf(tdata4,formatSpec);

A8 = fscanf(Adata8,formatSpec);
t8 = fscanf(tdata8,formatSpec);

A16 = fscanf(Adata16,formatSpec);
t16 = fscanf(tdata16,formatSpec);

A32 = fscanf(Adata32,formatSpec);
t32 = fscanf(tdata32,formatSpec);

A64 = fscanf(Adata64,formatSpec);
t64 = fscanf(tdata64,formatSpec);

A128 = fscanf(Adata128,formatSpec);
t128 = fscanf(tdata128,formatSpec);

figure % make figure of all A profiles
plot(t0,A0,t1,A1,t2,A2,t4,A4,t8,A8,t16,A16,t32,A32,t64,A64,t128, ...
    A128,'LineWidth',2.0);
xlabel('time (au)');
ylabel('A (au)');
xlim([0 100])
grid on;
legend('k_4=0','k_4=1','k_4=2','k_4=4','k_4=8','k_4=16','k_4=32', ...
    'k_4=64','k_4=128')
exportgraphics(figure(1), './output/figures/A_merged.pdf');
```

b

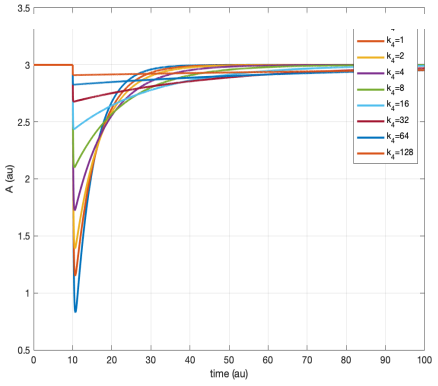

FIGURE B.2: MATLAB script (panel a) for generating m1's resetting kinetics (panel b). The resetting kinetics are similar to Fig. 3.3b. Run this script after producing the response amplitudes for k_4=0, 1, 2, 4, 8, 16, 32, 64, 128.

m2 controller

a

```
% matlab calculation of m2
clear all
warning('off','all')

% define matlab rate constant vector k; k(i),ith element in k;
% from fortran rate constants Ki;

% fortran <=> matlab (motif 1)
%-----------------------------
% K1=0.0    <=> k(1)
% K2=1.0    <=> k(2) step-perturbation:
%                  1 (phase 1, t<100)--> 5 (phase 2, t>=100)
% K3=1.e+4     <=> k(3) rate constant for compensatory flux
% K4         <=> k(4) background, variable
% K5=1.0    <=> k(5) defines set-point
% K6=3.0    <=> k(6) defines set-point
% KM=1.e-6  <=> k(7) KM or k7 to get zero-order removal of E
% KI=0.1    <=> k(8) inhibition constant

%vector of rate constant values:
 %   k1 k2  k3   k4  k5   k6     k7   k8
  k =[0  1  1.e+4  80  1.0  3.0  1.e-6  0.1];

%  total simulation time
T=[0 500.00];


%  assignments motif 2 zero-order controller:
%  y(1) <-> A
%  y(2) <-> E

%  initial concentrations:
y0=[3.0 4.02];


% options for numerical integration
options = odeset('RelTol',1.0e-4,'absTol',1e-7,'MaxStep',0.01);
% Solve model
[T, Y]=ode23s(@m2,T,y0,options,k);

[minValue, minIndex] = min(Y(:,1));
 Amax=3-minValue;
 mkdir ./output/A-data
 mkdir ./output/t-data
 mkdir ./output/figures

 Adata = fopen('./output/A-data/k4=80.txt','w');
 fprintf(Adata,'%f\n',Y(:,1));

 tdata = fopen('./output/t-data/k4=80.txt','w');
 fprintf(tdata,'%f\n',T);

figure % make a figure
plot(T,Y(:,1),'LineWidth',2.0);
xlabel('time (au)');
ylabel('A (au)');
grid on;
str1=sprintf('k_4=80, ΔAmax= %.4f \n ', Amax);
title(str1,'FontSize',16);
exportgraphics(figure(1), './output/figures/A_k4=80.pdf');
```

b

```
function dy=m2(T,y,k);

dy=zeros(2,1);

%  assignments motif 2 controller (Fig. 8):
%  y(1) <-> A
%  y(2) <-> E


%k2 step increase from t>= 100.0:
if T >= 100.00
    k(2)=5.0;
end


dy(1)=k(1)-(k(2)+k(4))*y(1)+(k(3)*k(8))/(k(8)+y(2));
dy(2)=k(5)*y(1)-(k(6)*y(2))/(k(7)+y(2));
```

c

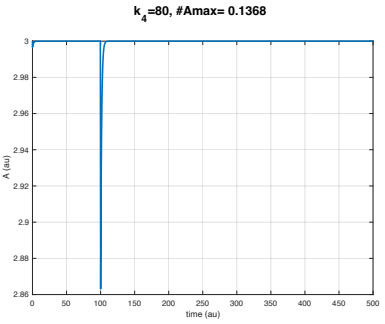

FIGURE B.3: MATLAB scripts for generating m2's response amplitude of A at background k_4=80. Run the script in panel a in order to generate the response amplitude of A in panel c. This can be run at different backgrounds by changing the k_4 value in panel a, and inserting the corresponding initial concentrations of A and E. Panel b contains the rate equations.

a

```
% opens and reads files in 'A-data' and 't-data' directories
% and plots an overlay of all A-data/A-profiles as a function
% of time.

formatSpec = '%f'; %format specifier

%assign FileIDs/FileHandles for files:
Adata0 = fopen('./output/A-data/k4=0.txt','r');
tdata0 = fopen('./output/t-data/k4=0.txt','r');

Adata1 = fopen('./output/A-data/k4=1.txt','r');
tdata1 = fopen('./output/t-data/k4=1.txt','r');

Adata5 = fopen('./output/A-data/k4=5.txt','r');
tdata5 = fopen('./output/t-data/k4=5.txt','r');

Adata10 = fopen('./output/A-data/k4=10.txt','r');
tdata10 = fopen('./output/t-data/k4=10.txt','r');

Adata20 = fopen('./output/A-data/k4=20.txt','r');
tdata20 = fopen('./output/t-data/k4=20.txt','r');

Adata40 = fopen('./output/A-data/k4=40.txt','r');
tdata40 = fopen('./output/t-data/k4=40.txt','r');

Adata80 = fopen('./output/A-data/k4=80.txt','r');
tdata80 = fopen('./output/t-data/k4=80.txt','r');


%read files, both A and t values:
A0 = fscanf(Adata0,formatSpec);
t0 = fscanf(tdata0,formatSpec);

A1 = fscanf(Adata1,formatSpec);
t1 = fscanf(tdata1,formatSpec);

A5 = fscanf(Adata5,formatSpec);
t5 = fscanf(tdata5,formatSpec);

A10 = fscanf(Adata10,formatSpec);
t10 = fscanf(tdata10,formatSpec);

A20 = fscanf(Adata20,formatSpec);
t20 = fscanf(tdata20,formatSpec);

A40 = fscanf(Adata40,formatSpec);
t40 = fscanf(tdata40,formatSpec);

A80 = fscanf(Adata80,formatSpec);
t80 = fscanf(tdata80,formatSpec);


figure % make figure of all A profiles
plot(t0,A0,t1,A1,t5,A5,t10,A10,t20,A20,t40,A40,t80,A80,'LineWidth',2.0);
xlabel('time (au)');
ylabel('A (au)');
%xlim([0 100])
grid on;
legend('k_4=0','k_4=1','k_4=5','k_4=10','k_4=20','k_4=40','k_4=80')
exportgraphics(figure(1), './output/figures/A_merged.pdf');
```

b

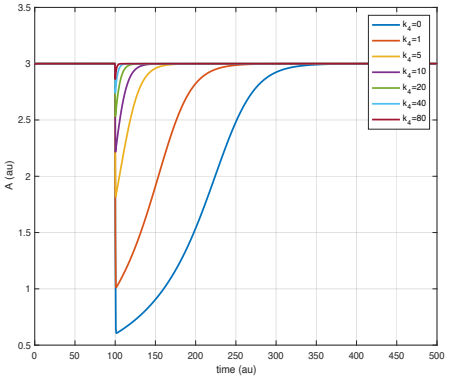

FIGURE B.4: MATLAB script (panel a) for generating m2's resetting kinetics (panel b). The resetting kinetics are similar to Fig. 3.7b. Run this script after producing the response amplitudes for k_4=0, 1, 5, 10, 20, 40, 80.

m3 controller

a

```
% matlab calculation of m2
clear all
warning('off','all')

% define matlab rate constant vector k; k(i),ith element in k;
% from fortran rate constants Ki;

% fortran <==> matlab (motif 1)
%-------------------------------
% K1=0.0     <==> k(1)
% K2=1.0     <==> k(2) step-perturbation:
%                  1 (phase 1, t<100)--> 5 (phase 2, t>=100)
% K3=1.0     <==> k(3) rate constant for compensatory flux
% K4         <==> k(4) background, variable
% K5=31      <==> k(5) defines set-point
% K6=1.0     <==> k(6) defines set-point
% KM=1.e-6   <==> k(7) KM or k7 to get zero-order removal of E
% KI=0.1     <==> k(8) inhibition constant

%vector of rate constant values:
 %   k1 k2  k3 k4  k5  k6     k7    k8
 k =[0  1  1.0  128  31  1.0  1.e-6  0.1];

%  total simulation time
T=[0 200.00];


%  assignments motif 3 zero-order controller:
%  y(1) <-> A
%  y(2) <-> E

%  initial concentrations:
y0=[3.0 387.0];


% options for numerical integration
options = odeset('RelTol',1.0e-4,'absTol',1e-7,'MaxStep',0.01);
% Solve model
[T, Y]=ode23s(@m3,T,y0,options,k);

[minValue, minIndex] = min(Y(:,1));
 Amax=3-minValue;
 mkdir ./output/A-data
 mkdir ./output/t-data
 mkdir ./output/figures

 Adata = fopen('./output/A-data/k4=128.txt','w');
 fprintf(Adata,'%f\n',Y(:,1));

 tdata = fopen('./output/t-data/k4=128.txt','w');
 fprintf(tdata,'%f\n',T);

figure % make a figure
plot(T,Y(:,1),'LineWidth',2.0);
xlabel('time (au)');
ylabel('A (au)');
grid on;
str1=sprintf('k_4=128, ΔAmax= %.4f \n ', Amax);
title(str1,'FontSize',16);
exportgraphics(figure(1), './output/figures/A_k4=128.pdf');
```

b

```
function dy=m2(T,y,k);

dy=zeros(2,1);

%  assignments motif 3 controller (Fig. S2):
%  y(1) <-> A
%  y(2) <-> E


%k2 step increase from t>= 10.0:
if T >= 10.00
    k(2)=5.0;
end



dy(1)=k(1)-(k(2)+k(4))*y(1)+k(3)*y(2);
dy(2)=((k(5)*k(8))/(k(8)+y(1)))-((k(6)*y(2))/(k(7)+y(2)));
```

c

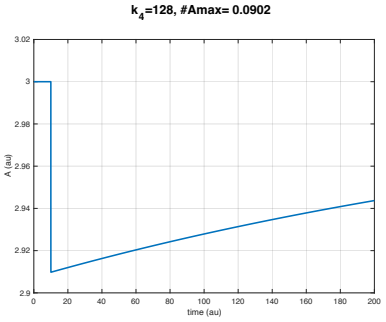

FIGURE B.5: MATLAB scripts for generating m3's response amplitude of A at background k_4=128. Run the script in panel a in order to generate the response amplitude of A in panel c. This can be run at different backgrounds by changing the k_4 value in panel a, and inserting the corresponding initial concentrations of A and E. Panel b contains the rate equations.

```
% opens and reads files in 'A-data' and 't-data' directories
% and plots an overlay of all A-data/A-profiles as a function
% of time.

formatSpec = '%f'; %format specifier

%assign FileIDs/FileHandles for files:
Adata0 = fopen('./output/A-data/k4=0.txt','r');
tdata0 = fopen('./output/t-data/k4=0.txt','r');

Adata1 = fopen('./output/A-data/k4=1.txt','r');
tdata1 = fopen('./output/t-data/k4=1.txt','r');

Adata2 = fopen('./output/A-data/k4=2.txt','r');
tdata2 = fopen('./output/t-data/k4=2.txt','r');

Adata4 = fopen('./output/A-data/k4=4.txt','r');
tdata4 = fopen('./output/t-data/k4=4.txt','r');

Adata8 = fopen('./output/A-data/k4=8.txt','r');
tdata8 = fopen('./output/t-data/k4=8.txt','r');

Adata16 = fopen('./output/A-data/k4=16.txt','r');
tdata16 = fopen('./output/t-data/k4=16.txt','r');

Adata32 = fopen('./output/A-data/k4=32.txt','r');
tdata32 = fopen('./output/t-data/k4=32.txt','r');

Adata64 = fopen('./output/A-data/k4=64.txt','r');
tdata64 = fopen('./output/t-data/k4=64.txt','r');

Adata128 = fopen('./output/A-data/k4=128.txt','r');
tdata128 = fopen('./output/t-data/k4=128.txt','r');

%read files, both A and t values:
A0 = fscanf(Adata0,formatSpec);
t0 = fscanf(tdata0,formatSpec);

A1 = fscanf(Adata1,formatSpec);
t1 = fscanf(tdata1,formatSpec);

A2 = fscanf(Adata2,formatSpec);
t2 = fscanf(tdata2,formatSpec);

A4 = fscanf(Adata4,formatSpec);
t4 = fscanf(tdata4,formatSpec);

A8 = fscanf(Adata8,formatSpec);
t8 = fscanf(tdata8,formatSpec);

A16 = fscanf(Adata16,formatSpec);
t16 = fscanf(tdata16,formatSpec);

A32 = fscanf(Adata32,formatSpec);
t32 = fscanf(tdata32,formatSpec);

A64 = fscanf(Adata64,formatSpec);
t64 = fscanf(tdata64,formatSpec);

A128 = fscanf(Adata128,formatSpec);
t128 = fscanf(tdata128,formatSpec);

figure % make figure of all A profiles
plot(t0,A0,t1,A1,t2,A2,t4,A4,t8,A8,t16,A16,t32,A32,t64,A64,t128,A128, ...
    'LineWidth',2.0);
xlabel('time (au)');
ylabel('A (au)');
xlim([0 100])
grid on;
legend('k_4=0','k_4=1','k_4=2','k_4=4','k_4=8','k_4=16','k_4=32', ...
    'k_4=64','k_4=128')
exportgraphics(figure(1), './output/figures/A_merged.pdf');
```

a b

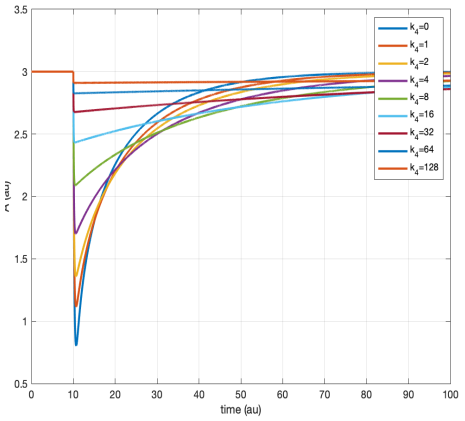

FIGURE B.6: MATLAB script (panel a) for generating m3's resetting kinetics (panel b). The resetting kinetics are similar to Fig. 3.4b. Run this script after producing the response amplitudes for k_4=0, 1, 2, 4, 8, 16, 32, 64, 128

m4 controller

a

```
% matlab calculation of m4
clear all
warning('off','all')

% define matlab rate constant vector k; k(i),ith element in k;
% from fortran rate constants Ki;

% fortran <=> matlab (motif 1)
%-----------------------------
% K1=0.0     <=> k(1)
% K2=1.0     <=> k(2) step-perturbation:
%                   1 (phase 1, t<100)--> 5 (phase 2, t>=100)
% K3=1.e+4   <=> k(3) rate constant for compensatory flux
% K4         <=> k(4) background, variable
% K5=1.0     <=> k(5) defines set-point
% K6=31      <=> k(6) defines set-point
% KM=1.e-6   <=> k(7) KM or k7 to get zero-order removal of E
% KI=0.1     <=> k(8) inhibition constant
% K9=0.1     <=> k(9) inhibition constant

%vector of rate constant values:
 %   k1 k2  k3   k4  k5   k6   k7     k8  k9
 k =[0  1  1.e+4  80  1.0  31  1.e-6  0.1  0.1];

%  total simulation time
T=[0 600.00];


%  assignments motif 2 zero-order controller:
%  y(1) <-> A
%  y(2) <-> E

%  initial concentrations:
y0=[3.0 4.02];


% options for numerical integration
options = odeset('RelTol',1.0e-4,'absTol',1e-7,'MaxStep',0.01);
% Solve model
[T, Y]=ode23s(@m4,T,y0,options,k);

[minValue, minIndex] = min(Y(:,1));
 Amax=3-minValue;
 mkdir ./output/A-data
 mkdir ./output/t-data
 mkdir ./output/figures

 Adata = fopen('./output/A-data/k4=80.txt','w');
 fprintf(Adata,'%f\n',Y(:,1));

 tdata = fopen('./output/t-data/k4=80.txt','w');
 fprintf(tdata,'%f\n',T);

figure % make a figure
plot(T,Y(:,1),'LineWidth',2.0);
xlabel('time (au)');
ylabel('A (au)');
grid on;
str1=sprintf('k_4=80, ΔAmax= %.4f \n ', Amax);
title(str1,'FontSize',16);
exportgraphics(figure(1), './output/figures/A_k4=80.pdf');
```

b

```
function dy=m4(T,y,k);

dy=zeros(2,1);

%  assignments motif 4 controller (Fig. S2):
%  y(1) <-> A
%  y(2) <-> E


%k2 step increase from t>= 100.0:
if T >= 100.00
    k(2)=5.0;
end


dy(1)=k(1)-(k(2)*y(1))-(k(4)*y(1))+((k(3)*k(8))/(k(8)+y(2)));
dy(2)=k(5)-((k(6)*y(2))/(k(7)+y(2)))*(k(9)/(k(9)+y(1)));
```

c

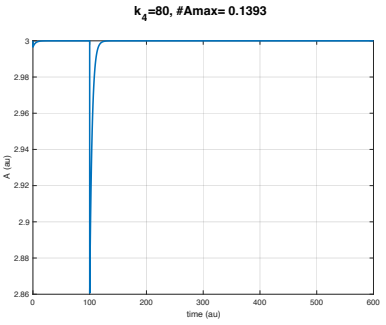

FIGURE B.7: MATLAB scripts for generating m4's response amplitude of A at background k_4=80. Run the script in panel a in order to generate the response amplitude of A in panel c. This can be run at different backgrounds by changing the k_4 value in panel a, and inserting the corresponding initial concentrations of A and E. Panel b contains the rate equations.

a

```
% opens and reads files in 'A-data' and 't-data' directories
% and plots an overlay of all A-data/A-profiles as a function
% of time.

formatSpec = '%f'; %format specifier

%assign FileIDs/FileHandles for files:
Adata0 = fopen('./output/A-data/k4=0.txt','r');
tdata0 = fopen('./output/t-data/k4=0.txt','r');

Adata2 = fopen('./output/A-data/k4=2.txt','r');
tdata2 = fopen('./output/t-data/k4=2.txt','r');

Adata5 = fopen('./output/A-data/k4=5.txt','r');
tdata5 = fopen('./output/t-data/k4=5.txt','r');

Adata10 = fopen('./output/A-data/k4=10.txt','r');
tdata10 = fopen('./output/t-data/k4=10.txt','r');

Adata20 = fopen('./output/A-data/k4=20.txt','r');
tdata20 = fopen('./output/t-data/k4=20.txt','r');

Adata40 = fopen('./output/A-data/k4=40.txt','r');
tdata40 = fopen('./output/t-data/k4=40.txt','r');

Adata80 = fopen('./output/A-data/k4=80.txt','r');
tdata80 = fopen('./output/t-data/k4=80.txt','r');


%read files, both A and t values:
A0 = fscanf(Adata0,formatSpec);
t0 = fscanf(tdata0,formatSpec);

A2 = fscanf(Adata2,formatSpec);
t2 = fscanf(tdata2,formatSpec);

A5 = fscanf(Adata5,formatSpec);
t5 = fscanf(tdata5,formatSpec);

A10 = fscanf(Adata10,formatSpec);
t10 = fscanf(tdata10,formatSpec);

A20 = fscanf(Adata20,formatSpec);
t20 = fscanf(tdata20,formatSpec);

A40 = fscanf(Adata40,formatSpec);
t40 = fscanf(tdata40,formatSpec);

A80 = fscanf(Adata80,formatSpec);
t80 = fscanf(tdata80,formatSpec);


figure % make figure of all A profiles
plot(t0,A0,t2,A2,t5,A5,t10,A10,t20,A20,t40,A40,t80,A80,'LineWidth',2.0);
xlabel('time (au)');
ylabel('A (au)');
%xlim([0 100])
grid on;
legend('k_4=0','k_4=2','k_4=5','k_4=10','k_4=20','k_4=40','k_4=80')
exportgraphics(figure(1), './output/figures/A_merged.pdf');
```

b

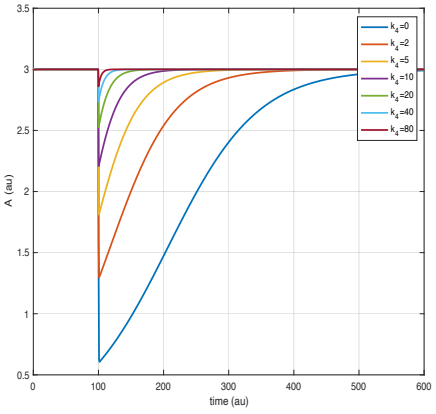

FIGURE B.8: MATLAB script (panel a) for generating m4's resetting kinetics (panel b). The resetting kinetics are similar to Fig. 3.9b. Run this script after producing the response amplitudes for k_4=0, 2, 5, 10, 20, 40, 80

m5 controller

a

```
% matlab calculation of m5
clear all
warning('off','all')

% define matlab rate constant vector k; k(i),ith element in k;
% from fortran rate constants Ki;

% fortran <=> matlab (motif 5)
%-------------------------------
% K1=1.0    <=> k(1) step-perturbation:
%                   1 (phase 1, t<100)--> 5 (phase 2, t>=100)
% K2=0      <=> k(2)
% K3        <=> k(3) background, variable
% K4=0.005   <=> k(4) rate constant for compensatory flux
% K5=1.0    <=> k(5) defines set-point
% K6=3.0    <=> k(6) defines set-point
% KM=1.e-6  <=> k(7) KM or k7 to get zero-order removal of E


%vector of rate constant values:
 %   k1 k2 k3  k4    k5   k6   k7
 k =[1  0  128  0.005  1.0  3.0  1.e-6];

%  total simulation time
T=[0 500.00];


%  assignments motif 6 zero-order controller:
%  y(1) <-> A
%  y(2) <-> E

%  initial concentrations:
y0=[3.0 8600.0];


% options for numerical integration
options = odeset('RelTol',1.0e-4,'absTol',1e-7,'MaxStep',0.01);
% Solve model
[T, Y]=ode23s(@m5,T,y0,options,k);

[maxValue, maxIndex] = max(Y(:,1));
 Amax=maxValue-3;
 mkdir ./output/A-data
 mkdir ./output/t-data
 mkdir ./output/figures

 Adata = fopen('./output/A-data/k3=128.txt','w');
 fprintf(Adata,'%f\n',Y(:,1));

 tdata = fopen('./output/t-data/k3=128.txt','w');
 fprintf(tdata,'%f\n',T);

figure % make a figure
plot(T,Y(:,1),'LineWidth',2.0);
xlabel('time (au)');
ylabel('A (au)');
grid on;
str1=sprintf('k_3=128, ΔAmax= %.4f \n ', Amax);
title(str1,'FontSize',16);
exportgraphics(figure(1), './output/figures/A_k3=128.pdf');
```

b

```
function dy=m5(T,y,k);

dy=zeros(2,1);

%  assignments motif 5 controller (Fig. 12):
%  y(1) <-> A
%  y(2) <-> E


%k1 step increase from t>= 100.0:
if T >= 100.00
    k(1)=5.0;
end


dy(1)=k(1)+k(3)-(k(2)+(k(4)*y(2)))*y(1);
dy(2)=k(5)*y(1)-((k(6)*y(2))/(k(7)+y(2)));
```

c

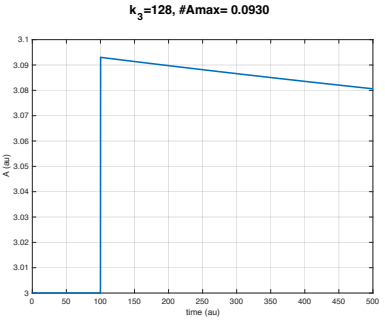

FIGURE B.9: MATLAB scripts for generating m5's response amplitude of A at background k_3=128. Run the script in panel a in order to generate the response amplitude of A in panel c. This can be run at different backgrounds by changing the k_3 value in panel a, and inserting the corresponding initial concentrations of A and E. Panel b contains the rate equations.

a

```
% opens and reads files in 'A-data' and 't-data' directories
% and plots an overlay of all A-data/A-profiles as a function
% of time.

formatSpec = '%f'; %format specifier

%assign FileIDs/FileHandles for files:
Adata0 = fopen('./output/A-data/k3=0.txt','r');
tdata0 = fopen('./output/t-data/k3=0.txt','r');

Adata1 = fopen('./output/A-data/k3=1.txt','r');
tdata1 = fopen('./output/t-data/k3=1.txt','r');

Adata2 = fopen('./output/A-data/k3=2.txt','r');
tdata2 = fopen('./output/t-data/k3=2.txt','r');

Adata4 = fopen('./output/A-data/k3=4.txt','r');
tdata4 = fopen('./output/t-data/k3=4.txt','r');

Adata8 = fopen('./output/A-data/k3=8.txt','r');
tdata8 = fopen('./output/t-data/k3=8.txt','r');

Adata16 = fopen('./output/A-data/k3=16.txt','r');
tdata16 = fopen('./output/t-data/k3=16.txt','r');

Adata32 = fopen('./output/A-data/k3=32.txt','r');
tdata32 = fopen('./output/t-data/k3=32.txt','r');

Adata64 = fopen('./output/A-data/k3=64.txt','r');
tdata64 = fopen('./output/t-data/k3=64.txt','r');

Adata128 = fopen('./output/A-data/k3=128.txt','r');
tdata128 = fopen('./output/t-data/k3=128.txt','r');

%read files, both A and t values:
A0 = fscanf(Adata0,formatSpec);
t0 = fscanf(tdata0,formatSpec);

A1 = fscanf(Adata1,formatSpec);
t1 = fscanf(tdata1,formatSpec);

A2 = fscanf(Adata2,formatSpec);
t2 = fscanf(tdata2,formatSpec);

A4 = fscanf(Adata4,formatSpec);
t4 = fscanf(tdata4,formatSpec);

A8 = fscanf(Adata8,formatSpec);
t8 = fscanf(tdata8,formatSpec);

A16 = fscanf(Adata16,formatSpec);
t16 = fscanf(tdata16,formatSpec);

A32 = fscanf(Adata32,formatSpec);
t32 = fscanf(tdata32,formatSpec);

A64 = fscanf(Adata64,formatSpec);
t64 = fscanf(tdata64,formatSpec);

A128 = fscanf(Adata128,formatSpec);
t128 = fscanf(tdata128,formatSpec);

figure % make figure of all A profiles
plot(t0,A0,t1,A1,t2,A2,t4,A4,t8,A8,t16,A16,t32,A32,t64,A64,t128,A128, ...
    'LineWidth',2.0);
xlabel('time (au)');
ylabel('A (au)');
grid on;
legend('k_3=0','k_3=1','k_3=2','k_3=4','k_3=8','k_3=16','k_3=32', ...
    'k_3=64','k_3=128')
exportgraphics(figure(1), './output/figures/A_merged.pdf');
```

b

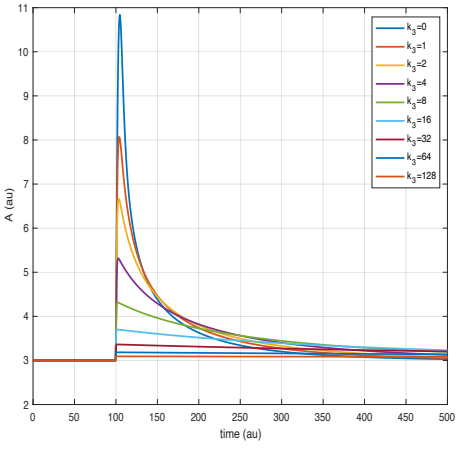

FIGURE B.10: MATLAB script (panel a) for generating m5's resetting kinetics (panel b). The resetting kinetics are similar to Fig. 3.5b. Run this script after producing the response amplitudes for k_3=0, 1, 2, 4, 8, 16, 32, 64, 128

m6 controller

a

```
% matlab calculation of m6
clear all
warning('off','all')

% define matlab rate constant vector k; k(i),ith element in k;
% from fortran rate constants Ki;

% fortran <=> matlab (motif 6)
%-------------------------------
% K1=1.0     <=> k(1) step-perturbation:
%                   1 (phase 1, t<100)--> 5 (phase 2, t>=100)
% K2=0       <=> k(2)
% K3         <=> k(3) background, variable
% K4=1.e4    <=> k(4) rate constant for compensatory flux
%                 high, to avoid oscillations
% K5=6.0     <=> k(5) defines set-point
% K6=2.0     <=> k(6) defines set-point
% KM=1.e-6   <=> k(7) KM or k7 to get zero-order removal of E
% KI=0.1     <=> k(8) inhibition constant

%vector of rate constant values:
 %  k1  k2 k3  k4   k5   k6   k7      k8
 k =[1  0  80  1.e4  6.0  2.0  1.e-6  0.1];

%  total simulation time
T=[0 600.00];


%  assignments motif 6 zero-order controller:
%  y(1) <-> A
%  y(2) <-> E

%  initial concentrations:
y0=[3.0 36.94];


% options for numerical integration
options = odeset('RelTol',1.0e-4,'absTol',1e-7,'MaxStep',0.01);
% Solve model
[T, Y]=ode23s(@m6,T,y0,options,k);

[maxValue, maxIndex] = max(Y(:,1));
 Amax=maxValue-3;
 mkdir ./output/A-data
 mkdir ./output/t-data
 mkdir ./output/figures

 Adata = fopen('./output/A-data/k3=80.txt','w');
 fprintf(Adata,'%f\n',Y(:,1));

 tdata = fopen('./output/t-data/k3=80.txt','w');
 fprintf(tdata,'%f\n',T);

figure % make a figure
plot(T,Y(:,1),'LineWidth',2.0);
xlabel('time (au)');
ylabel('A (au)');
grid on;
str1=sprintf('k_3=80, ΔAmax= %.4f \n ', Amax);
title(str1,'FontSize',16);
exportgraphics(figure(1), './output/figures/A_k3=80.pdf');
```

b

```
function dy=m6(T,y,k);

dy=zeros(2,1);

%  assignments motif 2 controller (Fig. 12):
%  y(1) <-> A
%  y(2) <-> E


%k1 step increase from t>= 100.0:
if T >= 100.00
    k(1)=5.0;
end


dy(1)=k(1)-k(2)*y(1)+k(3)-k(4)*k(8)*y(1)/(k(8)+y(2));
dy(2)=k(5)-k(6)*y(2)*y(1)/(k(7)+y(2));
```

c

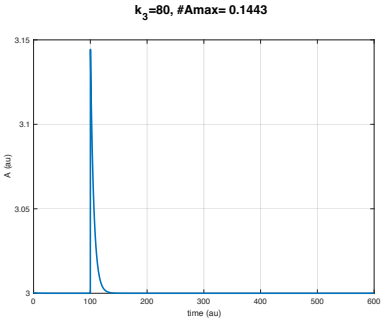

FIGURE B.11: MATLAB scripts for generating m6's response amplitude of A at background k_3=80. Run the script in panel a in order to generate the response amplitude of A in panel c. This can be run at different backgrounds by changing the k_3 value in panel a, and inserting the corresponding initial concentrations of A and E. Panel b contains the rate equations.

a

```
% opens and reads files in 'A-data' and 't-data' directories
% and plots an overlay of all A-data/A-profiles as a function
% of time.

formatSpec = '%f'; %format specifier

%assign FileIDs/FileHandles for files:
Adata0 = fopen('./output/A-data/k3=0.txt','r');
tdata0 = fopen('./output/t-data/k3=0.txt','r');

Adata1 = fopen('./output/A-data/k3=1.txt','r');
tdata1 = fopen('./output/t-data/k3=1.txt','r');

Adata2 = fopen('./output/A-data/k3=2.txt','r');
tdata2 = fopen('./output/t-data/k3=2.txt','r');

Adata5 = fopen('./output/A-data/k3=5.txt','r');
tdata5 = fopen('./output/t-data/k3=5.txt','r');

Adata10 = fopen('./output/A-data/k3=10.txt','r');
tdata10 = fopen('./output/t-data/k3=10.txt','r');

Adata20 = fopen('./output/A-data/k3=20.txt','r');
tdata20 = fopen('./output/t-data/k3=20.txt','r');

Adata40 = fopen('./output/A-data/k3=40.txt','r');
tdata40 = fopen('./output/t-data/k3=40.txt','r');

Adata80 = fopen('./output/A-data/k3=80.txt','r');
tdata80 = fopen('./output/t-data/k3=80.txt','r');

%read files, both A and t values:
A0 = fscanf(Adata0,formatSpec);
t0 = fscanf(tdata0,formatSpec);

A1 = fscanf(Adata1,formatSpec);
t1 = fscanf(tdata1,formatSpec);

A2 = fscanf(Adata2,formatSpec);
t2 = fscanf(tdata2,formatSpec);

A5 = fscanf(Adata5,formatSpec);
t5 = fscanf(tdata5,formatSpec);

A10 = fscanf(Adata10,formatSpec);
t10 = fscanf(tdata10,formatSpec);

A20 = fscanf(Adata20,formatSpec);
t20 = fscanf(tdata20,formatSpec);

A40 = fscanf(Adata40,formatSpec);
t40 = fscanf(tdata40,formatSpec);

A80 = fscanf(Adata80,formatSpec);
t80 = fscanf(tdata80,formatSpec);

figure % make figure of all A profiles
plot(t0,A0,t1,A1,t2,A2,t5,A5,t10,A10,t20,A20,t40,A40,t80,A80, ...
    -'LineWidth',2.0);
xlabel('time (au)');
ylabel('A (au)');
grid on;
legend('k_3=0','k_3=1','k_3=2','k_3=5','k_3=10','k_3=20','k_3=40','k_3=80')
exportgraphics(figure(1), './output/figures/A_merged.pdf');
```

b

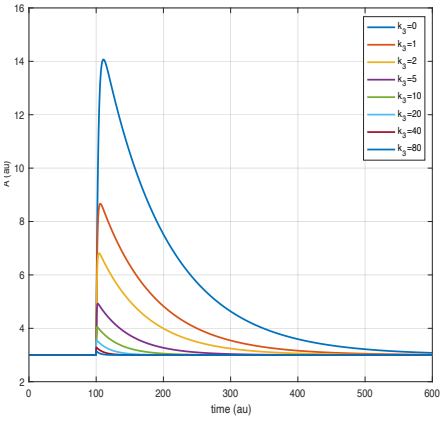

FIGURE B.12: MATLAB script (panel a) for generating m6's resetting kinetics (panel b). The resetting kinetics are similar to Fig. 3.10b. Run this script after producing the response amplitudes for k_3=0, 1, 2, 5, 10, 20, 40, 80

m7 controller

a

```
% matlab calculation of m7
clear all
warning('off','all')

% define matlab rate constant vector k; k(i),ith element in k;
% from fortran rate constants Ki;

% fortran <=> matlab (motif 6)
%-------------------------------
% K1=1     <=> k(1) step-perturbation:
%                  1 (phase 1, t<100)--> 5 (phase 2, t>=100)
% K2=0       <=> k(2)
% K3         <=> k(3) background, variable
% K4=0.03    <=> k(4) rate constant for compensatory flux
% K5=1.0     <=> k(5) defines set-point
% K6=31      <=> k(6) defines set-point
% KM=1.e-6   <=> k(7) KM or k7 to get zero-order removal of E
% KI=0.1     <=> k(8) inhibition constant

%vector of rate constant values:
 %   k1 k2 k3  k4   k5   k6  k7     k8
 k =[1  0  128  0.03  1.0  31  1.e-6  0.1];

%  total simulation time
T=[0 500.00];


%  assignments motif 7 zero-order controller:
%  y(1) <-> A
%  y(2) <-> E

%  initial concentrations:
y0=[3.0 1433.33];


% options for numerical integration
options = odeset('RelTol',1.0e-4,'absTol',1e-7,'MaxStep',0.01);
% Solve model
[T, Y]=ode23s(@m7,T,y0,options,k);

[maxValue, maxIndex] = max(Y(:,1));
 Amax=maxValue-3;
 mkdir ./output/A-data
 mkdir ./output/t-data
 mkdir ./output/figures

 Adata = fopen('./output/A-data/k3=128.txt','w');
 fprintf(Adata,'%f\n',Y(:,1));

 tdata = fopen('./output/t-data/k3=128.txt','w');
 fprintf(tdata,'%f\n',T);

figure % make a figure
plot(T,Y(:,1),'LineWidth',2.0);
xlabel('time (au)');
ylabel('A (au)');
grid on;
str1=sprintf('k_3=128, ΔAmax= %.4f \n ', Amax);
title(str1,'FontSize',16);
exportgraphics(figure(1), './output/figures/A_k3=128.pdf');
```

b

```
function dy=m7(T,y,k);

dy=zeros(2,1);

%  assignments motif 7 controller (Fig. 6):
%  y(1) <-> A
%  y(2) <-> E


%k1 step increase from t>= 100.0:
if T >= 100.00
    k(1)=5.0;
end


dy(1)=k(1)+k(3)-(k(2)*y(1))-(k(4)*y(1)*y(2));
dy(2)=k(5)-((k(6)*y(2))/(k(7)+y(2)))*(k(8)/(k(8)+y(1)));
```

c

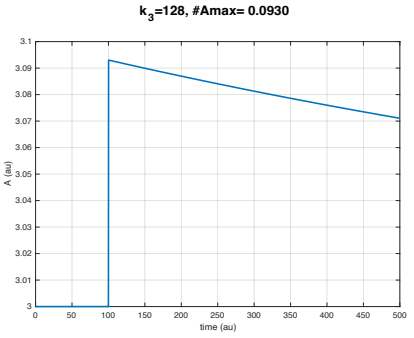

FIGURE B.13: MATLAB scripts for generating m7's response amplitude of A at background k_3=128. Run the script in panel a in order to generate the response amplitude of A in panel c. This can be run at different backgrounds by changing the k_3 value in panel a, and inserting the corresponding initial concentrations of A and E. Panel b contains the rate equations.

a

```
% opens and reads files in 'A-data' and 't-data' directories
% and plots an overlay of all A-data/A-profiles as a function
% of time.

formatSpec = '%f'; %format specifier

%assign FileIDs/FileHandles for files:
Adata0 = fopen('./output/A-data/k3=0.txt','r');
tdata0 = fopen('./output/t-data/k3=0.txt','r');

Adata1 = fopen('./output/A-data/k3=1.txt','r');
tdata1 = fopen('./output/t-data/k3=1.txt','r');

Adata2 = fopen('./output/A-data/k3=2.txt','r');
tdata2 = fopen('./output/t-data/k3=2.txt','r');

Adata4 = fopen('./output/A-data/k3=4.txt','r');
tdata4 = fopen('./output/t-data/k3=4.txt','r');

Adata8 = fopen('./output/A-data/k3=8.txt','r');
tdata8 = fopen('./output/t-data/k3=8.txt','r');

Adata16 = fopen('./output/A-data/k3=16.txt','r');
tdata16 = fopen('./output/t-data/k3=16.txt','r');

Adata32 = fopen('./output/A-data/k3=32.txt','r');
tdata32 = fopen('./output/t-data/k3=32.txt','r');

Adata64 = fopen('./output/A-data/k3=64.txt','r');
tdata64 = fopen('./output/t-data/k3=64.txt','r');

Adata128 = fopen('./output/A-data/k3=128.txt','r');
tdata128 = fopen('./output/t-data/k3=128.txt','r');

%read files, both A and t values:
A0 = fscanf(Adata0,formatSpec);
t0 = fscanf(tdata0,formatSpec);

A1 = fscanf(Adata1,formatSpec);
t1 = fscanf(tdata1,formatSpec);

A2 = fscanf(Adata2,formatSpec);
t2 = fscanf(tdata2,formatSpec);

A4 = fscanf(Adata4,formatSpec);
t4 = fscanf(tdata4,formatSpec);

A8 = fscanf(Adata8,formatSpec);
t8 = fscanf(tdata8,formatSpec);

A16 = fscanf(Adata16,formatSpec);
t16 = fscanf(tdata16,formatSpec);

A32 = fscanf(Adata32,formatSpec);
t32 = fscanf(tdata32,formatSpec);

A64 = fscanf(Adata64,formatSpec);
t64 = fscanf(tdata64,formatSpec);

A128 = fscanf(Adata128,formatSpec);
t128 = fscanf(tdata128,formatSpec);

figure % make figure of all A profiles
plot(t0,A0,t1,A1,t2,A2,t4,A4,t8,A8,t16,A16,t32,A32,t64,A64,t128,A128, ...
    'LineWidth',2.0);
xlabel('time (au)');
ylabel('A (au)');
grid on;
legend('k_3=0','k_3=1','k_3=2','k_3=4','k_3=8','k_3=16','k_3=32', ...
       'k_3=64','k_3=128')
exportgraphics(figure(1), './output/figures/A_merged.pdf');
```

b

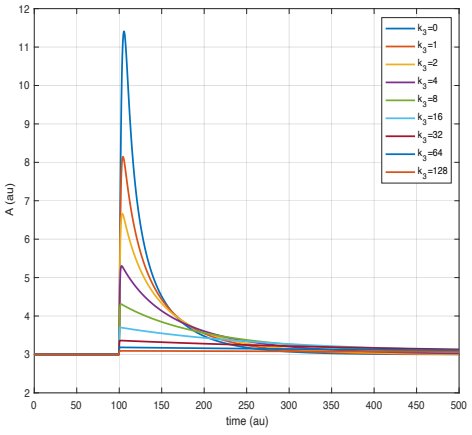

FIGURE B.14: MATLAB script (panel a) for generating m7's resetting kinetics (panel b). The resetting kinetics are similar to Fig. 3.6b. Run this script after producing the response amplitudes for k_3=0, 1, 2, 4, 8, 16, 32, 64, 128

m8 controller

a

```
% matlab calculation of m8
clear all
warning('off','all')

% define matlab rate constant vector k; k(i),ith element in k;
% from fortran rate constants Ki;

% fortran <=> matlab (motif 8)
%-------------------------------
% K1=1.0     <=> k(1) step-perturbation:
%                    1 (phase 1, t<100)--> 5 (phase 2, t>=100)
% K2=0       <=> k(2)
% K3         <=> k(3) background, variable
% K4=1.e4    <=> k(4) rate constant for compensatory flux
%                 high, to avoid oscillations
% K5=620     <=> k(5) defines set-point
% K6=20    <=> k(6) defines set-point
% KM=1.e-6  <=> k(7) KM or k7 to get zero-order removal of E
% KI=0.1     <=> k(8) inhibition constant
% K9=0.1     <=> k(9) inhibition constant

%vector of rate constant values:
 %   k1 k2 k3  k4   k5   k6   k7    k8   k9
 k =[1  0  80  1.e4  620  20  1.e-6  0.1  0.1];

%  total simulation time
T=[0 500.00];

%  assignments motif 8 zero-order controller:
%  y(1) <-> A
%  y(2) <-> E

%  initial concentrations:
y0=[3.0 36.94];

% options for numerical integration
options = odeset('RelTol',1.0e-4,'absTol',1e-7,'MaxStep',0.01);
% Solve model
[T, Y]=ode23s(@m8,T,y0,options,k);

[maxValue, maxIndex] = max(Y(:,1));
 Amax=maxValue-3;
 mkdir ./output/A-data
 mkdir ./output/t-data
 mkdir ./output/figures

 Adata = fopen('./output/A-data/k3=80.txt','w');
 fprintf(Adata,'%f\n',Y(:,1));

 tdata = fopen('./output/t-data/k3=80.txt','w');
 fprintf(tdata,'%f\n',T);

figure % make a figure
plot(T,Y(:,1),'LineWidth',2.0);
xlabel('time (au)');
ylabel('A (au)');
grid on;
str1=sprintf('k_3=80, ΔAmax= %.4f \n ', Amax);
title(str1,'FontSize',16);
exportgraphics(figure(1), './output/figures/A_k3=80.pdf');
```

b

```
function dy=m8(T,y,k);

dy=zeros(2,1);

%  assignments motif 8 controller (Fig. 11):
%  y(1) <-> A
%  y(2) <-> E


%k1 step increase from t>= 100.0:
if T >= 100.00
    k(1)=5.0;
end


dy(1)=k(1)-k(2)*y(1)+k(3)-k(4)*y(1)*(k(9)/(k(9)+y(2)));
dy(2)=k(5)*(k(8)/(k(8)+y(1)))-((k(6)*y(2))/(k(7)+y(2)));
```

c

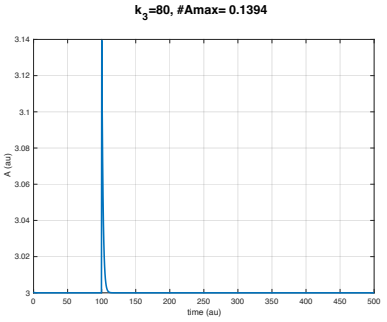

FIGURE B.15: MATLAB scripts for generating m8's response amplitude of A at background k_3=80. Run the script in panel a in order to generate the response amplitude of A in panel c. This can be run at different backgrounds by changing the k_3 value in panel a, and inserting the corresponding initial concentrations of A and E. Panel b contains the rate equations.

a

```
% opens and reads files in 'A-data' and 't-data' directories
% and plots an overlay of all A-data/A-profiles as a function
% of time.

formatSpec = '%f'; %format specifier

%assign FileIDs/FileHandles for files:
Adata0 = fopen('./output/A-data/k3=0.txt','r');
tdata0 = fopen('./output/t-data/k3=0.txt','r');

Adata1 = fopen('./output/A-data/k3=1.txt','r');
tdata1 = fopen('./output/t-data/k3=1.txt','r');

Adata5 = fopen('./output/A-data/k3=5.txt','r');
tdata5 = fopen('./output/t-data/k3=5.txt','r');

Adata10 = fopen('./output/A-data/k3=10.txt','r');
tdata10 = fopen('./output/t-data/k3=10.txt','r');

Adata20 = fopen('./output/A-data/k3=20.txt','r');
tdata20 = fopen('./output/t-data/k3=20.txt','r');

Adata40 = fopen('./output/A-data/k3=40.txt','r');
tdata40 = fopen('./output/t-data/k3=40.txt','r');

Adata80 = fopen('./output/A-data/k3=80.txt','r');
tdata80 = fopen('./output/t-data/k3=80.txt','r');

%read files, both A and t values:
A0 = fscanf(Adata0,formatSpec);
t0 = fscanf(tdata0,formatSpec);

A1 = fscanf(Adata1,formatSpec);
t1 = fscanf(tdata1,formatSpec);

A5 = fscanf(Adata5,formatSpec);
t5 = fscanf(tdata5,formatSpec);

A10 = fscanf(Adata10,formatSpec);
t10 = fscanf(tdata10,formatSpec);

A20 = fscanf(Adata20,formatSpec);
t20 = fscanf(tdata20,formatSpec);

A40 = fscanf(Adata40,formatSpec);
t40 = fscanf(tdata40,formatSpec);

A80 = fscanf(Adata80,formatSpec);
t80 = fscanf(tdata80,formatSpec);

figure % make figure of all A profiles
plot(t0,A0,t1,A1,t5,A5,t10,A10,t20,A20,t40,A40,t80,A80,'LineWidth',2.0);
xlabel('time (au)');
ylabel('A (au)');
grid on;
legend('k_3=0','k_3=1','k_3=5','k_3=10','k_3=20','k_3=40','k_3=80')
exportgraphics(figure(1), './output/figures/A_merged.pdf');
```

b

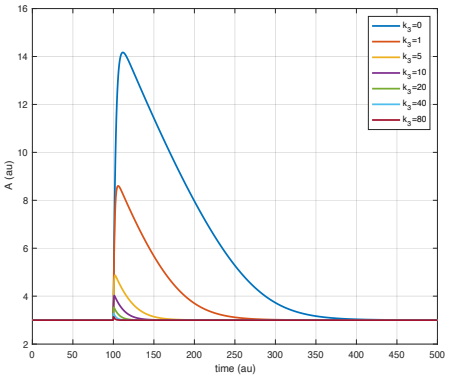

FIGURE B.16: MATLAB script (panel a) for generating m8's resetting kinetics (panel b). The resetting kinetics are similar to Fig. 3.11b. Run this script after producing the response amplitudes for k_3=0, 1, 5, 10, 20, 40, 80

Appendix C

Homeostasis at different backgrounds: The roles of overlayed feedback structures in vertebrate photoadaptation

PLOS ONE

RESEARCH ARTICLE

Homeostasis at different backgrounds: The roles of overlayed feedback structures in vertebrate photoadaptation

Jonas V. Grini[☯], **Melissa Nygård**[☯], **Peter Ruoff***

Department of Chemistry, Bioscience, and Environmental Engineering, University of Stavanger, Stavanger, Norway

☯ These authors contributed equally to this work.
* peter.ruoff@uis.no

Citation: Grini JV, Nygård M, Ruoff P (2023) Homeostasis at different backgrounds: The roles of overlayed feedback structures in vertebrate photoadaptation. PLoS ONE 18(4): e0281490. https://doi.org/10.1371/journal.pone.0281490

Editor: Paolo Cazzaniga, University of Bergamo: Universita degli Studi di Bergamo, ITALY

Received: January 23, 2023

Accepted: March 30, 2023

Published: April 28, 2023

Peer Review History: PLOS recognizes the benefits of transparency in the peer review process; therefore, we enable the publication of all of the content of peer review and author responses alongside final, published articles. The editorial history of this article is available here: https://doi.org/10.1371/journal.pone.0281490

Data Availability Statement: All relevant data are within the paper and its Supporting information files.

Funding: The author(s) received no specific funding for this work.

Abstract

We have studied the resetting behavior of eight basic integral controller motifs with respect to different but constant backgrounds. We found that the controllers split symmetrically into two classes: one class, based on derepression of the compensatory flux, leads to more rapid resetting kinetics as backgrounds increase. The other class, which directly activates the compensatory flux, shows a slowing down in the resetting at increased backgrounds. We found a striking analogy between the resetting kinetics of vertebrate photoreceptors and controllers based on derepression, i.e. vertebrate rod or cone cells show decreased sensitivities and accelerated response kinetics as background illuminations increase. The central molecular model of vertebrate photoadaptation consists of an overlay of three negative feedback loops with cytosolic calcium (Ca_i^{2+}), cyclic guanosine monophosphate (cGMP) and cyclic nucleotide-gated (CNG) channels as components. While in one of the feedback loops the extrusion of Ca_i^{2+} by potassium-dependent sodium-calcium exchangers (NCKX) can lead to integral control with cGMP as the controlled variable, the expected robust perfect adaptation of cGMP is lost, because of the two other feedback loops. They avoid that Ca_i^{2+} levels become too high and toxic. Looking at psychophysical laws, we found that in all of the above mentioned basic controllers Weber's law is followed when a "just noticeable difference" (threshold) of 1% of the controlled variable's set-point was considered. Applying comparable threshold pulses or steps to the photoadaptation model we find, in agreement with experimental results, that Weber's law is followed for relatively high backgrounds, while Stephens' power law gives a better description when backgrounds are low. Limitations of our photoadaption model, in particular with respect to potassium/sodium homeostasis, are discussed. Finally, we discuss possible implication of background perturbations in biological controllers when compensatory fluxes are based on activation.

Competing interests: The authors have declared that no competing interests exist.

Introduction

In 1929 Walter B. Cannon [1] defined homeostasis as the sum of the physiological processes which keep the steady states in a cell or organism within narrow limits [2]. Since then many facets of homeostatic regulation has been discovered and alternative concept names have been suggested. For example, Mrosovsky [3] argued that the term *rheostasis* would be more appropriate since there is often a change in a defended set-point, for example, the elevated (and controlled) temperature when we are running a fever. He further argues (see [3], ch. 1) that homeostasis has often been equated to a single negative feedback loop. The term *allostasis* [4–6] was introduced to focus on changing environmental conditions, feedforward loops, and on the control mechanisms which deviate from a simple negative feedback loop with a single set-point [5]. With respect to circadian adaptation and anticipation mechanisms Moore-Ede [7] coined the term *predictive homeostasis*. As adaptation mechanisms are highly dynamic Lloyd [8] argued for the use of the term *homeodynamics* instead of homeostasis. While all these aspects point to important properties of homeostatic regulation, we agree with Carpenter that the term *homeostasis* still stands as an unified approach [9]. We believe, that when multiple feedback and feedforward loops are studied theoretically in more detail, many of the above mentioned homeostatic facets can be accounted for, such as rheostatic control can be observed in a model of p53 regulation upon variable stress conditions [10].

In this paper we explore the influence of background perturbations on a set of eight basic negative feedback (controller) motifs [11]. We found that some of the motifs show an astonishing analogy to retinal photoreceptor adaptation when various background illuminations are applied.

The paper consists of two major parts. In the first part results from a systematic study of all eight controller motifs are shown. In the second part we show how certain of these controller motifs can provide an understanding about the kinetics of retinal photoreceptor adaptation. All eight feedback motifs show robust perfect homeostasis due to the implementation of integral control.

Integral control is a control-engineering concept [12], which allows a controlled variable to reset precisely at its set-point when step perturbations are applied. In biochemical systems several kinetic requirements have been identified which lead to integral control. Among them we have zero-order kinetics in the removal of the manipulated (controller) variable [11, 13], antithetic control in which two controller variables are removed by second-order [14, 15] or enzyme [16] kinetics, or a (first-order) autocatalytic synthesis combined with first-order removal kinetics of the manipulated variable [17–19]. When dealing with the different basic controller motifs we will introduce integral control mostly by zero-order kinetics, but also by antithetic control (see 'Results and discussion' below).

Psychophysical laws

Psychophysical laws relate the intensity of a physical stimulus with its perceived magnitude, for example a human (or a receptor cell) perceived brightness of light in relation to a certain applied light intensity. We will use the concept of a "just noticeable perturbation" (alternatively "just noticeable difference" or "threshold") in order to compare computational results with corresponding experimental data. The concept of a "just noticeable difference" was first introduced by Weber [20] in order to understand the relationship between an applied physical stimulus and its (human) perception. We will focus on two well-known psychophysical laws, i.e. on Weber's law and on Stephens' power law, because these laws are often applied in adaptation studies (see for example Part IV in [21])).

Weber's law. Ernst Heinrich Weber [20, 22] found that the human perception of a just noticeable difference $dw = w' - w$ between a reference weight w and a slightly heavier weight w' is approximately proportional to the reference weight w, i.e.,

$$dw = w' - w = k \cdot w \tag{1}$$

with k being a constant. Weber's law implies a linear relationship between a just noticeable perturbation (threshold perturbation) and an applied background perturbation. It was Gustav Fechner [23] who made Weber's law public and gave it its name, but expanded the perception of a just noticeable difference dw to $dp = dw/w$ (termed by Fechner as *Contrast*) and stated its logarithmic form, i.e.,

$$dp = \alpha \cdot \frac{dw}{w} \quad \Rightarrow \quad p = \alpha \ln \frac{w}{w_0} + C \tag{2}$$

where α and C are constants. Instead of weight, w can generally be any other stimulus. The logarithmic form of Eq 2 is termed as *Fechner's law*.

Stevens' power law. Stevens [24] suggested (and revived) a power-law formulation between the magnitude of a sensation/perception p and its stimulus s, i.e.

$$p = k \cdot s^{\alpha} + p_0 \tag{3}$$

where k, α, and p_0 are constants depending respectively on the units used and the type of stimulation. MacKay [25] suggested a model of perceived intensities by an adaptive "counterbalancing" response mechanism. This "negative feedback" approach enabled MacKay to make connections between the Weber-Fechner law and Stevens' law. In a model of retinal light adaptation we will show that Stephens' power law or Weber's law are followed dependent whether the background perturbation range is either low or high, respectively.

Materials and methods

Calculations and parameter estimations

Computations were performed by using LSODE [26], which is part of a set of Fortran solvers at the Lawrence Livermore National Laboratory (https://computing.llnl.gov/projects/odepack). Graphical results were generated with gnuplot (www.gnuplot.info). Composite figures and additional annotations were done with Adobe Illustrator (https://www.adobe.com/).

To make notations simpler, concentrations of compounds are denoted by compound names without square brackets. Time derivatives are generally indicated by the 'dot' notation. For the basic feedback loops m1-m8 (next section) concentrations and rate parameter values are given in arbitrary units (au), while for the light adaptation model concentrations are in μM (or nM) and time scale is in seconds (s). Rate parameters are presented as k_i's ($i = 1, 2, 3, \ldots$) irrespective of their kinetic nature, i.e. whether they represent turnover numbers, Michaelis constants, or inhibition/activation constants.

For the light adaptation model some parameter values were estimated by using gnuplot's fit function with respect to experimental literature data. Graphical experimental data were extracted with the program GraphClick (https://macdownload.informer.com/graphclick/).

To make the computations more accessible supporting information 'S1 Programs' in S1 File contains python scripts of Fortran results.

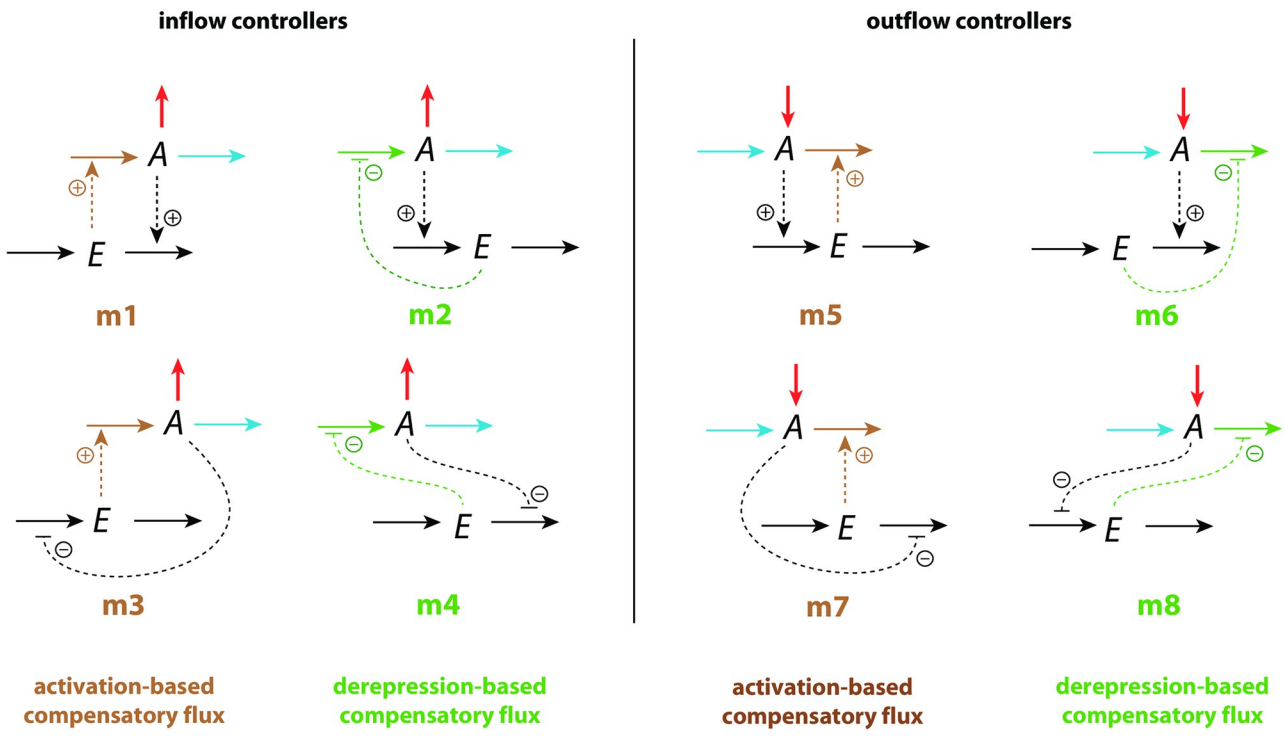

Fig 1. Set of basic negative feedback motifs m1-m8. Red and blue arrows indicate, respectively, a step perturbation and a constant background reaction. Integral control is implemented either by zero-order kinetics [11, 13] or by antithetic control [14, 16]. Outlined in brown and green we have activating or derepressing compensatory fluxes, respectively.

https://doi.org/10.1371/journal.pone.0281490.g001

Feedback motifs investigated

Fig 1 shows the investigated negative feedback loops. These are eight basic motifs (m1-m8), which divide equally into a set of inflow and outflow controllers [11]. Compound *A* is the homeostatic controlled variable, while *E* is the controller variable (or manipulated variable). Red arrows indicate a step perturbation while blue arrows represent a constant background. Black arrows indicate synthesis and removal of the controller variable *E*. Dashed lines represent signaling events which lead to the activation (plus signs) or inhibition (minus signs) of target reactions.

We have applied step perturbations, because integral controllers are generally capable to compensate them perfectly (for a proof see ch. 10.3.1 in Ref. [27]). Note however, that some feedback loop kinetics, such as in m2, are capable to oppose even rapidly increasing perturbations, such as hyperbolic growth [28, 29].

In the inflow controllers m1-m4 the manipulated variable *E* leads to the increase of a compensatory inflow flux either by direct activation (brown plus signs) or by derepression (green minus signs) and thereby opposing the step perturbations which remove *A* (red arrows). In the outflow controllers m5-m8 the compensatory (outflow) flux compensates step perturbations (red arrows) which increase *A* [30].

Results and discussion

Analyses of controller motifs

We have analyzed the eight controller schemes (Fig 1) with regard to step perturbations at different but constant backgrounds. Fig 2 shows the two idealized responses. In panel (a) the

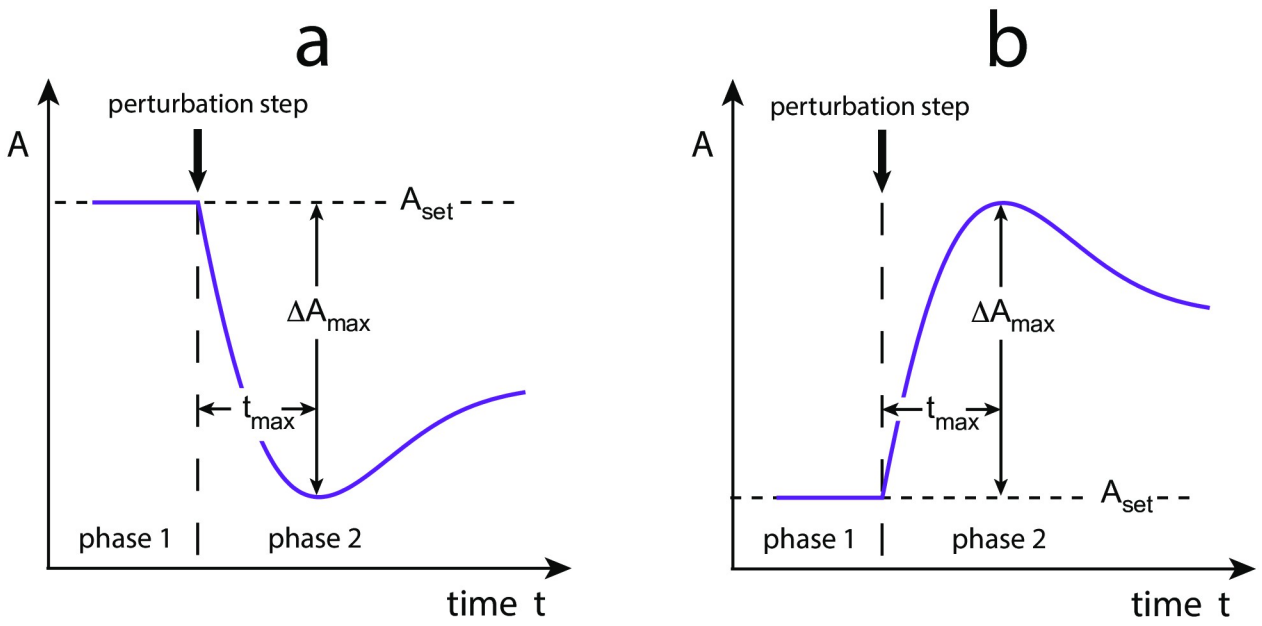

Fig 2. Idealized response kinetics of (a) inflow and (b) outflow controllers upon step perturbations. Indicated are the set-point of the controlled variable A, A_{set}, the maximum excursion of A, ΔA_{max}. t_{max} is the time between the start of the perturbation until ΔA_{max} is reached.

https://doi.org/10.1371/journal.pone.0281490.g002

resetting for inflow controllers is shown. In this case a step perturbation removes the controlled variable A and temporarily decreases it. Panel (b) shows the behavior of an outflow controller. When integral control is operative the controllers will defend the set-point of A (A_{set}) and move the level of A during the on-going step perturbation precisely back to A_{set}.

The *resetting period* is rather loosely defined as the time required to reach A_{set} after a step perturbation has been applied. Fig 2 also indicates the parameter ΔA_{max}, which is the maximum excursion of A after the applied step. t_{max} is the time the controller needs to reach ΔA_{max} after the perturbation has been applied.

We found that the controllers' response kinetics split into two classes independent whether they are inflow or outflow controllers. In both classes an increase of a background reaction leads to a reduced excursion ΔA_{max}. In the class where the compensatory flux is based on activation (controllers m1, m3, m5, and m7; outlined in brown in Fig 1), the controllers slow down in their resetting with increasing backgrounds and decreasing t_{max} values. In the other class, when compensatory fluxes are based on derepression, the controllers show an accelerated resetting (controllers m2, m4, m6, and m8; outlined in green in Fig 1).

In the following we describe in more detail how the two classes of controllers differ in their resetting behavior.

Controllers with activated compensatory fluxes

We show here the results for motifs m1 and m7. The supporting information 'S1 Text' shows corresponding details for controllers m3 and m5.

Controller m1. In the m1 controller the compensatory flux $j_3 = k_3 \cdot E$ is activated by E while A activates the removal of E (Fig 3). Step-wise perturbations removing A are mediated by k_2 while k_4 is a constant background outflow. For simplicity, we assume that activation kinetics are first-order with respect to the concentration of the activating species. This

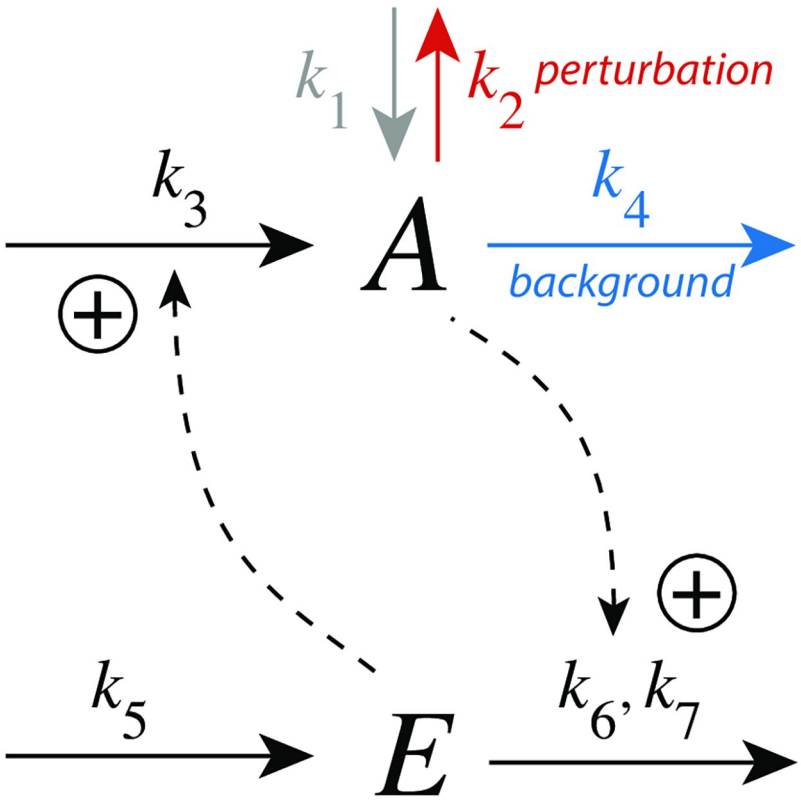

Fig 3. Inflow controller m1 with integral control implemented as a zero-order Michaelis-Menten (MM) type removal of *E*. k_2 undergoes a step perturbation, k_3 is a rate constant for the inflow of A, while k_4 is a constant background reaction. k_6 and k_7 are MM parameters analogous to V_{max} and K_M, respectively. In the calculations the grayed-out rate constant k_1 will be set to zero.

https://doi.org/10.1371/journal.pone.0281490.g003

assumption neglects possible saturation and controller breakdown at high activator concentrations [31].

The rate equations are:

$$\dot{A} = k_1 - (k_2 + k_4) \cdot A + k_3 \cdot E \tag{4}$$

$$\dot{E} = k_5 - A\left(\frac{k_6 \cdot E}{k_7 + E}\right) \tag{5}$$

Integral control is incorporated by a zero-order kinetic removal of E, i.e. $E/(k_7 + E) \approx 1$, with the result that E becomes proportional to the integrated error $\epsilon = A_{set} - A$:

$$\dot{E} = k_6(\underbrace{\frac{k_5}{k_6}}_{A_{set}} - A) = k_6 \cdot \epsilon \;\Rightarrow\; E(t) = k_6 \int_0^t \epsilon(t') \cdot dt' \tag{6}$$

Fig 4 shows the response kinetics of the m1 controller with set-point A_{set}=3.0. Panel (a) shows the concentration of A as a function of time when a k_2 step 1→5 is applied. Clearly, ΔA_{max} (see definition in Fig 2) decreases with increasing background k_4. Typically for controllers where the compensatory flux is based on activation, we observe that for increased backgrounds the

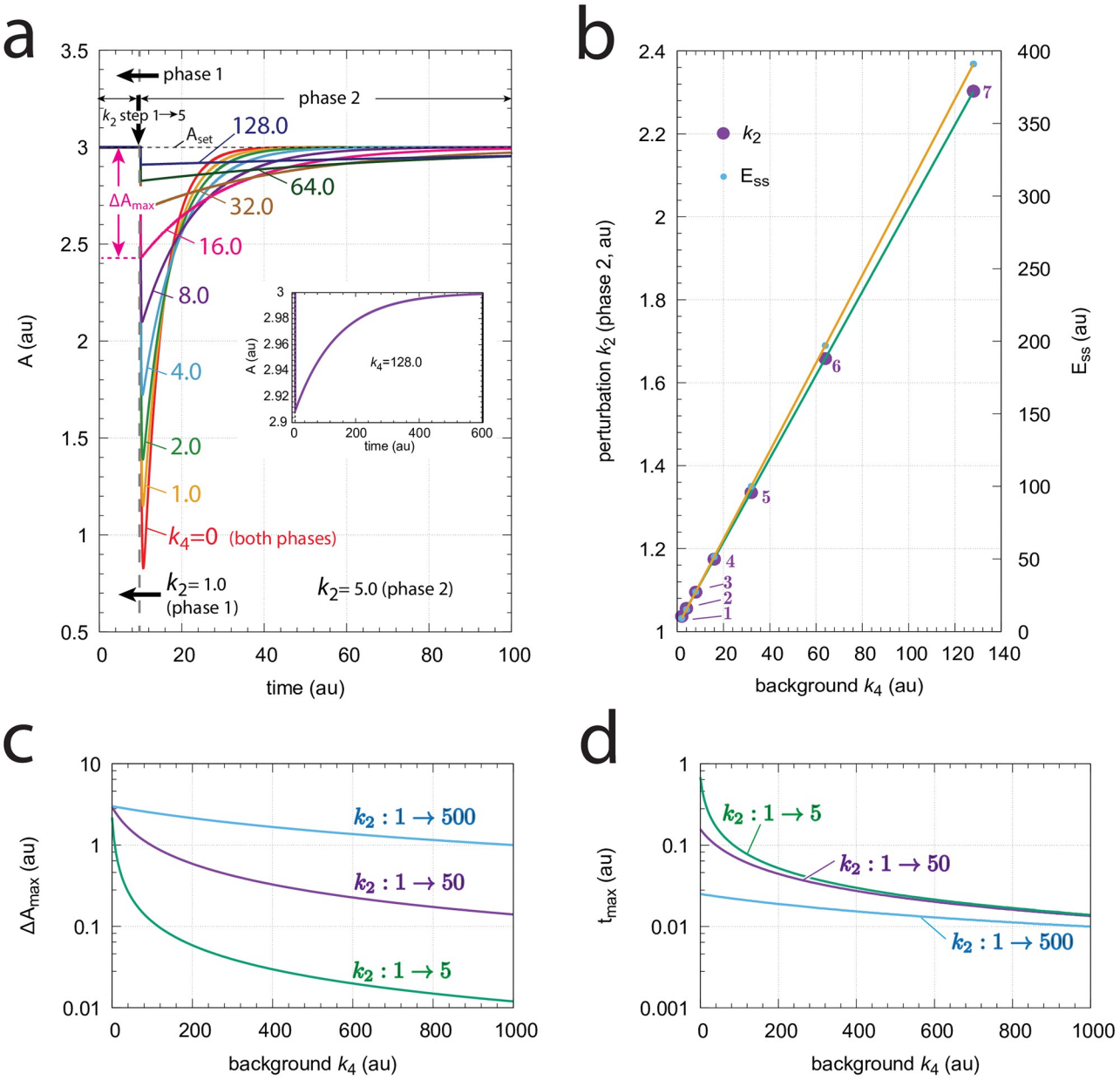

Fig 4. Response kinetics and relationship to Weber's law in the m1 controller (Fig 3). The set-point of A is 3.0. (a) Step-wise increase of k_2 from 1.0 to 5.0 at time t=10 at different but constant backgrounds k_4 (0–128.0, phases 1 and 2). Note the successive decrease in the maximum excursion of A (ΔA_{max}) with slowed-down A resetting kinetics as k_4 backgrounds increase. ΔA_{max} for k_4=16.0 is indicated. The inset shows that even at high backgrounds the controller is fully operative. Rate constants (in au): k_1=0.0, k_2=1.0 (phase 1), k_2=5.0 (phase 2), k_3=1.0, k_4 variable, k_5=3.0, k_6=1.0, k_7=1 × 10^{-6}. Initial concentrations (in au): A_0=3.0, E_0=3.0 (k_4=0); A_0=3.0, E_0=6.0 (k_4=1); A_0=3.0, E_0=9.0 (k_4=2); A_0=3.0, E_0=15.0 (k_4=4); A_0=3.0, E_0=27.0 (k_4=8); A_0=3.0, E_0=51.0 (k_4=16); A_0=3.0, E_0=99.0 (k_4=32); A_0=3.0, E_0=195.0 (k_4=64); A_0=3.0, E_0=387.0 (k_4=128). The inset shows the full adaptation response when k_4=128.0 (b) Relationship to Weber's law: When perturbation k_2 in phase 2 is adjusted such that the maximum (just noticeable) excursion in A is 0.03 (i.e. 1% of A_{set}) then both k_2 and the "perception" E_{ss} are linear functions of different but constant backgrounds k_4. Rate constants and initial concentrations as in (a), except that k_2 in phase 2 has the following values: **1**, k_2 = 1.0367 (k_4 = 2); **2**, k_2 = 1.0559 (k_4 = 4); **3**, k_2 = 1.0950 (k_4 = 8); **4**, k_2 = 1.1745 (k_4 = 16); **5**, k_2 = 1.3350 (k_4 = 32); **6**, k_2 = 1.6581 (k_4 = 64); **7**, k_2 = 2.3030 (k_4 = 128). (c) ΔA_{max} as a function of background k_4 at three different k_2 steps. (d) t_{max} as a function of background k_4 at three different k_2 steps. Rate constants are as in panel (a), except for k_2 and k_4. Initial concentrations are the steady state values of A and E prior to the step in k_2.

https://doi.org/10.1371/journal.pone.0281490.g004

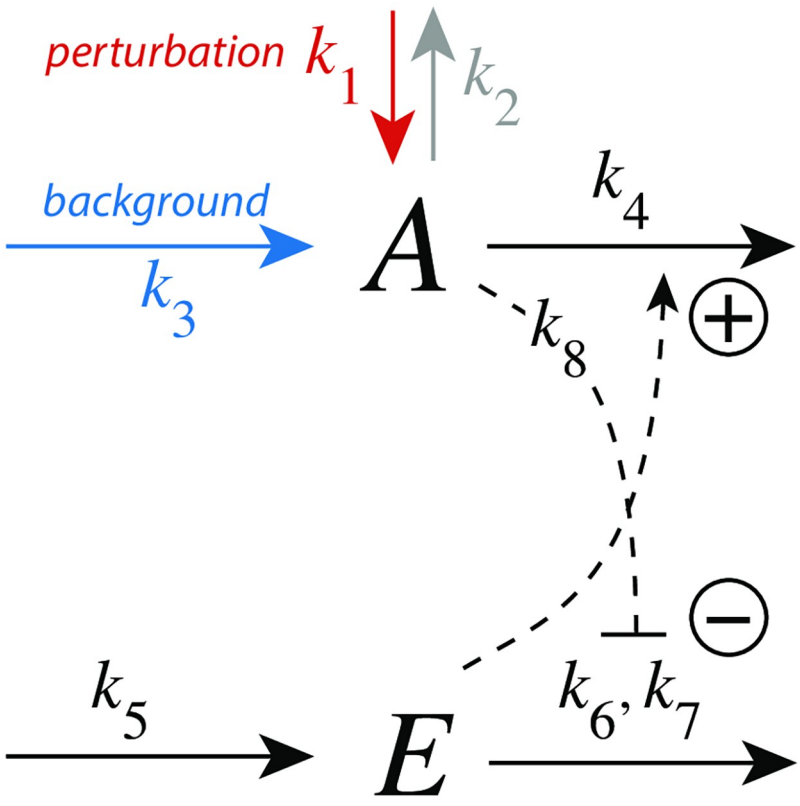

Fig 5. Outflow controller motif m7 with integral control implemented as a zero-order Michaelis-Menten (MM) type degradation of *E*. The perturbation k_1 changes step-wise (1.0→5.0), while k_3 is a constant background. Rate constant k_4 relates to the outflow of A, and k_8 is an inhibition constant. k_6 and k_7 are MM parameters analogous to V_{max} and K_M, respectively. In the calculations the grayed-out rate constant k_2 is, for the sake of simplicity, set to zero.

https://doi.org/10.1371/journal.pone.0281490.g005

resetting period is lengthend. Despite the increase in the resetting period the inset in panel (a) shows that the controller is fully operational and is able to defend its set-point.

Fig 4b shows the response kinetics related to Weber's law when probing a "just noticeable" excursion in ΔA of 0.03 (1% of A_{set}=3.0) by applying appropriate k_2 values in phase 2. We observe that the different k_2 values (in phase 2) and the corresponding steady-state values of E (E_{ss}) are linear functions of the background k_4.

Fig 4c and 4d show the values of ΔA_{max} and t_{max} for three different k_2 steps with increasing backgrounds k_4. Reflecting the behavior from Fig 4a, panel (c) shows that ΔA_{max} values decrease monotonically as background increases, but that the magnitude of ΔA_{max} depends on the size of the applied step. Despite that the resetting period increases with increasing backgrounds we observe that t_{max} decreases with increasing k_4 (panel (d)). The increase of the resetting period at increased k_4 levels can be explained by the high steady state levels of E in phase 1 when k_4 backgrounds become high and that the system needs more time to reach the steady state of E in phase 2 by zero-order kinetics.

Controller m7. m7 is an outflow controller which opposes inflow perturbations k_1 at different background reactions k_3 by E-activation of the compensatory flux j_4 (=$k_4 \cdot A \cdot E$). The negative feedback is closed by inhibiting the removal of E through A (Fig 5). The rate equations are

$$\dot{A} = k_1 + k_3 - k_2 \cdot A - k_4 \cdot A \cdot E \tag{7}$$

$$\dot{E} = k_5 - \left(\frac{k_6 \cdot E}{k_7 + E}\right) \cdot \left(\frac{k_8}{k_8 + A}\right) \tag{8}$$

The set-point for A is calculated from the steady-state condition of Eq 8 by using zero-order degradation of E, i.e. $E/(k_7 + E) \approx 1$.

$$\dot{E} = 0 \;\Rightarrow\; k_5 = \frac{k_6 k_8}{(k_8 + A_{ss})} \;\Rightarrow\; A_{set} = A_{ss} = k_8\left(\frac{k_6}{k_5} - 1\right) \tag{9}$$

Fig 6 shows the response kinetics of the m7 controller. Since the controller opposes inflow perturbations excursions of A are above the set-point A_{set} (=3.0). Panel a shows the slowed-down responses during the resetting in phase 2 as background k_3 increases. The inset shows that the controller is still operative even at the highest k_3 and slowest resetting. Panel b shows that a k_1 step perturbation which results in a just noticeable maximum excursion ΔA_{max} of 0.03 (1% of A_{set}) increases, together with the corresponding steady state E_{ss} values in phase 2, linearly with the background k_3. ΔA_{max} in creases with increasing k_1 step (Fig 6c), while for a given background we find, somewhat surprisingly, that t_{max} is independent on the magnitude of the k_1 step (Fig 6d). Both ΔA_{max} and t_{max} decrease monotonically with increasing background k_3.

We explain the delay in the resetting of A for large k_3 backgrounds as the increased time needed to change the high steady state values of E from phase 1 to its new steady state in phase 2 after the step.

Controllers with compensatory fluxes based on derepression

We show here the results for controllers m2 and m8 (Fig 1). Corresponding results for m4 and m6 are given in supporting information 'S2 Text'.

Controller m2. In the m2 controller scheme (Fig 7) activation of E by A is proportional to the concentration of A, while the inhibition term on the compensatory flux is formulated as $k_8/(k_8 + E)$. The rate equations are:

$$\dot{A} = k_1 - k_2 \cdot A - k_4 \cdot A + \frac{k_3 k_8}{k_8 + E} \tag{10}$$

$$\dot{E} = k_5 \cdot A - \frac{k_6 \cdot E}{k_7 + E} \tag{11}$$

To achieve homeostasis in A a perturbation (removal) of A is counteracted by a decrease of E ("derepression"), which increases the compensatory flux $j_3 = k_3 k_8/(k_8 + E)$ and moves, in the presence of integral control, A to its set-point.

The set-point of A (A_{set}) is determined how integral control is implemented in the feedback loop. In Fig 7 we use zero-order kinetics with respect to the removal of E, i.e. $k_7 \ll E_{ss}$. This implies that the steady state of A is also the set-point of A (A_{set}) and is given as the ratio k_6/k_5, i.e.

$$\dot{E} = 0 = k_5 \cdot A_{ss} - k_6 \cdot \underbrace{f_E}_{\approx 1} = -k_5\Big(\underbrace{\frac{k_6}{k_5}}_{A_{set}} - A_{ss}\Big) \tag{12}$$

with $f_E = E/(k_7 + E) \approx 1$.

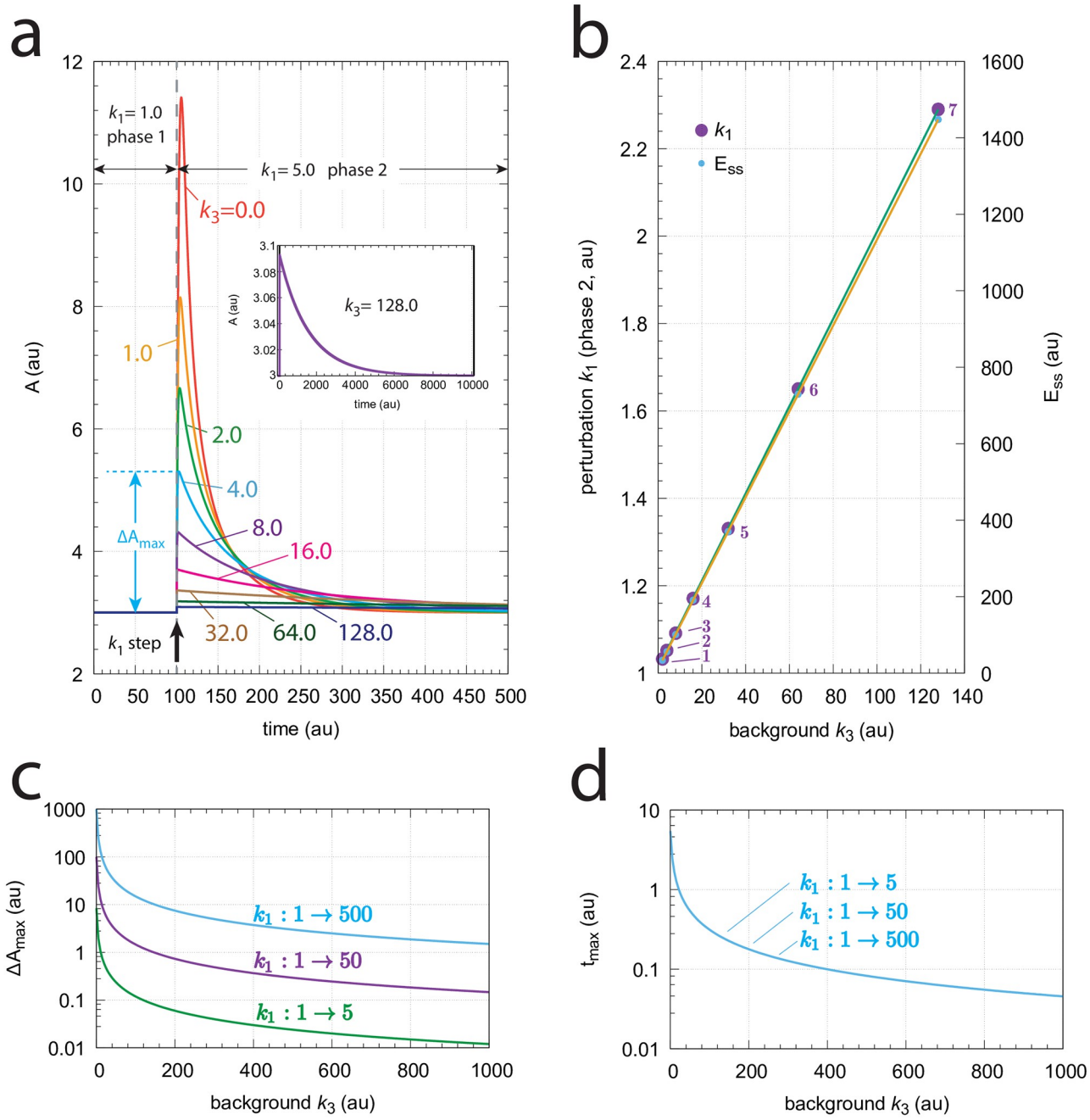

Fig 6. Response kinetics and relationship to Weber's law in the m7 controller (Fig 5). The set-point of A is 3.0. (a) Step-wise increase of k_1 from 1.0 to 5.0 at time t=100 at different and constant background perturbations k_3 (0–128.0, applied in phases 1 and 2). Note the successive decrease in the maximum excursion of A (ΔA_{max}) with slowed-down A resetting kinetics as k_3 values increase. ΔA_{max} for k_3=4.0 is indicated. Rate constants (in au): k_1=1.0, k_2=0.0 (phases 1 and 2), k_1=5.0 (phase 2), k_3 variable, k_4=0.03, k_5=1.0, k_6=31.0, k_7=1×10^{-6}, k_8=0.1. Initial concentrations (in au): A_0=3.0, E_0=11.11 (k_3=0); A_0=3.0, E_0=22.22 (k_3=1); A_0=3.0, E_0=33.33 (k_3=2); A_0=3.0, E_0=55.55 (k_3=4); A_0=3.0, E_0=100.0 (k_3=8); A_0=3.0, E_0=188.89 (k_3=16); A_0=3.0, E_0=366.67 (k_3=32); A_0=3.0, E_0=722.22 (k_3=64); A_0=3.0, E_0=1433.33 (k_3=128). The inset shows the full adaptation response when k_3=128.0 (b) Relationship to Weber's law: When perturbation k_1 in phase 2 is adjusted such that the maximum (just noticeable) excursion ΔA_{max} is 0.03 (i.e. 1% of A_{set}) then both k_1 and the "perception" E_{ss} are linear functions of the background k_3. Rate constants and initial concentrations as in (a), except that k_1 in phase 2 has the following values: **1**, k_1 = 1.0325 (k_3 = 2); **2**, k_1 = 1.0520 (k_3 = 4); **3**, k_1 = 1.0914 (k_3 = 8); **4**, k_1 = 1.1709 (k_3 = 16); **5**, k_1 = 1.3306 (k_3 = 32); **6**, k_1 = 1.6503 (k_3 = 64); **7**, k_1 = 2.2900 (k_3 = 128). (c) ΔA_{max} values as a function of background k_3 for three step perturbations in k_1. Note that the three curves are congruent, i.e., their identical shape can be precisely moved onto each other. (d) t_{max} as a function of background k_3. For a given background t_{max} is practically the same and independent of the three k_1 steps.

https://doi.org/10.1371/journal.pone.0281490.g006

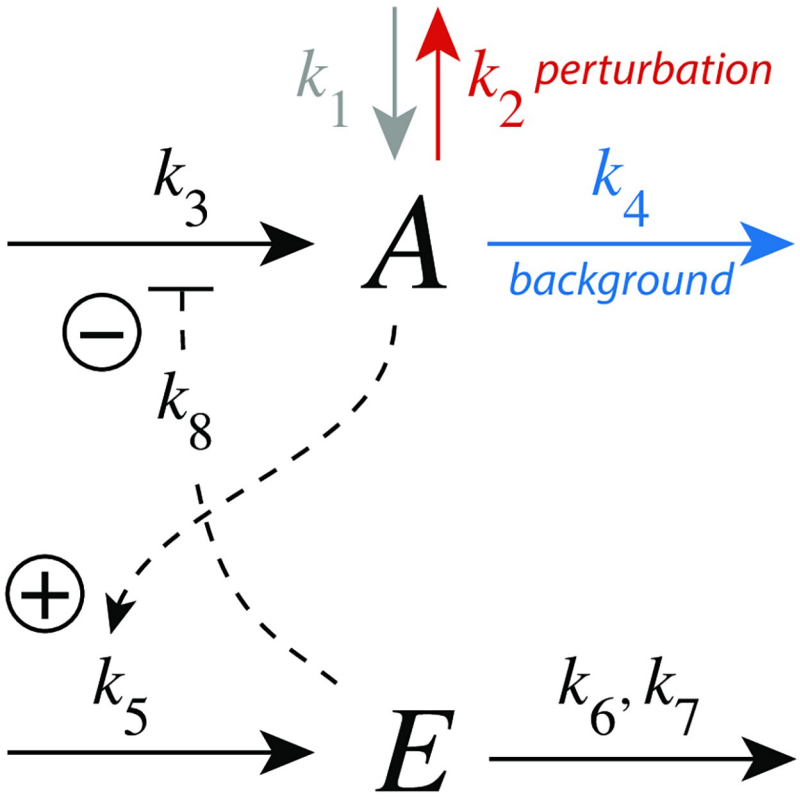

Fig 7. Controller motif m2 with integral control implemented as a zero-order Michaelis-Menten (MM) type degradation of E. Rate constant k_2 undergoes a step-wise change (perturbation), k_3 represents the maximum inflow of A, while k_4 is a (constant) background reaction. Rate constant k_8 is an inhibition constant. k_6 and k_7 are MM parameters analogous to V_{max} and K_M, respectively. The grayed-out rate constant k_1 is set in the calculations to zero.

https://doi.org/10.1371/journal.pone.0281490.g007

Fig 8a shows the response for step-wise changes in k_2 from 1.0 (phase 1) to 5.0 (phase 2) at different but constant background perturbations k_4. Typically for derepression controllers is both the decrease of ΔA_{max} at increasing backgrounds when a constant step perturbation is applied and a *decreasing* response time.

We were interested to see how the m2 controller would respond when a just noticeable excursion in A (ΔA_{max}) was applied for different background perturbations k_4. For that purpose we determined in phase 2 the steady state values of E and the k_2 values when the excursion of A was 1% of A_{set}(=3.0), i.e. $\Delta A_{max} = 0.03$. Fig 8b shows that $(1/E_{ss})$ and k_2 increase linearly with increasing k_4, a manifestation of Weber's law. In this view, $(1/E_{ss})$ could be interpreted as a "perceived" variable. Fig 8c and d show how ΔA_{max} and t_{max} depend on the background k_4, respectively.

Controller m2 with antithetic integral control. Since we later will use bimolecular (antithetic) control [14, 19] to describe the simultaneous removal of Ca^{2+} and K^+ out of a photoreceptor cell by potassium-dependent sodium-calcium exchangers (NCKX), we illustrate here how scheme m2 works with antithetic integral control (Fig 9).

The rate equations are:

$$\dot{A} = k_1 - k_2 \cdot A - k_4 \cdot A + \frac{k_3 k_8}{k_8 + E_1} \tag{13}$$

$$\dot{E}_1 = k_5 \cdot A - k_7 \cdot E_1 \cdot E_2 \tag{14}$$

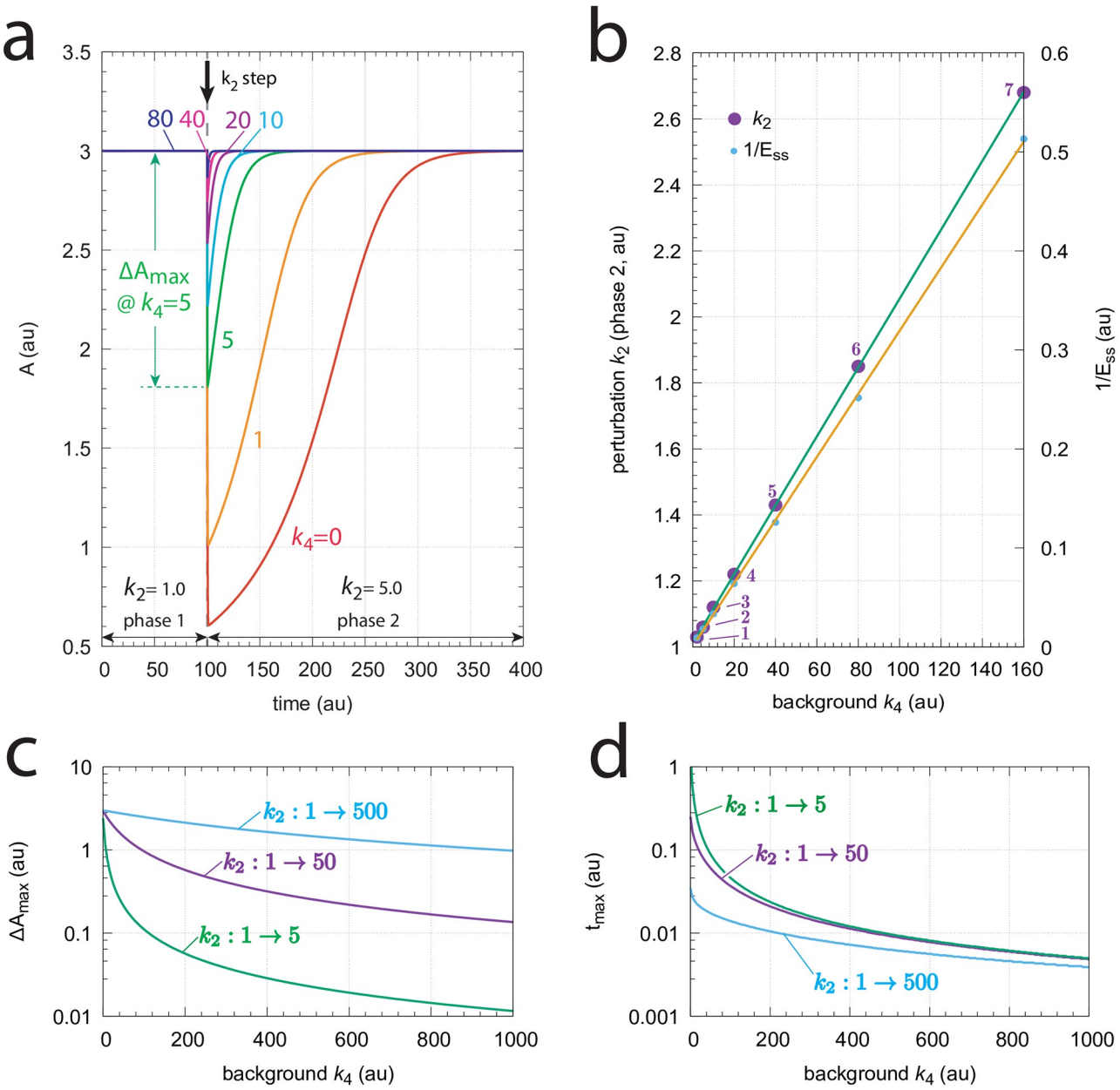

Fig 8. Response kinetics and relationship to Weber's law in the m2 controller (Fig 7). The set-point of A is A_{set}=3.0 (a) Step-wise increase of k_2 from 1.0 to 5.0 at time t=100 at different and constant background perturbations k_4 (0–80). The maximum excusion in A, ΔA_{max}, for k_4=5 is indicated. Note the successive decrease in ΔA_{max} and the more rapid resetting of A at increased k_4 values. Rate constants (in au): k_1=0.0, k_2=1.0 (phase 1), k_2=5.0 (phase 2), k_3=1×10^4, k_4 variable, k_5=1.0, k_6=3.0, k_7=1×10^{-6}, k_8=0.1. Initial concentrations (in au): A_0=3.0, E_0=333.23 (k_4=0); A_0=3.0, E_0=166.62 (k_4=1); A_0=3.0, E_0=55.46 (k_4=5); A_0=3.0, E_0=30.20 (k_4=10); A_0=3.0, E_0=15.77 (k_4=20); A_0=3.0, E_0=8.03 (k_4=40); A_0=3.0, E_0=4.02 (k_4=80). (b) Relationship to Weber's law: in phase 2 the perturbation k_2 and ($1/E_{ss}$) are linear functions of the background perturbation k_4 when the "just noticable difference" ΔA_{max} is 0.03. Rate constants and initial concentrations as in (a), except that k_2 in phase 2 has the following values: **1**, k_2 = 1.0314 (k_4 = 2); **2**, k_2 = 1.0627 (k_4 = 5); **3**, k_2 = 1.1150 (k_4 = 10); **4**, k_2 = 1.2195 (k_4 = 20); **5**, k_2 = 1.4285 (k_4 = 40); **6**, k_2 = 1.8465 (k_4 = 80); **7**, k_2 = 2.6820 (k_4 = 160). (c) Monotonic decrease of ΔA_{max} as a function of background k_4 for three different steps. At constant background ΔA_{max} increases with increasing step size. (d) t_{max} decreases monotonically with increasing backgrounds k_4. At constant background t_{max} decreases with increasing step size. Rate constants in panels (c) and (d) are the same as for panel (a), apart from k_2 and k_4. Initial concentrations were taken as the steady state values of A and E at the different backgrounds k_4 prior to the applied step in k_2.

https://doi.org/10.1371/journal.pone.0281490.g008

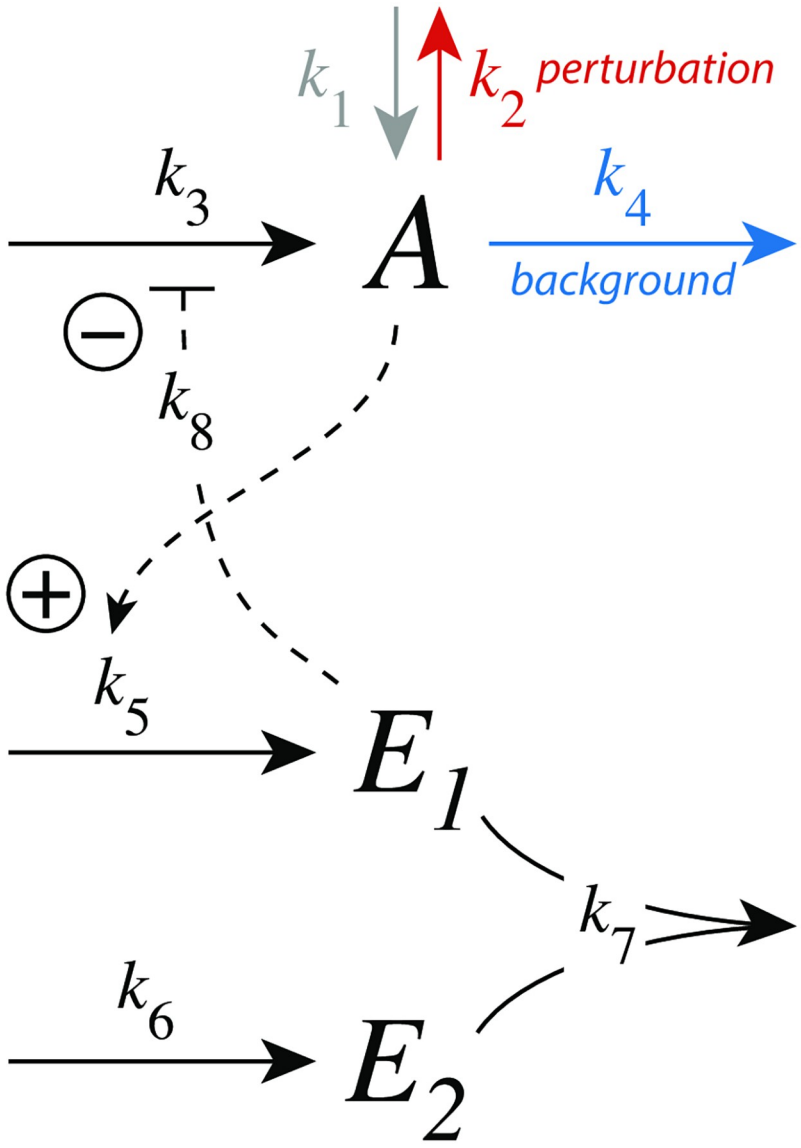

Fig 9. Controller motif m2 with antithetic integral control. Here, antithetic control is implemented as a bimolecular second-order reaction which removes the two controller molecules E_1 and E_2. See text on how A's set-point is calculated.

https://doi.org/10.1371/journal.pone.0281490.g009

$$\dot{E}_2 = k_6 - k_7 \cdot E_1 \cdot E_2 \tag{15}$$

From the steady-state conditions for E_1 ($k_5 \cdot A_{ss} = k_7 \cdot E_1 \cdot E_2$) and E_2 ($k_6 = k_7 \cdot E_1 \cdot E_2$) the set-point for A (A_{set}) is given by:

$$k_5 \cdot A_{ss} = k_7 \cdot E_1 \cdot E_2 = k_6 \quad \Rightarrow \quad A_{ss} = A_{set} = \frac{k_6}{k_5} \tag{16}$$

In many respects robust perfect adaptation by zero-order or bimolecular (antithetic) kinetics, i.e., E (Eq 12) and E_1 (Eq 14) behave dynamically identical. In fact, both E and E_1 show zero-

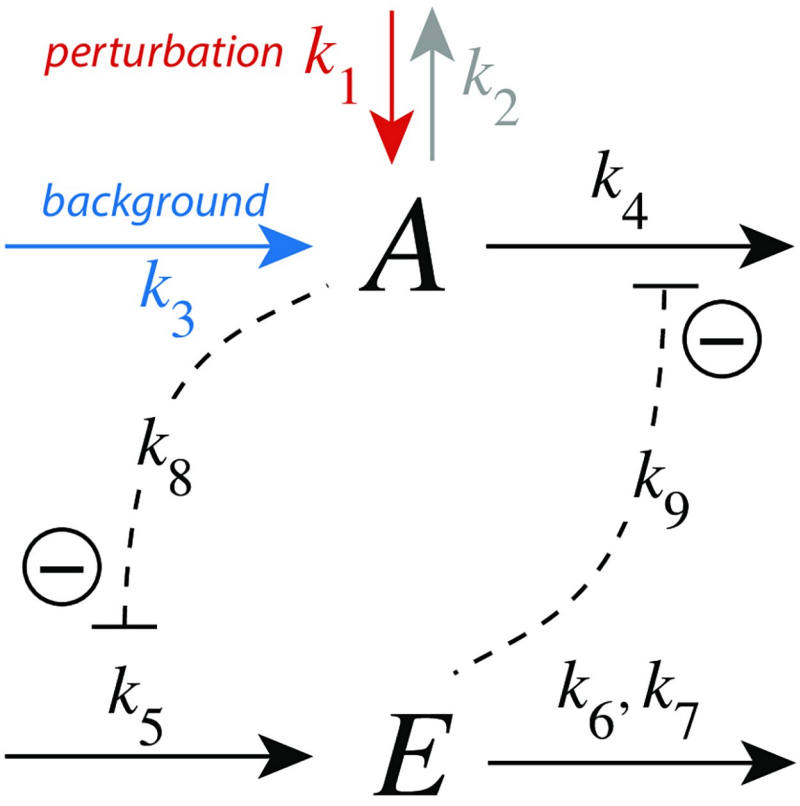

Fig 10. Outflow controller motif m8 with integral control implemented as a zero-order Michaelis-Menten (MM) type degradation of E. Rate constant k_1 undergoes a perturbation, while k_3 is a background inflow rate. k_8 and k_9 are inhibition constants. k_6 and k_7 are MM parameters analogous to V_{max} and K_M, respectively. For simplicity, the grayed-out rate constant k_2 is set to zero.

https://doi.org/10.1371/journal.pone.0281490.g010

order kinetics with respect to E and E_1, respectively. In the supporting information 'S3 Text' we show the identical antithetic behavior of the m2 scheme when using step perturbations at various backgrounds in comparison with the above m2 calculations using zero-order kinetics.

Controller m8. Fig 10 shows the scheme of controller m8. The compensatory outflow flux $j_4 = k_4 \cdot k_9 \cdot A/((k_9 + E))$ and the signaling from A to E are based on derepression.

The rate equations are:

$$\dot{A} = k_1 - k_2 \cdot A + k_3 - k_4 \cdot A \cdot \left(\frac{k_9}{k_9 + E}\right) \tag{17}$$

$$\dot{E} = k_5 \cdot \left(\frac{k_8}{k_8 + A}\right) - \frac{k_6 \cdot E}{k_7 + E} \tag{18}$$

The set-point of A is derived from the steady-state condition $\dot{E} = 0$ together with the assumption that E is removed by zero-order kinetics, i.e. $E/(k_7 + E) \approx 1$:

$$\dot{E} = 0 \;\Rightarrow\; k_5 \cdot \left(\frac{k_8}{k_8 + A_{ss}}\right) = k_6 \;\Rightarrow\; A_{set} = A_{ss} = k_8\left(\frac{k_5}{k_6} - 1\right) \tag{19}$$

Fig 11a shows the response of the m8 derepression controller at different but constant backgrounds k_3. Note the typical, more rapid, resetting when backgrounds are increased. Panel b

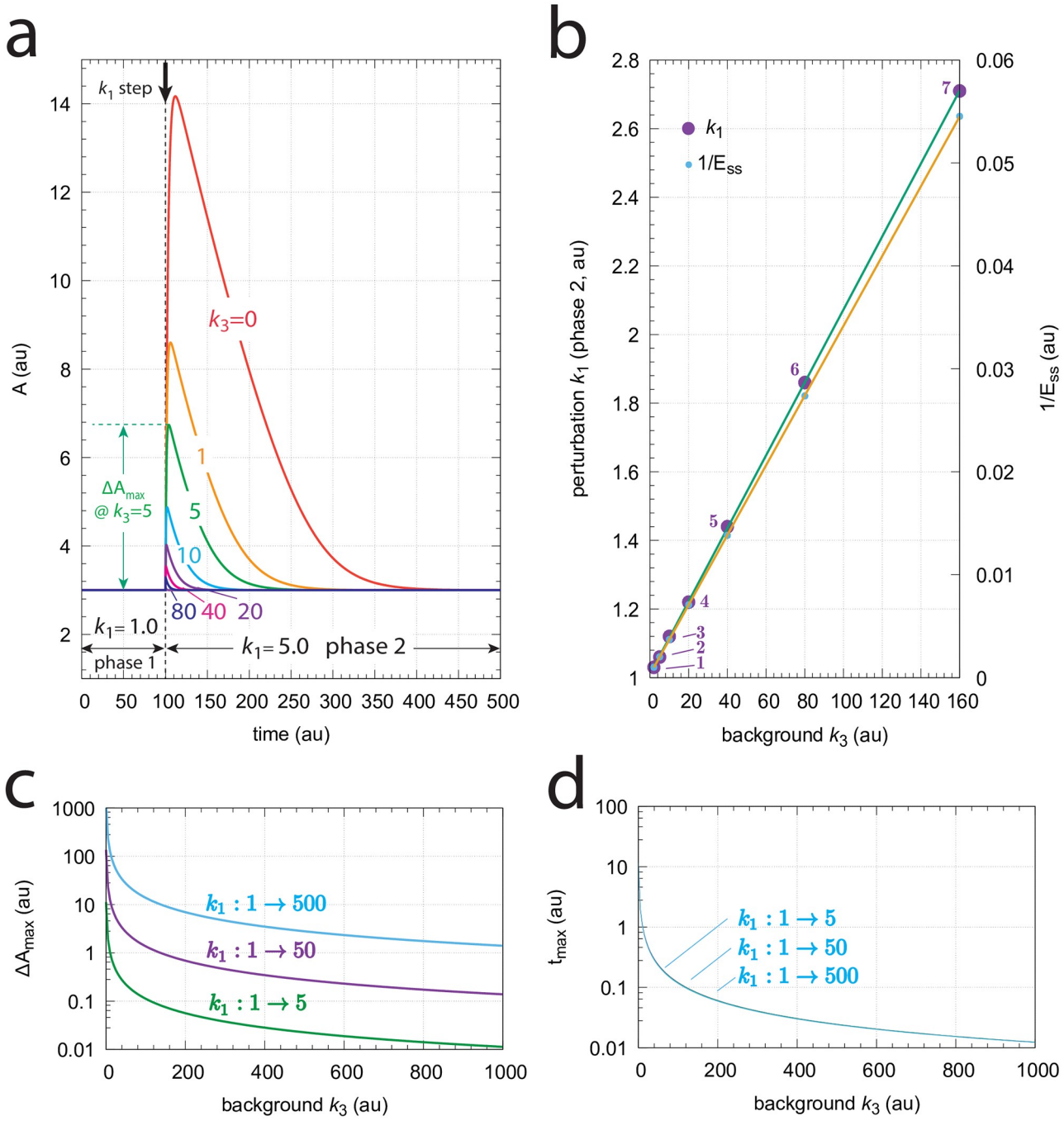

Fig 11. Response kinetics and relationship to Weber's law in the m8 controller (Fig 10). The set-point of A is A_{set}=3.0. (a) Step-wise increase of k_1 from 1.0 to 5.0 at time t=100 at different and constant background perturbations k_3 (0–80). Note the successive decrease in the excursion of A (ΔA_{max}) and the more rapid A resetting to the set-point at increased k_3 values. Rate constants (in au): k_1=1.0 (phase 1), k_1=5.0 (phase 2), k_2=0.0, k_3 variable, k_4 = 1×10^4, k_5=620.0, k_6=20.0, k_7=1×10^{-6}, k_8=k_9=0.1. Initial concentrations (in au): A_0=3.0, E_0=2999.90 (k_3=0); A_0=3.0, E_0=1499.90 (k_3=1); A_0=3.0, E_0=499.90 (k_3=5); A_0=3.0, E_0=272.63 (k_3=10); A_0=3.0, E_0=142.76 (k_3=20); A_0=3.0, E_0=73.07 (k_3=40); A_0=3.0, E_0=36.94 (k_3=80). (b) Relationship to Weber's law: the perturbation k_1 and ($1/E_{ss}$) in phase 2 are linear functions of the background perturbation k_3 when k_1 is adjusted such that a "just noticable difference" of ΔA_{max}=0.03 is observed. Rate constants and initial concentrations as in (a), except that k_1 in phase 2 has the following values: **1**, k_1 = 1.0319 (k_3 = 2); **2**, k_1 = 1.0637 (k_3 = 5); **3**, k_1 = 1.1169 (k_3 = 10); **4**, k_1 = 1.2231 (k_3 = 20); **5**, k_1 = 1.4356 (k_3 = 40); **6**, k_1 = 1.8604 (k_3 = 80); **7**, k_1 = 2.7111 (k_3 = 160). (c) ΔA_{max} values as a function of background k_3 for three step perturbations in k_1. Like for the m7 controller the three curves are congruent and their shape can be moved onto each other. (d) t_{max} as a function of background k_3. For a given background t_{max} values are practically the same independent of the three steps. Rate constants in panels (c) and (d) are the same as for panel (a), apart from k_1 and k_3. Initial concentrations are taken as the steady state values for A and E at the different backgrounds k_3 prior to the applied step in k_1.

https://doi.org/10.1371/journal.pone.0281490.g011

shows that the controller follows Weber's law (Eq 1), i.e. when setting a "just noticeable difference" of ΔA_{max} to 1% of the set-point of A (A_{set}=3.0) the required perturbations k_1 in phase 2 needed to achieve ΔA_{max}=0.03 become a linear function of the background k_3. Similarly, plotting ($1/E_{ss}$) against the background is likewise linear, suggesting that ($1/E_{ss}$) may be interpreted as the "perception" of ΔA_{max}. Fig 11c and 11d show how ΔA_{max} and t_{max} depend on the background k_3, respectively.

Implications to photoreceptor adaptation

As a biological example, we found a striking analogy between the resetting kinetics of the derepression controllers m2, m4, m6, and m8 and the responses in vertebrate photoreceptors. In mammals and other animals photoadaptation occurs mainly in the retina, which consists of five basic classes of neurons: photoreceptors, bipolar cells, ganglion cells, horizontal cells, and amacrine cells, where each of them come in different subclasses. These neurons are arranged in layers and form a complex interaction network [21, 32, 33]. Our focus here is on the light-sensitive photoreceptor cells, which according to their physical shape are characterized as rods and cones, and differ in their sensitivity to light. Rods and cones occur in all retinas with the exception of the skate [33].

Fig 12 shows voltage responses of a rod cell to 10 ms light flashes at different background light intensities [34]. The experiments show that increased backgrounds lead to diminished

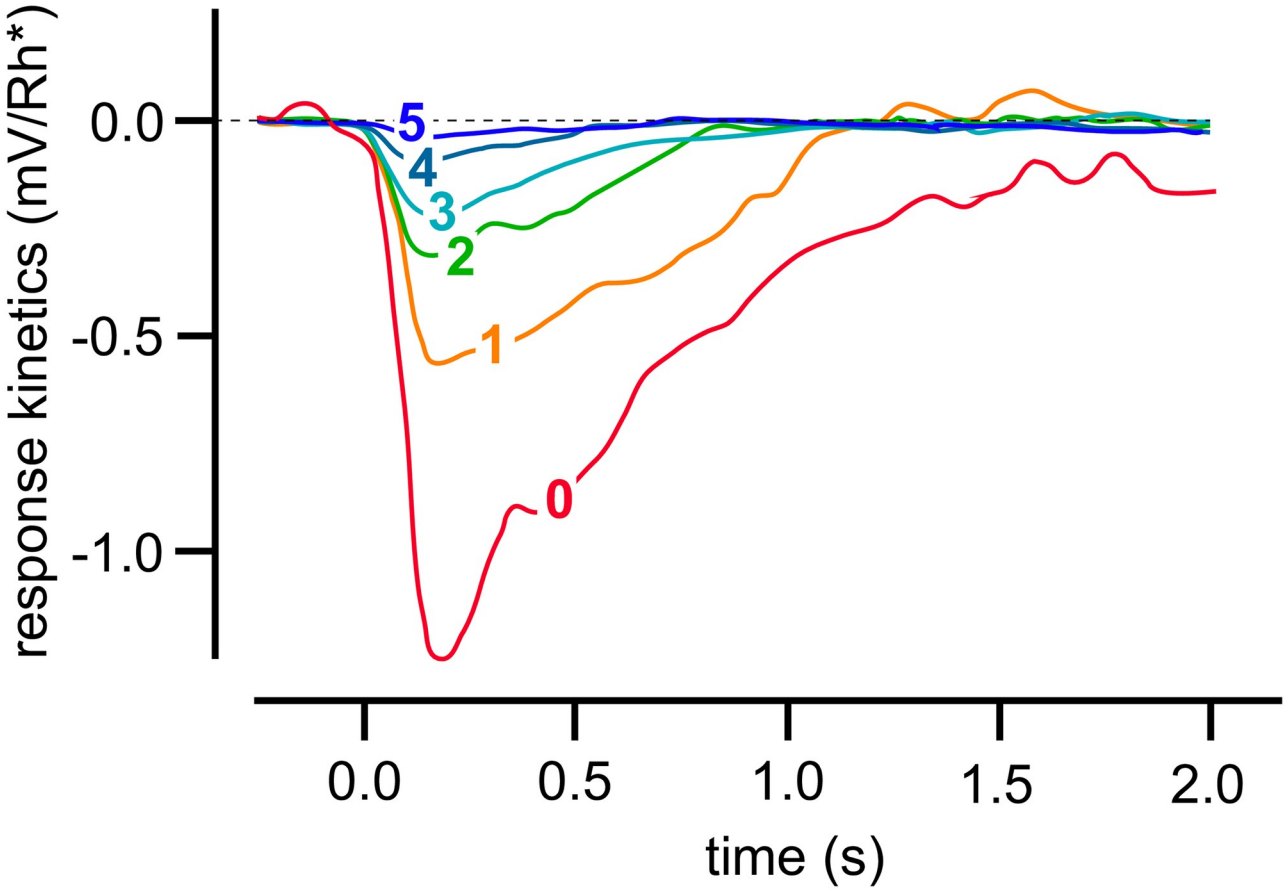

Fig 12. Light adaptation in a Macaque monkey's rod cell. 10 ms light flashes were applied to different light background intensities. Background intensities (in photons $\mu m^{-2}s^{-1}$) were: **0**, 0; **1**, 3.1; **2**, 12; **3**, 41; **4**, 84; **5**, 162. Redrawn after Fig 2A from Ref [34].

https://doi.org/10.1371/journal.pone.0281490.g012

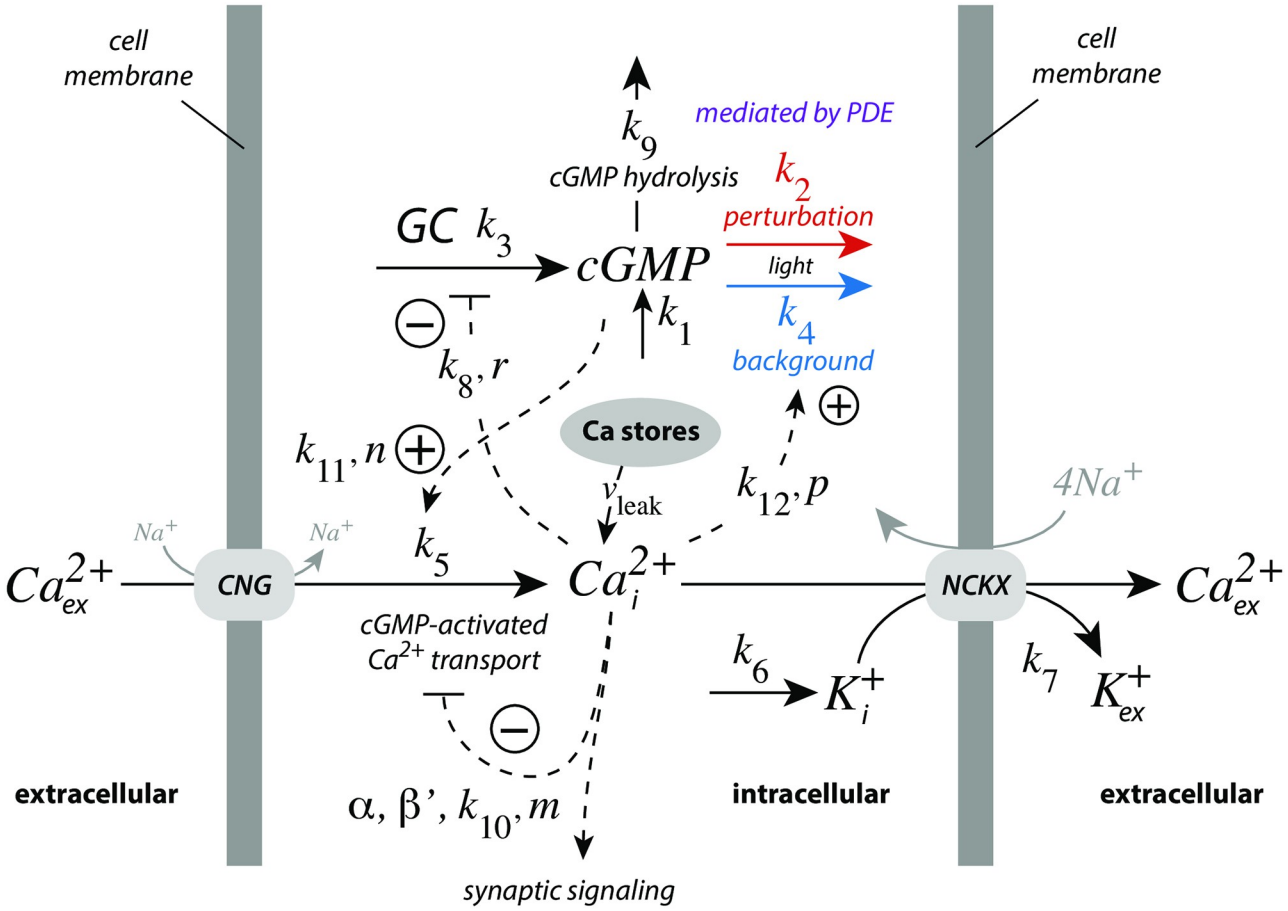

Fig 13. Model with the main regulatory elements of vertebrate photoreceptor adaptation. Light leads to the removal of cyclic guanosine monophosphate (cGMP) by phosphodiesterases (PDE), via transducin and the activation of PDE by internal Ca^{2+} (Ca^{2+}_i). In the figure this path is split into two components, one background with rate constant k_4 (outlined in blue), and a perturbation on top of the background (rate constant k_2, outlined in red). cGMP is formed by guanylate cyclase (GC). cGMP's constitutive non-light induced hydrolysis is described by a first-order reaction with rate constant k_9. GC is inhibited/derepressed by Ca^{2+}_i to keep cGMP under homeostatic control. cGMP activates cyclic nucleotide-gated (CNG) channels, which leads to the inflow of Ca^{2+} into the cell, while high Ca^{2+}_i levels inhibit CNG channels. Calcium is removed from the cell by potassium-dependent sodium-calcium exchangers (NCKX). Rate equations and used rate parameter values are described in the main text. Grayed reaction arrows indicate reactions which are not included in the model.

https://doi.org/10.1371/journal.pone.0281490.g013

response excursions, while the resetting to the initial steady state levels were found to be faster. This behavior, a decreased sensitivity but accelerated response kinetics at increased background light intensities is considered typical for the light adaptation in vertebrate rod or cone cells [35]. When corresponding photocurrents are studied as a function of different background light levels the observed resetting behavior is close to that found for m8 or m6 controllers (for experimental data see Fig 1 in Ref [36]).

In photoreceptor cells cytosolic calcium has been found to be the major regulator in vertebrate light adaptation [37]. There, calcium takes part in a derepressing feedback loop analogous as E in m2. Fig 13 shows a model with its main regulatory elements. In comparison with extracellular Ca^{2+} concentrations, which are in the 10–100 mM range, cytosolic (internal) Ca^{2+} levels (Ca^{2+}_i) are considerably lower, around in the 100 nM range since too high cytosolic Ca^{2+}_i concentrations are toxic and may lead to apoptosis. While Ca^{2+} is a versatile cellular signal its levels are also tightly regulated [38]. In photoreceptor cells dark Ca^{2+}_i levels are in the

range around 300–500 nM [37], which is sufficient to regulate photo-transduction, but at the same time low enough to avoid cytotoxic Ca^{2+} effects.

In vertebrate photoreceptor cells Ca_i^{2+} is part of a negative feedback regulation of cyclic guanosine monophosphate (cGMP), where cGMP activates the inflow of Ca^{2+} into the cytosol by cyclic nucleotide-gated (CNG) channels [37–39]. Analogous to a m2 controller, Ca_i^{2+} on its side inhibits guanylate cyclase (GC), which synthesizes cGMP. In addition, Ca^{2+} inhibits its inflow by CNG channels and takes part, analogous to a m5 controller, in the light-dependent removal of cGMP (with rate constants k_2 and k_4) by activating phosphodiesterases (PDE). Potassium-dependent sodium-calcium exchangers (NCKX) pump Ca_i^{2+} out of the cell. In the model the removal of Ca_i^{2+} by NCKX is formulated, for the sake of simplicity, as a bimolecular second-order reaction, where K^+ is removed together with Ca_i^{2+}, while keeping NCKX constant. For certain feedback combinations the bimolecular (or a zero-order) removal of Ca_i^{2+} and K^+ by NCKX will lead to robust perfect adaptation of cGMP, which is discussed below. k_1 represents an inflow perturbation with respect to cGMP. We have mostly ignored k_1, except in section "Roles of the feedback loops", where k_1 is used to test the homeostatic behaviors of the individual feedback loops.

The rate equations of the model are:

$$\dot{\mathrm{cGMP}} = k_1 + k_3\left(\frac{k_8^r}{k_8^r + (\mathrm{Ca}_i^{2+})^r}\right) - k_9 \cdot \mathrm{cGMP} - \underbrace{(k_2 + k_4) \cdot (cGMP) \cdot \frac{(\mathrm{Ca}_i^{2+})^p}{k_{12}^p + (\mathrm{Ca}_i^{2+})^p}}_{light\ \ induced} \tag{20}$$

$$\dot{\mathrm{Ca}_i^{2+}} = k_5 \cdot \frac{(\mathrm{cGMP})^n}{k_{11}^n + (\mathrm{cGMP})^n}\left(\alpha \cdot \frac{k_{10}^m}{k_{10}^m + (\mathrm{Ca}_i^{2+})^m} + \beta'\right) - k_7(\mathrm{Ca}_i^{2+})(\mathrm{K}^+) + v_{\mathrm{leak}} \tag{21}$$

$$\dot{\mathrm{K}^+} = k_6 - k_7(\mathrm{Ca}_i^{2+})(\mathrm{K}^+) \tag{22}$$

Estimation of model parameters. Fig 14 gives an overview of the experimental data used to estimate some of the model parameters. Panel a shows the results by Koutalos et al. (Fig 3 in [40]; see also Fig 3 in [41]), who studied the influence of Ca^{2+} on the light-stimulated PDE activity in salamander rods. The experimental data were described by the function

$$f(\mathrm{Ca}_i^{2+}) = \frac{V_{max} \cdot (\mathrm{Ca}_i^{2+})^p}{k_{12}^p + (\mathrm{Ca}_i^{2+})^p} \tag{23}$$

with V_{max}=(100.01±2.53)%, p=0.894±0.0534, and k_{12}=(622.612±55.01)nM.

Also using salamander rods, Fig 14b shows the inhibition of GC activity by Ca^{2+} when using 0.5 mM GTP (Fig 13 in [42]). The function

$$g(\mathrm{Ca}_i^{2+}) = \frac{k_8^r}{k_8^r + (\mathrm{Ca}_i^{2+})^r} \tag{24}$$

was fitted to the data with k_8=(57.49±2.53)nM and r=1.65±0.12.

Using bovine retinae, Hsu and Molday [39] determined the influence of cGMP and Ca^{2+} on CNG channel activity in the presence of calmodulin (Fig 14, panels c and d, respectively).

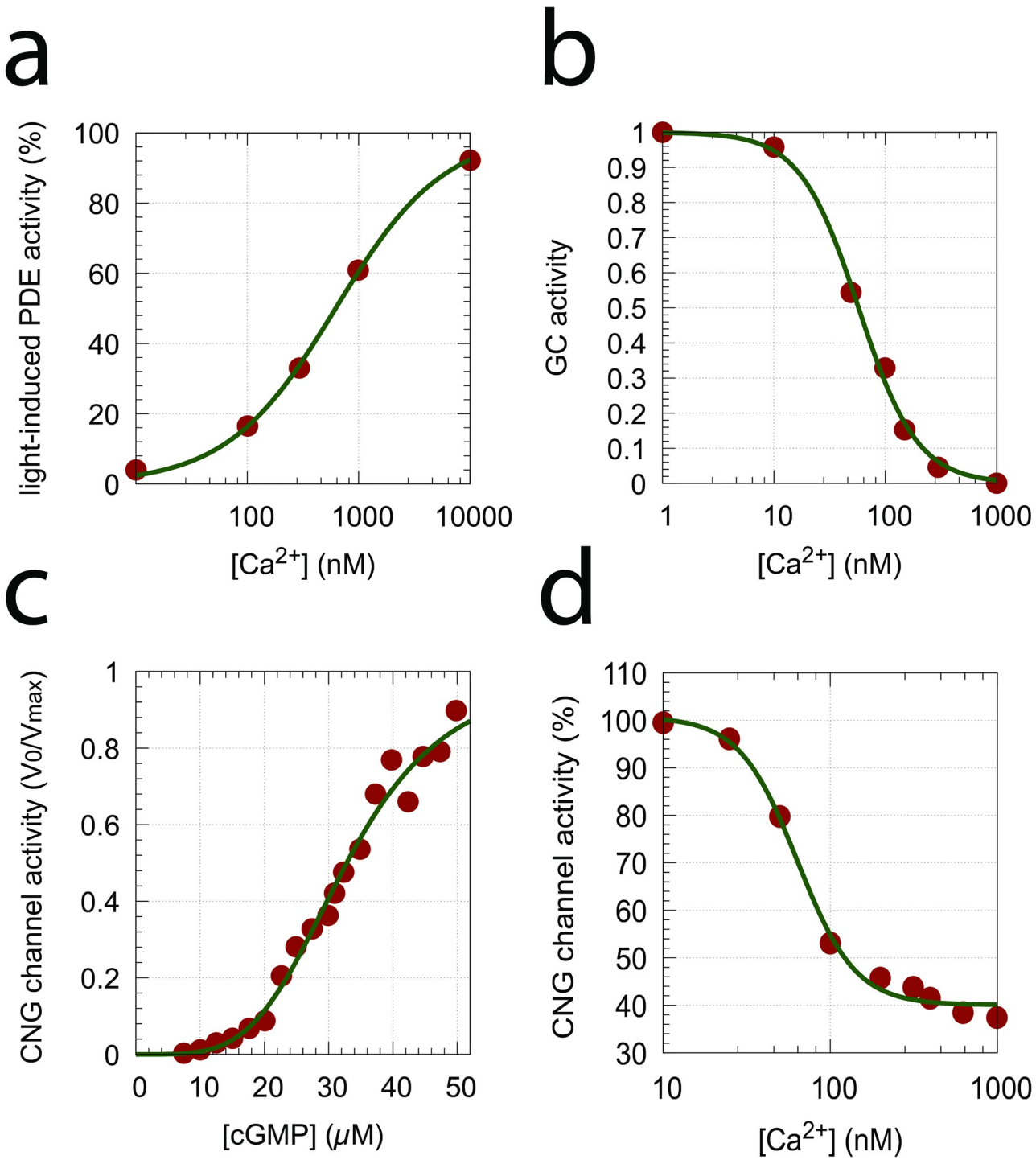

Fig 14. Normalized experimental data used to extract parameter values. (a) Light-induced PDE activity as a function of Ca^{2+} concentration [40, 41]; (b) Inhibition of GC activity by Ca^{2+} [42]; (c) CNG channel activity as a function of cGMP concentration [39]; (d) CNG channel activity as a function of Ca^{2+} concentration [39].

https://doi.org/10.1371/journal.pone.0281490.g014

For CNG channel activation by cGMP (panel c) the following trial function

$$h(cGMP) = \frac{(\mathrm{cGMP})^n}{k_{11}^n + (\mathrm{cGMP})^n} \tag{25}$$

described the experimental data with k_{11}=(32.81±0.39)μM and n=4.14±0.23 quite well. For the inhibition of the CNG channel by Ca^{2+} (panel d) we fitted the function

$$k(\alpha, \beta, \mathrm{Ca}_i^{2+}) = 100 \cdot \alpha \cdot \frac{k_{10}^m}{k_{10}^m + (\mathrm{Ca}_i^{2+})^m} + \beta \tag{26}$$

to the experimental data obtaining α=0.6067±0.0295, k_{10}=(63.57±4.44)nM, m=2.50±0.38, and β=40.07±1.29. In Eq 21 β' is given by β/100.

Organelles, such as mitochondria and the endoplasmatic reticulum (ER), store calcium with relative high concentrations (100–800μM). There is evidence that intracellular Ca stores leak Ca into the cytosol [43–46]. Analyzing the data by Camello et al. [45] and Luik et al. [46], we observed (S4 Text and [47]) that the kinetics of the two recorded leaks were surprisingly different. While Camello et al. [45] found practically zero-order kinetics with respect to ER calcium and leak rates at around 0.25 μM/s, the data by Luik et al. [46] show clean *first-order* kinetics with respect to ER calcium. Here Ca-dependent leak velocities between 5.5 and 0.36 μM/s were observed (S4 Text). Also the results by Oldershaw et al. [43] and Missiaen et al. [44] indicate single or dual first-order kinetics in the decrease of store Ca. We wondered how calcium leaks may influence the photoadaptation of the model. As we will show in the section "Roles of the feedback loops" calcium leaks will have an influence on the steady state level of cGMP. In particular, when the leak rate v_{leak} becomes larger than the K^+ inflow rate k_6 in the NCKX-based calcium pump, then uncontrolled growth in Ca_i^{2+} may occur (S4 Text).

cGMP hydrolysis in darkness (rate constant k_9) is described as a first-order reaction with respect to cGMP. The value of k_9 is taken from the modeling work by Nikonov et al. (Table IV in [48]) with k_9=1.0s^{-1}. The rates for the light-induced removal of cGMP (described by k_2 and k_4) are variable (light-dependent) parameters.

Parameter k_3 represents the maximum rate of cGMP synthesis at low Ca_i^{2+} concentrations. Its value (k_3=50 μM/s) has been taken from the work by Nikonov et al. [48].

The extrusion of Ca_i^{2+} by NCKX is simplified as a second-order process with rate constant k_7, i.e. $v_{\mathrm{extrude}} = k_7 \cdot (\mathrm{K}^+) \cdot (\mathrm{Ca}_i^{2+})$. Apart from that, we have not considered sodium ion and potassium ion currents.

It is interesting to note that in the absence of the CNG channel inhibition by Ca_i^{2+} the NCKX pump would lead to robust perfect adaptation in cGMP by antithetic feedback [14], like the zero-order removal of E in the above idealized controllers (see for example, Eq 12). However, such an antithetic control of cGMP without CNG channel inhibition by Ca_i^{2+} would lead to high Ca_i^{2+} concentrations and thereby to possible apoptosis of photoreceptor cells [49].

The remaining parameters k_5, k_6, and k_7 have been chosen such that cGMP and Ca_i^{2+} levels are close to the observed experimental values [35, 37, 50, 51], i.e., using k_5=100 μM/s, k_6=0.5 μM/s, and k_7=2.0 $\mu M^{-1}s^{-1}$. While k_7 has no influence on the steady state values of cGMP and Ca_i^{2+} it has a significant influence on how fast steady state levels are approached after light perturbations are applied (S5 Text).

Application of pulse perturbations. In the majority of experiments on rod or cone cells light perturbations are applied in form of flashes in the millisecond range (see for example Fig 12). Fig 15 shows the application of 10 ms pulses of light in the model. A k_2 pulse from $1 \rightarrow 50\ s^{-1}$ is applied at time t=1.0 s for different k_4 backgrounds. In panel a the graphs are

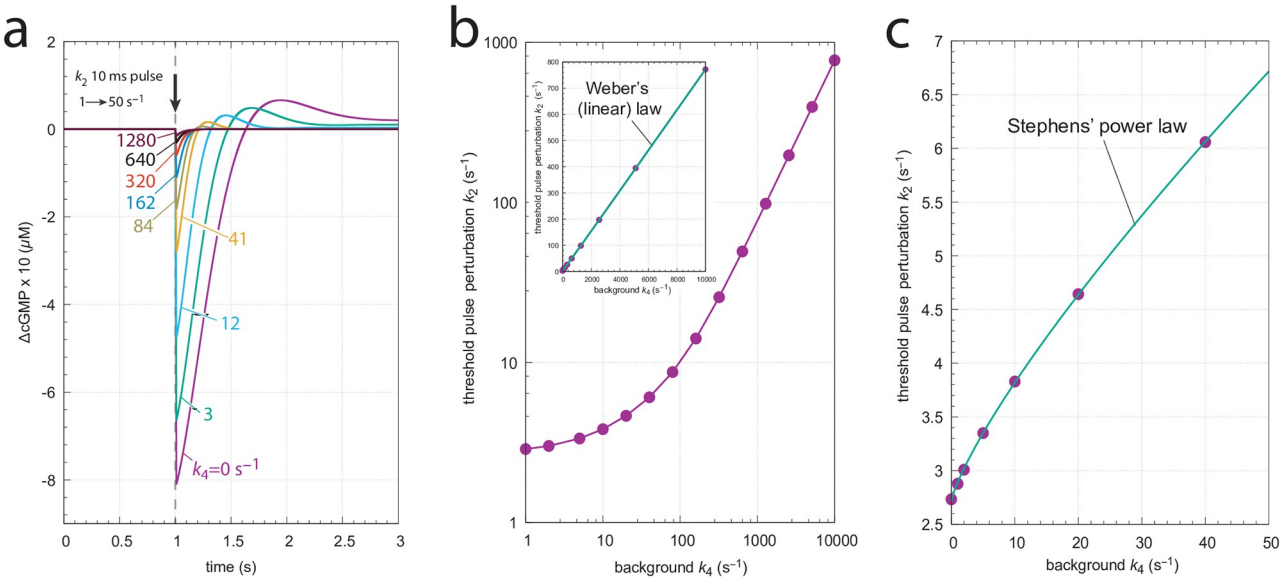

Fig 15. Application of 10 ms k_2 pulses (1 → 50 s^{-1}) at different k_4 backgrounds. (a) the scaled ΔcGMP levels against time. Colored numbers indicate the different background levels in s^{-1}. Initial concentrations (in μM): cGMP$_0$=9.04191, $Ca^{2+}_{i,0} = 1.25717 \times 10^{-1}$, $K^+_0 = 1.25717$ (k_4=0 s^{-1}); cGMP$_0$=8.80039, $Ca^{2+}_{i,0} = 9.89550 \times 10^{-2}$, $K^+_0 = 2.52640$ (k_4=3 s^{-1}); cGMP$_0$=8.36375, $Ca^{2+}_{i,0} = 6.80242 \times 10^{-2}$, $K^+_0 = 3.67516$ (k_4=12 s^{-1}); cGMP$_0$=7.86039, $Ca^{2+}_{i,0} = 3.83237 \times 10^{-2}$, $K^+_0 = 6.52333$ (k_4=41 s^{-1}); cGMP$_0$=7.67946, $Ca^{2+}_{i,0} = 2.34638 \times 10^{-2}$, $K^+_0 = 1.06543 \times 10^{1}$ (k_4=84 s^{-1}); cGMP$_0$=7.61322, $Ca^{2+}_{i,0} = 1.31981 \times 10^{-2}$, $K^+_0 = 1.89421 \times 10^{1}$ (k_4=162 s^{-1}); cGMP$_0$=7.59537, $Ca^{2+}_{i,0} = 6.58562 \times 10^{-3}$, $K^+_0 = 3.79615 \times 10^{1}$ (k_4=320 s^{-1}); cGMP$_0$=7.59210, $Ca^{2+}_{i,0} = 3.09110 \times 10^{-3}$, $K^+_0 = 8.087735 \times 10^{1}$ (k_4=640 s^{-1}); cGMP$_0$=7.59160, $Ca^{2+}_{i,0} = 1.42894 \times 10^{-3}$, $K^+_0 = 1.74954 \times 10^{2}$ (k_4=1280 s^{-1}). Panel b shows the threshold perturbation k_2, which leads to a ΔcGMP of 0.03 μM as a function of background. The overall curved log-log plot turns out to be linear and follows Weber's law (inset) as: threshold perturbation $k_2 = a{\cdot}(k_4)^n + b$ with a=(0.069±0.001)s^{n-1}, n=1.012±0.002, and b=(2.73±0.20)s^{-1}. Panel c shows that at low backgrounds the threshold-background relationship follows Stephens' power law, i.e., threshold perturbation $k_2 = a{\cdot}(k_4)^n + b$ with a=(0.175±0.006)s^{n-1}, n=0.800±0.009, and b=(2.72±0.01)s^{-1}. Parameter and rate constant values are as described in the previous section. See also 'S1 Programs' in S1 File.

https://doi.org/10.1371/journal.pone.0281490.g015

scaled such that the steady state levels of cGMP are set to zero and the individual excursions in cGMP can be compared. As for the above derepression controllers m2, m4, m6 and m8 the excursion $\Delta cGMP_{max}$ of the controlled variable cGMP decreases with increasing backgrounds while the speed of resetting to its original steady state increases with increasing backgrounds (Fig 15a). These changes are considered to be typical for the light adaptation in vertebrate photoreceptors (for example, see Ch. V in [35] and Fig 22–19C in [21]).

Fig 15b shows threshold light pulse (10 ms) perturbations k_2 with a ΔcGMP of 0.03 μM as a function of background light intensity k_4. The main graph shows the log-log plot which resembles the experimental results with rods or cones (see Fig 22–19B in [21]). The inset shows that the threshold-background relationship is linear in agreement with Weber's law, at least for large backgrounds. Panel c shows, on the other hand, that for small backgrounds the threshold-background relationship follows Stephens' power law. In fact, replotting the original experimental data [52] shown in Fig 22–19B of Ref [21], indicates that Stephens' law describes best the situation at low backgrounds, while at higher backgrounds the threshold-background relationship tends towards Weber's law (S6 Text).

Application of step perturbations. We applied step perturbations in the model to see to what extent the CNG channel inhibition by calcium affects cGMP homeostasis and avoids robust perfect adaptation. Fig 16a shows the influence of k_{21}→ 50 s^{-1} steps at different backgrounds. The steps occur at time t=0.5 s and changes in cGMP are followed for 3 s. We also measured the maximum excursion of cGMP ($\Delta cGMP_{max}$) from its initial steady state level and the time t_{max} at which $\Delta cGMP_{max}$ occurs (see inset).

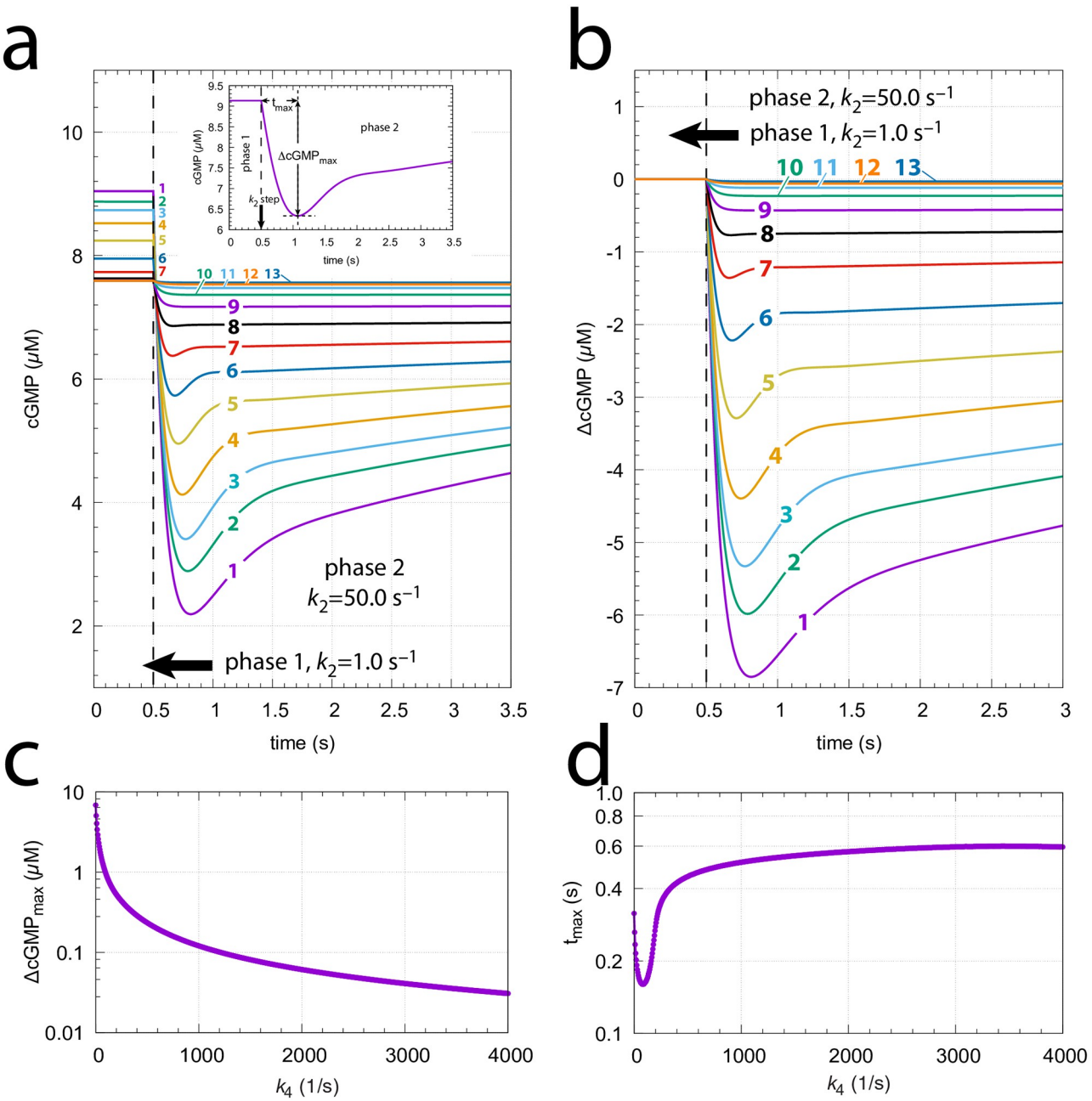

Fig 16. The model's response towards k_{21}→ 50 s^{-1} steps at different backgrounds k_4. (a) Unscaled cGMP concentrations as a function of time. The steps occur at t=0.5 s. Background k_4 values (s^{-1}): **1**, 0.0; **2**, 2.0; **3**, 4.0; **4**, 8.0; **5**, 16.0; **6**, 32.0; **7**, 64.0; **8**, 128.0; **9**, 256.0; **10**, 512.0; **11**, 1024.0; **12**, 2048.0; **13**, 4096.0. Initial concentrations (in μM): cGMP$_0$=9.04191, $Ca^{2+}_{i,0}$ = 1.25717, K^+_0 = 1.25717 (k_4=0 s^{-1}); cGMP$_0$=8.87243, $Ca^{2+}_{i,0}$ = 1.05733, K^+_0 = 2.36445 (k_4=2 s^{-1}); cGMP$_0$=8.73490, $Ca^{2+}_{i,0}$ = 9.33822, K^+_0 = 2.67717 (k_4=4 s^{-1}); cGMP$_0$=8.52196, $Ca^{2+}_{i,0}$ = 7.79015, K^+_0 = 3.20918 (k_4=8 s^{-1}); cGMP$_0$=8.24168, $Ca^{2+}_{i,0}$ = 6.08968, K^+_0 = 4.10531 (k_4=16 s^{-1}); cGMP$_0$=7.95044, $Ca^{2+}_{i,0}$ = 4.40458, K^+_0 = 5.67591 (k_4=32 s^{-1}); cGMP$_0$=7.73313, $Ca^{2+}_{i,0}$ = 2.87344, K^+_0 = 8.70036 (k_4=64 s^{-1}); cGMP$_0$=7.62877, $Ca^{2+}_{i,0}$ = 1.64393, K^+_0 = 1.52075 × 10^1 (k_4=128 s^{-1}); cGMP$_0$=7.59845, $Ca^{2+}_{i,0}$ = 8.33466, K^+_0 = 2.99952 × 10^1 (k_4=256 s^{-1}); cGMP$_0$=7.59259, $Ca^{2+}_{i,0}$ = 3.95393, K^+_0 = 6.3228 × 10^1 (k_4=512 s^{-1}); cGMP$_0$=7.59165, $Ca^{2+}_{i,0}$ = 1.83312, K^+_0 = 1.36379 × 10^2 (k_4=1024 s^{-1}); cGMP$_0$=7.59154, $Ca^{2+}_{i,0}$ = 8.44877, K^+_0 = 2.95901 × 10^2 (k_4=2048 s^{-1}); cGMP$_0$=7.59152, $Ca^{2+}_{i,0}$ = 3.88973, K^+_0 = 6.42718 × 10^2 (k_4=4096 s^{-1}). Inset: Defining ΔcGMP$_{max}$ and t_{max}. (b) cGMP data as in (a), but scaled relative to their initial steady state concentrations. (c) and (d) ΔcGMP$_{max}$ and t_{max} values as a function of backgrounds k_4, respectively. Parameter and rate constant values are as described in section "Estimation of model parameters" (see also S1 Programs in S1 File).

https://doi.org/10.1371/journal.pone.0281490.g016

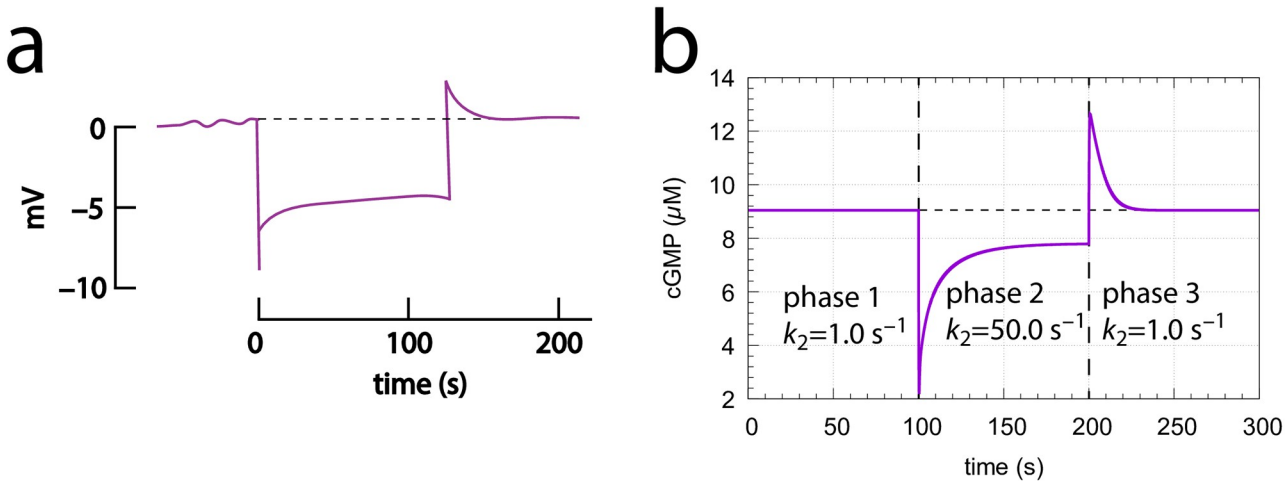

Fig 17. Experimental and model behaviors when applying step perturbations. (a) Experimental response of a red-sensitive turtle cone to a long step of light. Redrawn from Ref [53] (Fig 14, trace 2). (b) Model calculation using a $k_{21}\rightarrow$ 50 s^{-1} step at time t=100s. After 100 s k_2 returned to its original value. Background k_4=0.0 s^{-1}. All other rate parameters are as described in section "Estimation of model parameters". Initial concentrations: cGMP = 9.04μM, Ca_i^{2+} = 125.7nM, K^+=2.0μM. See also S1 Programs in S1 File.

https://doi.org/10.1371/journal.pone.0281490.g017

Fig 16b shows the same data as in (a), but scaled relative to their initial steady states. Due to the inhibition of CNG channels by calcium (Fig 13) the model does not show robust perfect adaptation (S5 Text, Fig 17). cGMP steady state levels during the step become significantly lower than their initial values before the step. This is seen in Fig 16a, where the pre-step steady state levels decrease as the background k_4 increases. Not unexpected we see that with increasing backgrounds the $\Delta cGMP_{max}$ excursions decrease monotonically (Fig 16c). Surprisingly, however, we find that t_{max} first decreases, but then increases again (Fig 16d). Interestingly, when studying turtle photoreceptors, an increase of t_{max} at increasing backgrounds has also been reported by Baylor and Hodgkin [53]. They studied both flashes and steps [54, 55] and provided several models [56] to explain the lengthening of the peak time t_{max}.

Fig 17a shows experimental results by Baylor and Hodgkin [53] when long steps of light are applied to red-sensitive turtle cones. The behavior of our model (panel b) is analogous with a typical overshooting when the step ends.

Roles of the feedback loops. Outlined in Fig 18 are the three feedback loops in the model. Feedback loops 1 and 2, both based on the inflow activation of Ca_i^{2+} by cGMP (outlined in purple), feed respectively back to cGMP by a Ca_i^{2+}-based inhibition (derepression) of cGMP synthesis (loop 1, analogous to m2, outlined in red) and by a Ca_i^{2+}-based activation of cGMP turnover (loop 2, analogous to m5, outlined in blue). Both loops 1 and 2 promote robust perfect cGMP homeostasis by antithetic control and oppose perturbations on cGMP. Feedback 3 (outlined in orange) keeps Ca_i^{2+} levels low to avoid high and cytotoxic calcium levels inside the cell.

When feedback loop 3 is absent, for example by low Ca_i^{2+} levels, the Ca_i^{2+}-inhibition term in Eq 21 becomes 1, because

$$\left(\alpha \cdot \frac{k_{10}^m}{k_{10}^m + (Ca_i^{2+})^m} + \beta'\right) \xrightarrow{\text{low } Ca_i^{2+}} \alpha + \beta' = 1 \tag{27}$$

The remaining feedbacks 1 and 2 will provide robust perfect adaptation of cGMP, provided that there are sufficiently high GC and PDE activities to work as compensatory fluxes. This

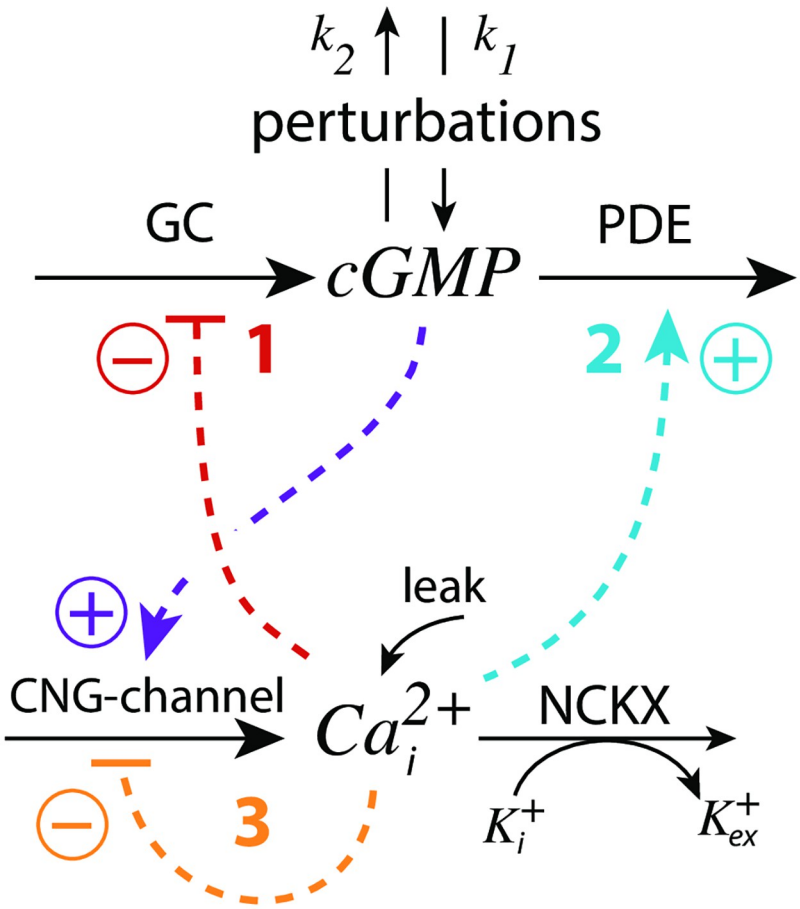

Fig 18. Schematic outline of the feedback loops 1–3 in the model (Fig 13). CNG: cyclic nucleotide-gated; GC: guanylate cyclase; PDE: phospho-diesterase; NCKX: potassium-dependent sodium-calcium exchangers (without the sodium part).

https://doi.org/10.1371/journal.pone.0281490.g018

robust perfect adaptation in cGMP is due to the simultaneous NCKX-based removal of Ca_i^{2+} and K^+ described by the term $k_7(Ca_i^{2+})(K^+)$ in Eqs 21 and 22. The $k_7(Ca_i^{2+})(K^+)$ transport term leads to robust antithetic integral control [14]. Instead of using the term $k_7(Ca_i^{2+})(K^+)$, one could have explicitly included the NCKX transporter protein, as generally outlined in [16] for catalyzed antithetic controllers. Anyway, using the $k_7(Ca_i^{2+})(K^+)$ term, the set-point of cGMP ($cGMP_{set}$) is calculated by setting Eqs 21 and 22 to zero and solving for cGMP. The resulting steady state concentration of cGMP becomes cGMP's set-point:

$$cGMP_{set} = cGMP_{ss} = k_{11}\sqrt[n]{\frac{b}{1-b}} \quad \text{with } b = \frac{k_6 - v_{\text{leak}}}{k_5} \tag{28}$$

Using the experimentally determined rate parameters (see section "Estimation of model parameters") leads to $cGMP_{set} = 7.61\mu M$. The two feedback loops 1 and 2 act as an *antagonistic* pair as they will defend $cGMP_{set}$ robustly against both inflow and outflow perturbations, respectively. Fig 19a shows the homeostatic behavior of the loop 1–2 antagonistic feedback during three different phases where either inflow perturbation k_1 or outflow perturbation k_2 dominate. Although the antagonistic feedback can deal well with both inflow and outflow

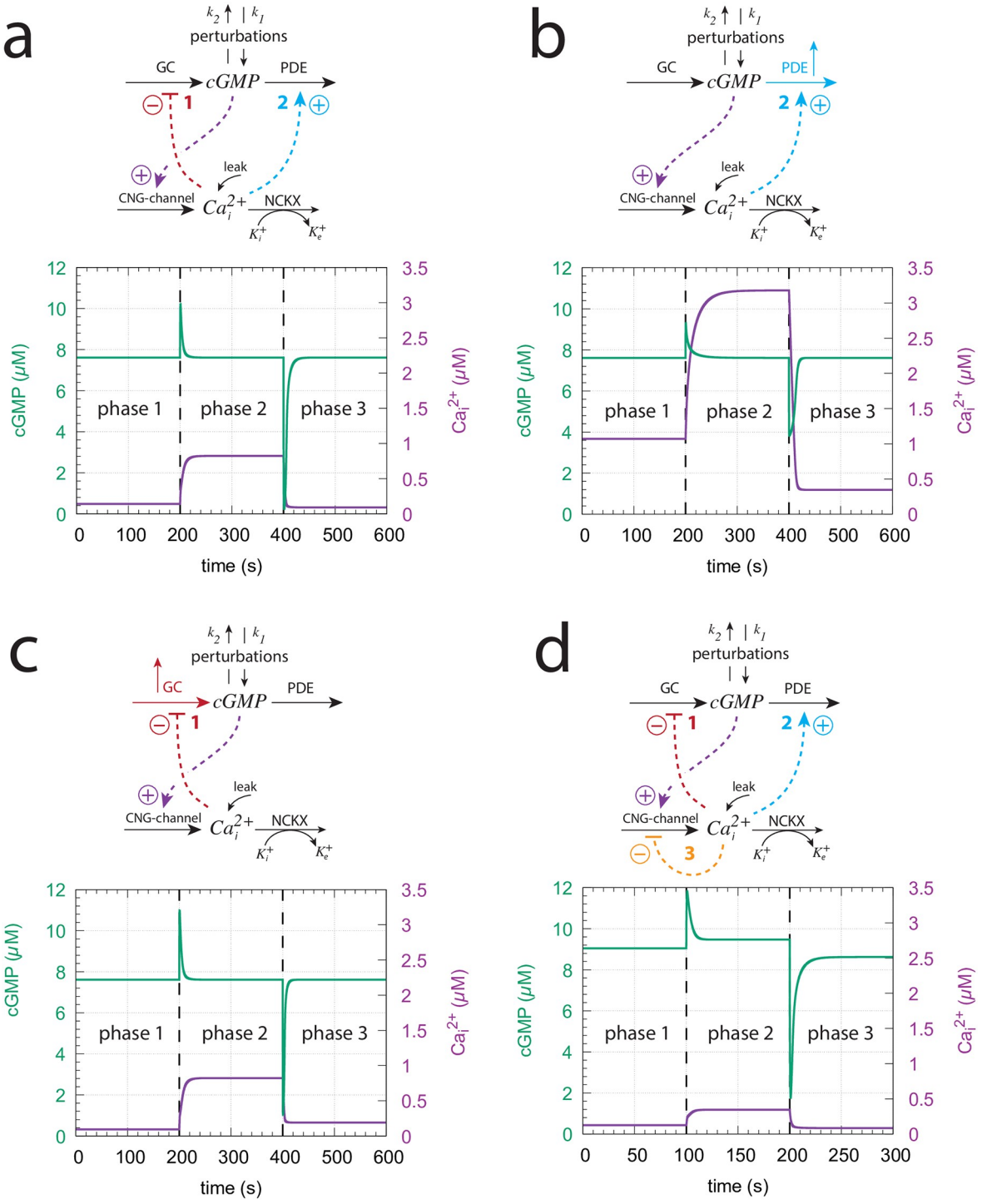

Fig 19. Influence of the model's three feedback loops on the homeostatic behavior of cGMP and Ca_i^{2+}. Perturbation profile in panels (a)-(d): phase 1: k_1=0.0μM/s, k_2=1.0s^{-1}, k_4=0.0s^{-1}; phase 2: k_1=7.0μM/s, k_2=0.0s^{-1}, k_4=0.0s^{-1}; phase 3: k_1=0.0μM/s, k_2=7.0s^{-1}, k_4=0.0s^{-1}. (a) Both feedback 1 and 2 are operative. Robust homeostasis of cGMP is observed with $cGMP_{set}$ = 7.61μM. Other rate constants values are as described in section "Estimation of model parameters". Initial concentrations: cGMP = 7.612μM, Ca_i^{2+} = 141.7 nM, K^+=1.760μM. (b) Feedback 2 is only operative. In order to keep cGMP at its set-point k_4 needs to be increased to 8.0 μM/s in all three phases (indicated in the scheme by the blue upright arrow). Initial concentrations: cGMP = 7.612μM, Ca_i^{2+} = 1.071 μM, K^+=2.335μM. (c) Feedback 1 is only operative. To keep cGMP at its set-point k_3 has been increased from 50.0 μM/s to 500.0 μM/s in phase 3 (indicated in the scheme by the red upright arrow). Initial concentrations: cGMP = 7.612μM, Ca_i^{2+} = 94.9 nM, K^+=2.64μM. (d) All feedback loops are operative with rate constants as in panel (a). Although perfect adaptation in cGMP is lost both cGMP and Ca_i^{2+} undergo only small variations when the perturbations are applied with lowest Ca_i^{2+} levels. Initial concentrations: cGMP = 9.042μM, Ca_i^{2+} = 125.7 nM, K^+=1.989μM. See S4 Text how the leak term affects this configuration.

https://doi.org/10.1371/journal.pone.0281490.g019

perturbations it needs sufficiently large GC and PDE activities, reflected by sufficiently high k_2, k_3, and k_4 values, in order to provide the necessary compensatory fluxes.

Fig 19b shows the system's behavior when only feedback loop 2 is operative. To achieve control by only feedback 2 the condition in Eq 27 needs to hold and the inhibition of GC by Ca_i^{2+} has to be abolished by using a high inhibition constant k_8. We have used k_8=1×10^9μM with r = 1.0. When applying the same perturbation profile as in Fig 19a it turned out that the PDE activity from Fig 19a was not sufficient to keep cGMP homeostasis at $cGMP_{set}$ = 7.61μM. The reason for this is that the lack of feedback loop 1 causes a higher cGMP and Ca^{2+} inflow into the cell. When becoming too high the Ca^{2+} inflow cannot be absorbed by the constant Ca_i^{2+} removal speed k_6 of NCKX. In other words, the antithetic zero-order removal kinetics of Ca_i^{2+} by NCKX will become too slow and thereby lead to a steady increase (windup) in the concentration of Ca_i^{2+} (S5 Text). To avoid this and to keep cGMP robustly at $cGMP_{set}$ = 7.61μM we have in Fig 19b increased the background k_4 to 8 μM/s (indicated by the blue upright arrow). Alternatively, one may increase the constant removal speed k_6 of the NCKX pump, but this will result in a change of $cGMP_{set}$ (see also S6 Text).

Fig 19c shows the system's behavior when only feedback loop 1 is present. To get only loop 1 operative the condition of Eq 27 is imposted and the activation constant k_{12} (Fig 13) is set to zero. To act as a robust inflow controller cGMP homeostasis requires sufficiently high k_3 values. With the perturbation profile from panel (a) k_3 needs to be increased in phase 3 by one order of magnitude to k_3=500μ/s (indicated by the red upright arrow in Fig 19c) in order to avoid cGMP levels below $cGMP_{set}$ = 7.61μM (see also S6 Text).

When all three loops are operative (Fig 19d) the robust perfect adaptation of cGMP is lost due to the presence of feedback loop 3. However, with respect to the applied perturbations cGMP levels show only small variations and Ca_i^{2+} steady state concentrations have their lowest values. The results in Fig 19 show that the antagonistic feedback between loops 1 and 2 is more efficient than when loops 1 or 2 are isolated. Although the robust perfect adaptation of cGMP is lost in the presence of feedback loop 3, the overlayed feedback structure between all three feedbacks provides a compromise between robust perfect adaptation of cGMP and the need to avoid high cytotoxic Ca_i^{2+} levels.

Another aspect of the three feedbacks' overlay concerns the resetting times at varying/increasing backgrounds. While a faster resetting with increasing backgrounds has been described as a typical property of vertebrate photoadaptation (see section V in [35]), in turtle photoreceptors Baylor et al. [53] found that increasing backgrounds first lead to a decrease in peak time (analogous to t_{max}), but further increases of the background eventually lead to an increase of the peak time (t_{max}), as qualitatively observed in Fig 16d. The increase of the time to peak was explained by Baylor et al. [56] by a hypothetical autocatalytic reaction which removed particles blocking the ionic channels. An additional factor could be a differential dominance between feedback loops 1 and 2, since loop 1 and loop 2 affect the resetting differently analogous as described for the m2 (Fig 8) and m5 (S1 Text) controllers.

Fig 20 shows ΔcGMP and t_{max} as a function of the feedback arrangement. In panel (a) we have feedback loops 1 and 3 combined, while in panel (b) we have only feedback loop 2. When testing a 1.0 → 50.0 μM/s k_2 step for increasing backgrounds both feedback arrangements show a monotonic decline of ΔcGMP as a function of background k_4 (middle panels), but differ in their t_{max} responses (bottom panels). While combined feedback loop 1 and 3 show a monotonic shortening of t_{max}, in the feedback 2 arrangement t_{max} first decreases, but then increases again as background k_4 increases, as found experimentally by Baylor et al. [53] and when all three feedback loops are combined (Fig 16c and 16d). Since the single feedback 2 behavior (Fig 20b) resembles that of all three feedbacks combined (Fig 19c and 19d) we

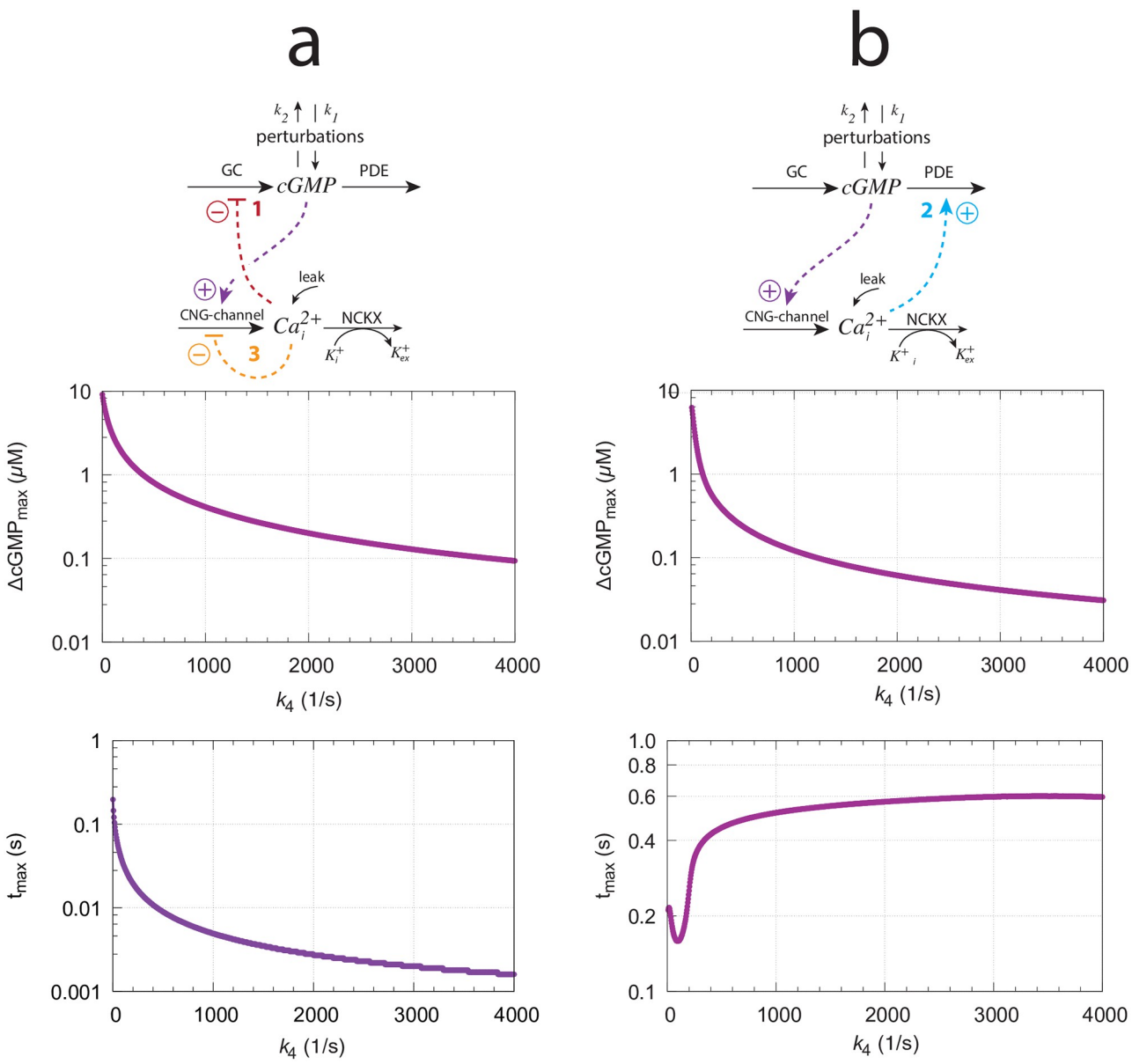

Fig 20. The model's resetting behavior for different feedback arrangements when applying a 1.0 → 50.0 s^{-1} step in k_2 as a function of backgrounds k_4. (a) Feedback loops 1 and 3 are combined. (b) Feedback 2 only. Used parameter values, rate constants, and definition of ΔcGMP and t_{max} are as in Fig 16.

https://doi.org/10.1371/journal.pone.0281490.g020

conclude that in our model with the used parameter values feedback 2 is dominating over the two other feedbacks with respect to the system's resetting behavior. In organisms where the photoadaptation shows faster resettings (decreasing or constant t_{max}) with increasing backgrounds, as found in Ref. [34] and highlighted in the review by Fain et al. [35], the feedback loop 2 may be weakened and loops 1 and 3 may become more dominant. Since the rate parameters of our model were taken from different organisms it is possible that these combined parameters reflect a situation closer to turtles [53] than, for example, to Macaque monkeys [34].

Other model approaches. There is an extensive literature in theoretical and computational approaches to understand various aspects of vertebrate photoadaptation. The approaches range from phenomenological mathematical descriptions to reaction kinetic and stochastic model calculations. For an overview we refer to chapter 19 in the book by Keener and Sneyd [57], to the review by Roberts et al. [58] and to Pan et al. [59]. Although phenomenological models can provide quantitative descriptions and predictions [60], they generally lack knowlegde of the involved chemical processes and their regulations. Due to this, the need for reaction kinetic descriptions has been emphasized [59, 61, 62].

Our approach, although primarily kinetic in nature, differs from previous adaptation models by looking at photoadaptation from a robust homeostatic viewpoint. In this respect we agree with Billman [63] that homeostatic approaches are still underappreciated and are far too often ignored as a central organizing principle in physiology.

Conclusion and outlook

Studying perturbations with backgrounds on eight basic feedback loops m1-m8 with integral control show that these homeostatic controllers divide into two classes dependent on how the compensatory flux is activated. In the class where the compensatory flux is based on derepression faster resetting with respect to a standard step perturbation is observed when backgrounds increase. In the other class when compensatory fluxes are based on direct activation the resetting to the set-point slows down as backgrounds increase. In both cases the maximum excursion of the controlled variable following the perturbation decrease monotonically as backgrounds increase. We originally thought that vertebrate photoadaptation would be a nice example of using sole derepression kinetics in a robust control of cGMP with cellular calcium as the controller. However, the situations turned out to be more complex with an overlay of three feedback loops, one based on derepression by Ca^{2+} on GC (feedback 1) and one based on Ca^{2+}-based light activation of PDE (feedback 2). The antagonistic pair of combined feedbacks 1 and 2 show more improved properties than each of the individual controllers alone. In addition, there is a third Ca^{2+}-controlling feedback (feedback 3) which apparently avoids high cytotoxic Ca^{2+} levels. This combination of three feedback loops indicates that robust perfect adaptation of cGMP by feedback loops 1 and 2 is not by itself an evolutionary target, but that a compromise between these three controllers has developed by keeping both cGMP *and* cytosolic Ca^{2+} levels at narrow limits, but not by robust perfect adaptation mechanisms. Furthermore, there is also evidence that photoadaptation with increasing backgrounds may both accelerate or slow down the resetting kinetics dependent on the dominance of feedback 1 or feedback 2.

The findings that controllers m1-m8 react so differently on perturbations with respect to backgrounds may be of importance also in other physiological systems. For example, blood sugar levels are controlled by two major feedback loops involving insulin and glucagon. Since glucose control by insulin is based by an activation of beta cells via glucose (see Supporting Material in Ref. [11]), constantly high glucose levels ("glucose overload") [64, 65], for example, may lead to a slower resetting of the insulin-based control loop in comparison with more rapid anticipated adaptations at lower glucose levels. Such a slowing-down response may be one of the causes that could participate in the mechanisms leading to insulin resistance and early diabetes. To what extent these aspects of background perturbations in homeostatic systems apply to the development of diabetes or have implications in other homeostatic systems needs certainly further investigations.

Supporting information

S1 File. Documentation. (part 1). A zip-file with python scripts describing the results for motifs m1 (Fig 4a), m7 (Fig 6a), m2 (Fig 8a), m8 (Fig 11a), m3 and m5 (S1 Text, Figs S2a and S4a), m4 (S2 Text, Fig S2), and m6 (S2 Text, Fig S4a). (part 2). A zip-file with python scripts describing the results for Figs 15, 16a, 16b, 17b and 19.
(ZIP)

S1 Text. Response kinetics of controllers m3 and m5. Applied step perturbations lead to slower resetting kinetics for increasing backgrounds.
(ZIP)

S2 Text. Response kinetics of controllers m4 and m6. Applied step perturbations lead to faster resetting kinetics for increasing backgrounds.
(ZIP)

S3 Text. Response kinetics controller m2 with antithetic integral control. The behavior is dynamically identical to that of m2 with zero-order kinetics.
(ZIP)

S4 Text. Influence of Ca leak kinetics on photoadaptation. A comparison how experimentally observed zero-order and first-order Ca leak kinetics affect photoadaptation in the model and when homeostatic breakdown occurs.
(ZIP)

S5 Text. Influence of k_5, k_6, and k_7 on the model's photoadaptation. By using a k_1-k_2 perturbation profile influences of k_5, k_6, and k_7 on the model's resetting kinetics are shown.
(ZIP)

S6 Text. Experimental light adaptation data. Replots of experimental data show, as indicated by model calculations, that Stephens' law is followed at low backgrounds, while at higher backgrounds the response tends towards Weber's law.
(ZIP)

Author Contributions

Conceptualization: Peter Ruoff.

Formal analysis: Jonas V. Grini, Melissa Nygård, Peter Ruoff.

Investigation: Jonas V. Grini, Melissa Nygård, Peter Ruoff.

Methodology: Peter Ruoff.

Project administration: Peter Ruoff.

Software: Jonas V. Grini, Melissa Nygård.

Supervision: Peter Ruoff.

Validation: Jonas V. Grini, Melissa Nygård.

Visualization: Peter Ruoff.

Writing – original draft: Peter Ruoff.

Writing – review & editing: Peter Ruoff.

References

1. Cannon W. Organization for Physiological Homeostatics. Physiol Rev. 1929; 9:399–431. https://doi.org/10.1152/physrev.1929.9.3.399
2. Langley LL, editor. Homeostasis. Origins of the Concept. Stroudsbourg, Pennsylvania: Dowden, Hutchinson & Ross, Inc.; 1973.
3. Mrosovsky N. Rheostasis. The Physiology of Change. New York: Oxford University Press; 1990.
4. Sterling P, Eyer J. Allostasis: A new paradigm to explain arousal pathology. In: Fisher S and Reason J, editor. Handbook of Life Stress, Cognition and Health. New York: John Wiley & Sons; 1988. p. 629–49.
5. Schulkin J. Rethinking Homeostasis. Allostatic Regulation in Physiology and Pathophysiology. Cambridge, Massachusetts: MIT Press; 2003.
6. Schulkin J. Allostasis, Homeostasis and the Costs of Physiological Adaptation. Cambridge, Massachusetts: Cambridge University Press; 2004.
7. Moore-Ede M. Physiology of the circadian timing system: Predictive versus reactive homeostasis. Am J Physiol. 1986; 250:R737–52. PMID: 3706563
8. Lloyd D, Aon M, Cortassa S. Why Homeodynamics, Not Homeostasis? The Scientific World. 2001; 1:133–145. https://doi.org/10.1100/tsw.2001.20 PMID: 12805697
9. Carpenter R. Homeostasis: A plea for a unified approach. Advances in Physiology Education. 2004; 28 (4):180–187. https://doi.org/10.1152/advan.00012.2004 PMID: 15545346
10. Ruoff P, Nishiyama N. Frequency switching between oscillatory homeostats and the regulation of p53. PloS One. 2020; 15(5):e0227786. https://doi.org/10.1371/journal.pone.0227786 PMID: 32433703
11. Drengstig T, Jolma IW, Ni XY, Thorsen K, Xu XM, Ruoff P. A Basic Set of Homeostatic Controller Motifs. Biophys J. 2012; 103:2000–2010. https://doi.org/10.1016/j.bpj.2012.09.033 PMID: 23199928
12. Wilkie J, Johnson M, Reza K. Control Engineering. An Introductory Course. New York: Palgrave; 2002.
13. Ni XY, Drengstig T, Ruoff P. The control of the controller: Molecular mechanisms for robust perfect adaptation and temperature compensation. Biophys J. 2009; 97:1244–53. https://doi.org/10.1016/j.bpj.2009.06.030 PMID: 19720012
14. Briat C, Gupta A, Khammash M. Antithetic integral feedback ensures robust perfect adaptation in noisy biomolecular networks. Cell Systems. 2016; 2(1):15–26. https://doi.org/10.1016/j.cels.2016.01.004 PMID: 27136686
15. Aoki SK, Lillacci G, Gupta A, Baumschlager A, Schweingruber D, Khammash M. A universal biomolecular integral feedback controller for robust perfect adaptation. Nature. 2019; 570(7762):533–537. https://doi.org/10.1038/s41586-019-1321-1 PMID: 31217585
16. Waheed Q, Zhou H, Ruoff P. Kinetics and mechanisms of catalyzed dual-E (antithetic) controllers. PloS One. 2022; 17(8):e0262371. https://doi.org/10.1371/journal.pone.0262371 PMID: 35980978
17. Shoval O, Goentoro L, Hart Y, Mayo A, Sontag E, Alon U. Fold-change detection and scalar symmetry of sensory input fields. PNAS. 2010; p. 201002352. https://doi.org/10.1073/pnas.1002352107 PMID: 20729472
18. Drengstig T, Ni XY, Thorsen K, Jolma IW, Ruoff P. Robust Adaptation and Homeostasis by Autocatalysis. J Phys Chem B. 2012; 116:5355–5363. https://doi.org/10.1021/jp3004568 PMID: 22506960
19. Briat C, Zechner C, Khammash M. Design of a synthetic integral feedback circuit: dynamic analysis and DNA implementation. ACS Synthetic Biology. 2016; 5(10):1108–1116. https://doi.org/10.1021/acssynbio.6b00014 PMID: 27345033
20. Ross HE, Murray DJ. EH Weber on the Tactile Senses. Psychology Press; 2018.
21. Kandel ER, Koester JD, Mack SH, Siegelbaum S, editors. Principles of Neural Science. Sixth Edition. McGraw-Hill; 2021.
22. Eisler H, Eisler AD, Hellström A. Psychophysical Issues in the Study of Time Perception. In: Grondin S, editor. Psychology of Time. Emerald Group Publishing Limited; 2008. p. 75–76.
23. Fechner GT. Elemente der Psychophysik. Zweiter Theil. Breitkopf und Härtel; 1860.
24. Stevens SS. On the psychophysical law. Psychological Review. 1957; 64(3):153. https://doi.org/10.1037/h0046162 PMID: 13441853
25. MacKay DM. Psychophysics of perceived intensity: A theoretical basis for Fechner's and Stevens' laws. Science. 1963; 139(3560):1213–1216. https://doi.org/10.1126/science.139.3560.1213.b
26. Radhakrishnan K, Hindmarsh AC. Description and Use of LSODE, the Livermore Solver for Ordinary Differential Equations. NASA Reference Publication 1327, Lawrence Livermore National Laboratory

Report UCRL-ID-113855. Cleveland, OH 44135-3191: National Aeronautics and Space Administration, Lewis Research Center; 1993.

27. Warwick K. An Introduction to Control Systems. Second Edition. World Scientific; 2019.
28. Fjeld G, Thorsen K, Drengstig T, Ruoff P. Performance of homeostatic controller motifs dealing with perturbations of rapid growth and depletion. The Journal of Physical Chemistry B. 2017; 121(25):6097–6107. https://doi.org/10.1021/acs.jpcb.7b01989 PMID: 28571313
29. Drobac G, Waheed Q, Heidari B, Ruoff P. An amplified derepression controller with multisite inhibition and positive feedback. PLoS One. 2021; 16(3):e0241654. https://doi.org/10.1371/journal.pone.0241654 PMID: 33690601
30. Drengstig T, Jolma I, Ni X, Thorsen K, Xu X, Ruoff P. A basic set of homeostatic controller motifs. Biophys J. 2012; 103(9):2000–2010. https://doi.org/10.1016/j.bpj.2012.09.033 PMID: 23199928
31. Ang J, McMillen DR. Physical constraints on biological integral control design for homeostasis and sensory adaptation. Biophys J. 2013; 104(2):505–515. https://doi.org/10.1016/j.bpj.2012.12.015 PMID: 23442873
32. Purves D, Augustine GJ, Fitzpatrick D, Hall WC, LaMantia AS, McNamara JO, et al. Neuroscience. 4th Edition. Sunderland, Mass.: Sinauer; 2008.
33. Dowling JE. The Retina: An approachable Part of the Brain. Revised Edition. Harvard University Press; 2012.
34. Schneeweis D, Schnapf J. Noise and light adaptation in rods of the macaque monkey. Visual Neuroscience. 2000; 17(5):659–666. https://doi.org/10.1017/S0952523800175017 PMID: 11153647
35. Fain GL, Matthews HR, Cornwall MC, Koutalos Y. Adaptation in vertebrate photoreceptors. Physiological Reviews. 2001; 81(1):117–151. https://doi.org/10.1152/physrev.2001.81.1.117 PMID: 11152756
36. Baylor DA, Nunn B, Schnapf J. The photocurrent, noise and spectral sensitivity of rods of the monkey Macaca fascicularis. The Journal of Physiology. 1984; 357(1):575–607. https://doi.org/10.1113/jphysiol.1984.sp015518 PMID: 6512705
37. Krizaj D, Copenhagen DR. Calcium regulation in photoreceptors. Frontiers in Bioscience—Landmark. 2002; 7(4):d2023–d2044. https://doi.org/10.2741/a896 PMID: 12161344
38. Marks F, Klingmüller U, Müller-Decker K. Cellular Signal Processing: An Introduction to the Molecular Mechanisms of Signal Transduction. Second Edition. Garland Science; 2017.
39. Hsu YT, Molday RS. Modulation of the cGMP-gated channel of rod photoreceptor cells by calmodulin. Nature. 1993; 361(6407):76–79. https://doi.org/10.1038/361076a0 PMID: 7678445
40. Koutalos Y, Nakatani K, Yau K. The cGMP-phosphodiesterase and its contribution to sensitivity regulation in retinal rods. The Journal of General Physiology. 1995; 106(5):891–921. https://doi.org/10.1085/jgp.106.5.891 PMID: 8648297
41. Koutalos Y, Yau KW. Regulation of sensitivity in vertebrate rod photoreceptors by calcium. Trends in Neurosciences. 1996; 19(2):73–81. https://doi.org/10.1016/0166-2236(96)89624-X PMID: 8820871
42. Koutalos Y, Nakatani K, Tamura T, Yau K. Characterization of guanylate cyclase activity in single retinal rod outer segments. The Journal of General Physiology. 1995; 106(5):863–890. https://doi.org/10.1085/jgp.106.5.863 PMID: 8648296
43. Oldershaw KA, Nunn D, Taylor CW. Quantal Ca^{2+} mobilization stimulated by inositol 1, 4, 5-trisphosphate in permeabilized hepatocytes. Biochemical Journal. 1991; 278(3):705–708. https://doi.org/10.1042/bj2780705 PMID: 1898359
44. Missiaen L, Smedt HD, Parys JB, Raeymaekers L, Droogmans G, Bosch LVD, et al. Kinetics of the non-specific calcium leak from non-mitochondrial calcium stores in permeabilized A7r5 cells. Biochemical Journal. 1996; 317(3):849–853. https://doi.org/10.1042/bj3170849 PMID: 8760372
45. Camello C, Lomax R, Petersen OH, Tepikin A. Calcium leak from intracellular stores—the enigma of calcium signalling. Cell Calcium. 2002; 32(5-6):355–361. https://doi.org/10.1016/S0143416002001926 PMID: 12543095
46. Luik RM, Wang B, Prakriya M, Wu MM, Lewis RS. Oligomerization of STIM1 couples ER calcium depletion to CRAC channel activation. Nature. 2008; 454(7203):538–542. https://doi.org/10.1038/nature07065 PMID: 18596693
47. Selstø CH, Ruoff P. A basic model of calcium homeostasis in non-excitable cells. bioRxiv. 2022. https://doi.org/10.1101/2022.x.y
48. Nikonov S, Lamb T, Pugh EN Jr. The role of steady phosphodiesterase activity in the kinetics and sensitivity of the light-adapted salamander rod photoresponse. The Journal of General Physiology. 2000; 116(6):795–824. https://doi.org/10.1085/jgp.116.6.795 PMID: 11099349
49. He L, Poblenz AT, Medrano CJ, Fox DA. Lead and calcium produce rod photoreceptor cell apoptosis by opening the mitochondrial permeability transition pore. Journal of Biological Chemistry. 2000; 275(16):12175–12184. https://doi.org/10.1074/jbc.275.16.12175 PMID: 10766853

50. Nakatani K, Yau K. Guanosine 3', 5'-cyclic monophosphate-activated conductance studied in a truncated rod outer segment of the toad. The Journal of Physiology. 1988; 395(1):731–753. https://doi.org/10.1113/jphysiol.1988.sp016943 PMID: 2457686

51. Cote RH, Brunnock M. Intracellular cGMP concentration in rod photoreceptors is regulated by binding to high and moderate affinity cGMP binding sites. Journal of Biological Chemistry. 1993; 268 (23):17190–17198. https://doi.org/10.1016/S0021-9258(19)85321-8 PMID: 8394335

52. Wyszecki G, Stiles WS. Color Science. Second edition. Wiley New York; 1982.

53. Baylor D, Hodgkin A. Changes in time scale and sensitivity in turtle photoreceptors. The Journal of Physiology. 1974; 242(3):729–758. https://doi.org/10.1113/jphysiol.1974.sp010732 PMID: 4449053

54. Baylor D, Hodgkin A. Detection and resolution of visual stimuli by turtle photoreceptors. The Journal of Physiology. 1973; 234(1):163–198. https://doi.org/10.1113/jphysiol.1973.sp010340 PMID: 4766219

55. Baylor D, Hodgkin A, Lamb T. The electrical response of turtle cones to flashes and steps of light. The Journal of Physiology. 1974; 242(3):685–727. https://doi.org/10.1113/jphysiol.1974.sp010731 PMID: 4449052

56. Baylor D, Hodgkin A, Lamb T. Reconstruction of the electrical responses of turtle cones to flashes and steps of light. The Journal of Physiology. 1974; 242(3):759–791. https://doi.org/10.1113/jphysiol.1974.sp010733 PMID: 4449054

57. Keener J, Sneyd J. Mathematical Physiology. II: Systems Physiology. Springer; 2009.

58. Roberts PA, Gaffney EA, Luthert PJ, Foss AJ, Byrne HM. Mathematical and computational models of the retina in health, development and disease. Progress in Retinal and Eye Research. 2016; 53:48–69. https://doi.org/10.1016/j.preteyeres.2016.04.001 PMID: 27063291

59. Pan G, Tan J, Guo Y. Modeling and simulation of phototransduction cascade in vertebrate rod photoreceptors. BMC Ophthalmology. 2019; 19:1–8. https://doi.org/10.1186/s12886-019-1048-7 PMID: 30786871

60. Clark DA, Benichou R, Meister M, Azeredo da Silveira R. Dynamical adaptation in photoreceptors. PLoS Computational Biology. 2013; 9(11):e1003289. https://doi.org/10.1371/journal.pcbi.1003289 PMID: 24244119

61. Sneyd J, Tranchina D. Phototransduction in cones: An inverse problem in enzyme kinetics. Bulletin of Mathematical Biology. 1989; 51:749–784. https://doi.org/10.1007/BF02459659 PMID: 2573396

62. Tranchina D, Sneyd J, Cadenas ID. Light adaptation in turtle cones. Testing and analysis of a model for phototransduction. Biophysical Journal. 1991; 60(1):217–237. https://doi.org/10.1016/S0006-3495(91)82045-8 PMID: 1653050

63. Billman GE. Homeostasis: The underappreciated and far too often ignored central organizing principle of physiology. Frontiers in Physiology; 11:200. https://doi.org/10.3389/fphys.2020.00200 PMID: 32210840

64. Moreira PI. High-sugar diets, type 2 diabetes and Alzheimer's disease. Current Opinion in Clinical Nutrition & Metabolic Care. 2013; 16(4):440–445. https://doi.org/10.1097/MCO.0b013e328361c7d1 PMID: 23657152

65. Joubert M, Manrique A, Cariou B, Prieur X. Diabetes-related cardiomyopathy: The sweet story of glucose overload from epidemiology to cellular pathways. Diabetes & Metabolism. 2019; 45(3):238–247. https://doi.org/10.1016/j.diabet.2018.07.003 PMID: 30078623

Appendix D

Coherent feedback leads to robust background compensation in oscillatory and non-oscillatory homeostats

Coherent feedback leads to robust background compensation in oscillatory and non-oscillatory homeostats

Melissa Nygård, Peter Ruoff*

Department of Chemistry, Bioscience, and Environmental Engineering, University of Stavanger, Stavanger, Norway

* peter.ruoff@uis.no

Abstract

When in an integral feedback controller a step perturbation is applied at a constant background, the controlled variable (described here as A) will in general respond with decreased response amplitudes ΔA as backgrounds increase. The controller variable E will at the same time provide the necessary compensatory flux to move A back to its set-point. A typical example of decreased response amplitudes at increased backgrounds is found in retinal light adaptation. Due to remarks in the literature that retinal light adaptation would also involve a compensation of backgrounds we became interested in conditions how background compensation could occur. In this paper we describe how background influences can be robustly eliminated. When such a background compensation is active, oscillatory controllers will respond to a defined perturbation with always the same (damped or undamped) frequency profile, or in the non-oscillatory case, with the same response amplitude ΔA, irrespective of the background level. To achieve background compensation we found that two conditions need to apply: (i) an additional set of integral controllers (here described as I_1 and I_2) have to be employed to keep the manipulated variable E at a defined set-point, and (ii), I_1 and I_2 need to feed back to the A-E signaling axis directly through the controlled variable A. In analogy to a similar feedback applied in quantum control theory, we term these feedback conditions as 'coherent feedback'. When analyzing retinal light adaptations in more detail, we find no evidence in the presence of background compensation mechanisms. Although robust background compensation, as described theoretically here, appears to be an interesting regulatory property, relevant biological or biochemical examples still need to be identified.

Introduction

Homeostatic mechanisms play important roles in physiology and in the adaptation of organisms to their environments [1]. For example in the vertebrate retina, photoreceptor cells contain negative feedback loops which participate in light adaptation [2–5]. A hallmark of vertebrate photoadaptation is that resetting kinetics accelerate and response amplitudes decrease as backgrounds increase [5, 6]. This behavior is seen in Fig 1 for a macaque monkey's rod cell response towards a single light flash applied at different background light levels.

Fig 1. Light adaptation in a Macaque monkey's rod cell. 10 ms light flashes were applied to different light background intensities. Background intensities (in photons $\mu m^{-2}s^{-1}$) were: **0**, 0; **1**, 3.1; **2**, 12; **3**, 41; **4**, 84; **5**, 162. The influence of the background on the response amplitude and the speed of resetting is clearly seen. V_0 is the response amplitude for background **0**. Redrawn and modified after Fig 2A from Ref [7]. For a theoretical description of this behavior see Ref [5] and references therein.

Another retinal light adaptation example is shown in Fig 2. Here, the mean maximum firing rates of a cat ganglion cell was measured with respect to different step light perturbations (test spot luminance) which are applied at six different backgrounds [8].

Fig 2. Light adaptation of an on-center ganglion cell in the cat retina (redrawn from Fig 8, Ref [8]). Averaged maximum ganglion cell frequencies are shown as a function of six different background illuminations in response to applied light step perturbations (test spot luminance). The three colored curves show the averaged maximum frequencies at background illuminations 10^{-3}, 10^{-2} and 10^{-1} cd/m^2. A test spot luminance (perturbation) of 9×10^{-2} cd/m^2 is indicated as the vertical dashed black line. The colored intersection points and vertical dashed lines indicate that for this perturbation strength the maximum mean response frequency decreases with increasing background illumination.

In Kandel et al. [2] it was commented (see page 540, section *Light Adaptation Is Apparent in Retinal Processing and Visual Perception*) that Fig 2 would indicate a compensation of the background illumination and thereby causing the same response due to a lateral shifting along the perturbation (test spot luminance) axis. Based on this comment we became interested in mechanisms which would allow to compensate for background levels and thereby give the same response for a given perturbation irrespective of the applied background.

In this paper we present results on how such a robust background compensation can be achieved in both oscillatory and non-oscillatory homeostats.

The paper is structured in the following way: We first show that a feedback type similar to what quantum physicists have termed 'coherent feedback' [9, 10] is required to obtain background compensation in both oscillatory and non-oscillatory homeostats. For oscillatory homeostats we show that coherent feedback control leads to, besides background compensation, also to frequency control. In fact, robust frequency control was previously observed by us [11], but without having recognized the background-compensating property of coherent feedback. For non-oscillatory controllers or homeostats with damped oscillations, coherent feedback leads to conserved response profiles in the controlled variables, independent of an applied background. We then look at the situation of a 'incoherent feedback', where background compensation is lost, but oscillatory homeostats may still show robust frequency control. Finally we analyze photoreceptor responses in terms of a Michaelis-Menten model [3] and show that parallel lines as in Fig 2 or as log-log plots do not require the postulation of background compensation or additional adaptation mechanisms.

Materials and methods

Computations were performed with the Fortran subroutine LSODE [12], which can be downloaded from https://computing.llnl.gov/projects/odepack. Graphical output was

generated with gnuplot (www.gnuplot.info) and annotated with Adobe Illustrator (https://www.adobe.com/).

To make notations simpler, concentrations of compounds are denoted by compound names without square brackets. Time derivatives are generally indicated by the 'dot' notation. Rate parameters are in arbitrary units (au) and are presented as k_i's (i=1, 2, 3, ...) irrespective of their kinetic nature, i.e. whether they represent turnover numbers, Michaelis constants, or inhibition/activation constants. To allow readers to redo calculations, the supporting information S1 Programs contains python scripts for a set of selected results.

Usage of integral control

In the calculations robust homeostasis of concentrations and frequencies is achieved by implementing integral control into the negative feedbacks, a concept which comes from control engineering [13–16], and has been indicated to occur in and being applied to biological systems [17–21]. Briefly, in integral control the difference (also termed error) between the actual concentration of a controlled variable A and its set-point is integrated in time. The integrated error can then be used to compensate precisely for step-wise perturbations [15,16]. Fig 3a shows the control scheme of integral control. An example is given in panel b using 'motif 2', one of eight basic feedback loops [22]. Panel c shows how zero-order removal of controller species E leads to integral control with a defined set-point of the controlled variable A.

Fig 3. Principle of integral control. Panel a: The controlled variable A (outlined in blue) is compared with its set-point and the difference/error ($A_{set}-A$) is integrated. This leads to the integrated error E, which is able to compensate precisely for step-wise perturbations [15]. Panel b: Basic negative feedback loop (motif 2, [22]). Solid lines are chemical reactions, while dashed lines represent activations (plus sign) and inhibitions (negative sign). Panel c: Rate equation of controller E. The zero-order removal of E introduces integral control. The set-point for A is given as k_5/k_4, and the concentration of E becomes proportional to the integrated error. For details, see for example Ref [22].

In the below calculations we have used zero-order kinetics to implement integral control [17,22–24]. However, it should be mentioned that there are other kinetics conditions to achieve integral control, such as antithetic control [21,25,26], which generally will show identical resetting behaviors as in zero-order control [5,26]. Also, autocatalytic reactions can be used to obtain integral control [27–29], which will generally show much faster resetting kinetics in comparison when integral control is introduced by zero-order kinetics [30,31].

Results and discussion

Background compensation in negative feedback oscillators by coherent feedback

In this section we describe feedback conditions which can achieve background compensation in oscillatory homeostats. The type of oscillators we here focus on show frequency homeostasis due to a two-layered negative feedback structure. The center negative feedback layer ensures that the time average value of a controlled variable A, defined by Eq 1, is kept robustly at a certain set-point by a controller species E via

integral control.

$$<A>(t) = \frac{1}{t}\int_0^t A(t')\cdot dt' \tag{1}$$

A second 'outer' negative feedback layer keeps on its side the time average value of E, i.e. $<E>$ (Eq 2), under robust homeostatic control by two additional controller variables I_1 and I_2.

$$<E>(t) = \frac{1}{t}\int_0^t E(t')\cdot dt' \tag{2}$$

We previously showed [11] that these two-layered negative feedback structures enable robust frequency homeostasis. Here we now report the additional finding that when the I_1 and I_2 controllers feed back directly via A to control E, the oscillator has the capability to neutralize backgrounds. In analogy to a closely related feedback definition employed in quantum control theory and optics we call this type of feedback for 'coherent feedback' (see [9, 10] and references therein).

Background compensation in a motif 2 based oscillatory homeostat

Fig 4a shows an example of a frequency-compensated oscillator, but now with the novel finding that it can also compensate for different but constant backgrounds.

Fig 4. Frequency-compensated oscillator with background compensation by coherent feedback. Panel a: Reaction system based on derepression motif 2 (m2) [22] in the inner *A*-*e*-*E*-*A* negative feedback. Figs S12-S14 in the supporting information of Ref [11] describe some properties of this oscillator, but without having recognized at that time the ability to robustly compensate for backgrounds. Solid arrows indicate chemical reactions, while dashed lines show activations (plus signs) and one inhibition (minus sign). Panel b: Flow scheme indicating the additional control of E via A by controllers I_1 and I_2.

The center oscillator in Fig 4a is given by the *A*-*e*-*E*-*A* feedback loop based on derepression motif 2 [22], where E keeps $<A>$ under homeostatic control (see rate equations and definitions of set-points below). Oscillations occur, because the removals of A and E are zero-order with respect to A and E and thereby construct a quasi-conservative oscillator. The intermediate e has been included to obtain limit-cycle oscillations [11]. I_1 and I_2 are controller species, which keep $<E>$ under homeostatic control. It is the control of $<E>$ by I_1 and I_2, which allows for the frequency homeostasis of the oscillator [11]. Their A-coherent feedback directly to A allows for robust background compensation. Since the central *A*-*e*-*E*-*A* negative feedback is an inflow controller it principally can only compensate for outflow perturbations [22]. The outflow perturbation considered here splits into two components: a constant (zero-order) background with rate constant k_{10} (Fig 4a outlined in blue) and a (zero-order) perturbation part where rate constant k_2 undergoes a step-wise change (in Fig 4a outlined in red). Zero-order kinetics with respect to A are achieved by small k_8 and k_{17} values, i.e. $A/(k_8{+}A) \approx 1$ and $A/(k_{17}{+}A) \approx 1$. Fig 4b shows the flow scheme and the control of E by I_1 and I_2 via the A-coherent part of the controller.

The rate equations are:

$$\dot{A} = k_{g3}\cdot I_2 + \frac{k_3\cdot k_5}{k_5{+}E} - \frac{k_g\cdot A\cdot I_1}{k_{17}{+}A} - \underbrace{\frac{k_2\cdot A}{k_8{+}A}}_{\text{perturbation}} - \underbrace{\frac{k_{10}\cdot A}{k_8{+}A}}_{\text{background}} \tag{3}$$

$$\dot{e} = k_4{\cdot}A - k_9{\cdot}e \tag{4}$$

$$\dot{E} = k_9{\cdot}e - \frac{k_6{\cdot}E}{k_7{+}E} \tag{5}$$

$$\dot{I}_1 = k_{11}{\cdot}E - \frac{k_{12}{\cdot}I_1}{k_{13}{+}I_1} \tag{6}$$

$$\dot{I}_2 = k_{14} - \left(\frac{k_{15}{\cdot}I_2}{k_{16}{+}I_2}\right){\cdot}E \tag{7}$$

The set-point of $<A>$ (A_{set}) by controller E can be calculated from the steady state condition of the time averages:

$$k_4{\cdot}<A_{ss}> = k_9{\cdot}<e_{ss}> = k_6 \cdot \underbrace{\left(\frac{E_{ss}}{k_7{+}E_{ss}}\right)}_{\approx 1\,(\mathrm{zero-order})} \;\Rightarrow\; <A_{ss}>{=}A_{set}{=}\frac{k_6}{k_4} \tag{8}$$

The zero-order condition with respect to E in Eq 8 ensures a robust perfect adaptation of $<A_{ss}>$ to A_{set} when the system oscillates, or of A to A_{set} in case the feedback loop is non-oscillatory [11]. Since the control of A by E is an inflow controller based on derepression of the flux $k_3{\cdot}k_5/(k_5{+}E)$ the controller is active whenever $<A>$ is below A_{set}.

E is controlled by I_1 and I_2. They act as respectively outflow or inflow controllers [22] with respect to $<E>$ (if oscillatory) or E (if non-oscillatory). Also here zero-order removals of both I_1 and I_2 ensure robust set-points. For controller I_1 the steady state condition gives:

$$k_{11}{\cdot}<E_{ss}> = k_{12} \cdot \underbrace{\left(\frac{I_{1,ss}}{k_{13}{+}I_{1,ss}}\right)}_{\approx 1\,(\mathrm{zero-order})} \;\Rightarrow\; <E_{ss}>{=}E^{I_1}_{set}{=}\frac{k_{12}}{k_{11}} \tag{9}$$

The I_1 outflow controller becomes active whenever $<E>$ is higher than $E^{I_1}_{set}$.

The set-point for the I_2 inflow controller is determined by the steady state condition:

$$k_{14} = k_{15}{\cdot}<E_{ss}> \underbrace{\left(\frac{I_{2,ss}}{k_{16}{+}I_{2,ss}}\right)}_{\approx 1\,(\mathrm{zero-order})} \;\Rightarrow\; <E_{ss}>{=}E^{I_2}_{set}{=}\frac{k_{14}}{k_{15}} \tag{10}$$

The I_2 controller becomes active whenever $<E>$ is lower than $E^{I_2}_{set}$. It should be noted that the values of the inflow/outflow set-points $E^{I_1}_{set}$ and $E^{I_2}_{set}$ need to follow certain rules to guarantee that inflow and outflow controllers cooperate. In this case $E^{I_2}_{set}$ should be lower than $E^{I_1}_{set}$, otherwise I_1 and I_2 will work against each other and windup will occur. For a discussion about windup in combined controllers, see Ref [22].

In the following we show how the above oscillator behaves in presence of a step-wise perturbation at different but constant backgrounds.

Fig 5 shows the oscillator's behavior for a step-wise perturbation in k_2 from 1.0 (phase 1) to 10.0 (phase 2) at a background k_{10}=0.0. The time of change in k_2 is indicated in each panel by a vertical arrow. Panel a shows the oscillations in A together with its average $<A>$ (Eq 1), while panel b shows E and $<E>$ (Eq 2). Panel c shows the changes in I_1 and I_2, and panel d shows the frequency (inverse of the period length). The resetting of the frequency to its pre-perturbation value is clearly seen. If I_1 and I_2 would not be present, $<A>$ would be kept at A_{set}=2.0 by a reduced

(derepressed) E as seen in panel b at 100 time units. However, since $<E>$ is also controlled by I_1 and I_2, i.e. between 5.0 ($E_{set}^{I_1}$=5.0) and 4.99 ($E_{set}^{I_2}$=4.99), I_1 and I_2 take over both for the control of $<A>$ and of $<E>$.

Fig 5. Frequency compensation of feedback scheme in Fig 4a for a step-wise change in k_2 from 1.0 to 10.0 at a background of k_{10}=0.0. Vertical arrows indicate the change in k_2. Other rate constants: k_3=100.0, k_4=1.0, k_5=0.1, k_6=2.0, k_7=k_8=k_{13}=k_{16}=k_{17}=1×10^{-6}, k_9=20.0, k_{11}=1.0, k_{12}=5.0, k_{14}=4.99, k_{15}=1.0, and k_g=k_{g3}=1×10^{-2}. Initial concentrations: A_0=0.3780, E_0=2.4784, e_0=1.5993×10^{-2}, $I_{1,0}$=4.5727×10^{2}, $I_{2,0}$=2.9817×10^{2} (see S1 Programs for python script).

Fig 6 shows the same perturbation in k_2 as in Fig 5 but with a background of k_{10}=2048.0. The increased removal of A by the background is compensated by an increase of I_2 and a decrease of I_1, which keep $<A>$ and $<E>$ at their respective set-points. The maximum frequency, which occurs directly after the k_2 step is not affected. In other words, the sensitivity of the oscillator with respect to k_2-step perturbations is compensated by I_1 and I_2 and is independent of the background k_{10}.

Fig 6. Frequency compensation of feedback scheme in Fig 4a for a step-wise change in k_2 from 1.0 to 10.0 at a background of k_{10}=2048.0. Vertical arrows indicate the change in k_2. Other rate constants as in Fig 5. Initial concentrations: A_0=2.1377, E_0=7.6720, e_0=1.0996×10^{-1}, $I_{1,0}$=3.4304, $I_{2,0}$=2.0465×10^{5} (see S1 Programs for python script).

Fig 7 shows how the maximum frequency depends on k_2 steps at different but constant backgrounds k_{10}. The parallel lines indicate that the maximum frequency responses are independent of the background ("background compensation").

Fig 7. Background frequency compensation in the oscillator of Fig 4. The maximum frequency (see Fig 5d or Fig 6d) is plotted as a function of k_2^{ph2}+k_{10}, where k_2^{ph2} is the k_2 value during phase 2. The maximum frequency is determined for different step-wise k_2 changes, i.e. for 1.0→2.0, 1.0→3.0,..., 1.0→9.0, up to 1.0→10.0, which occur at time t=100 at different but constant k_{10} backgrounds (bgs). Calculations have been performed analogous to Fig 5 and Fig 6. The k_{10} background values are 0, 1, 2, 4, up to 2048 (indicated in the figure). Other rate constants as in Fig 5. Initial concentrations: bgs 0-128, as in Fig 5; bg 256, A_0=0.9866, E_0=7.3508, e_0=5.2447×10^{-2}, $I_{1,0}$=5.8243, $I_{2,0}$=2.5447×10^{4}; bg 512, A_0=8.3872×10^{-4}, E_0=4.8793, e_0=3.9572×10^{-5}, $I_{1,0}$=7.6544, $I_{2,0}$=5.1046×10^{4}; bg 1024, A_0=1.7657, E_0=7.6866, e_0=9.1430×10^{-2}, $I_{1,0}$=4.2379, $I_{2,0}$=1.0225×10^{5}; bg 2048, as in Fig 6.

Background compensation in a motif 8 (m8) based oscillatory homeostat

To provide an additional example of a frequency-compensated negative feedback oscillator with background compensation we use a m8 outflow control motif [22] for the center feedback. In this motif, A the controlled variable, inhibits the generation of the controller E. E on its side inhibits the removal of A. The outer controllers, I_1 and I_2, feed directly back to A. As for the m2 controller, oscillations in the central m8 oscillator are facilitated by removing A and E by zero-order processes. The scheme of this oscillator is shown in Fig 8. The rate equations are ('pert' stands for perturbation and 'bg' for background):

$$\dot{A} = \underbrace{k_1}_{\text{pert}} + \underbrace{k_3}_{\text{bg}} - \left(\frac{k_{g2}\cdot A}{k_{18}+A}\right)\cdot I_2 + k_{g1}\cdot I_1 - \left(\frac{k_4\cdot A}{k_5+A}\right)\cdot\left(\frac{k_9}{k_9+E}\right) \qquad (11)$$

$$\dot{e} = \frac{k_6 \cdot k_{10}}{k_{10}+A} - k_{11} \cdot e \tag{12}$$

$$\dot{E} = k_{11} \cdot e - \frac{k_7 \cdot E}{k_8+E} \tag{13}$$

$$\dot{I}_1 = k_{12} \cdot E - \frac{k_{13} \cdot I_1}{k_{14}+I_1} \tag{14}$$

$$\dot{I}_2 = k_{15} - \left(\frac{k_{16} \cdot I_2}{k_{17}+I_2} \right) \cdot E \tag{15}$$

The inflow to A is divided into a step-wise perturbative component k_1 (indicated in Eq 11 by 'pert' and outlined in red in Fig 8) and a background k_3 (indicated in Eq 11 by 'bg' and outlined in blue in Fig 8). All other in- and outflows to and from A are compensatory fluxes.

Fig 8. Frequency-compensated oscillator with background compensation by coherent feedback based on derepression motif m8 in the inner A-e-E-A negative feedback. Solid arrows indicate chemical reactions, while dashed lines show activations (plus signs) and inhibitions (minus sign).

As for the m2 oscillator above, we can calculate the set-points for $<E>$ by I_1 and I_2 by setting Eqs 14 and 15 to zero and assume that I_1 and I_2 are removed by zero-order reactions, i.e.:

$$E_{set}^{I_1} = \frac{k_{13}}{k_{12}} \quad ; \quad E_{set}^{I_2} = \frac{k_{15}}{k_{16}} \tag{16}$$

Unfortunately, for this scheme the oscillatory A_{set} cannot be calculated analytically. The closest analytical expression we can obtain is by setting Eqs 12 and 13 to zero, eliminating the $k_{11} \cdot e$ term, and then calculating the time average of $1/(k_{10}+A)$:

$$\frac{k_6 \cdot k_{10}}{k_{10}+A} = k_{11} \cdot e = k_7 \cdot \underbrace{\frac{E}{k_8+E}}_{\approx 1} \Rightarrow \left\langle \frac{1}{k_{10}+A} \right\rangle (t) = \frac{1}{t} \int_0^t \frac{dt'}{k_{10}+A(t')} \xrightarrow{\text{large } t} \frac{k_7}{k_6 \cdot k_{10}} \tag{17}$$

While calculations easily verify the right-hand side of Eq 17, $<A>$ needs to be calculated numerically.

Fig 9. Frequency compensation/homeostasis in the oscillator described in Fig 8. In both panels a step-wise perturbation in k_1 from 1.0 (phase 1) to 100.0 (phase 2) is applied (the step is indicated by the vertical arrows on top of the plots). In panel a, a constant background of k_3=0.0 is applied (at both phases 1 and 2), while in panel b the background is 1024.0. Other rate constant values are: k_4=1×10^4, k_5=k_8=k_{14}=k_{17}=k_{18}=1×10^{-6}, k_6=1×10^3, k_7=50.0, k_9=0.1, k_{11}=1.0, k_{12}=5.0, k_{13}=50.00, k_{15}=50.0, k_{16}=1.0 and k_{g1}=k_{g2}=1×10^{-2}. Initial concentrations (k_3=0.0): A_0=3.3568×10^2, E_0=2.6209×10^1, e_0=7.3942, $I_{1,0}$=2.4840×10^4, $I_{2,0}$=1.2768×10^4. Initial concentrations (k_3=1024.0): A_0=3.6188, E_0=1.8696×10^1, e_0=1.7115×10^2, $I_{1,0}$=4.6869, $I_{2,0}$=9.0420×10^4. Two python scripts, which in addition show the variations of A, E, I_1, and I_2, are included in S1 Programs.

Fig 9 shows that the oscillator described in Fig 8 shows frequency homeostasis at different but constant k_3 backgrounds. In panel a the background is k_3=0.0, while in panel b we have k_3=1024.0. In both cases the maximum frequency for a k_1 step of

1.0→100.0 is the same, indicating that the maximum frequency is background compensated.

Fig 10 shows maximum frequencies for different k_1 steps and k_3 backgrounds. There, different but constant k_3 backgrounds are applied with values 0, 2, 4, 8, 16, 32, 64, 128, 256, 512, and 1024. Step perturbations in k_1 are applied starting with a 1.0 (phase 1) to 10.0 (phase 2) step and ends with a 1.0 (phase 1) to 500.0 (phase 2) step by successively increasing the k_1 values in phase 2 by 10.0. As the parallel lines in Fig 10 show, once the oscillator has reached steady state for a certain background, the maximum frequencies, although dependent on the k_1 step become independent of the background k_3.

Fig 10. Background (bg) frequency compensation in the oscillator of Fig 8. The maximum frequency (see Fig 9) is plotted as a function of the sum of k_1^{ph2} and background k_3, where k_1^{ph2} is the k_1 value in phase 2. In analogy with the calculations in Fig 5 and Fig 6 the maximum frequency is determined for different step-wise k_1 changes, i.e. for 1.0→10.0, 1.0→20.0,..., 1.0→30.0, up to 1.0→500.0, which occur at time t=100 at different but constant k_3 backgrounds (bgs). The k_3 background values are 0, 2, 4, up to 1024 (indicated in the figure). Other rate constants as in Fig 9. Initial concentrations: bg 0: as in Fig 9a; bg 2: A_0=3.4008×10^2, E_0=2.3906×10^1, e_0=7.0224, $I_{1,0}$=2.4739×10^4, $I_{2,0}$=1.2869×10^4; bg 4: A_0=3.4461×10^2, E_0=2.1393×10^1, e_0=6.6417, $I_{1,0}$=2.4637×10^4, $I_{2,0}$=1.2971×10^4; bg 8: A_0=4.8073×10^2, E_0=6.0165×10^1, e_0=1.0914×10^2, $I_{1,0}$=2.4401×10^4, $I_{2,0}$=1.3207×10^4; bg 16: A_0=4.3570, E_0=1.9953×10^1, e_0=1.6964×10^2, $I_{1,0}$=2.4005×10^4, $I_{2,0}$=1.3603×10^4; bg 32: A_0=3.9151×10^1, E_0=5.4663×10^1, e_0=1.1875×10^2, $I_{1,0}$=2.3201×10^4, $I_{2,0}$=1.4407×10^4; bg 64: A_0=3.0270×10^2, E_0=4.1000×10^1, e_0=1.0456×10^1, $I_{1,0}$=2.1646×10^4, $I_{2,0}$=1.5962×10^4; bg 128: A_0=3.2021×10^2, E_0=3.3534×10^1, e_0=8.7470, $I_{1,0}$=1.8443×10^4, $I_{2,0}$=1.9165×10^4; bg 256: A_0=6.4511×10^1, E_0=6.8158×10^1, e_0=9.3623×10^1, $I_{1,0}$=1.2002×10^4, $I_{2,0}$=2.5606×10^4; bg 512: A_0=2.6297×10^2, E_0=5.5584×10^1, e_0=1.5294×10^1, $I_{1,0}$=3.2525×10^3, $I_{2,0}$=4.2375×10^4; bg 1024: as in Fig 9b. Panel a shows an overview of the maximum frequencies up to background 64, while panel b shows a blown-up part indicated in panel a. Panel c shows the maximum frequencies for backgrounds from 64 up to 1024.

Background compensation in non-oscillatory homeostats

In this section we look at background compensation in non-oscillatory homeostats where E is controlled by I_1 and I_2 via coherent feedback. We show two examples: in the first one the controller's response after a step perturbation is significantly damped, while in the other example the response shows a larger train of (damped) oscillations. In both cases the response profiles of the controlled variables A and E are preserved, independent of the background.

For the first example we use the oscillator scheme from Fig 4a. To go over to a non-oscillatory mode, we change the kinetics for all A-removing reactions from zero-order to first-order kinetics with respect to A. The rate equation of A becomes (compare with Eq 3):

$$\dot{A} = k_1 + k_{g3}\cdot I_2 + \frac{k_3\cdot k_5}{k_5+E} - \frac{k_g\cdot A\cdot I_1}{k_{17}+A} - \underbrace{k_2\cdot A}_{\text{perturbation}} - \underbrace{k_{10}\cdot A}_{\text{background}} \tag{18}$$

while the rate equations for the other components (Eqs 4-7) remain the same.

Fig 11. Same scheme as Fig 4a, but to facilitate a non-oscillatory homeostat all A-removing reactions are changed to first-order kinetics with respect to A.

Fig 12 gives an overview of the results. In panel a the maximum excursions ΔA after the step (see inset) are plotted for different backgrounds k_{10} as a function of the sum of the phase 2 k_2 value and k_{10}. For each background, the nine k_2 steps 1→2, 1→3, ...,1→9, and 1→10 are applied and ΔA is determined. The parallel lines indicate robust background compensation, i.e. ΔA is the same for a certain defined step, independent of the background. Panel b shows the situation for a k_2 1→ 10 step when background k_{10}=0. In panel c the same step is applied, but the background has been increased to k_{10}=10. Comparing Figs 12b and 12c shows that profiles in both A and E are the same with A_{set}=2.0 and E_{set}=100.

Fig 12. Background compensation in the non-oscillatory feedback scheme of Fig 11. Panel a: Each colored curve shows the values of ΔA for the nine k_2 steps: 1→2, 1→3,...,1→10 at k_{10} background levels: 0, 2, 4,...,8, 10. Inset shows how ΔA is defined. k_2^{ph2} is the value of k_2 during phase 2. Panels in b: Time profiles of A, E (left panel) and I_1, I_2 (right panel) for a 1→10 k_2 step at background k_{10}=0.0. The change in k_2 is applied at time t=500 indicated by the vertical arrow. Panels in c are similar to the panels in b with the difference that background k_{10} is 10.0. Other rate constants: k_3=5×10^3, k_4=1.0, k_5=0.5, k_6=2.0, k_7=1×10^{-5}, k_9=2.0, k_{11}=0.1, k_{12}=10.0, k_{13}=k_{16}=1×10^{-4}, k_{14}=1.0, k_{15}=0.01, k_g=0.01, k_{g3}=1×10^{-3}. Initial concentrations for panel b: A_0=2.0, E_0=100.0, e_0=1.0, $I_{1,0}$=2.5684×10^3, $I_{2,0}$=2.8492×10^4. Initial concentrations for panel c: A_0=2.0, E_0=100.0, e_0=1.0, $I_{1,0}$=1.5734×10^3, $I_{2,0}$=2.8592×10^4. For python scripts showing the results of panels b and c, please see Supporting information S1 Programs.

Fig 13 shows another example of coherent feedback. Here we have two inflow controllers E_1 and E_2, but only E_2 is connected to A via I_1 and I_2 through a coherent feedback. The reason why we looked at two E-controllers was to see whether E_2 alone, i.e. without the help of I_1 and I_2, was able to compensate backgrounds. This, however, turned out not to be the case and I_1 and I_2 were included to control E_2.

Fig 13. Coherent feedback loop A-E_2-(I_1,I_2)-A with an additional inflow control of A by E_1.

The rate equations are:

$$\dot{A} = k_g \cdot I_2 - k_{g3} \cdot A \cdot I_1 - k_2 \cdot A - k_{10} \cdot A + k_9 \cdot a + k_{11} \cdot E_2 \tag{19}$$

$$\dot{a} = \frac{k_3 \cdot k_5}{k_5 + E_1} - k_9 \cdot a \tag{20}$$

$$\dot{E_1} = k_4 \cdot A - \frac{k_6 \cdot E_1}{k_7 + E_1} \tag{21}$$

$$\dot{E_2} = k_{12} - A \cdot \left(\frac{k_{13} \cdot E_2}{k_{14} + E_2} \right) \tag{22}$$

$$\dot{I_1} = k_{15} - \left(\frac{k_{16} \cdot I_1}{k_{17} + I_1} \right) \cdot E_2 \tag{23}$$

$$\dot{I_2} = k_{18} \cdot E_2 - \frac{k_{19} \cdot I_2}{k_{20} + I_2} \tag{24}$$

E_1 and E_2 provide two set-points for A: one, $A_{set}^{E_1}$, by setting Eq 21 to zero and solving for the steady state level of A under zero-order conditions, and the other, $A_{set}^{E_2}$, by doing the same for Eq 22. This gives:

$$A_{set}^{E_1} = \frac{k_6}{k_4} \quad (k_7 \ll E_1) \tag{25}$$

and

$$A_{set}^{E_2} = \frac{k_{12}}{k_{13}} \quad (k_{14} \ll E_2) \tag{26}$$

In the calculations we have set $A_{set}^{E_1}$=2.1 and $A_{set}^{E_2}$=2.0. Since the E_2 inflow controller has a lower set-point in comparison with E_1, E_2 will take over the control of A [22], while E_1 will be inactive and allow a constant inflow to A via a.

Fig 14 shows that in this system a 1→10 perturbation in k_2 induces a train of damped oscillations with background (k_{10}) independent concentration profiles. In panels a and b ΔA (for definition see inset in Fig 12) is shown as a function of increasing k_2 steps at different but constant k_{10} backgrounds. Panel c shows the time profile in A for a 1→10 k_2 step with a k_{10} background of 0. In panel d the same step is applied but now with a background of k_{10}=1024. One clearly sees the conserved background-independent transition profiles in A.

Fig 14. Background compensation by coherent feedback in the scheme of Fig 13. Panels a and b: ΔA as a function of $k_2^{ph2}+k_{10}$ for different but constant backgrounds. k_2^{ph2} is the k_2 value in phase 2. The background values (k_{10}) are indicated above the colored curves. Panels c and d: Concentration profiles in A when a k_2 1→10 step is applied at respective backgrounds of k_{10}=0.0 and 1024.0. Other rate constants: k_3=2.5×10^3, k_4=1.0, k_5=0.1, k_6=2.1, k_7=1×10^{-5}, k_9=0.5, k_{11}=0.5, k_{12}=200.0, k_{13}=100, k_{14}=k_{17}=k_{20}=1×10^{-5}, k_{15}=1×10^3, k_{16}=10.0, k_{18}=1.0, k_{19}=99.99, k_g=k_{g3}=0.1. Initial concentrations for c: A_0=2.0, $E_{1,0}$=2.0×10^{-4}, $E_{2,0}$=100.0, a_0=4.99×10^3, $I_{1,0}$=2.5684×10^3, $I_{2,0}$=2.8492×10^4. Initial concentrations for d: A_0=2.0, $E_{1,0}$=2.0×10^{-4}, $E_{2,0}$=100.0, a_0=4.99×10^3, $I_{1,0}$=3.5195×10^3, $I_{2,0}$=2.0888×10^3. Supporting information S1 Programs includes the python scripts showing the results of panels c and d.

Frequency homeostasis without background compensation

Fig 15a shows an oscillator scheme which we described previously in relation to robust frequency homeostasis [11]. We wondered whether frequency homeostasis would imply background compensation, but found out that this is not the case. In this case I_1, I_2, and E do not feed back coherently to A, but (incoherently) to a, which is a precursor of A.

Fig 15. Oscillator based on motif 2 [11, 22] with A-incoherent feedback, where E, I_1, and I_2 feed back to a, a precursor of A. Panel a: reaction scheme. Panel b: Flow scheme. For rate equations, see main text.

The rate equations are ('pert' stands for perturbation and 'bg' for background):

$$\dot{A} = k_9 \cdot a - \underbrace{k_2 \cdot A}_{\text{pert}} - \underbrace{k_{10} \cdot A}_{\text{bg}} \tag{27}$$

$$\dot{a} = \left(\frac{k_{g3} \cdot I_2 + k_3}{k_5 + E} \right) \cdot k_5 - k_g \cdot a \cdot I_1 - k_9 \cdot a \tag{28}$$

$$\dot{E} = k_4 \cdot A - \frac{k_6 \cdot E}{k_7 + E} \tag{29}$$

$$\dot{I}_1 = k_{11} \cdot E - \frac{k_{12} \cdot I_1}{k_{13} + I_1} \tag{30}$$

$$\dot{I}_2 = k_{14} - \left(\frac{k_{15} \cdot I_2}{k_{16} + I_2} \right) \cdot E \tag{31}$$

Fig 16 shows an example of oscillations for the scheme in Fig 15 with background k_{10}=0 and a step perturbation in k_2 from 1 (phase 1) to 10 (phase 2). It may be noted that in this case oscillations occur although the removal reactions of a and A are first-order with respect to a and A, indicating that first-order processes are only a 'weak' condition to abolish oscillatory behavior, as has been indicated in the above section 'Background compensation in non-oscillatory homeostats'.

Fig 16 clearly shows the occurrence of frequency homeostasis. However, when the oscillator is tested for different but constant k_{10} backgrounds with changed k_2 steps the maximum frequency decreases with increasing backgrounds. Fig 17a shows the decrease of the maximum frequency and loss of robust background compensation at four different k_{10} backgrounds when k_2 steps are applied from 1→2 up to 1→10 in analogy to the calculation shown in Fig 16. When using a logarithmic ordinate (Fig 17b) lines appear more or less parallel, which may give the illusion that the system responds in a background compensated way.

Fig 16. Frequency homeostasis in the oscillator of Fig 15. Background k_{10}=0.0. A k_2 step 1→10 occurs at time t=500 indicated by the vertical arrows. Panel a: Concentration of A and average $<A>$ as a function of time. Panel b: Concentration of E and average $<E>$ as a function of time. Panel c: Concentrations of I_1 and I_2 as a function of time. Panel d: Frequency as a function of time. Other rate constants: k_3=1×10^6, k_4=1.0, k_5=1×10^{-6}, k_6=2.0, k_7=k_{13}=k_{16}=1×10^{-6}, k_9=2.0, k_{11}=5.0, k_{12}=100.0, k_{14}=99.99, k_{15}=5.0, k_g=1×10^{-3}, and k_{g3}=100.0. Initial concentrations: A_0=5.6920×10^{-3}, E_0=6.1163, a_0=3.6221×10^{-3}, $I_{1,0}$=4.4051×10^4, $I_{2,0}$=2.7566×10^2. See S1 Programs for python scripts.

Fig 17. Maximum frequencies as a function of k_2^{ph2}+k_{10}, where k_2^{ph2} is the k_2 value in phase 2. Calculations were performed with rate constants as described in Fig 16. Panel a show results with linear scaling of axes, while panel b shows the same data set as double-logarithmic plots. Initial concentrations: bg (k_{10})=0.0, see legend of Fig 16; bg (k_{10})=1.0, A_0=2.5946×10^{-3}, E_0=25.4830, a_0=2.6844×10^{-3}, $I_{1,0}$=3.0980×10^4, $I_{2,0}$=1.3296×10^4; bg (k_{10})=2.0, A_0=5.0041×10^{-3}, E_0=15.8930, a_0=7.8102×10^{-3}, $I_{1,0}$=2.2995×10^4, $I_{2,0}$=2.1181×10^4; bg (k_{10})=4.0, A_0=4.7328×10^{-3}, E_0=21.6050, a_0=1.2043×10^{-2}, $I_{1,0}$=1.3516×10^4, $I_{2,0}$=3.0610×10^4.

Is retinal light adaptation background compensated?

Based on the comment in Ref [2] that the parallel lines in Fig 2 indicate the same response at different backgrounds and involve a form of compensation mechanism, we became interested to look into the conditions how background compensation could occur. This requires of course how the term 'background compensation' is defined. We have applied the following, we think rather intuitive definition, where background compensation for a negative feedback system means the presence of a compensatory mechanism, which, when a perturbation is applied, the same response in a controlled

variable occurs *independent* of an applied constant background in relationship to the perturbation. This definition is, however, not in agreement with the results shown in Fig 2, for example for the backgrounds indicated by the red, blue and green curves. Increasing the background from the red, blue to the green curve leads to a reduction in the average maximum frequency when a test spot luminance of 1×10^{-2} cd/m^2 is applied, as indicated by the vertical dashed bar. In fact, the adaptation behavior shown in Fig 1 can show an analogous behavior as in Fig 2.

To see this we use the model where the response amplitude V of retinal cells with respect to a light perturbation I are described by a Hill-type Michaelis-Menten equation of the form

$$V = \frac{V_{max} I^{\alpha}}{I^{\alpha}+\sigma^{\alpha}} \tag{32}$$

The cooperativity α is 1.0 for photoreceptor cells, but found to be 0.7 to 0.8 for horizontal cells, 1.2-1.4 for bipolar and sustained ganglion cells, and about 3.4 for transient ganglion cells (for an overview see [3]).

We consider here the response kinetics of rods and cones, i.e. σ=1 with

$$V = \frac{V_{max} I}{I+\sigma} \tag{33}$$

As pointed out by Naka and Rushton [32], in the presence of a background I_0 the response V_1 upon a perturbation I_1 of a single pigment system will follow Eq 33, but with an increase of σ to σ_1=σ+I_0 and a scaling of V_{max} by a factor of $\sigma/(\sigma+I_0)$. This can be shown as follows:

In the presence of a constant background I_0 Eq 33 gives

$$V_0 = \frac{V_{max} I_0}{I_0+\sigma} \tag{34}$$

If a light perturbation I_1 is applied in addition to background I_0 the total response amplitude is

$$V_1 + V_0 = \frac{V_{max}(I_0+I_1)}{I_0+I_1+\sigma} \tag{35}$$

Subtracting Eq 34 from Eq 35 gives

$$\begin{aligned} V_1 &= V_{max}\left[\frac{(I_0+I_1)}{I_0+I_1+\sigma} - \frac{I_0}{I_0+\sigma}\right] = V_{max}\left[\frac{(I_0+I_1)\cdot(I_0+\sigma) - I_0\cdot(I_0+I_1+\sigma)}{(I_0+I_1+\sigma)\cdot(I_0+\sigma)}\right] \\ &= V_{max}\left[\frac{I_1\cdot\sigma}{(I_0+I_1+\sigma)\cdot(I_0+\sigma)}\right] = \frac{V_{max}\cdot\sigma}{I_0+\sigma}\left(\frac{I_1}{I_0+I_1+\sigma}\right) \\ &= V_{max,1}\left(\frac{I_1}{I_1+\sigma_1}\right) \end{aligned} \tag{36}$$

Fig 18 shows Eq 33 with six different σ values which mimick six different background levels. For the sake of simplicity we have set V_{max}=1. In panel a both axes are linear, while in panel b the ordinate is logarithmic and the abscissa is linear. In panel c the ordinate is linear and the abscissa is logarithmic. Finally, in panel d both axes are logarithmic.

Fig 18. Photoadaptation behaviors in rods and cones described by the Michaelis-Menten equation. The colored lines in the panels show Eq 33 with σ values ranging over six orders of magnitudes from σ=1×10^{-4} up to σ=10. For simplicity, V_{max}=1. Panel a: Both axes are linear. Panel b: Ordinate is logarithmic and abscissa is linear. Panel c: Ordinate is linear and abscissa is logarithmic. Panel d: Both axes are logarithmic. The dashed vertical lines indicate an perturbation intensity of I=1. The colored intersection points with the vertical dashed lines show the responses of V for the different backgrounds with the same color.

Fig 18c is analogous to the results in Fig 2 when for a given perturbation (indicated by the vertical dashed lines) an increased background or an increased σ leads to a reduction in the averaged maximum frequency. No background compensation, as indicated by Kandel et al. in Ref 2, appears necessary.

When studying the photoadaptation of gecko photoreceptors, Kleinschmidt and Dowling 33 showed log-log relationships analogous to Fig 18d. Dowling interpreted the parallel lines as follows: *A second adaptive mechanism in the receptor shifts the photoreceptor intensity-response curves along the intensity axis, thus extending the range over which the receptor responds* (cited from Ref 3, page 222, bottom section).

Clearly, as Fig 18 shows, the parallel lines in panels c or d neither require the need for a compensation mechanism of a background or other additional adaptive mechanisms. While adaptation mechanisms compensating for a background cannot be excluded, the observation of parallel lines in semi-logarithmic or double-logarithmic plots appear not sufficient to indicate additional background compensation mechanisms besides the negative feedbacks, which lead to the responses in Fig 1, 5.

Conclusion and outlook

We have shown how robust background compensation in oscillatory and non-oscillatory homeostatic controllers can be realized. The needed feedback condition has been termed 'coherent feedback' in analogy to a corresponding concept applied in quantum control theory. Although the property of robust background compensation appears interesting, we are presently not aware of any biological or biochemical example that shows or applies this property. Background compensation may become of interest in synthetic biology to design cellular responses, which by some reason are needed to become background independent. Concerning the case of retinal light adaptation, parallel lines in semi-logarithmic or double-logarithmic plots do not necessarily imply the presence of background compensating mechanisms as defined in this paper.

Supporting information

S1 Programs. Documentation. A zip-file with python scripts describing the results for Figs 5, 6, 9a, 9b, 12b, 12c, 14c, 14d, and 16.

References

1. Clancy J, McVicar AJ. Physiology and Anatomy. A Homeostatic Approach. Hodder Arnold; 2002.
2. Kandel ER, Koester JD, Mack SH, Siegelbaum S, editors. Principles of Neural Science. Sixth Edition. McGraw-Hill; 2021.
3. Dowling JE. The Retina: An Approachable Part of the Brain. Revised Edition. Harvard University Press; 2012.
4. Purves D, Augustine GJ, Fitzpatrick D, Hall WC, LaMantia AS, McNamara JO, et al. Neuroscience. Fourth Edition. Sinauer Associates, Inc.; 2008.
5. Grini JV, Nygård M, Ruoff P. Homeostasis at different backgrounds: The roles of overlayed feedback structures in vertebrate photoadaptation. PLoS One. 2023;18(4):e0281490.

6. Fain GL, Matthews HR, Cornwall MC, Koutalos Y. Adaptation in vertebrate photoreceptors. Physiological Reviews. 2001;81(1):117–151.

7. Schneeweis D, Schnapf J. Noise and light adaptation in rods of the macaque monkey. Visual Neuroscience. 2000;17(5):659–666.

8. Sakmann B, Creutzfeldt OD. Scotopic and mesopic light adaptation in the cat's retina. Pflügers Archiv. 1969;313:168–185.

9. Lloyd S. Coherent quantum feedback. Physical Review A. 2000;62(2):022108.

10. Fan B, Ning J, Xie M, Liu C, Guan S. Coherent feedback induced transparency. Optics Express. 2020;28(19):28243–28251.

11. Thorsen K, Agafonov O, Selstø CH, Jolma IW, Ni XY, Drengstig T, et al. Robust concentration and frequency control in oscillatory homeostats. PLoS One. 2014;9(9):e107766. doi:10.1371/journal.pone.0107766.

12. Radhakrishnan K, Hindmarsh AC. Description and Use of LSODE, the Livermore Solver for Ordinary Differential Equations. NASA Reference Publication 1327, Lawrence Livermore National Laboratory Report UCRL-ID-113855. Cleveland, OH 44135-3191: National Aeronautics and Space Administration, Lewis Research Center; 1993.

13. Lewis FL. Applied Optimal Control & Estimation. Englewood Cliffs, NJ: Prentice Hall; 1992.

14. Bennett S. A brief history of automatic control. IEEE Control Systems Magazine. 1996;16(3):17–25.

15. Warwick K. An Introduction to Control Systems. Second Edition. World Scientific; 1996.

16. Wilkie J, Johnson M, Reza K. Control Engineering. An Introductory Course. New York: Palgrave; 2002.

17. Yi TM, Huang Y, Simon MI, Doyle J. Robust perfect adaptation in bacterial chemotaxis through integral feedback control. PNAS. 2000;97(9):4649–4653.

18. Iglesias PA, Ingalls BP. Control Theory and Systems Biology. MIT Press; 2010.

19. Ang J, Bagh S, Ingalls B, McMillen D. Considerations for using integral feedback control to construct a perfectly adapting synthetic gene network. J Theor Biol. 2010;266(4):723–738.

20. Del Vecchio D, Dy AJ, Qian Y. Control theory meets synthetic biology. Journal of The Royal Society Interface. 2016;13(120):20160380.

21. Aoki SK, Lillacci G, Gupta A, Baumschlager A, Schweingruber D, Khammash M. A universal biomolecular integral feedback controller for robust perfect adaptation. Nature. 2019;570(7762):533–537.

22. Drengstig T, Jolma I, Ni X, Thorsen K, Xu X, Ruoff P. A basic set of homeostatic controller motifs. Biophys J. 2012;103(9):2000–2010.

23. Ni XY, Drengstig T, Ruoff P. The control of the controller: Molecular mechanisms for robust perfect adaptation and temperature compensation. Biophys J. 2009;97:1244–53.

24. Ang J, McMillen D. Physical constraints on biological integral control design for homeostasis and sensory adaptation. Biophys J. 2013;104(2):505–15.

25. Briat C, Gupta A, Khammash M. Antithetic integral feedback ensures robust perfect adaptation in noisy biomolecular networks. Cell Systems. 2016;2(1):15–26.

26. Waheed Q, Zhou H, Ruoff P. Kinetics and mechanisms of catalyzed dual-E (antithetic) controllers. PLoS One. 2022;17(8):e0262371.

27. Shoval O, Goentoro L, Hart Y, Mayo A, Sontag E, Alon U. Fold-change detection and scalar symmetry of sensory input fields. PNAS. 2010; p. 201002352.

28. Drengstig T, Ni XY, Thorsen K, Jolma IW, Ruoff P. Robust adaptation and homeostasis by autocatalysis. J Phys Chem B. 2012;116:5355–5363.

29. Briat C, Zechner C, Khammash M. Design of a synthetic integral feedback circuit: dynamic analysis and DNA implementation. ACS Synthetic Biology. 2016;5(10):1108–1116.

30. Fjeld G, Thorsen K, Drengstig T, Ruoff P. Performance of homeostatic controller motifs dealing with perturbations of rapid growth and depletion. J Phys Chem B. 2017;121(25):6097–6107.

31. Nishiyama N, Ruoff P, Jimenez JC, Miwakeichi F, Nishiyama Y, Yata T. Modeling the interaction between donor-derived regulatory T cells and effector T cells early after allogeneic hematopoietic stem cell transplantation. Biosystems. 2023;227-228:104889. doi:https://doi.org/10.1016/j.biosystems.2023.104889.

32. Naka KI, Rushton WA. S-potentials from luminosity units in the retina of fish (Cyprinidae). The Journal of Physiology. 1966;185(3):587–599.

33. Kleinschmidt J, Dowling JE. Intracellular recordings from Gecko photoreceptors during light and dark adaptation. The Journal of General Physiology. 1975;66(5):617–648.

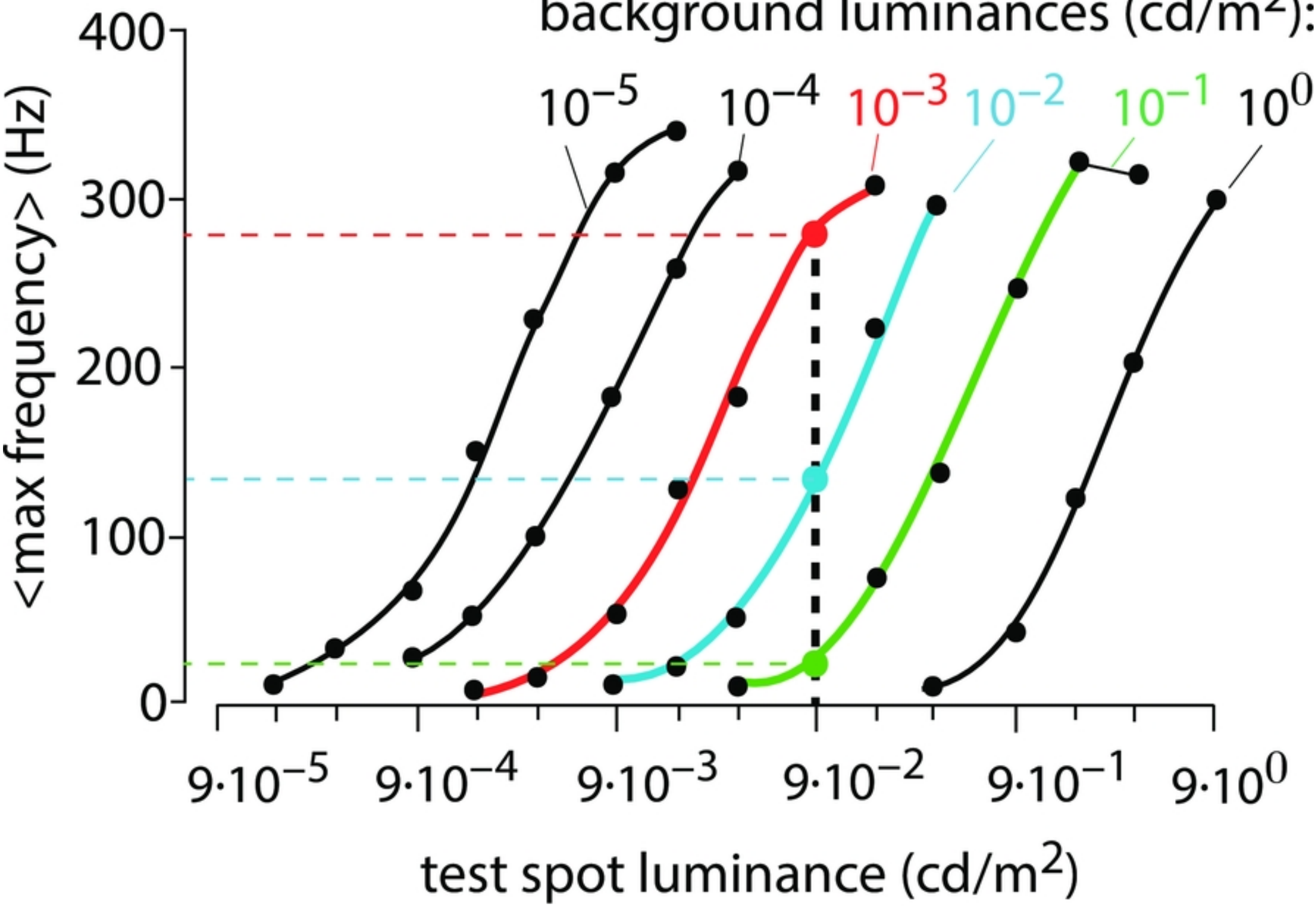
background luminances (cd/m²):
10⁻⁵
10⁻⁴
10⁻³
10⁻²
10⁻¹
10⁰
<max frequency> (Hz)
400
300
200
100
0
9·10⁻⁵
9·10⁻⁴
9·10⁻³
9·10⁻²
9·10⁻¹
9·10⁰
test spot luminance (cd/m²)

Figure 2

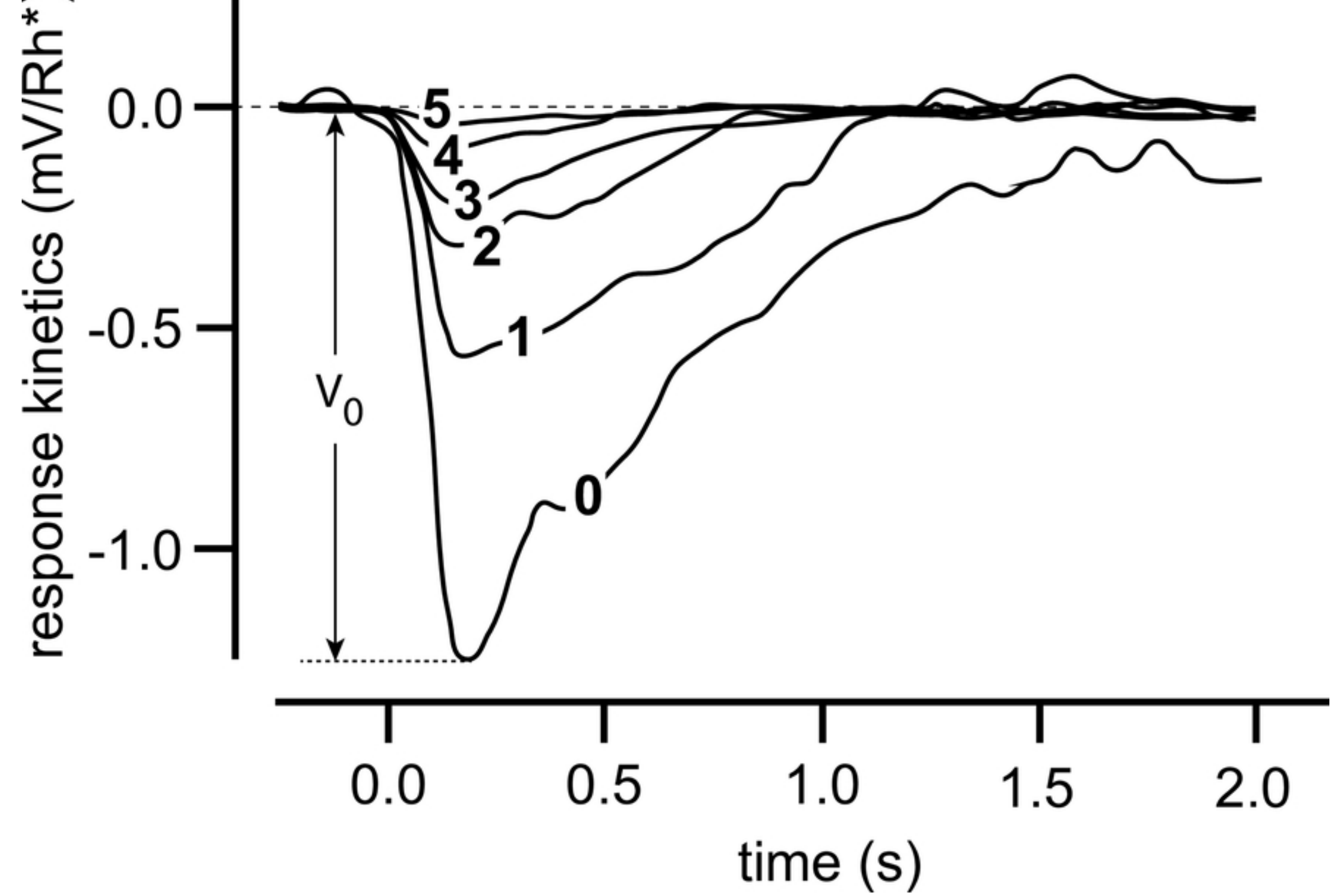

Figure 1

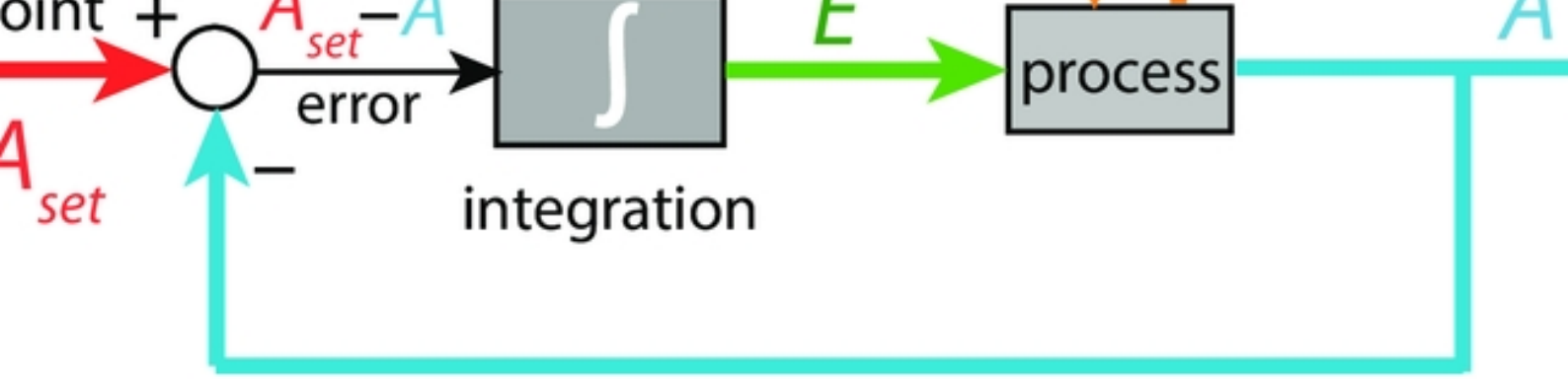

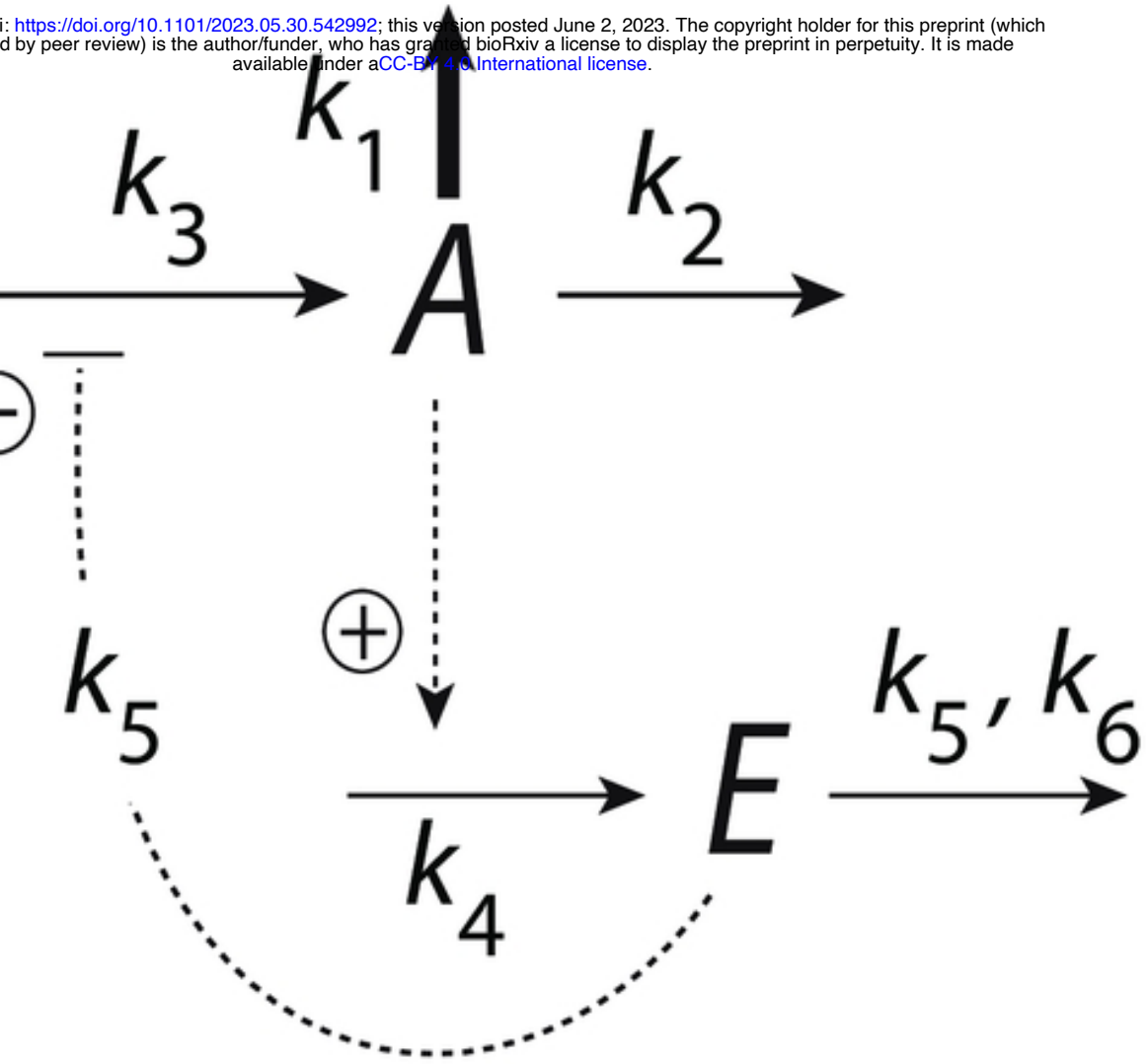

$$\dot{E} = k_4 \cdot A - k_5 \underbrace{\left(\frac{E}{k_6 + E} \right)}_{\approx 1} \approx -k_4 \underbrace{\left[\left(\frac{k_5}{k_4} \right.}_{A_{set}} \right.$$

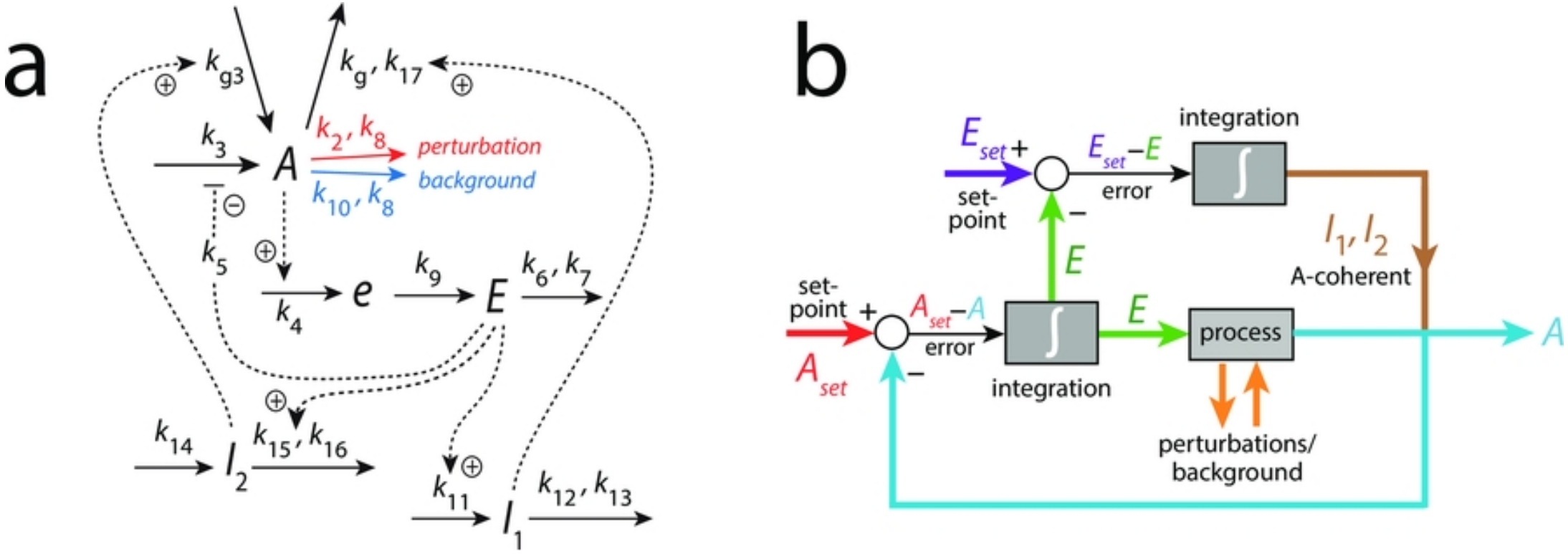
a
k_{g3}
k_g, k_{17}
k_3
A
k_2, k_8
perturbation
k_{10}, k_8
background
k_5
k_4
e
k_9
E
k_6, k_7
k_{14}
I_2
k_{15}, k_{16}
k_{11}
I_1
k_{12}, k_{13}
b
E_{set} +
set-point
E_{set} – E
error
integration
E
I_1, I_2
A-coherent
set-point +
A_{set} – A
error
A_{set}
integration
E
process
A
perturbations/ background

Figure 4

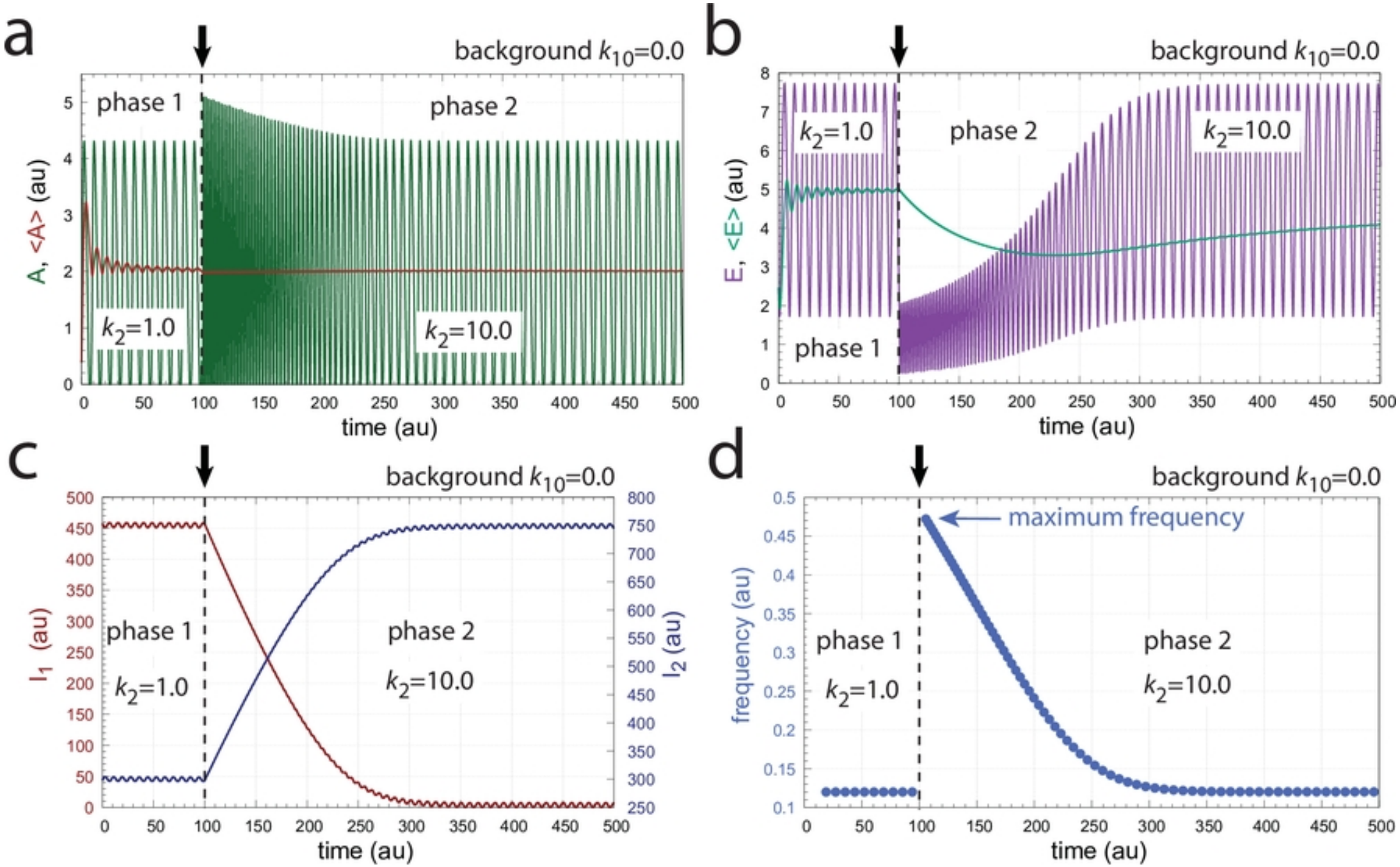
a
background k_{10}=0.0
phase 1
phase 2
A, <A> (au)
k_2=1.0
k_2=10.0
time (au)
b
background k_{10}=0.0
k_2=1.0
phase 2
k_2=10.0
E, <E> (au)
phase 1
time (au)
c
background k_{10}=0.0
I_1 (au)
phase 1
k_2=1.0
phase 2
k_2=10.0
I_2 (au)
time (au)
d
background k_{10}=0.0
maximum frequency
frequency (au)
phase 1
k_2=1.0
phase 2
k_2=10.0
time (au)

Figure 5

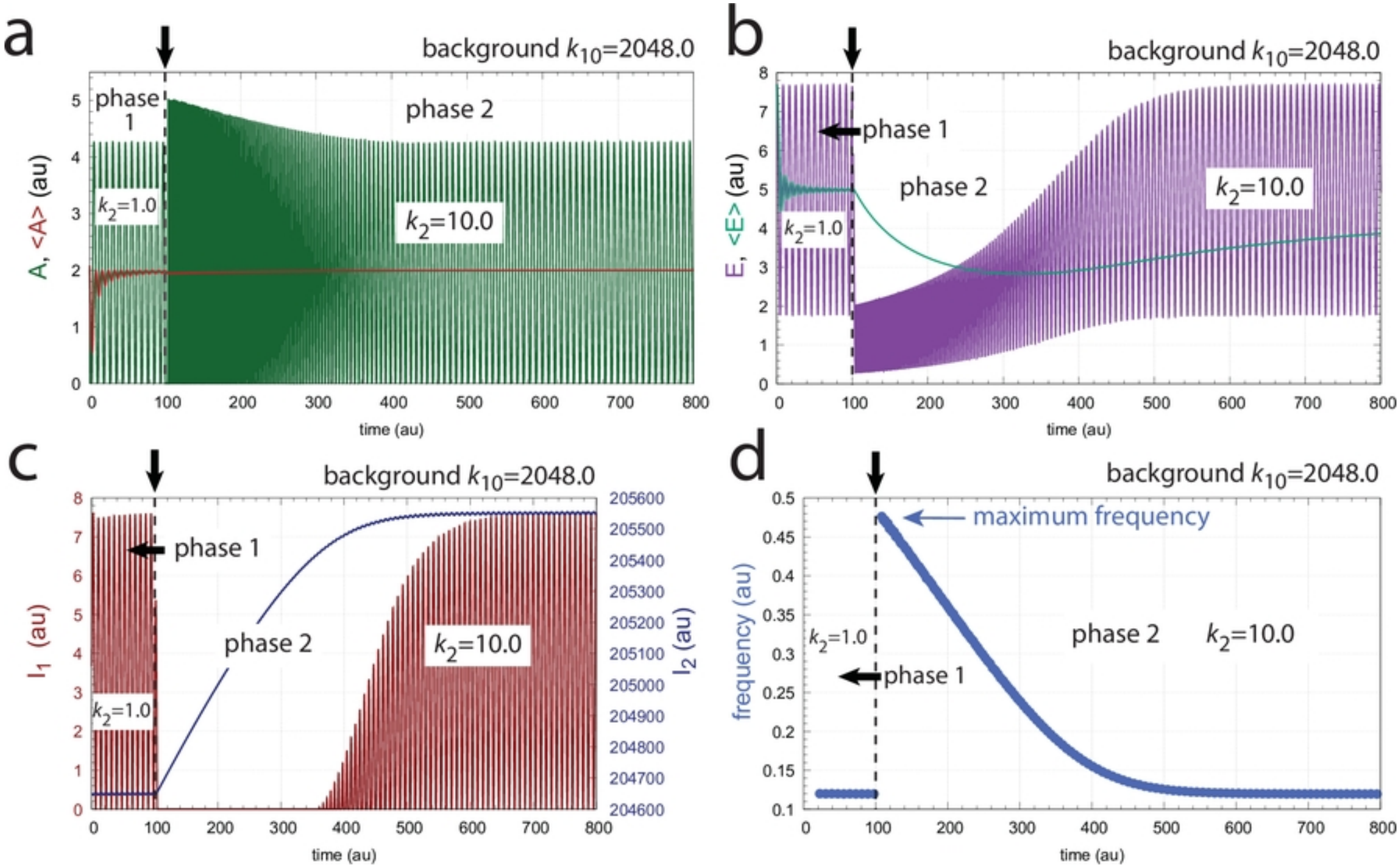
a
background k_{10}=2048.0
phase 1
phase 2
k_2=1.0
k_2=10.0
A, <A> (au)
time (au)
b
background k_{10}=2048.0
phase 1
phase 2
k_2=1.0
k_2=10.0
E, <E> (au)
time (au)
c
background k_{10}=2048.0
phase 1
phase 2
k_2=1.0
k_2=10.0
I_1 (au)
I_2 (au)
time (au)
d
background k_{10}=2048.0
maximum frequency
phase 2
k_2=10.0
k_2=1.0
phase 1
frequency (au)
time (au)

Figure 6

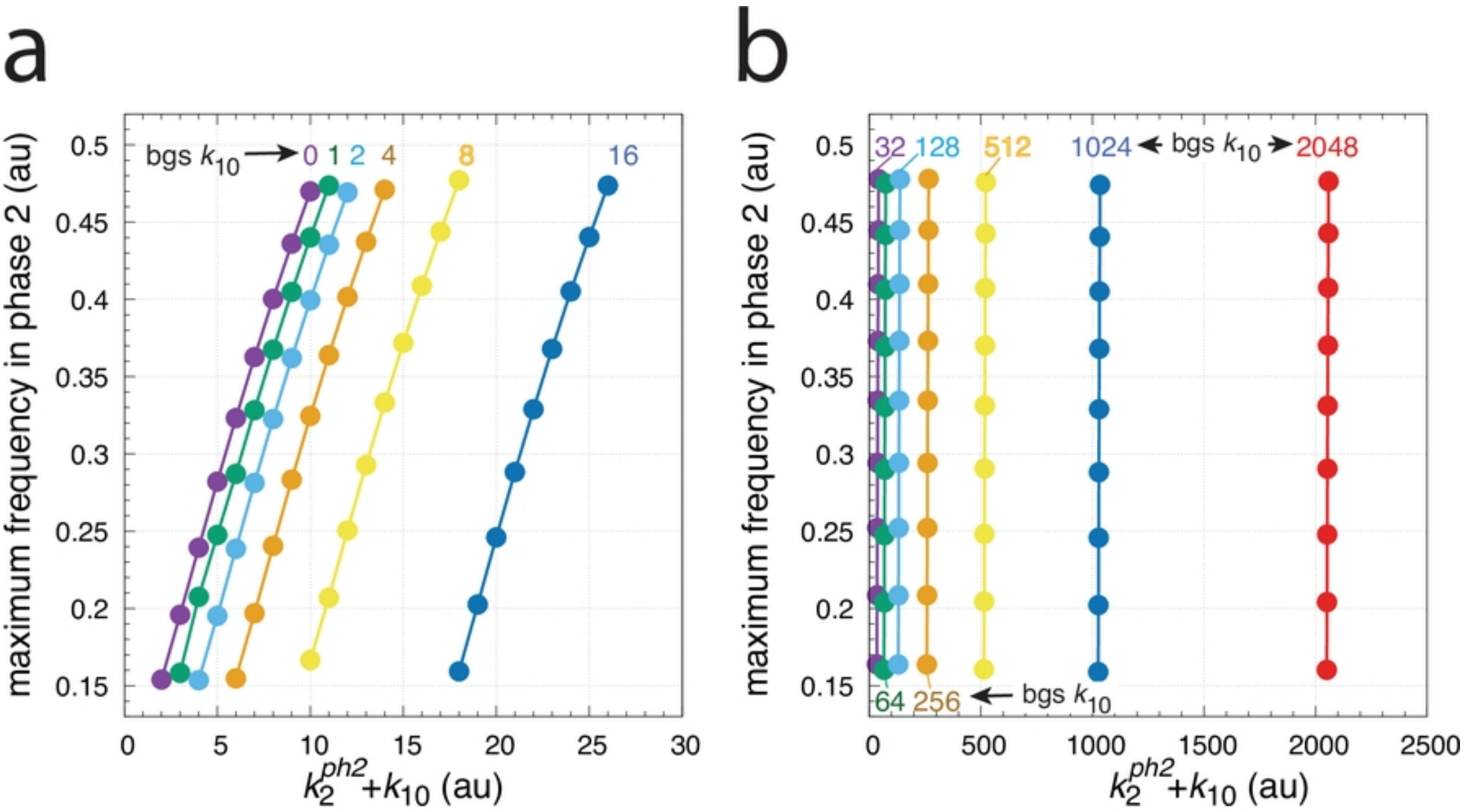
a
b
maximum frequency in phase 2 (au)
bgs k_{10}
0 1 2 4 8 16
32 128 512 1024 2048
64 256
$k_2^{ph2}+k_{10}$ (au)

Figure 7

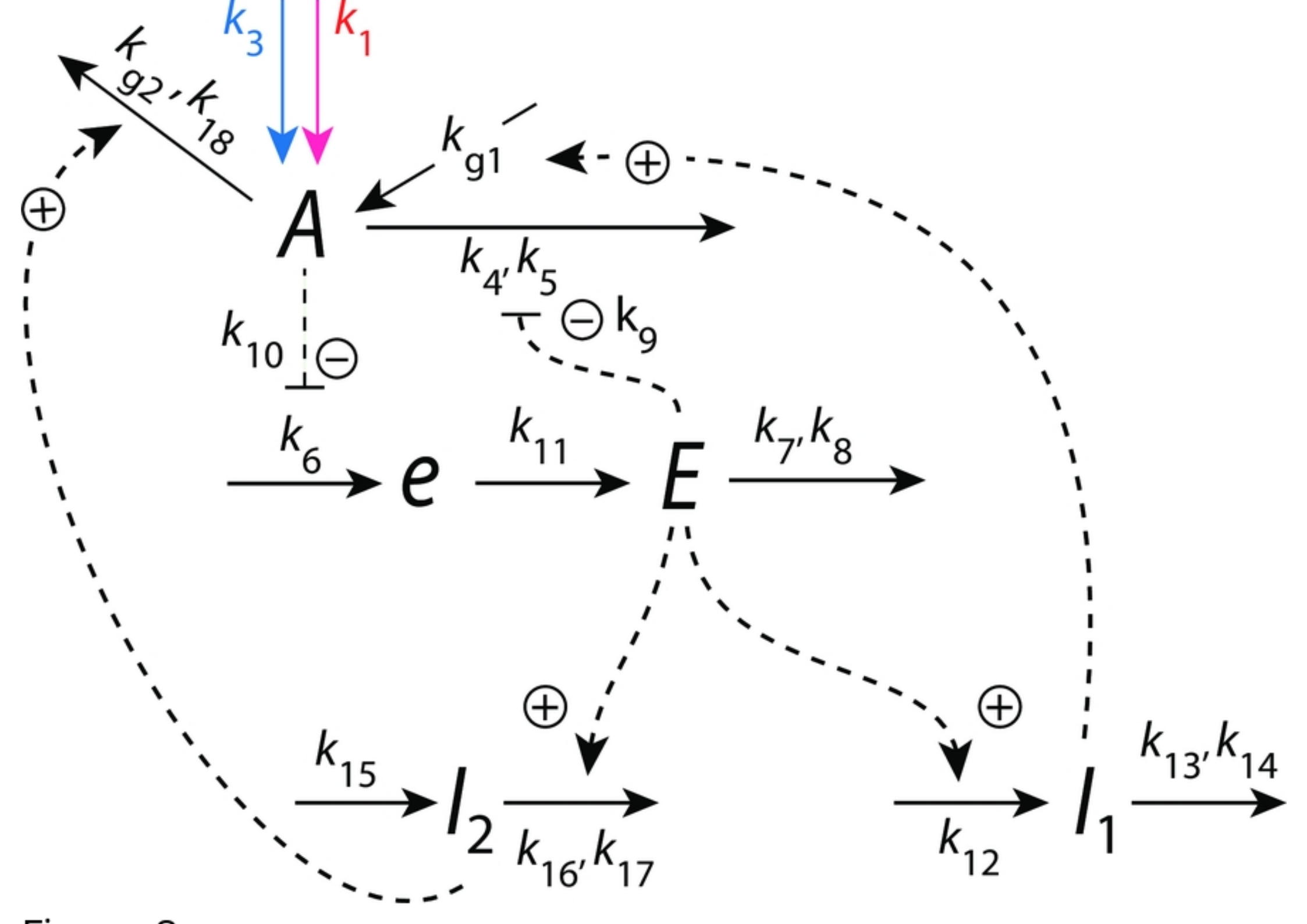
k_3
k_1
k_{g2}, k_{18}
k_{g1}
A
k_{4}, k_5
k_{10}
k_9
k_6
e
k_{11}
E
k_{7}, k_8
k_{15}
I_2
k_{16}, k_{17}
k_{12}
I_1
k_{13}, k_{14}

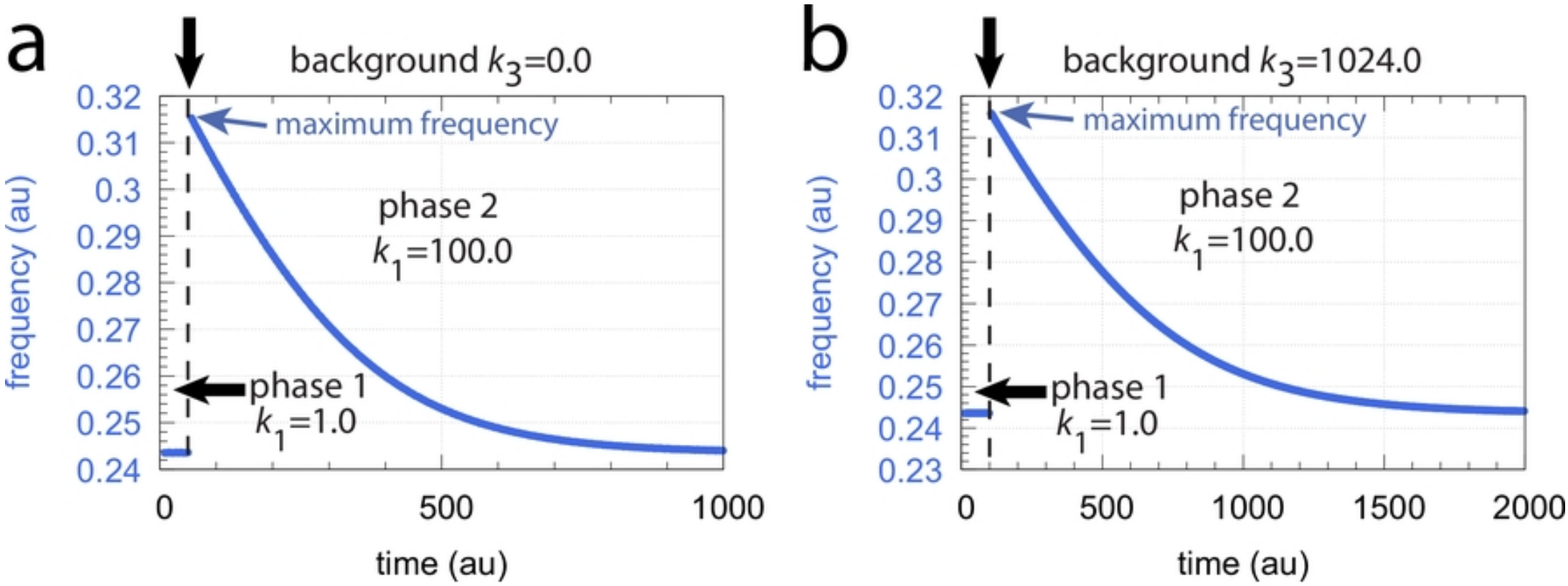
a
background k_3=0.0
maximum frequency
phase 2
k_1=100.0
phase 1
k_1=1.0
frequency (au)
0.32
0.31
0.3
0.29
0.28
0.27
0.26
0.25
0.24
0
500
1000
time (au)
b
background k_3=1024.0
maximum frequency
phase 2
k_1=100.0
phase 1
k_1=1.0
frequency (au)
0.32
0.31
0.3
0.29
0.28
0.27
0.26
0.25
0.24
0.23
0
500
1000
1500
2000
time (au)

Figure 9

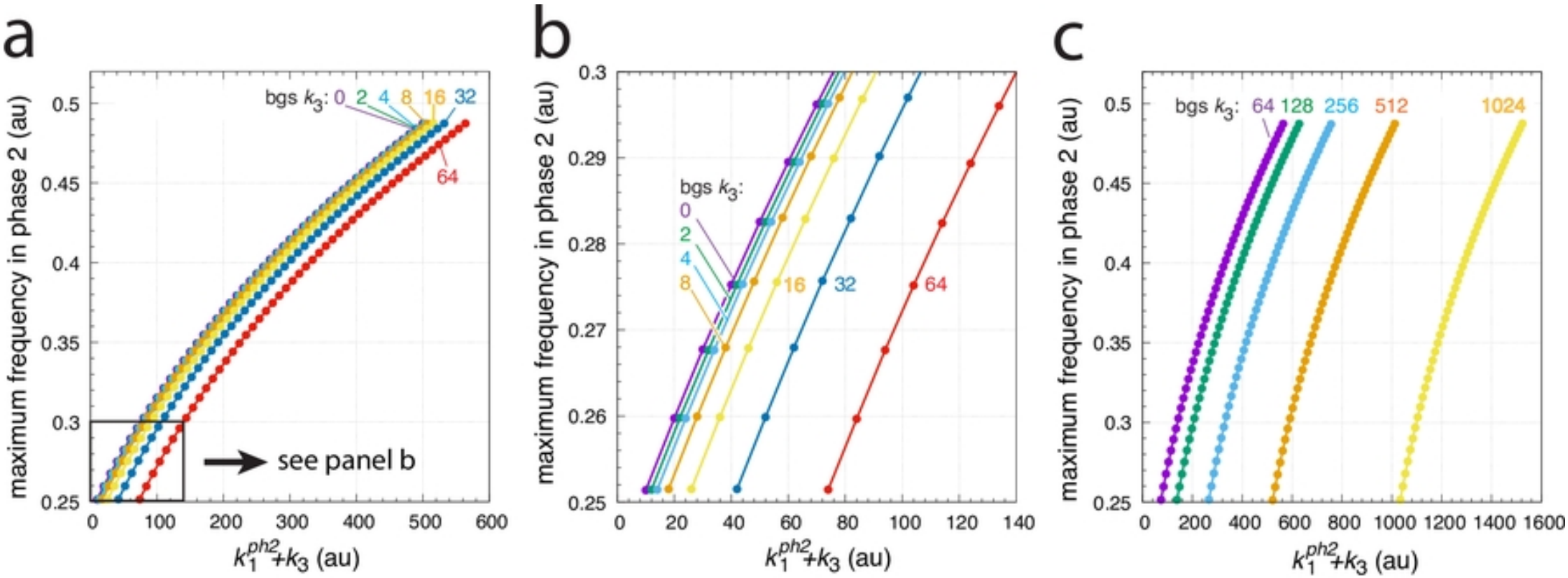
a
b
c
maximum frequency in phase 2 (au)
$k_1^{ph2}+k_3$ (au)
bgs k_3: 0 2 4 8 16 32
64
see panel b
bgs k_3:
0
2
4
8
16
32
64
bgs k_3: 64 128 256 512 1024

Figure 10

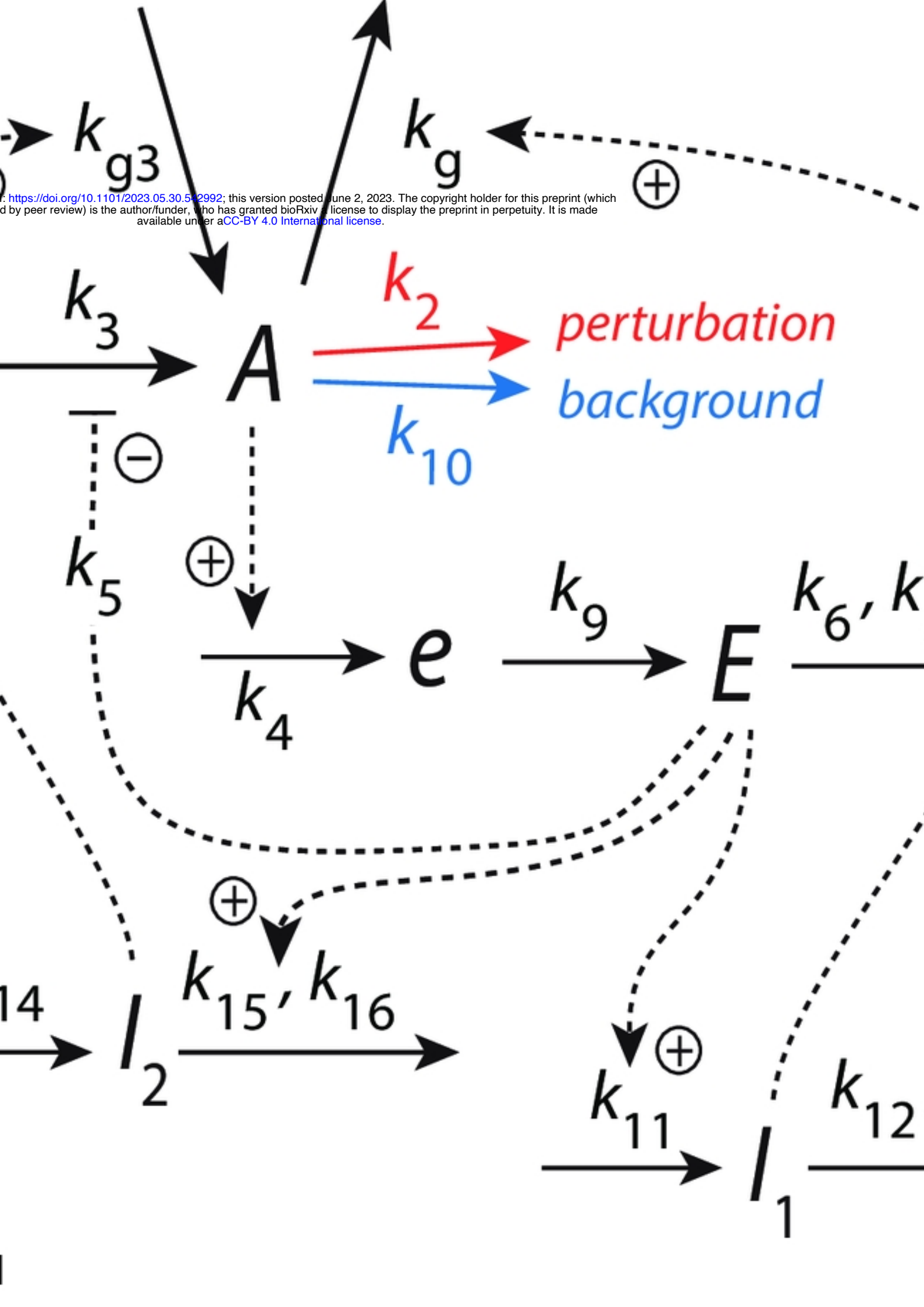

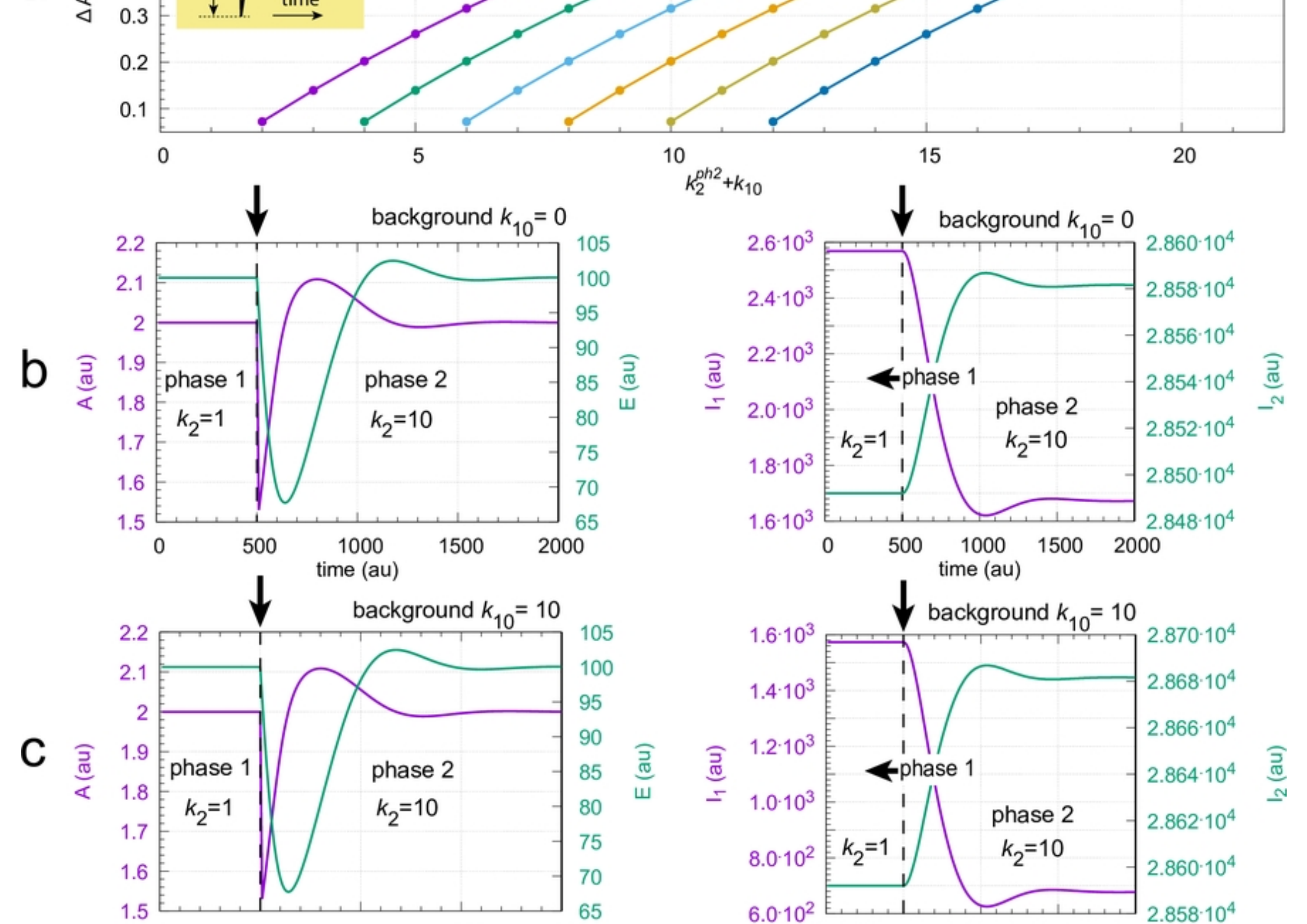
ΔA
0.3
0.2
0.1
0
5
10
15
20
$k_2^{ph2}+k_{10}$
b
background k_{10}= 0
phase 1
k_2=1
phase 2
k_2=10
A (au)
E (au)
time (au)
I_1 (au)
I_2 (au)
c
background k_{10}= 10

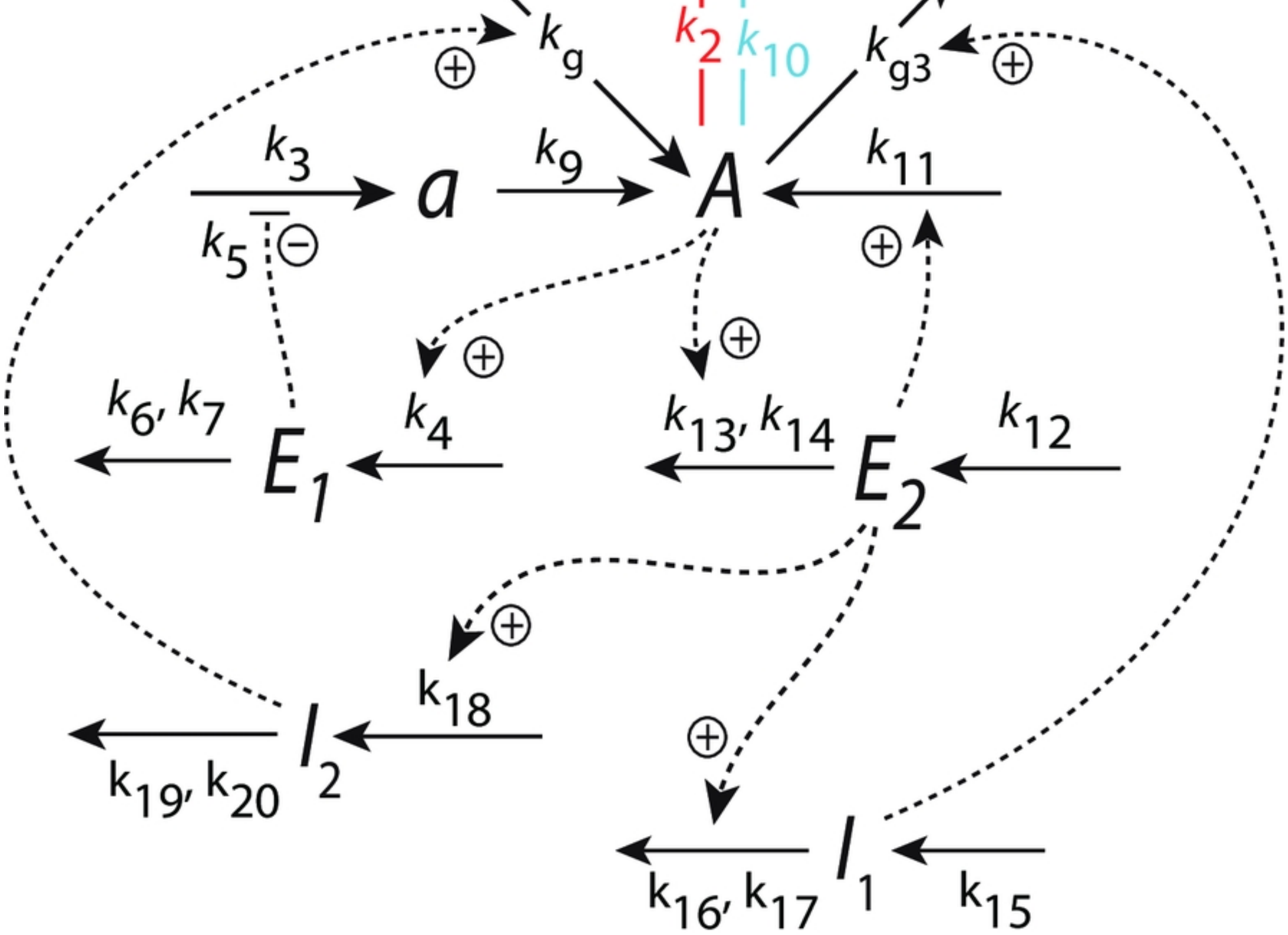
k_g
k_2
k_10
k_g3
k_3
a
k_9
A
k_11
k_5
k_6, k_7
E_1
k_4
k_13, k_14
E_2
k_12
k_18
I_2
k_19, k_20
k_16, k_17
I_1
k_15

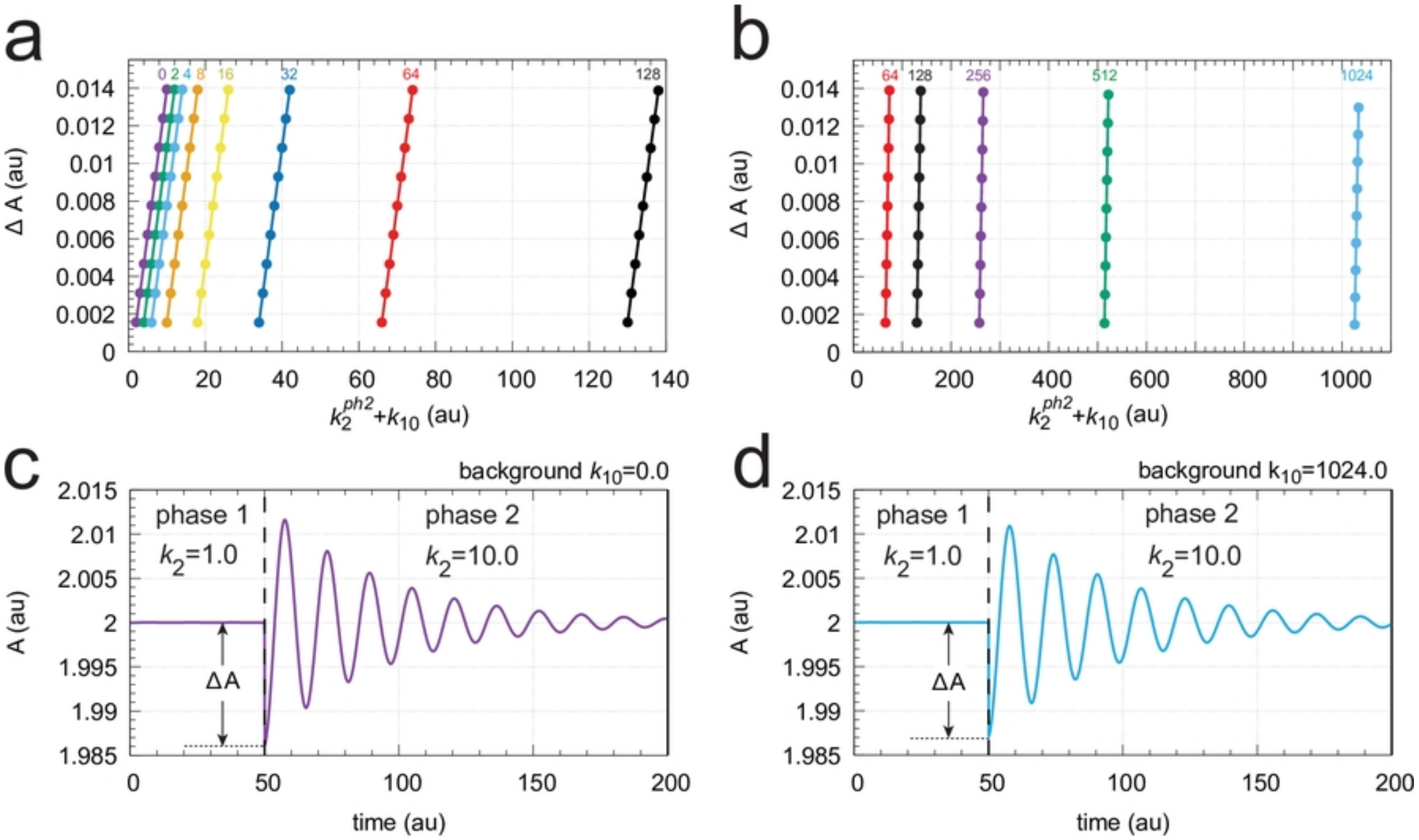
a
0 2 4 8 16 32 64 128
Δ A (au)
$k_2^{ph2}+k_{10}$ (au)
b
64 128 256 512 1024
Δ A (au)
$k_2^{ph2}+k_{10}$ (au)
c
background k_{10}=0.0
phase 1
k_2=1.0
phase 2
k_2=10.0
ΔA
A (au)
time (au)
d
background k_{10}=1024.0
phase 1
k_2=1.0
phase 2
k_2=10.0
ΔA
A (au)
time (au)

Figure 14

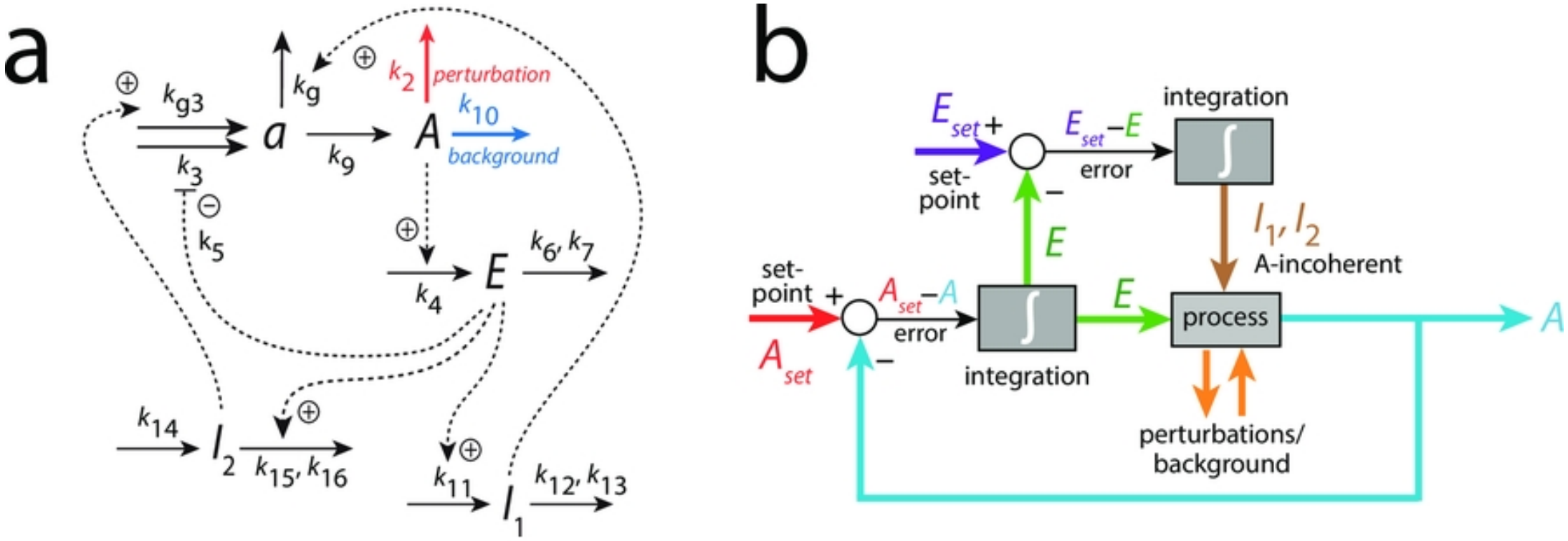
a
k_{g3}
k_g
k_2
perturbation
k_{10}
background
a
A
k_3
k_9
k_5
k_4
E
k_6, k_7
k_{14}
I_2
k_{15}, k_{16}
k_{11}
I_1
k_{12}, k_{13}
b
E_{set} +
$E_{set} - E$
integration
set-point
error
E
I_1, I_2
A-incoherent
set-point +
$A_{set} - A$
error
A_{set}
integration
process
A
perturbations/
background

Figure 15

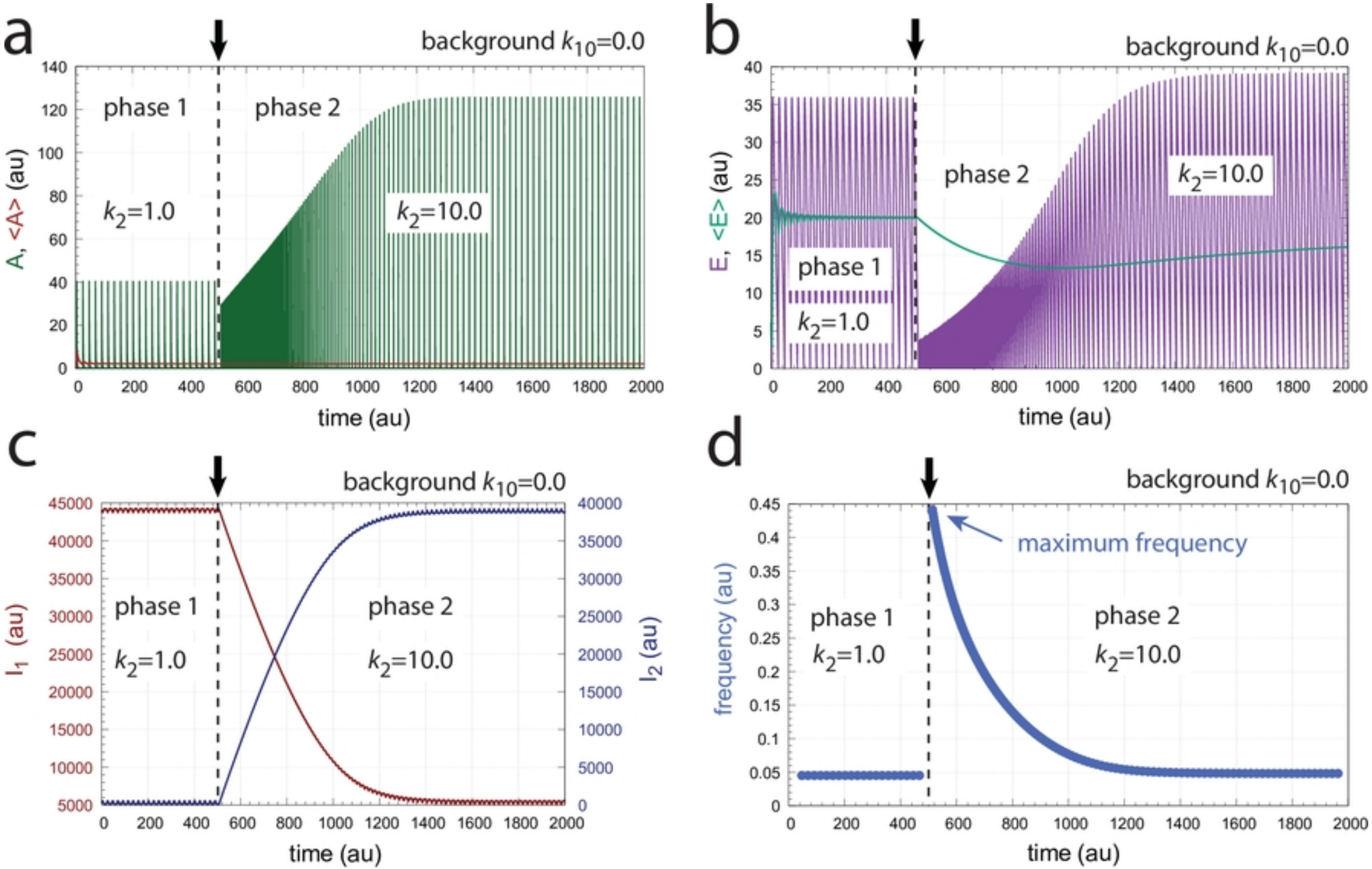
a
background k_{10}=0.0
phase 1
phase 2
k_2=1.0
k_2=10.0
A, <A> (au)
time (au)
b
background k_{10}=0.0
phase 2
k_2=10.0
phase 1
k_2=1.0
E, <E> (au)
time (au)
c
background k_{10}=0.0
phase 1
k_2=1.0
phase 2
k_2=10.0
I_1 (au)
I_2 (au)
time (au)
d
background k_{10}=0.0
maximum frequency
phase 1
k_2=1.0
phase 2
k_2=10.0
frequency (au)
time (au)

Figure 16

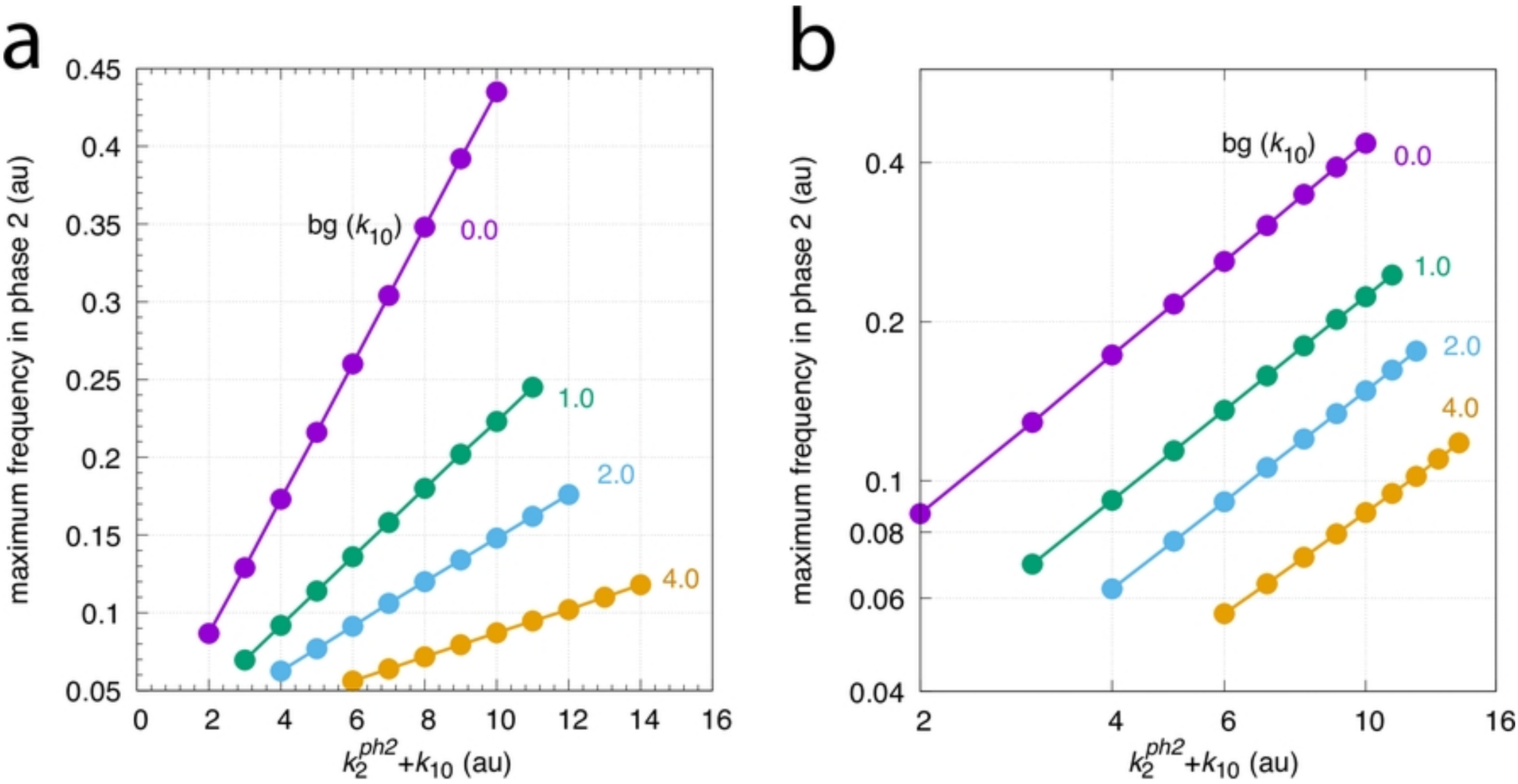
a
b
maximum frequency in phase 2 (au)
$k_2^{ph2}+k_{10}$ (au)
bg (k_{10})
0.0
1.0
2.0
4.0

Figure 17

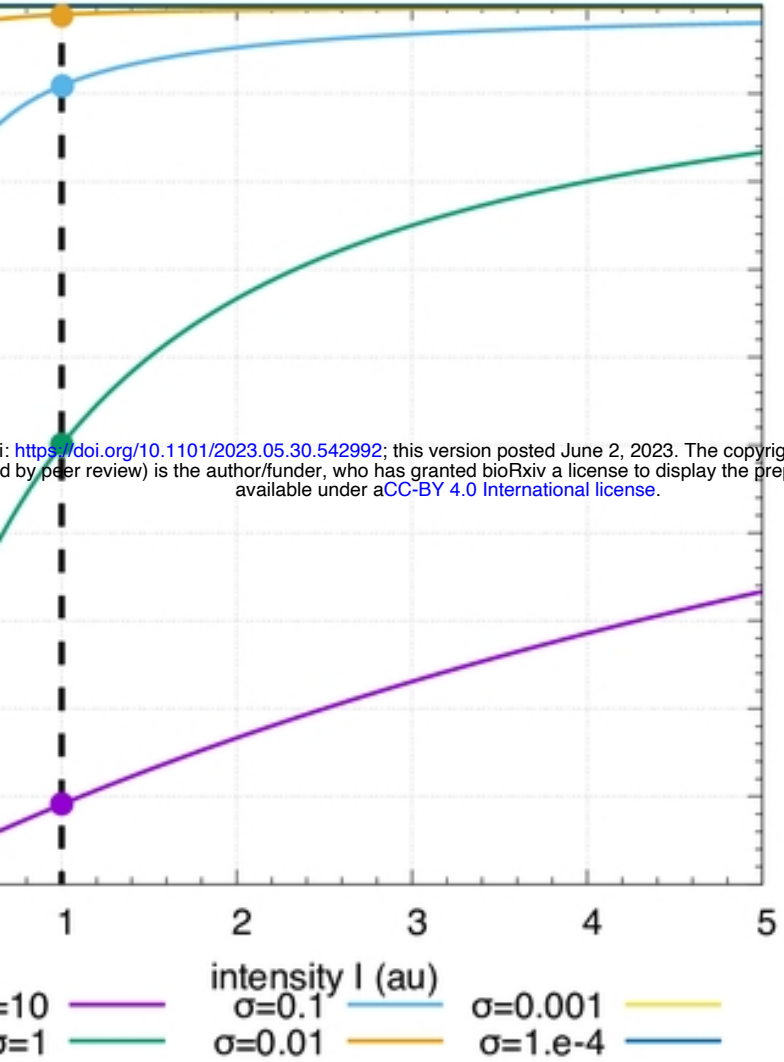

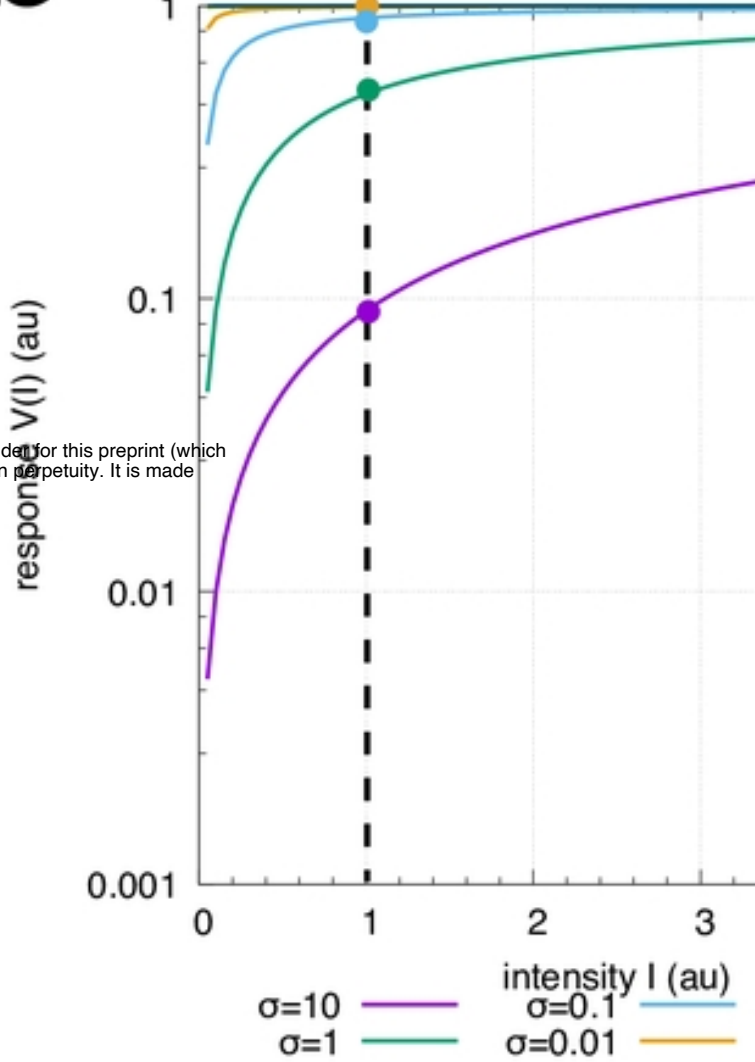

d

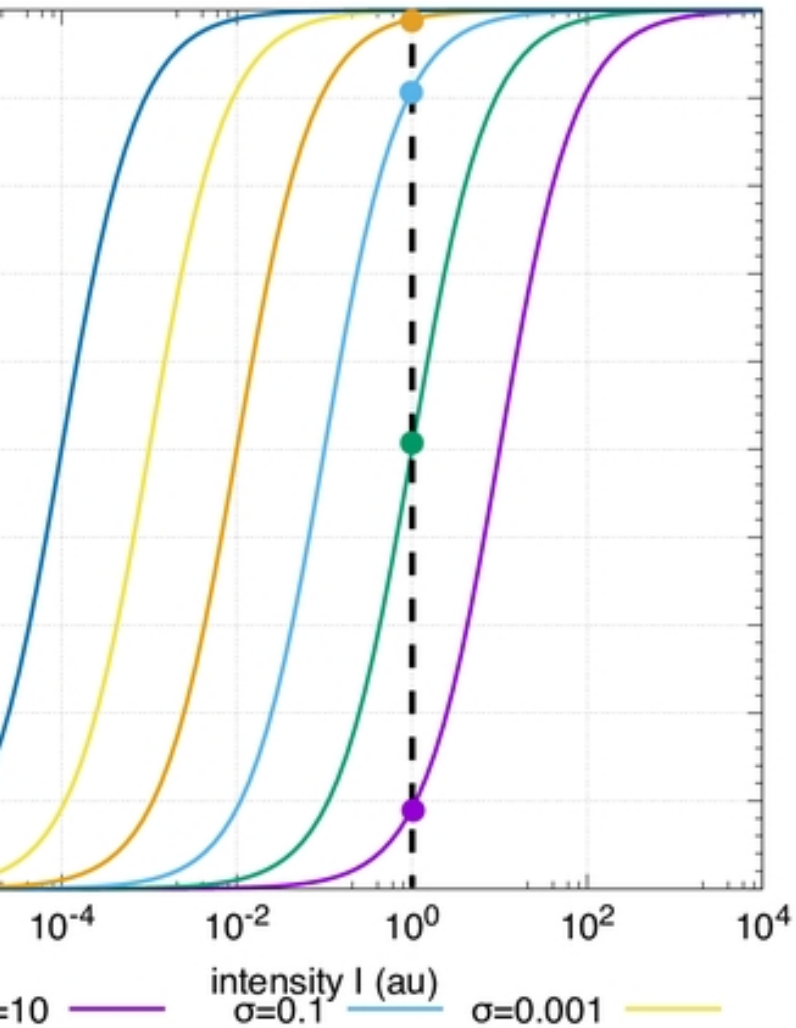

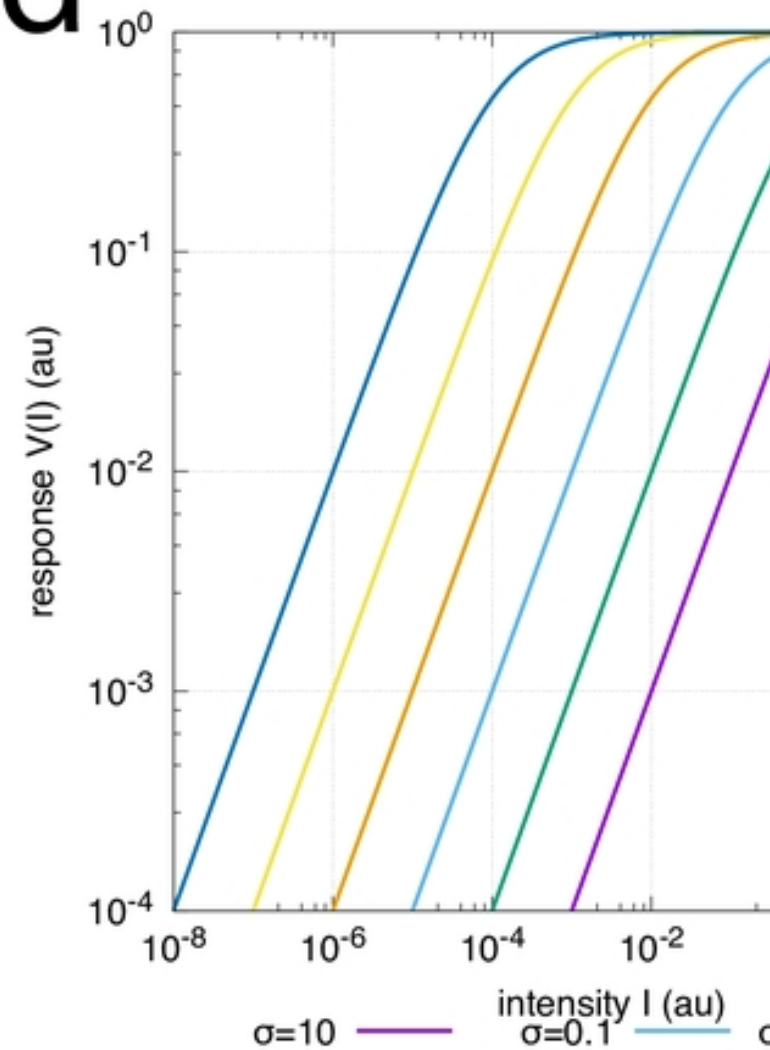

Bibliography

[1] J. Grini, M. Nygard, and P. Ruoff. Homeostasis at different backgrounds: The roles of overlayed feedback structures in vertebrate photoadaptation. *PLOS ONE*, 2023. doi: https://doi.org/10.1101/2023.01.25.525568.

[2] K. Thorsen, O. Agafonov, C. H Selstø, I. W Jolma, X. Y. Ni, T. Drengstig, and P. Ruoff. Robust concentration and frequency control in oscillatory homeostats. *PLOS ONE*, 9(9):e107766, 2014. doi: https://doi.org/10.1371/journal.pone.0107766.

[3] D. Purves, G. J. Augustine, D. Fitzpatric, W. Hall, A. LaMantia, J. McNamara, and L. E. White, editors. *Neuroscience fourth edition*. Sinauer Associates, Inc., 2008. ISBN 0878936971.

[4] Melissa Nygård and Peter Ruoff. Coherent feedback leads to robust background compensation in oscillatory and non-oscillatory homeostats. *bioRxiv*, pages 2023–05, 2023.

[5] Seth Lloyd. Coherent quantum feedback. *Physical Review A*, 62(2):022108, 2000.

[6] Bixuan Fan, Jiahui Ning, Min Xie, Cunjin Liu, and Shengguo Guan. Coherent feedback induced transparency. *Optics Express*, 28(19):28243–28251, 2020.

[7] T Drengstig, IW Jolma, XY Ni, K Thorsen, XM Xu, and P Ruoff. A basic set of homeostatic controller motifs. *Biophysical journal*, 103(9):2000–2010, 2012. doi: https://doi.org/10.1016/j.bpj.2012.09.033.

[8] Eric R Kande, John D Koester, Sarah H Mack, and Steven A Siegelbaum. *Principles of Neural Science*. McGraw-Hill's AccessNeurology. McGraw-Hill Education LLC, New York, N.Y, 6th edition. edition, 2021. ISBN 1259642232.

[9] Walter B. Cannon. Organization for physiological homeostasis. *Physiological Reviews*, IX(3):399–431, 1929. doi: https://doi.org/10.1152/physrev.1929.9.3.399.

[10] L. L. Langley, editor. *Homeostasis. Origins of the Concept.* Benchmark Papers in Human Physiology, v. [1]. Dowden, Hutchinson & Ross, Inc, Stroudsburg, Pennsylvania, USA, 1973. ISBN 0879330074.

[11] Charles Blagden. Xii. experiments and observations in an heated room. *Philosophical transactions of the Royal Society of London*, (65):111–123, 1775.

[12] Charles Blagden. Xlvii. further experiments and observations in an heated room. *Philosophical Transactions of the Royal Society of London*, (65):484–494, 1775.

[13] John Hunter. 1778 ii. of the heat, &c. of animals and vegetables phil. trans. r. soc. 68 7–49 http://doi. org/10.1098/rstl. 1778.0002.

[14] C. Bernard. *Introduction à l'étude de la médecine expérimentale.* Number 2. JB Baillière, 1865.

[15] L. L. Langley. *An Introduction to the Study of Experimental Medicine.* Dover Books ON Biology Ser. Dover Publications, New York, USA, 1957. ISBN 0486204006.

[16] Steven J. Cooper. From claude bernard to walter cannon. emergence of the concept of homeostasis. *Appetite*, 51(3):419–427, 2008. ISSN 0195-6663. doi: https://doi.org/10.1016/j.appet.2008.06.005.

[17] George E. Billman. Homeostasis: The underappreciated and far too often ignored central organizing principle of physiology. *Frontiers in Physiology*, 11, 2020. ISSN 1664-042X. doi: https://doi.org/10.3389/fphys.2020.00200.

[18] M. Moore-Ede. Physiology of the circadian timing system: Predictive versus reactive homeostasis. *The American journal of physiology*, 250:R737–52, 1986. doi: https://doi.org/10.1152/ajpregu.1986.250.5.R737.

[19] P. Sterling and J. Eyer. *Allostasis: A New Paradigm to Explain Arousal Pathology.* John Wiley & Sons, New York, 1988.

[20] Jay Schulkin et al. *Allostasis, homeostasis, and the costs of physiological adaptation.* Cambridge University Press, 2004.

[21] Jay Schulkin. *Rethinking homeostasis: Allostatic regulation in physiology and pathophysiology.* MIT Press, 2003.

[22] Bruce S McEwen and John C Wingfield. What's in a name. integrating homeostasis, allostasis and stress. *Hormones and behavior*, 57(2):105, 2010. doi: https://doi.org/10.1016/j.yhbeh.2009.09.011.

[23] D. Lloyd, M. Aon, and S. Cortassa. Why homeodynamics, not homeostasis? *The Scientific World Journal*, 1:133–145, 2001. doi: https://doi.org/10.1100/tsw.2001.20.

[24] N. Mrosovsky. *Rheostasis. The physiology of change.* Oxford University Press, 1990.

[25] George Fink. *Stress science: neuroendocrinology.* Academic Press, 2010.

[26] RHS Carpenter. Homeostasis: a plea for a unified approach. *Advances in physiology education*, 28(4):180–187, 2004.

[27] James C. Maxwell. On governors. *Proceedings of the Royal Society*, 16:270–283, 1868. doi: https://doi.org/10.1098/rspl.1867.0055.

[28] A. Rosenblueth, N. Wiener, and J. Bigelow. Behavior, purpose and teleology. *Philosophy of Science*, 10(1):18–24, 1943. doi: https://doi.org/10.1086/286788.

[29] W.S. McCulloch and W.A Pitts. A logical calculus of the ideas immanent in nervous activity. *Bulletin of Mathematical Biophysics*, 5:115–133, 1943. doi: https://doi.org/10.1007/BF02478259.

[30] N. Wiener. Cybernetics : Control and communication in the animal and the machine –2nd. ed. *Bulletin of Mathematical Biophysics*, 1961.

[31] S. Bennett. A brief history of automatic control. *IEEE Control Systems Magazine*, 16(3):17–25, 1996. doi: 10.1109/37.506394,.

[32] F. L Lewis. *Applied optimal control and estimation.* Prentice Hall PTR, 1992.

[33] T. Yi, Y. Huang, M. I. Simon, and J. Doyle. Robust perfect adaptation in bacterial chemotaxis through integral feedback control. *Proceedings of the National Academy of Sciences*, 97(9):4649–4653, 2000. doi: https://doi.org/10.1073/pnas.97.9.4649.

[34] S. K. Aoki, G. Lillacci, A. Gupta, A. Baumschlager, D. Schweingruber, and M. Khammash. A universal biomolecular integral feedback controller for robust perfect adaptation. *Nature*, 570(7762):533–537, 2019. doi: https://doi.org/10.1038/s41586-019-1321-1.

[35] Q. Waheed, H. Zhou, and P. Ruoff. Kinetics and mechanisms of catalyzed dual-e (antithetic) controllers. *PLOS ONE*, 17(8):e0262371, 2022.

[36] C. Briat, A. Gupta, and M. Khammash. Antithetic integral feedback ensures robust perfect adaptation in noisy biomolecular networks. *Cell systems*, 2(1):15–26, 2016.

[37] T. Drengstig, XY. Ni, K. Thorsen, IW. Jolma, and P. Ruoff. Robust adaptation and homeostasis by autocatalysis. *The Journal of Physical Chemistry B*, 116(18):5355–5363, 2012. doi: https://doi.org/10.1021/jp3004568.

[38] J. E Dowling. *The Retina. An approchabale part of the brain. Revised edition.* The Belknap Press of Harvard University Press, Cambridge, Massachusetts and London, England, 2012. ISBN 0674061543.

[39] Bert Sakmann and Otto D Creutzfeldt. Scotopic and mesopic light adaptation in the cat's retina. *Pflügers Archiv*, 313:168–185, 1969.

[40] Bruce M Koeppen and Bruce A Stanton. *Berne & Levy Physiology, Updated Edition E-Book.* Elsevier Health Sciences, 2009.

[41] A. R. Martin, D. A. Brown, M. E. Diamond, A. Cattaneo, and F. De-Miguel. *From Neuron to Brain sixth edition.* Sinauer Associates, Inc., 2020. ISBN 1605354392.

[42] Gordon L Fain, Hugh R Matthews, M Carter Cornwall, and Yiannis Koutalos. Adaptation in vertebrate photoreceptors. *Physiological reviews*, 81(1):117–151, 2001.

[43] DM Schneeweis and JL Schnapf. Noise and light adaptation in rods of the macaque monkey. *Visual neuroscience*, 17(5):659–666, 2000.

[44] Jacqueline Wilkie, Michael Johnson, and K Reza. *An Introductory Course.* Springer, 2002.

[45] Kevin Warwick. *An introduction to control systems*, volume 8. World Scientific, 1996.

[46] Xiao Yu Ni, Tormod Drengstig, and Peter Ruoff. The control of the controller: molecular mechanisms for robust perfect adaptation and temperature compensation. *Biophysical journal*, 97(5):1244–1253, 2009.

[47] Paula I Moreira. High-sugar diets, type 2 diabetes and alzheimer's disease. *Current Opinion in Clinical Nutrition & Metabolic Care*, 16(4):440–445, 2013.

[48] Michael Joubert, Alain Manrique, Bertrand Cariou, and Xavier Prieur. Diabetes-related cardiomyopathy: The sweet story of glucose overload from epidemiology to cellular pathways. *Diabetes & Metabolism*, 45(3):238–247, 2019.

[49] Ken-Ichi Naka and William AH Rushton. S-potentials from luminosity units in the retina of fish (cyprinidae). *The Journal of physiology*, 185(3):587–599, 1966.

[50] Jochen Kleinschmidt and John E Dowling. Intracellular recordings from gecko photoreceptors during light and dark adaptation. *The Journal of general physiology*, 66(5):617–648, 1975.